

Proteomics of *Aspergillus nidulans* sexually differentiated cells

Dissertation
for the award of the degree
“Doctor rerum naturalium”
Division of Mathematics and Natural Sciences
of the Georg-August University Göttingen

submitted by
Benedict Dirnberger
from Vienna (Austria)
Göttingen 2018

Es leuchtet! Seht! – Nun lässt sich wirklich hoffen, dass, wenn wir aus viel hundert Stoffen durch Mischung – denn auf Mischung kommt es an – den Menschenstoff gemächlich komponieren, in einen Kolben verlutieren und ihn gehörig kohobieren, so ist das Werk im Stillen abgetan.

Faust II (Johann Wolfgang von Goethe)

Thesis Committee Members:

Member of the Thesis Committee: **Professor Dr. Gerhard H. Braus** (Reviewer I)
Department of Molecular Microbiology and Genetics, Institute of Microbiology and Genetics, Georg-August University Goettingen

Member of the Thesis Committee: **Professor Dr. Stefanie Pöggeler** (Reviewer II)
Department of Genetics of Eukaryotic Microorganisms, Institute of Microbiology and Genetics, Georg-August University Goettingen

Member of the Thesis Committee: **Dr. Oliver Valerius**
Department of Molecular Microbiology and Genetics, Institute of Microbiology and Genetics, Georg-August University Goettingen

Examination Board Members:

Member of the Examination Board: **Professor Dr. Heike Krebber**
Department of Molecular Genetics, Institute of Microbiology and Genetics, Georg-August University Goettingen

Member of the Examination Board: **Professor Dr. Kai Heimel**
Department of Microbial Cell Biology, Institute of Microbiology and Genetics, Georg-August University Goettingen

Member of the Examination Board: **Privatdozent Dr. Michael Hoppert**
Department of General Microbiology, Institute of Microbiology and Genetics, Georg-August University Goettingen

Date of oral examination: 04.07.2018

This doctoral thesis was performed in the group of **Professor Dr. Gerhard H. Braus**. Department of Molecular Microbiology and Genetics, Institute of Microbiology and Genetics, Georg-August University Goettingen.

Affirmation

I declare that my doctoral thesis was written on my own having used only the listed resources and tools.

Erklärung

Die vorgelegte Arbeit wurde von mir selbständig angefertigt und nur die angegebenen Hilfsmittel wurden benutzt. Alle Stellen, die dem Wortlaut oder dem Sinne nach anderen Werken entnommen wurden, sind durch Angabe der Quelle kenntlich gemacht worden

Göttingen am 14.05.2018

Benedict Dirnberger

Table of contents

Summary.....	1
Zusammenfassung.....	2
1. Introduction	4
1.1. The genus <i>Aspergillus</i>	4
1.1.1. <i>Aspergillus</i> section <i>Nidulantes</i>	4
1.1.2. <i>Aspergillus nidulans</i> : A model organism for fungal development and secondary metabolism.....	5
1.1.3. Economic impact of <i>Aspergilli</i>	6
1.2. Morphological aspects	7
1.2.1. Hyphae.....	7
1.2.2. Hülle cells	7
1.2.3. Cleistothecia.....	9
1.2.4. Conidiophores.....	10
1.3. Factors influencing fungal development	11
1.3.1. Environmental factors	11
1.3.1.1. Light favors asexual differentiation.....	13
1.3.1.2. Sexual differentiation is promoted by darkness	13
1.3.1.3. Nutrients	14
1.3.2. Endogenous factors	14
1.3.2.1. Primary metabolism.....	15
1.3.2.2. Secondary metabolism.....	16
1.4. Specialized metabolism in fungal development.....	17
1.4.1. The monodictyphenone (<i>mdp</i>) / xanthone (<i>xpt</i>) secondary metabolite gene clusters.....	17
1.4.1.1. Monodictyphenone is a precursor for the synthesis of xanthones	18
1.4.2. LaeA as a factor that coordinates fungal development and secondary metabolism	21
1.4.2.1. LaeA methyltransferase	21
1.4.2.2. LaeA methyltransferase promotes Hülle cell formation	22
1.4.2.3. LaeA regulates the monodictyphenone (<i>mdp</i>) and other secondary metabolite gene clusters.....	24
1.4.3. Relationship between fungal development and secondary metabolism.....	25

1.4.3.1. Secondary metabolites that activate sporulation	25
1.4.3.2. Pigments	25
1.4.3.3. Secondary metabolites to protect the fungus against fungivory and other environmental threats	26
1.5. Aim of this work.....	27
2. Materials and methods	28
2.1. Materials.....	28
2.1.1. Strains	28
2.1.2. Plasmids	29
2.1.3. Primers.....	29
2.1.4. Chemicals and equipment	31
2.1.5. Solutions and growth media	35
2.1.5.1. Solutions.....	35
2.1.5.2. Growth media	36
2.2. Methods.....	37
2.2.1. Cultivation of <i>Aspergillus nidulans</i>	37
2.2.1.1. Hülle cells from solid agar plate: cleistothecia-rolling technique	37
2.2.1.2. Hülle cells from submerged cultures.....	39
2.2.2. DNA methods.....	40
2.2.2.1. Genetic transformation procedure.....	40
2.2.2.2. Plasmid DNA isolation from <i>Escherichia coli</i>	40
2.2.2.3. <i>Aspergillus nidulans</i> DNA extraction.....	41
2.2.2.4. Ligation of DNA fragments	41
2.2.2.5. PCR (Polymerase chain reactions)	42
2.2.2.6. Gelelectrophoresis of DNA.....	42
2.2.2.7. Purification of amplified DNA	43
2.2.2.8. Southern hybridization	43
2.2.2.9. Sequence analysis and oligonucleotides synthesis	44
2.2.2.10. <i>Aspergillus nidulans</i> strain construction	45
2.2.3. Protein methods	59
2.2.3.1. Protein extraction of Hülle cells from <i>Aspergillus nidulans</i>	59
2.2.3.2. Protein extraction of sexual mycelium from <i>Aspergillus nidulans</i>	59
2.2.3.3. Protein extraction of vegetative mycelium from <i>Aspergillus nidulans</i>	60

2.2.3.4. Protein extraction of asexual mycelium from <i>Aspergillus nidulans</i>	60
2.2.3.5. Protein concentration measurement.....	61
2.2.3.6. SDS-polyacrylamide gel electrophoresis	61
2.2.3.7. Colloidal Coomassie staining of proteins	61
2.2.3.8. In-gel protein digestion with trypsin.....	61
2.2.3.9. Liquid chromatography-mass spectrometry (LC-MS) and data analysis	63
2.2.3.10. Functional annotation of proteins	64
2.2.3.11. Fluorescence microscopy of fusion proteins	64
2.2.3.12. Immunoblotting.....	65
3. Results	66
3.1. Enrichment of sexual tissue and specialized Hülle cells.....	66
3.1.1. Hülle cells can be enriched from solid agar plates for comparative proteomics ...	66
3.1.2. Hülle cells can be enriched from submerged liquid cultures for comparative proteomics.....	67
3.2. Enzymes encoded by the monodictyphenone (<i>mdp</i>) / xanthone (<i>xpt</i>) secondary metabolite gene clusters are increased during sexual differentiation: proteome comparison of <i>Aspergillus nidulans</i> development grown on surfaces.....	68
3.2.1. Enrichment of surface Hülle cells enabled to perform a comparative proteome analysis	68
3.2.2. Comparative proteomics revealed that the proteome of surface Hülle cells overlaps especially to that of sexual mycelium.....	69
3.2.3. Comparative proteomics reveal six proteins found in enriched Hülle cells from solid agar plates	71
3.2.4. Surface Hülle cells contain increased enzyme levels for the mobilization of complex sugar molecules.....	73
3.2.5. Enzymes encoded by the monodictyphenone (<i>mdp</i>) / xanthone (<i>xpt</i>) gene clusters were found in Hülle cells and sexual mycelium from solid agar plates.....	73
3.2.6. Proteins encoded by the xanthone (<i>xpt</i>) gene cluster are enriched in the cytoplasm of Hülle cells.....	75
3.2.7. Comparative proteomics revealed that the proteome of surface Hülle cells overlaps to other fungal tissues besides of a sexual mycelium	78
3.2.8. Functional annotation reveals that surface Hülle cells are highly involved in carbohydrate and amino acid metabolism.....	80
3.3. Hülle cells from surface growth and liquid media differ in their composition by 28% beside a shared core proteome: Proteomes of <i>Aspergillus nidulans</i> development grown on surfaces compared to liquid cultures.....	81
3.3.1. Hülle cell formation in submerged liquid cultures for comparative proteomics.....	81

3.3.1.1. Submerged liquid cultures revealed the proteome for comparative analysis .	85
3.3.2. Quantification of proteins in submerged liquid cultures of a <i>laeA</i> Δ mycelium revealed two Hülle cells proteins	85
3.3.2.1. Quantitative determination of proteins in <i>laeA</i> Δ revealed that NptA is present in Hülle cells as well as in other fungal tissues.....	88
3.3.2.2. Quantitative protein analysis revealed the kinase RfeA enriched in Hülle cells and other fungal tissues	91
3.3.3. The core proteome revealed a 72% overlap between the identified proteins of both types of Hülle cells	94
3.3.4. The proteome of surface Hülle cells compared to Hülle cells from liquid media differ in composition by 28%.....	96
3.4. Functional analysis of genes for Hülle cell enriched proteins: A maltose permease-like protein of surface Hülle cells supports fungal growth and development	98
3.4.1. Comparative proteomics revealed two overlapping proteins found in Hülle cells from both approaches.....	98
3.4.2. A similar protein to a maltose transporter is enriched in surface Hülle cells and supports growth and fungal development	103
3.4.2.1. The sequence of MphA a maltose permease-like protein enriched in Hülle cells contains a distinctive sugar motif.....	103
3.4.2.2. MphA protein supports fungal growth and development	105
3.4.2.3. MphA protein is localized to the envelope of Hülle cells.....	107
3.4.2.4. The deletion of <i>mphA</i> prevents mycelia differentiation at higher concentration of carbohydrates in an early developmental time point.....	109
4. Discussion	111
4.1. Hülle cells and sexual tissue grown on solid agar plates revealed the presence of proteins for the synthesis of an antimicrobial substance.....	111
4.2. Submerged liquid cultures revealed the presence of the prenyltransferase NptA and the serine/threonine kinase RfeA in Hülle cells and in other fungal tissues ...	113
4.3. Hülle cells from surface and liquid cultures comprise shared proteins encoded by the monodictyphenone (<i>mdp</i>) / xanthone (<i>xpt</i>) gene clusters	117
4.4. Hülle cells from surface growth and liquid media comprise an ankyrin and a tyrosinase protein	120
4.5. A maltose permease-like protein enriched in surface Hülle cells supports fungal growth and development	123
4.6. Conclusion.....	127

References	129
Abbreviations	143
List of Figures	146
List of Tables	147
Acknowledgements	148
Curriculum vitae	149
Supplements	152

Summary

The homothallic mold *Aspergillus nidulans* produces as overwintering structures closed sexual fruiting bodies named cleistothecia, which contain ascospores as products of meiosis. Formation of fruiting bodies is linked to a specific secondary metabolism and includes a number of specialized cells like the globose-thick walled multinuclear Hülle cells. The LaeA methyltransferase represents an epigenetic regulator of numerous secondary metabolite clusters and is required for Hülle cell formation. Abolished Hülle cell formation correlates with a significantly reduced size of the cleistothecia, which suggested a nursing function of these cells for the growing fruiting body.

In this work, proteomes of fungal cells from different developmental programs and from enriched fractions of Hülle cells were compared to colonies grown on surfaces or in liquid medium. In a quantitative proteomics approach these results were compared to vegetative mycelia lacking the methyltransferase LaeA resulting in reduced Hülle cell formation and reduced secondary metabolism linked to the sexual program.

Comparative proteomics in combination with fluorescence microscopic investigations showed that the prenyltransferase XptB and other proteins encoded by the monodictyphenone (*mdp*) / xanthone (*xpt*) secondary metabolite gene clusters are found in sexual mycelium as well as in Hülle cells grown on surfaces or in submerged liquid cultures. NptA represents a second prenyltransferase, which could be identified in different fungal cell types including Hülle cells and quantitative proteomics revealed that the protein quantity of NptA is down-regulated in strains lacking LaeA.

Hülle cells grown on surfaces compared to liquid culture shared approximately 72% of the identified proteins in a core proteome. Besides the *mdp/xpt* protein, the ankyrin domain protein (AN8434) and the tyrosine domain protein (AN8435) are part of the core proteome and showed in fluorescence microscopic investigations a cellular localization in Hülle cells.

In contrast to Hülle cells derived from liquid culture, surface cells contained increased numbers of glucanase protein levels. Another specific protein, which was only identified in surface and not liquid Hülle cells was the maltose permease-like transporter of Hülle cells MphA. Genetic studies of the corresponding deletion strain revealed that the MphA protein, which is enriched in surface Hülle cells, promotes fungal growth, asexual and sexual development.

Zusammenfassung

Der homothallische Schimmelpilz *Aspergillus nidulans* produziert als Überwinterungsstrukturen geschlossene Fruchtkörper, welche man als Cleistothecien bezeichnet. Diese enthalten als Produkt der Meiose Ascosporen. Die Entwicklung der Fruchtkörper ist mit einem spezifischen sekundären Stoffwechsel verbunden, der mit der Bildung einer Reihe von spezialisierten Zellen, wie den dickwandigen globosen mehrkernigen Hülle-Zellen, gekoppelt ist. Die Methyltransferase LaeA ist als epigenetischer Regulator von zahlreichen sekundären Metabolit-Gen-Clustern für die Bildung von Hülle-Zellen erforderlich. Das Aussetzen der Bildung von Hülle-Zellen führt zu einer signifikanten Reduktion der Größe der Cleistothecien, woraus auf eine das Wachstum des Fruchtkörpers fördernde Funktion der Hülle-Zellen geschlossen werden kann.

In dieser Arbeit werden Proteome verschiedener Pilz-Zelltypen aus unterschiedlichen Entwicklungsprogrammen und aus angereicherten Fraktionen von Hülle-Zellen mit solchen verglichen, die aus Kolonien an der Oberfläche oder aus Flüssigmedien stammten. In einer quantitativen Proteom-Analyse wurden die Ergebnisse mit vegetativen Mycelien verglichen, denen die Methyltransferase LaeA fehlte. Das führte zu einer signifikanten Reduktion der Hülle-Zellen Bildung sowie des mit dem sexuellen Programm verbundenen Sekundärmetabolismus.

Vergleichende Proteomik in Verbindung mit fluoreszenzmikroskopischen Untersuchungen zeigte, dass zum Beispiel die Prenyltransferase XptB und andere Proteine, kodiert aus den Monodictyphenon (*mdp*) / Xanthon (*xpt*) sekundären Metabolit-Gen-Clustern, in Hülle-Zellen aus Fest- beziehungsweise Flüssigmedium sowie aus einem sexuellen Mycel gefunden werden. NptA repräsentiert die zweite Prenyltransferase und konnte in verschiedenen Pilz-Zelltypen sowie in Hülle-Zellen identifiziert werden. Durch quantitative Proteomik-Analysen wurde festgestellt, dass bei Fehlen von LaeA die Prenyltransferase NptA eine reduzierte Proteinmenge aufwies.

Das gemeinsame überlappende (Core-) Proteom der identifizierten Proteine stimmt zu cirka 72% bei an der Oberfläche gewachsenen Hülle-Zellen und jenen, die aus Flüssigmedium stammten, überein. Neben den *mdp/xpt* Proteinen zeigte das gemeinsame überlappende (Core-) Proteom noch zwei weitere Proteine, das Ankyrin-Domäne-Protein (AN8434) und das Tryosin-Domäne-Protein (AN8435), die eine

zelluläre Lokalisierung in Hülle-Zellen in fluoreszenzmikroskopischen Analysen aufweisen.

Im Gegensatz zu Hülle-Zellen, welche aus Flüssigmedium stammen, zeigen Hülle-Zellen, welche aus Oberflächen-Kulturen herrühren, eine erhöhte Protein-Anzahl an Glukanasen auf. Ein weiteres spezifisches Protein, das putative Maltose-Transport Protein MphA (Maltose Permease-artiges Protein von Hülle-Zellen) wurde ausschließlich in Hülle-Zellen aus Festmedium und nicht aus Flüssigmedium identifiziert. Genetische Studien zur Deletion von MphA zeigten, dass das MphA Protein, angereichert in Oberflächen-Hülle-Zellen, das Wachstum sowie die asexuelle und die sexuelle Entwicklung des Pilzes unterstützt.

1. Introduction

Fungi produce a wide range of secondary metabolites, some of which have properties that protect the fungus against harmful environmental influences. Secondary metabolite gene clusters that encode enzymes for the production of secondary metabolites are often activated under certain environmental conditions. The activation of secondary metabolite gene clusters is often linked to developmental processes. The transition of a rather undifferentiated vegetative growth to multicellular structures such as the cleistothecia activates certain secondary metabolite gene clusters (Bayram et al., 2016). The products of meiosis, the sexual spores, are protected by the cleistothecia. Cleistothecia are embedded in nest-like structures composed mainly of Hülle cells.

In order to protect the cleistothecia against harsh environmental conditions Hülle cells might have a key role in the process of secondary metabolism.

1.1. The genus *Aspergillus*

The fungal kingdom contains about eight different phyla. Ascomycetes represent the largest fungal phylum. Phylogenetic data suggest that fungi first appeared during the late Precambrian period and that the Ascomycota diverged from the Basidiomycota approximately 1206 million years ago (Heckman et al., 2001). The Ascomycota are divided into three different subphyla: (i) *Pezizomycotina*, (ii) *Saccharomycotina* and (iii) *Taphrinomycotina*. Genus *Aspergillus* belongs to the class *Eurotiomycetes* within the subphylum *Pezizomycotina*. It is presumed that the genus *Aspergillus* comprises over 350 species and sexual development is known for approximately 70 species (de Vries et al., 2017, Samson et. al., 2014).

1.1.1. *Aspergillus* section *Nidulantes*

Aspergillus species from section *Nidulantes* include a variety of morphological characteristics such as biseriate conidiophores and if present, sexual fruiting bodies embedded in masses of Hülle cells (Chen et al., 2016). *Aspergillus* species within the section *Nidulantes* are common in nature and play a central role in the decomposition processes in organic material. They colonize different habitats including terrestrial, freshwater and marine environments. *Aspergillus sydowii* is an example that colonizes

corals in marine habitats (Kirkwood et al., 2009, Rypien et al., 2008). Other members of the *Aspergillus* section *Nidulantes* are known to colonize humans and were reported in infectious diseases such as *Aspergillus versicolor* (Veraldi et al., 2010).

It was shown that different species of the section *Nidulantes* produce different mycotoxins (Kim et al., 2017). Secondary metabolites represent organic compounds that are important factors to protect and compete the fungus against harsh environmental conditions (Chang et al., 2017, Zhao et al., 2017, Caballero-Ortiz et al., 2013). Most of the species in the section *Nidulantes* produce the carcinogenic mycotoxin sterigmatocystin. Apart from the production of sterigmatocystin other mycotoxins are produced by different species in the section *Nidulantes* such as emestrin, fumitremorgins, asteltoxins and paxillin. *Aspergillus nidulans* is known to produce more than 100 different secondary metabolites including important pharmaceutically active compounds such as penicillin G (Chen et al., 2016).

1.1.2. *Aspergillus nidulans*: A model organism for fungal development and secondary metabolism

A. nidulans is a rapidly growing, saprophytic soil organism. The fungus is haploid and therefore, the organism is genetically better tractable. As a result, gene deletions and other mutations are possible. The fungus, therefore, can be used to answer research questions in the field of molecular biology. The presence of a sexual life cycle makes the fungus very attractive to study the molecular differences during various developmental programs.

A. nidulans was sequenced in the year 2005 (Galagan et al., 2005). The genome of *A. nidulans* contains 30 million base pairs, with eight haploid chromosomes and encodes 10555 proteins (Uniprot: Proteome ID UP00000056). Molecular biology, bioinformatics and comparative transcriptomics made it possible to study the expression of secondary metabolite gene clusters that are clustered within the genome and are often located near telomers (Clevenger et al., 2017). The well-studied products including important pharmaceuticals of *A. nidulans* like penicillin G made the fungus interesting for researchers (Itoh et al., 2017, Gerke and Braus 2014, Keller et al., 2005). Because *A. nidulans* produces different secondary metabolites in different developmental stages, it is crucial to study the life cycle of the fungus in more detail (Soukup et al., 2017).

1.1.3. Economic impact of *Aspergilli*

Some representatives of *Aspergillus* spp. are of significant economic benefit such as *Aspergillus niger* for the production of citric acid (Yu et al., 2018). *Aspergillus oryzae* is used in Asian cuisines for the fermentation of soya beans for the production of soya sauces or other traditional alcoholic beverages (Nishimura et al., 2018). Other representatives of *Aspergillus* spp. are of negative influence for their environment. For instance, *Aspergillus flavus* is an opportunistic, saprophytic fungus that infects maize and other feed crops. This leads to reduced harvest and can cause a substantial economic loss. *Aspergillus flavus* produces carcinogenic secondary metabolites. *Aspergillus flavus* which produces aflatoxins and herewith contaminates maize represents a serious threat to human health (Rajasekaran et al., 2018).

There are other *Aspergilli* with a negative impact on the health of human beings. For instance, *Aspergillus fumigatus* is a widespread fungus typically found in soil and decaying organic matter and represents a serious threat for immunocompromised patients such as organ transplant recipients and people with leukemia. Conidial germination of *Aspergillus fumigatus* into tissue-invasive hyphae can evoke life threatening infections (Shlezinger et al., 2017, Jöhnk et al., 2016). This can lead to an acute invasive and chronic pulmonary aspergillosis. *Aspergillus fumigatus* shows a high resistance against higher temperatures, dehydration and even disinfectants being able to survive in extremely harmful environmental conditions, even spores were isolated from the international space station (ISS); (Knox et al., 2016).

1.2. Morphological aspects

The filamentous fungus *A. nidulans* develops into a multicellular organism. The transition from undifferentiated growth, such as vegetative growth, to multicellular structures requires environmental and endogenous factors. Asexual and sexual development is linked to the formation of different spore-producing structures.

1.2.1. Hyphae

The initial and basic unit of filamentous fungi represents undifferentiated structures named hyphae. The formation of vegetative hyphae facilitates the habitation of various ecological niches. Hyphal growth requires cell surface expansion and cell wall disposition at the hyphal tip. Different types of hyphae are known and are formed during developmental processes.

Ascogenous dikaryotic hyphae are formed within cleistothecia. Through the fusion of two haploid nuclei a diploid meiotic nucleus is formed in an ascus mother cell. The ascus mother cell expands through a swelling process into an ascus (Kirk and Morris 1991).

Subtending hyphae are known to be attached to a spore from which the spore develops as a consequence of a swelling process. This is the case in Hülle cells.

1.2.2. Hülle cells

Eduard Eidam first described Hülle cells in 1883 where he termed Hülle cells as a “Blasenhülle” or bubble envelope (Eidam 1883). In different species, Hülle cell like structures are known such as in *Candida albicans* which produce at the very end of the hyphae globose blisters named chlamydospores (Navarathna et al., 2016). Eidam suggested that Hülle cells originate from the tip of “secondary hyphae” which in turn emerge from “primary hyphae” and develop as a consequence of a swelling process (Figure 1).

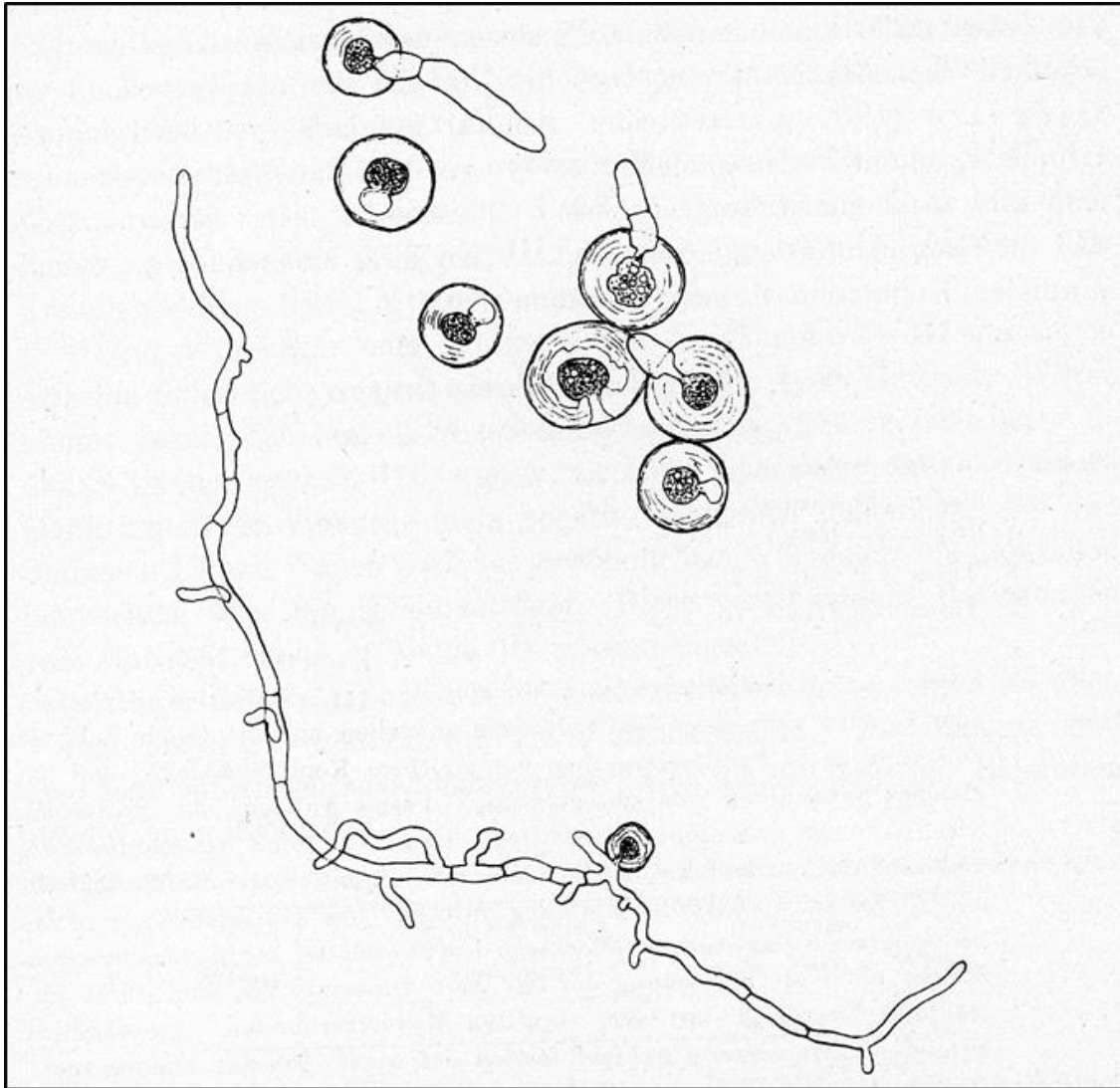


Figure 1. Adult Hülle cells and the subtending hyphae of Hülle cells.

Hülle cells are globose in shape with a thick cell wall and are often connected to subtending hyphae. These hyphae are of different size and length between very long and rather short and sometimes show a branch structure. Hyphae also contain subdividing septa. Within the globose structure of Hülle cells, a cytoplasm with metabolic activity is situated. The thick cell wall is ringshaped and open on one side. Two septa are visible in the open part of the ring (Raper and Fennel 1965).

Hülle cells and the subtending hyphae are connected via two distinct types of septa (Figure 2A). The inner one is a single perforate septum where woronin bodies can be observed and represents a typical ascomycetous septum. The second septum which separates Hülle cells from the subtending hyphae is unique and named basal septum (Figure 2B). At the basal septum vesicle fusion is observable. Consequently, to this fusion so called lomasome-like accumulations are visible. These lomasome-like structures are membrane-invaginations (Figure 2C). In Hülle cells several nuclei, mitochondria, lipid bodies and storage products can be observed (Ellis et al., 1973).

During initial Hülle cell formation, it was shown that several nuclei fuse to form a macronucleus (Carvalho et al., 2002). Different species of the *Aspergillus* genus produce Hülle cells, including *A. nidulans* and *Aspergillus heterothallicus* (Bayram and Braus 2012). Hülle cells have an average size of 12-20 µm, are of globose shape with an unusual thick cell wall and are mainly associated with the sexual developmental program. Hülle cells are known for all species in the section *Nidulantes* (Chen et al., 2016). In different species, Hülle cells vary in shape between the more elongated such as in *Aspergillus ustus* and the globose version like in *A. nidulans*. In *A. nidulans* and *Aspergillus heterothallicus* Hülle cells associate with the cleistothecia, whereas in *Aspergillus protuberus* and *Aspergillus ustus* Hülle cells are not in direct contact with the cleistothecia and are formed in masses (Muntanjola-Cvetkovic and Vukic 1972).

1.2.3. Cleistothecia

In *A. nidulans* the products of meiosis, the sexual spores, are situated and produced in the cleistothecia. The function of cleistothecia, therefore, is to protect the sexual spores against harsh environmental conditions. During sexual sporulation, certain hyphae develop to ascogenous hyphae. Ascogenous hyphae contain two haploid nuclei of opposite mating type. These hyphae form a hook shaped structure, named crozier, their nuclei divide synchronously. Different septae are formed thereby forming a dikaryotic top cell. After fusion of the end cell and the basal cell of the crozier karyogamy and further ascus development take place (Braus et al., 2002, Busch and Braus 2007). Hülle cells are most probably formed through a swelling process of certain vegetative hyphae. The first morphological manifestation of a visible structure is the appearance of cleistothecial initials, 40 hours after germination (Sohn and Yoon 2002). These structures are coiled lumps of cells, which undergo further coiling and become enlarged to approximately 10 µm. This is the stage where Hülle cells first appear (Sohn and Yoon 2002). *A. nidulans* produces dark reddish ascospores which are found in globose structures named asci (Dyer and O’Gorman 2012). These asci are protected by dark brown/violet ascomata. The ascomata are named cleistothecia in *Aspergillus nidulans*, due to its closed conformation (Greek: Kleistos = closed, theke = case). Cleistothecia are surrounded by numerous hyaline to pale brown globose Hülle cells.

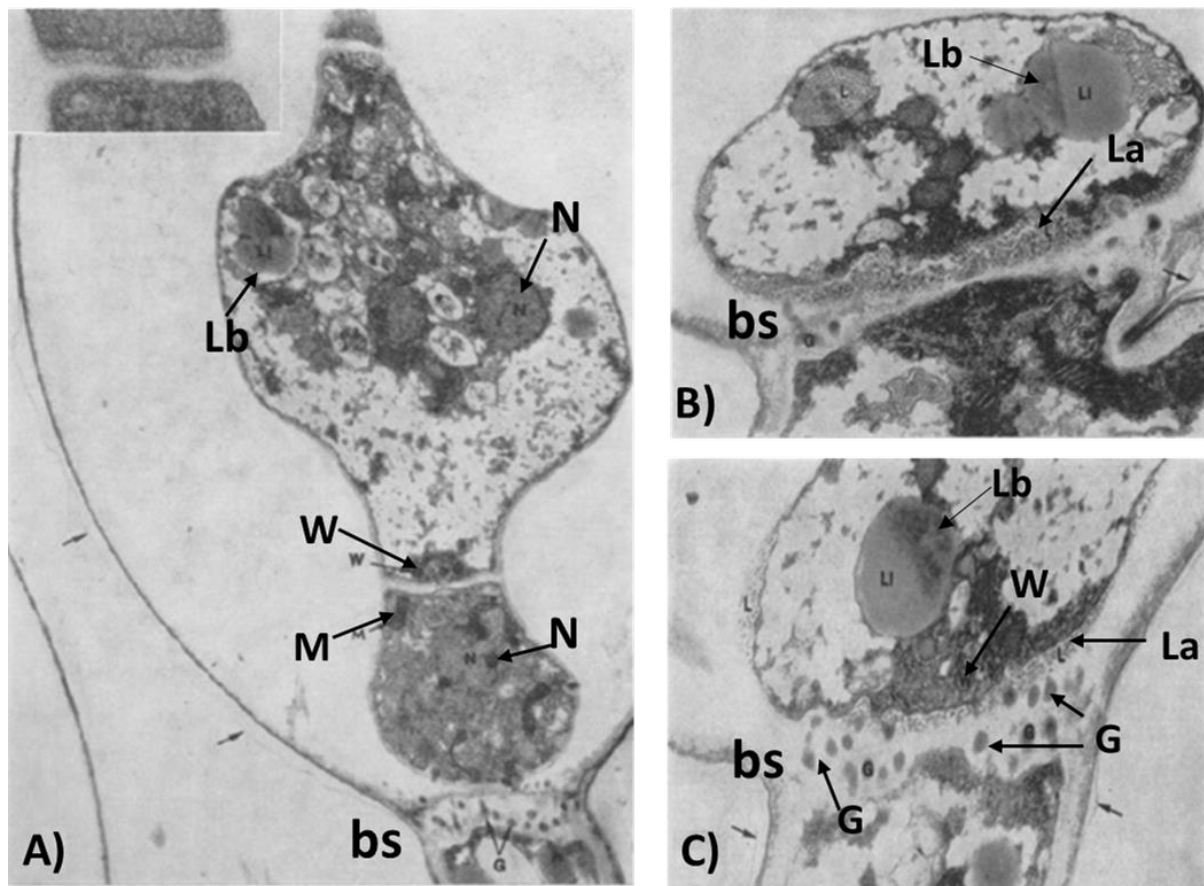


Figure 2. Electron microscope images of the content and septa found in Hülle cells of *Aspergillus nidulans*.

A) Overview picture of the content and the septa found in Hülle cells. The basal septum (bs) which separates Hülle cells from the subtending hyphae is unique. A second type of septum inside of Hülle cells is a typical ascomycetous septum where woronin bodies (W) and mitochondria (M) are observed. At the Hülle cell side (cytoplasm) lipid bodies (Lb) and nuclei (N) are visible. Further septa are possible in Hülle cells. B) The unique basal septum (bs) of Hülle cells. At the periphery of this septum (at Hülle cell side) lomasome-like accumulations (La) of the membrane are present (lomasome-like structures are invaginations of the membrane). In between the two septa woronin bodies (W), lipid bodies (Lb) and nuclei (N) are visible. Woronin bodies are close to the basal septum (bs). C) The basal septum (bs) contains globular structures (G). Image modified (Ellis et al., 1973).

1.2.4. Conidiophores

The *Aspergillus* species produces first foot cells from vegetative hyphae, which apically extend into a stalk. The very end of this cell swells to a so-called multinucleated vesicle. The vesicle produces a finger like metula as a first layer and a second layer, the phialides are formed by mitosis (Bayram and Braus 2012). These phialides undergo repeatedly asymmetric mitotically processes which lead to the production of haploid airborne conidiospores. After initial formation, conidiospores

undergo the maturation process. The progression of conidiospores is a separate process from the initial phase. The development of conidiospores contains several changes in cell wall structures and chemical modifications. During the maturation process, four different cell wall layers emerge. This enables impermeability of conidiospores, necessary to protect spores from harsh environmental conditions. Chemical modifications include the production of trehalose which serves as an energy source and protects against various environmental conditions such as dehydration, cold and oxidation (Elbein et al., 2003). Matured conidia are formed 15 hours after initial sporulation. The conidiophore represents the complete asexual structure which carries asexual spores called conidia.

1.3. Factors influencing fungal development

1.3.1. Environmental factors

Various environmental factors are important for *A. nidulans* to develop asexually on the surface (Figure 3A). Exposure to sunlight, in particular, represents a crucial factor (Dasgupta et al., 2016). Other environmental factors that induce the asexual developmental program are high oxygen concentrations, temperature shifts, osmotic stress and high concentrations of reactive oxygen species (ROS) (Bennett and Turgeon 2017, Noble and Andrianopoulos 2013). *A. nidulans* grow preferentially sexually and produce as overwintering structures, closed sexual fruiting bodies called cleistothecia in darkness under the soil (Dyer and O’Gorman 2012). Different environmental signals such as low oxygen concentrations, buffered temperature, humidity and low concentrations of ROS trigger sexual development. Asexual and sexual differentiation of *A. nidulans* is linked to significant changes in the formation of secondary metabolites and the formation of various distinct cell types of the respective developmental programs (Park et al., 2017). Asexual and sexual structures of *A. nidulans* are shown in Figure 3B.

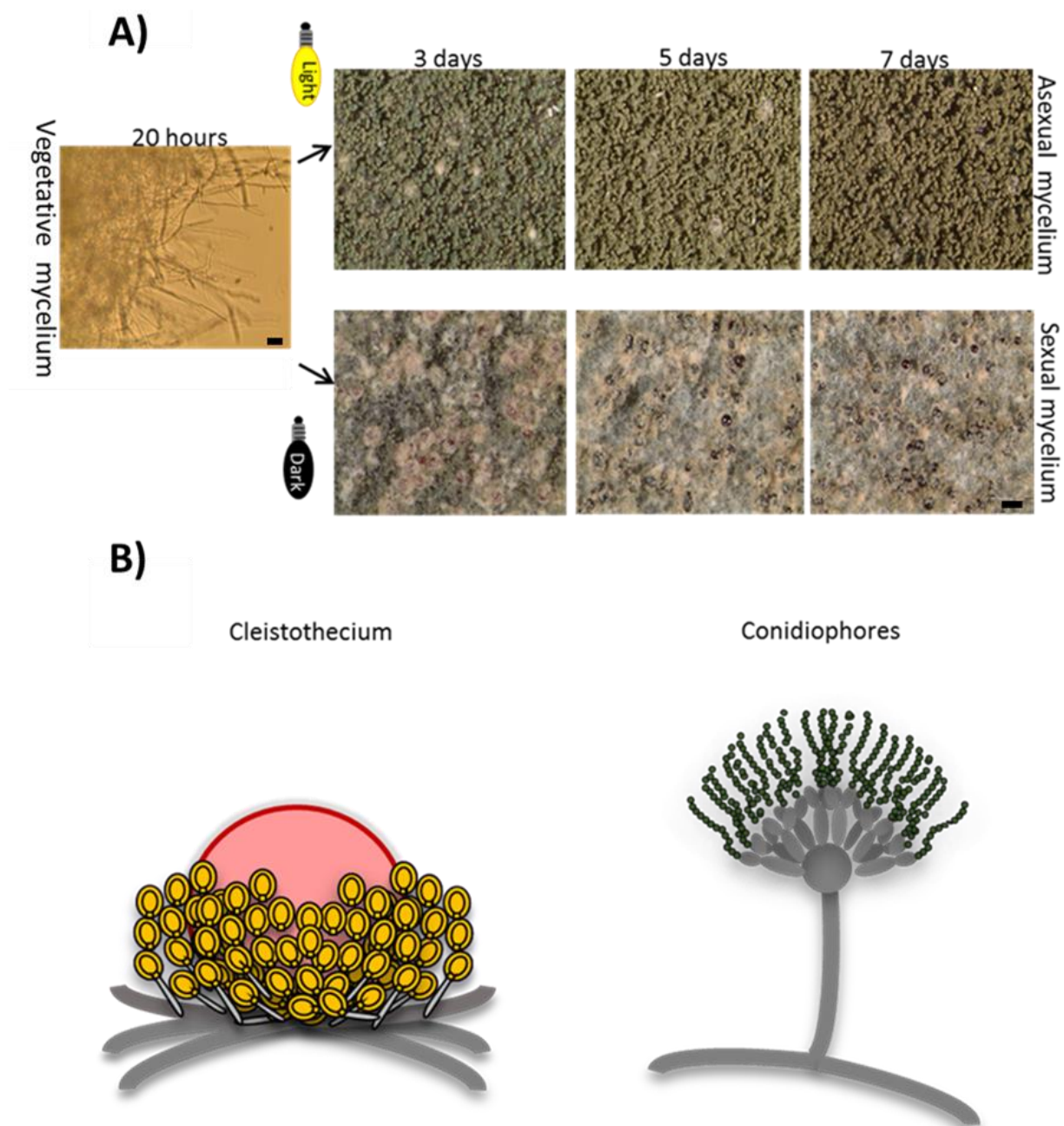


Figure 3. Asexual and sexual differentiation.

A) The fungus has to develop vegetative hyphae before cellular differentiation. This type of mycelium consists of relatively undifferentiated hyphae without other cell types. After the initial growth phase the fungus reaches a competence state, which defines a barrier to enter a differentiation capability. In light vegetative mycelium develops preferentially to asexual conidiophores, whereas in darkness the sexual developmental program is favored. Vegetative, asexual and sexual mycelia are shown at different time points. B) Different spore-producing structures of *Aspergillus nidulans*. Sexual differentiation increases sexual cell types such as cleistothecia. Hundreds of globose Hülle cells surround each cleistothecium. The cleistothecium contains sexual spores called ascospores. The asexual cell type is named conidiophore that carries the asexual spores called conidia. Scale bar is 200 μm . (Bennett and Turgeon 2017, Noble and Andrianopoulos 2013, Bayram and Braus 2012).

1.3.1.1. Light favors asexual differentiation

Light represents an important environmental factor that allows fungi to respond in different ways. Different processes are linked to light sensing in *A. nidulans*, including differentiation or changes in gene expression within primary and secondary metabolism. After the initial growth phase, the fungus reaches a competence state, that defines a barrier to enter a differentiation capability (Jiang et al., 2017, Ruger-Herreros et al., 2011). This allows to respond to different environmental factors. In light, *A. nidulans* preferentially develops asexually. The light-sensing function of fungi require a number of different, wave length specific receptors (Pöggeler et al., 2018). Cryptochromes (Cry) are a class of photolyase-like receptors sensitive to blue light. In *A. nidulans* the cryptochrome/photolyase CryA represses sexual differentiation beside its function in DNA-repair activities. Deletion of the corresponding gene *cryA* stimulated Hülle cell formation in submerged liquid cultures where usually no Hülle cells are formed. Asexual sporulation correlates with the production of few secondary metabolites. It was found that *A. nidulans* produces the antibiotic compound emericellamide (Chiang et al., 2008). The biosynthesis of the secondary metabolites emericellamide A, C and E, is initiated by light (Bayram et al., 2016). These types of antibiotics were shown to be present after 24 hours of growth in light, whereas in darkness, growth is extremely diminished (Bayram et al., 2016).

1.3.1.2. Sexual differentiation is promoted by darkness

Illumination mainly inhibits the production of certain secondary metabolites and favors asexual sporulation. Sexual reproduction is favored in darkness and low oxygen concentration. It is accompanied with the accumulation of secondary metabolites. The heterotrimeric velvet complex VelB/VeA/LaeA coordinates light signals with fungal development together with secondary metabolism (Bayram et al., 2008b). VeA bridges VelB to the methyltransferase LaeA. During illumination VeA is mostly situated in the cytoplasm where VelB supports asexual sporulation and LaeA shows low activity. In darkness VeA is imported into the nucleus by KapA (importin).

Additionally, VeA supports the transportation of VelB into the nucleus. VelB/VeA, forms together with *laeA* the heterotrimeric velvet complex VelB/VeA/LaeA. This complex regulates sexual sporulation and secondary metabolism. It was shown that

additional proteins associate with the heterotrimeric velvet complex and that specific secondary metabolite gene clusters are preferentially activated in darkness that lead to the accumulation of secondary metabolites like monodictyphenone, xanthone, asperthecin and sterigmatocystin (Sarıkaya-Bayram et al., 2014, Bayram et al., 2016).

1.3.1.3. Nutrients

Sexual and asexual development in *A. nidulans* is strongly affected by nutrients. Han and co-workers showed that the sexual development is favored in well-nourished growth conditions, whereas carbon limitation, light exposure and high concentration of salt promotes asexual development (Han et al., 2003). This suggests that stress conditions provoke asexual development, while well-nourished growth conditions favor sexual development. Chitins, carbohydrates and other compounds of the fungal cell wall are important factors for nutrient supply during development. During initial growth phase of the fungus α -1,3-glucans is accumulated in the fungal cell wall. Glucanases such as MutA or AngB degrade glucanes in the cell wall of storage hyphae to yield carbohydrates representing a carbon source (Zonneveld 1973, He et al., 2017, Wei et al., 2001) .

Amino acids are known to influence the growth of cleistothecia in *Aspergillus nidulans*. Amino acid starvation leads to impaired or stalled cleistothecia formation (Eckert et al., 1999, Serlupi et al., 1983). Storage lipids that represent carbon sources are present in lipid bodies and are found in Hülle cells (Ellis et al., 1973). It is known that fruiting body formation in various fungi is increased by addition of fatty acids (Pöggeler et al., 2006, Dyer et al., 1993; Goodrich-Tanrikulu et al., 1999).

1.3.2. Endogenous factors

Additional factors are required to allow the differentiation process of the fungus beside the above mentioned environmental factors. Primary as well as secondary metabolism are involved in this process. Primary and secondary metabolites are typically associated with different developmental programs. During initial growth phase primary metabolites are synthesized or obtained from the growth medium.

1.3.2.1. Primary metabolism

Primary metabolites such as amino acids, carbohydrates and lipids are molecules essential for growth, development and reproduction. Primary metabolites are mainly accumulated during initial growth phase and are processed during different developmental stages.

The process of sexual differentiation requires massive cell proliferation and as a result, increased carbon sources are required. Zonneveld and co-workers showed that α -1,3-glucans are accumulated during vegetative growth in the cell wall and that these polysaccharides are degraded during sexual development (Zonneveld 1973). The α -1,3-glucanase MutA was shown to be localized mainly in Hülle cells (Wei et al., 2001). The mobilization of α -1,3-glucans was affected in a *mutA* Δ strain although the cleistothecia were still able to grow similar to that of the wild-type (Wei et al., 2001). These results suggest that additional enzymes and carbon sources are most likely required as a nursing resource during the development of the cleistothecia (Yoshimi et al., 2017). It is assumed that Hülle cells comprise cell wall lytic enzymes that release monosaccharides (de Groot et al., 2009, Wei et al., 2001).

Furthermore, it is supposed that high affinity sugar transporters are involved to nurse the developing closed cleistothecia (Pöggeler et al., 2006). Wei and co-workers identified a putative hexose transporter, HxtA, that is expressed in Hülle cells and in ascogenous hyphae after starvation (Wei et al., 2004). The deletion of *hxtA* showed no effect on sexual development. The low affinity glucose transporter HxtB is suggested to be involved in fungal development (Dos Reis et al., 2017). Pantazopoulou and co-workers showed that the purine transporters UapA and AzgA are found in Hülle cells and on the surface of the cleistothecium (Pantazopoulou et al., 2007). The knockout of *uapA* and *azgA* showed no effect on the development of cleistothecia. This suggests that additional transporters are active during sexual development and required to supply nutrients or protective molecules to the maturing cleistothecia.

Amino acids, isopentenyl pyrophosphate and malonyl-CoA are building blocks for the synthesis of secondary metabolites. Malonyl-CoA represents in *A. nidulans* the initial unit for the synthesis of polyketides such as monodictyphenone which is a secondary metabolite (Klejnstrup et al., 2012).

1.3.2.2. Secondary metabolism

Primary and secondary metabolism merge into each other and as a result, the border is difficult to define. The morphological border to produce secondary metabolites is mainly determined by entering distinct developmental programs and thereby forming multicellular structures such as cleistothecia (Bayram et al., 2016).

Secondary metabolites are small-molecule metabolites produced by fungi, plants and bacteria. The production of secondary metabolites allows the fungus to colonize a multitude of environmental niches and allows to compete against other bacteria, fungi and insects (Demain and Fang 2000). Additionally, secondary metabolites production is connected to developmental processes of the fungus such as asexual and sexual sporulation.

Genes that encode enzymes for the production of secondary metabolites are often clustered and the expression of these genes are under the regulation of different factors (Hou et al., 2017, Brakhage 2013). Secondary metabolite gene clusters encode typically one of several backbone enzymes: (i) a polyketide synthase (PKS); (ii) a non-ribosomal peptide synthetase (NRPS); (iii) a polyketide synthase/non-ribosomal peptide synthetase hybrid (PKS-NRPS); (iv) a dimethyl-allyl-tryptophane synthase (DMATS) type aromatic prenyltransferase or (v) diterpene synthase (DTS) (Flores-Gallegos et al., 2016, Pan et al., 2017). The actions of the residual tailoring enzymes encoded by the residual genes from the gene cluster diversifies greatly the spectrum of the produced secondary metabolites of the gene cluster (Keller et al., 2005). The genome of *A. nidulans* encodes 29 polyketide synthases, eleven non-ribosomal peptide synthetases and seven prenyltransferases (de Vries et al., 2017, Galagan et al., 2005). Sequencing the genome of *A. nidulans*, proposes more than 40 different secondary metabolite pathways (Galagan et al., 2005).

In recent years, it was demonstrated that the expression of genes from secondary metabolite gene clusters and fungal development are coordinated through environmental factors (Cary et al., 2017, Röhrig et al., 2017). Bayram and co-workers showed that the transcripts of nine different genes from the monodictyphenone (*mdp*) / xanthone (*xpt*) gene clusters are specifically expressed during darkness in a sexual mycelium (Bayram et al., 2016).

1.4. Specialized metabolism in fungal development

Secondary metabolism, also called specialized metabolism, plays an important role in fungal development. Secondary metabolites are produced under special environmental conditions, in competition with other organisms and in special developmental stages.

1.4.1. The monodictyphenone (*mdp*) / xanthone (*xpt*) secondary metabolite gene clusters

The monodictyphenone (*mdp*) secondary metabolite gene cluster is found to contain twelve genes that are located near the rather silent telomeric region of chromosome VIII (Figure 4). It is known that chromatin remodeling factors are needed to influence the expression of genes that are responsible for the production of secondary metabolites (Gacek and Strauss 2012).

Bok and co-workers showed that CclA, a member of the histone 3 lysine 4 methylating COMPASS (complex associated with Set1) complex regulates the expression of secondary metabolite gene clusters such as the monodictyphenone (*mdp*) gene cluster (Bok et al., 2009). The deletion of *cclA* alters the expression of genes necessary for the production of monodictyphenone. Monodictyphenone represents a precursor for the synthesis of prenyl-xanthenes. The genes *xptA*, *xptB* and *xptC* required for the conversion of monodictyphenone into xanthenes are not embedded in the monodictyphenone gene cluster (Pockrandt et al., 2012, Sanchez et al., 2011). Instead, they are localized on two different chromosomes. The genes that encode the two prenyltransferases XptA and XptB are localized on chromosome I and II. The gene *xptC* that encodes an oxidoreductase that is localized on chromosome II and is separated from the gene that encodes the prenyltransferase XptB by the gene AN7998. Sanchez and co-workers showed that *mdpE* (encodes a putative C6 zinc finger transcription factor), *mdpI* (encodes a putative AMP-binding CoA ligase) and AN7998 (encodes a putative oxidoreductase) are not involved in the synthesis of prenyl-xanthenes (Sanchez et al., 2011).

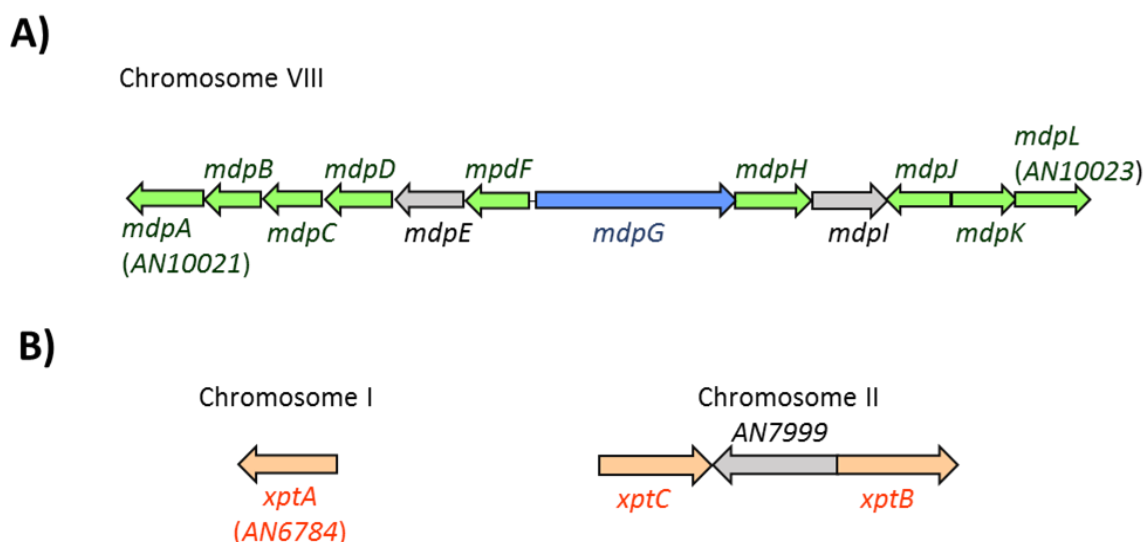


Figure 4. Secondary metabolite gene clusters which are involved in the production of monodictyphenone and xanthenes.

A) The monodictyphenone (*mdp*) gene cluster is located at the telomeric region of chromosome VIII and contains twelve genes. The gene *mdpG* (blue) encodes a polyketide synthase that is involved in the production of the polyketide backbone core structure of monodictyphenone. The enzymes encoded by the residual genes modify the core structure resulting in the production of emodin and finally in monodictyphenone and prenyl-xanthenes. The genes *mdpE* (encodes a C6 zinc finger transcription factor) and *mdpI* (encodes an AMP-binding CoA ligase) in grey are not essential for the production of prenyl-xanthenes.

B) Monodictyphenone represents a precursor for the production of prenyl-xanthenes. Two prenyltransferases XptA, XptB and an oxidoreductase XptC are involved in the conversion of monodictyphenone into prenyl-xanthenes. The genes that encode the prenyltransferases XptA and XptB are localized on chromosome I and II. The oxidoreductase XptC is localized on chromosome II and is situated next to the gene *AN7999* (grey) which encodes an oxidoreductase and is not essential for the production of prenyl-xanthenes (Sanchez et al., 2011, Chiang et al., 2010).

1.4.1.1. Monodictyphenone is a precursor for the synthesis of xanthenes

Xanthenes are organic compounds found in different species like the mangosteen tree *Garcinia mangostana* and are responsible for a yellow pigmentation. The chemical building block of xanthenes is composed of a core structure named xanthone nucleus (*9H-Xanthen-9-on*) that is an aromatic oxo compound. Different modifications of the xanthone nucleus lead to a variety of different xanthenes. A possible modification of the xanthone nucleus can be due to a prenylation event. Xanthenes found in *Garcinia mangostana* are known for anticancer activities (Alam and Khan 2018).

The polyketide synthase MdpG encoded by the monodictyphenone (*mdp*) gene cluster is required for the synthesis of anthraquinone emodin, monodictyphenone and related compounds (Klejstrup et al., 2012). The sequence of the polyketide synthase MdpG contains as many as 1806 amino acids with a predicted molecular mass of 196,8 kDa.

The polyketide synthase MdpG synthesizes the main polyketide backbone core structure. MdpG polyketide synthase consists of several domains with defined functions mentioned in Figure 5. These domains of MdpG are involved in the synthesis of the polyketide backbone.

Emodin and monodictyphenone are precursors for prenyl-xanthone. Sanchez and co-workers deleted *mdpG* and revealed that the product monodictyphenone and other compounds such as prenyl-xanthenes are no longer produced (Sanchez et al., 2011). The first step in the production of emodin and monodictyphenone requires MdpG. Malonyl-CoA represents a substrate for MdpG which synthesizes the polyketide backbone. The polyketide synthase MdpG lacks a thioesterase (TE) domain which hydrolyzes the newly formed polyketide backbone off the synthase. The gene *mdpF* that encodes a putative zinc dependent hydrolase, catalyzes most probably the release of the polyketide backbone from MdpG (Chiang et al., 2010). The gene *mdpH* that encodes a decarboxylase, catalyzes the conversion of atrochrysonic acid into atrochrysonic acid (Klejnstrup et al., 2012). The deletion of *mdpH* results in an inability of the above-mentioned conversion to atrochrysonic acid (Chiang et al., 2010). In order to convert atrochrysonic acid to emodin two unknown dehydrating and modifying enzymes are necessary. The following enzymes finally convert emodin into monodictyphenone, a dehydratase (MdpB), a ketoreductase (MdpC), a glutathione S transferase (MdpJ), an oxidoreductase (MdpK) and a Baeyer-Villiger oxidase (MdpL) (Simpson 2012, Klejnstrup et al., 2012). The monooxygenase MdpD is required for the hydroxylation of monodictyphenone (Bok et al., 2009).

As a next step the hydroxylated monodictyphenone is converted into prenyl-xanthenes. Klejnstrup and co-workers demonstrated that the two prenyltransferases XptA and XptB are involved in the prenylation of hydroxylated monodictyphenone (Klejnstrup et al., 2012). The biosynthesis of the stereoisomers shamixanthone and epishamixanthone is finally catalyzed by the oxidoreductase XptC (Sanchez et al., 2011).

It is known that monodictyphenone and xanthenes are antimicrobial agents that serve against fungivory and other environmental threats (Bok et al., 2009, Regulín and Kempken 2018). In a transcriptomic and metabolomic profiling study it was observed that after the addition of choline Hülle cell formation occurred in a vegetative mycelium and the secondary metabolite monodictyphenone was present in this liquid culture (Alves et al., 2016).

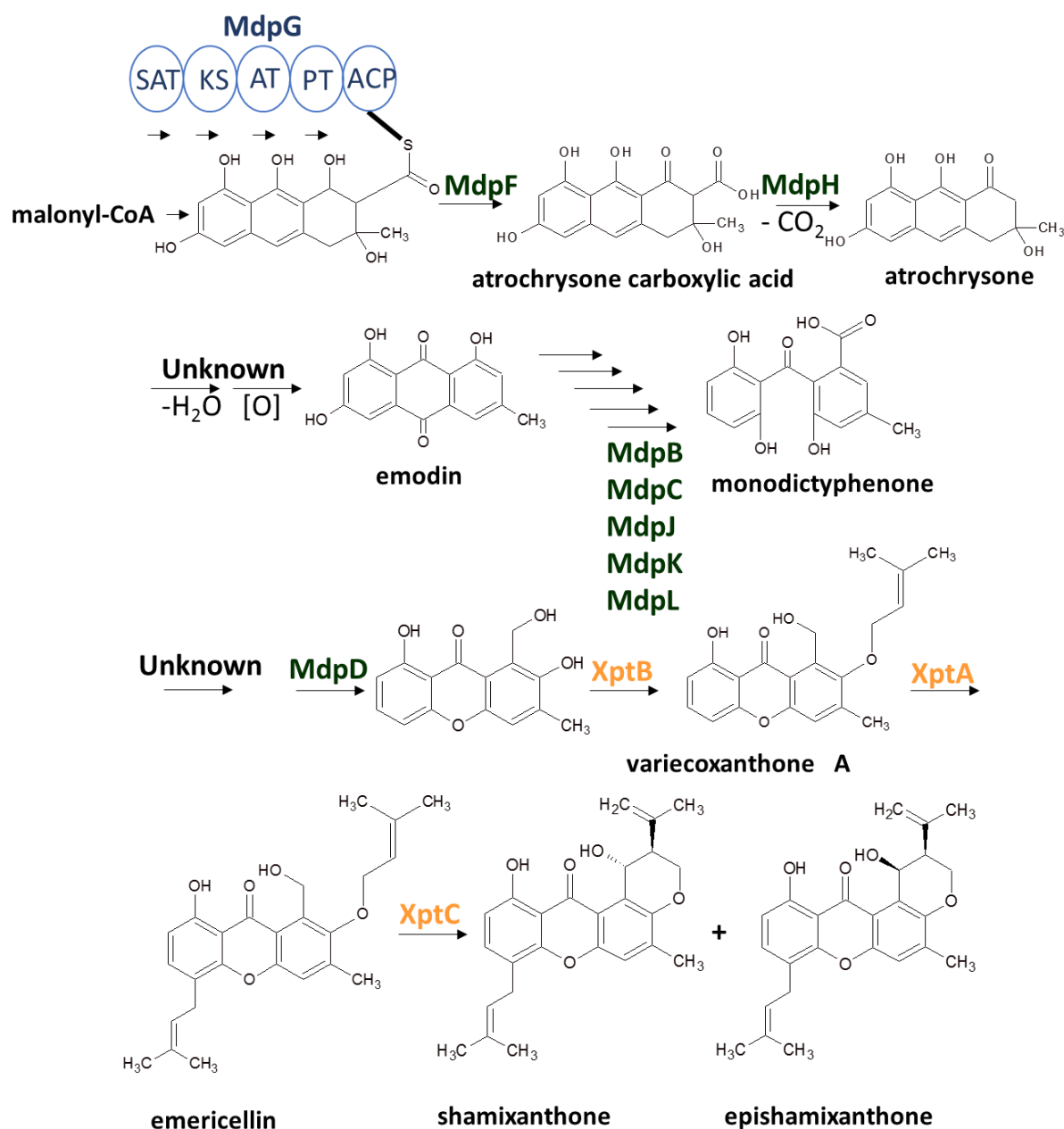


Figure 5. Biosynthesis of monodictyphenone and xanthenes.

The polyketide synthase MdpG synthesizes the main polyketide backbone core structure and uses malonyl-CoA as a substrate. Several domains of MdpG are involved in the synthesis of the polyketide backbone (SAT domain an ACP-transacylase as a starter unit, KS a β -ketoacyl synthase domain and AT an acetyltransferase domain). These three domains are involved in the synthesis of a polyketide backbone intermediate. The internal product template (PT) domain is responsible for folding and cyclization of the polyketide backbone intermediate. The ACP is an acryl carrier protein domain and represents a transiently holding domain for the polyketide backbone).

The putative zinc dependent hydrolase MdpF catalyzes most probably the release of the polyketide backbone from MdpG. The decarboxylase MdpH catalyzes the conversion of atrochrysonic acid to atrochryson. In the conversion of atrochryson to emodin unknown enzymes are involved. Several enzymes (MdpB (dehydratase), MdpC (ketoreductase), MdpJ (glutathione S transferase), MdpK (oxidoreductase), MdpL (Baeyer-Villiger oxidase) are required for the further synthesis of emodin to monodictyphenone. The monooxygenase MdpD hydroxylates monodictyphenone. The two prenyltransferases XptB and XptA are required for the prenylation of hydroxylated monodictyphenone. Giving rise to the compounds variecoxanthone A and emericellin. The oxidoreductase XptC converts emericellin into the stereoisomers shamixanthone and epishamixanthone (Simpson 2012; Klejnstrup et al., 2012).

1.4.2. LaeA as a factor that coordinates fungal development and secondary metabolism

Secondary metabolism and fungal development is known to be highly coordinated by several protein complexes (Sarıkaya-Bayram et al., 2014, Bok et al., 2009). The LaeA methyltransferase protein is a member of the velvet complex that regulates fungal development and secondary metabolism (Bayram et al., 2008b). In *A. nidulans* LaeA regulates not only secondary metabolism but also asexual and sexual sporulation. The coordination of fungal development and secondary metabolism through LaeA is known in different *Aspergilli* (Sarıkaya-Bayram et al., 2010, Dhingra et al., 2013, Zhao et al., 2017). In *Aspergillus flavus* it was demonstrated that *laeA* is required for sclerotia formation and crucial for aflatoxin synthesis (Zhao et al., 2017). The correlation between sclerotia formation and aflatoxin production enables *Aspergillus flavus* to grow in harsh environmental conditions (Chang et al., 2017). This indicates that secondary metabolism and fungal development is correlated in different species.

1.4.2.1. LaeA methyltransferase

The LaeA (loss of *afIR* expression of A) methyltransferase domain protein was first identified by a forward mutant screen and it was shown that *laeA* Δ is unable to express the AfIR transcriptional activator that controls the activation of numerous secondary metabolite gene clusters (Bok and Keller 2004). The LaeA protein of *A. nidulans* comprises 374 amino acids with a predicted molecular mass of 43.0 kDa. The protein sequence includes different domain architectures (Figure 6). At the N-terminal region, the protein sequence contains a nuclear localization signal (NLS). LaeA is known to interact with the VeA and VelB proteins in the nucleus (Bayram et al., 2008b). In the center a putative S-adenosylmethionine dependent (SAM) methyltransferase domain (MTD) is found and is typical for nuclear protein methyltransferase (Bok and Keller 2004). LaeA together with the velvet family proteins VeA and VelB represent a trimeric complex that is essential for fungal development and secondary metabolism (Bayram et al., 2008b). The deletion of *laeA* leads to a photoinhibition. Therefore *laeA* Δ strains are unable to repress sexual development in light (Sarıkaya-Bayram et al., 2010). This results in a phenotype that produces more cleistothecia in light. On the other hand, a *veA* Δ deletion results in total inability to enter the sexual program (Kim et al., 2009).

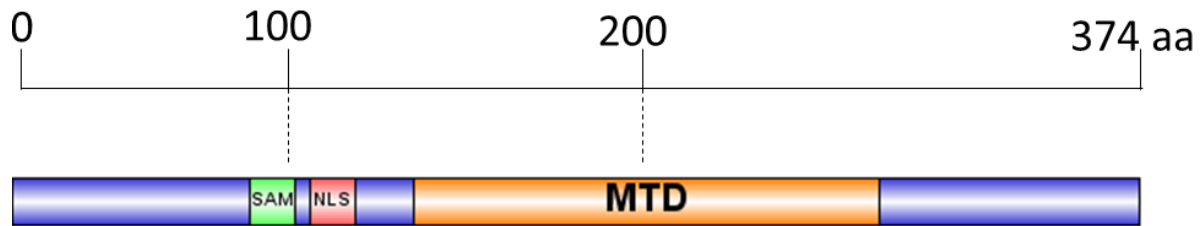


Figure 6. Domain architecture of the methyltransferase LaeA.

The sequence of the methyltransferase domain protein LaeA of *A. nidulans* comprises 374 amino acids with a molecular mass of 43.0 kDa and contains different domain architectures (SAM: S-adenosylmethionin- binding site, NLS: nuclear localization signal, MTD: methyltransferase domain).

1.4.2.2. LaeA methyltransferase promotes Hülle cell formation

LaeA methyltransferase is required for Hülle cell formation as shown in Figure 7. Abolished Hülle cell formation correlates with a significantly reduced size of the cleistothecia from around 200 μm to 40 μm (Sarıkaya-Bayram et al., 2010). This suggests a nursing function of Hülle cells for the growing cleistothecia. The growth of cleistothecia surrounded by Hülle cells are mainly observable under surface conditions since their growth is dependent on surface. Deleting the gene *laeA* led to abolished Hülle cell formation (Sarıkaya-Bayram et al., 2010). Genes which are expressed in sexual mycelia and Hülle cells were monitored in a *laeA* Δ strain. The expression of *mutA* that encodes an alpha-1,3-glucanase and which is localized in Hülle cells was monitored during sexual development in a *laeA* Δ strain (Sarıkaya-Bayram et al., 2010). The expression of *mutA* was reduced in a *laeA* Δ strain which causes significant reduction in Hülle cell formation. From other ascomycota such as *Aspergillus flavus* it is known that methyltransferases are crucial to coordinate fungal development and secondary metabolism (Satterlee et al., 2016).

Hülle cell formation in liquid media in *A. nidulans* FGSC A4 (Glasgow wild-type, *veA*⁺) is unobservable (Bayram et al., 2008a). Prolonging the growth of the fungus in submerged cultures has no effect on Hülle cell formation. The strain AGB552 (*pabaA1;yA;nkuA* Δ ::*argB*) contains a *nkuA* Δ mutation and an additional unknown mutation which results in increased Hülle cell formation in submerged liquid cultures. The gene *nkuA* encodes an ATP-dependent DNA helicase II that is involved in the process of non-homologous end joining (NHEJ) and is required for the repair of double-strand breaks in DNA. For improvement of gene targeting the *nkuA* Δ strain is used (Nayak et al., 2006).

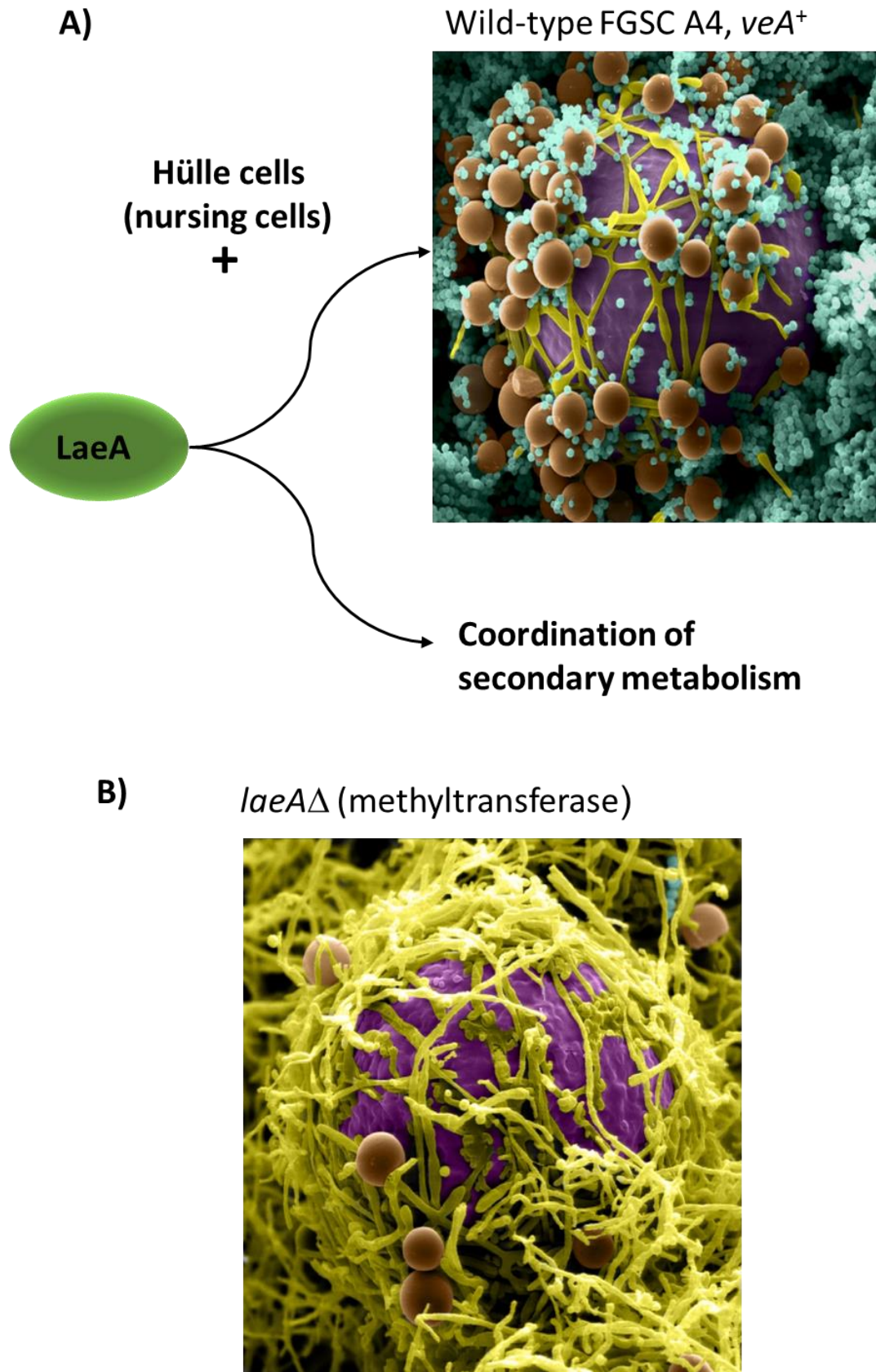


Figure 7. LaeA methyltransferase promotes Hülle cell formation.

A) LaeA methyltransferase domain protein coordinates fungal cell type specificity and secondary metabolism. Hundreds of Hülle cells (coloured beige) surround the cleistothecium. B) LaeA is required for Hülle cells formation. A Cleistothecium of a *laeA*Δ mycelium is shown. Abolished Hülle cells are observable and instead filamentous hyphae are covering the cleistothecium. Image modified (Sarikaya-Bayram et al., 2010).

1.4.2.3. LaeA regulates the monodictyphenone (*mdp*) and other secondary metabolite gene clusters

It is suggested that LaeA regulates more than 50% of all secondary metabolite gene clusters in *Aspergillus nidulans*, *Aspergillus fumigatus* and *Aspergillus flavus* (Sarıkaya-Bayram et al., 2010, Dhingra et al., 2013, Zhao et al., 2017). Different secondary metabolite gene clusters are regulated by LaeA in *A. nidulans* including monodictyphenone (*mdp*), terrequinone A, penicillin and sterigmatocystin (Bok et al., 2009, Bok et al., 2006, Bok and Keller 2004). Bok and co-workers indicated a role of LaeA in interaction with the CclA (H3K4 methyltransferase) complex which regulates the expression of the monodictyphenone (*mdp*) gene cluster (Bok et al., 2016, Bok et al., 2009). This shows that LaeA regulates the monodictyphenone (*mdp*) gene cluster. The deletion of *laeA* gene leads to more heterochromatin formation with an increased histone 3 (H3) lysine (K9) trimethylation (H3K9me3) in the sterigmatocystin gene cluster (Reyes-Domingues et al., 2010). This suggests that chromatin structures are changed in *laeA*Δ. In order to investigate methylation substrates of LaeA a biochemical study was performed. Patananan and co-workers were not able to find a specific methylation substrate and investigated an automethylation reaction of LaeA (Patananan et al., 2013). The methylating function of LaeA is so far unknown.

The LaeA protein regulates several secondary metabolite gene clusters that encode prenyltransferases (Bok et al., 2006, Kale et al., 2008). Seven different prenyltransferases are encoded by the genome of *A. nidulans* (Galagan et al., 2005). Prenyltransferases are involved in the prenylation of aromatic substrates and thereby modifying different secondary metabolites. LaeA regulated prenyltransferase has been characterized in *A. nidulans* (Bok et al., 2006). The terrequinone A biosynthetic pathway involves prenylation events (Bouhired et al., 2007). Bok and co-workers showed that the prenyltransferase *tidB* is not expressed in a *laeA*Δ mycelium in comparison to the wild-type and is up-regulated in a *laeA* overexpression strain (Bok et al., 2006).

1.4.3. Relationship between fungal development and secondary metabolism

Secondary metabolite production is commonly associated with the progression of sporulation and fulfills different functions during this process. First, secondary metabolites are needed in order to activate sporulation, such as hydroxylated oleic acid and linoleic acid produced by *Aspergillus nidulans*. Second, the process of sporulation is linked to the production of pigments. Third, mycotoxins and other toxic metabolites are crucial to protect the fungus against fungivory and other environmental threats.

1.4.3.1. Secondary metabolites that activate sporulation

A wide range of secondary metabolites are produced after the fungus has finalized its initial vegetative growth phase (Calvo et al., 2002). In *A. nidulans* endogenous factors such as the oxylipins, hydroxylated oleic acid and linoleic acid also called psi (precocious sexual inducer), are factors that regulate the balance between early sexual and asexual sporulation (Tsitsigiannis et al., 2004b). The oxygenase-like enzymes PpoA, PpoB and PpoC, are involved in the production of psi factors. Localization studies of these enzymes revealed that PpoA::GFP is localized to lipid bodies in Hülle cells and other fungal tissues (Tsitsigiannis and Keller 2004a). Deletion of *ppoA* gene resulted in increased asexual development. Thereby forming less cleistothecia in a sexual mycelium. The number of Hülle cells and ascospores were not affected by the deletion of *ppoA* (Tsitsigiannis and Keller 2004a).

1.4.3.2. Pigments

The production of the pigment melanin is known to be involved in the pigmentation process of fruiting bodies and/or ascospores (Engh et al., 2007). *Aspergilli* that produce no Hülle cells such as *Aspergillus tonophilus* and *Aspergillus fisheri*, also produce non-pigmented cleistothecia (Hermann et al., 1983). In *Aspergilli* it is known that laccases are involved in the melanin production (Upadhyay et al., 2013). Scherer and co-workers showed that the type II laccase CpeA is highly expressed in Hülle cells (Scherer et al., 2002). The expression of *cpeA* in Hülle cells enables the production of

the cleistin matrix of the cleistothecia, which is possibly a polymeric product of phenolic material. Scanning and transmission electron microscopy revealed that the cleistin matrix is an electron dense material and forms an outer layer of the cleistothecia which are pigmented (Champe and Simon 1992). Pigmentation protects most likely the cleistothecia against negative environmental influences.

1.4.3.3. Secondary metabolites to protect the fungus against fungivory and other environmental threats

A secondary metabolite-based defence mechanism provides a benefit to fungi (Döll et al., 2013, Drott et al., 2017, Caballero-Ortiz et al., 2013). In a recent study it was shown that the production of different secondary metabolites influenced the development of *Drosophila melanogaster* (Regulin and Kempken 2018). Analyzing effects of wild-type (FGSC A4, Glasgow wild-type, *veA*⁺) *A. nidulans* compared to the deletion of the polyketide synthase *mdpG* which is required for the biosynthesis of monodictyphenone showed a 95% higher egg laying activity of *Drosophila melanogaster* on the deletion strain. The egg laying activity of *Drosophila melanogaster* was additionally analyzed in a *laeA* Δ strain and was compared to *mdpG* Δ and wild-type. This resulted in an 57% egg laying activity on a *laeA* Δ mycelium. Döll and co-workers showed that the cleistothecia of *A. nidulans* covered with Hülle cells are more resistant against fungivory when comparing to a vegetative or asexual tissue (Döll et al., 2013). Therefore, secondary metabolites are crucial for the protection against environmental threats and provide resistance against fungivory.

1.5. Aim of this work

The central aim of this thesis was to get more insight into the proteomes and their biological functions of specialized fungal cells and during sexual development with a special focus on the accessory Hülle cells. The methyltransferase *LaeA* is required for Hülle cell formation and normally sized closed fruiting bodies named cleistothecia. Enrichment procedures for Hülle cells were established to gain more specific access to their proteomes. Tissues without and with Hülle cells were compared and analyzed. Identified proteins from an enriched Hülle cell fraction were compared to the identified proteins from a vegetative mycelium, asexual mycelium and sexual mycelium. Two proteomic approaches were performed during this study to investigate which proteins are enriched in Hülle cells. In the first proteomic approach proteins found in surface cultures were analyzed. An enriched Hülle cell fraction was compared to a vegetative, asexual and sexual mycelium. In the second proteomic investigation proteins were analyzed and quantified from submerged liquid cultures. Therefore, a *laeA* Δ strain was used that causes significant reduction in Hülle cells and was compared to a *nkuA* Δ strain with an additional unknown mutation that cause increased numbers of Hülle cells both in submerged liquid cultures. Furthermore, proteins identified in enriched Hülle cells were analyzed and functional gene studies were performed.

2. Materials and methods

2.1. Materials

2.1.1. Strains

Aspergillus nidulans strains *nkuA*Δ (AGB552) and *lysA*Δ; *nkuA*Δ (AGB1092) served as transformation host for deletion, complementation and GFP (green fluorescent protein) tagging. Strains used in this study are listed in Table 1.

Table 1. Strains used in this study.

Aspergillus nidulans strains are denominated AGB or FGSC, p.c. = personal communication.

Strain	Genotype	Reference
<i>Escherichia coli</i>		
DH5α TM	F ⁻ , Δ(<i>argF-lac</i>)169, φ80d <i>lacZ</i> 58(M15), Δ <i>phoA</i> 8, <i>glnX</i> 44(AS), λ ⁻ , <i>deoR</i> 481, <i>rfbC</i> 1, <i>gyrA</i> 96(NalR), <i>recA</i> 1, <i>endA</i> 1, <i>thiE</i> 1, <i>hsdR</i> 17	Invitrogen, Germany
Top10	F ⁻ <i>mcrA</i> Δ(<i>mrr-hsdRMS-mcrBC</i>) Φ80 <i>lacZ</i> ΔM15 Δ <i>lacX</i> 74 <i>recA</i> 1 <i>araD</i> 139 Δ <i>ara-leu</i>) 7697 <i>galU galK rpsL</i> (Str ^R) <i>endA</i> 1 <i>nupG</i> λ ⁻	Invitrogen, Germany
Strain	Genotype	Reference
<i>Aspergillus nidulans</i>		
A4	Glasgow wilde type, <i>veA</i> ⁺	FGSC
AGB596	<i>pgpdA::sgfp::phleoR;pabaA1;yA;veA</i> ⁺	Bayram et al., 2012
AGB552	<i>pabaA1;yA;nkuAΔ::argB</i>	Bayram et al., 2012
AGB1092	<i>lysAΔ;pabaA1;yA;nkuAΔ::argB</i>	Meister. p.c.
AGB1073	<i>laeAΔ;pabaA1;yA;nkuAΔ::argB</i>	This study
AGB1074	<i>laeAΔ;lysAΔ;pabaA1;yA;nkuAΔ::argB</i>	This study
AGB1075	<i>laeAΔ::laeA;pabaA1;yA;nkuAΔ::argB</i>	This study
AGB1076	<i>laeAΔ::laeA;lysAΔ;pabaA1;yA;nkuAΔ::argB</i>	This study
AGB1077	<i>mphAΔ;pabaA1;yA;nkuAΔ::argB</i>	This study
AGB1078	<i>mphAΔ::mphA::gfp;pabaA1;yA;nkuAΔ::argB</i>	This study
AGB1079	<i>mphA::gfp;pabaA1;yA;nkuAΔ::argB</i>	This study
AGB1080	<i>mphAΔ::mphA;pabaA1;yA;nkuAΔ::argB</i>	This study
ABG1081	<i>laeAΔ;mphA::gfp;pabaA1;yA;nkuAΔ::argB</i>	This study
AGB1082	<i>lysAΔ;nptA::gfp;pabaA1;yA;nkuAΔ::argB</i>	This study
AGB1083	<i>laeAΔ;lysAΔ;nptA::gfp;pabaA1;yA;nkuAΔ::argB</i>	This study
AGB1084	<i>lysAΔ;rfeA::gfp;pabaA1;yA;nkuAΔ::argB</i>	This study
AGB1085	<i>laeAΔ;lysAΔ;rfeA::gfp;pabaA1;yA;nkuAΔ::argB</i>	This study
AGB1086	<i>lysAΔ;xptB::gfp;pabaA1;yA;nkuAΔ::argB</i>	This study
AGB1088	<i>xptC::gfp;pabaA1;yA;nkuAΔ::argB</i>	This study
AGB1089	<i>AN8434::gfp;pabaA1;yA;nkuAΔ::argB</i>	This study
AGB1090	<i>AN8435::gfp;pabaA1;yA;nkuAΔ::argB</i>	This study

2.1.2. Plasmids

Plasmids used in this study are listed in Table 2.

Table 2. Plasmids used in this study.

RM: recyclable marker, *phleoRM* = recyclable *phleoRM* resistance cassette from pME4305 or pJG292, ^R = resistance, ^P = promoter, ^t = terminator, p.c = personal communication.

Plasmid	Description	Reference
pBluescript sk +	Cloning plasmid	Fermentas
pME4305	<i>six</i> ^{-P} <i>xyIP</i> :: <i>B-rec</i> :: <i>trpc</i> ^t - <i>phleo</i> ^R - <i>six</i>	Gerke, p.c.
pJG292	<i>swal</i> :: <i>six</i> ^{-P} <i>xyIP</i> :: <i>B-rec</i> :: <i>trpc</i> ^t - <i>phleo</i> ^R - <i>six</i> :: <i>Eco74I</i>	Gerke, p.c.
pME4292	Plasmid contains <i>gfp</i>	Jöhnk, p.c.
pME4636	<i>ANlaeAΔ</i> :: <i>phleoRM</i>	This study
pME4637	<i>ANlaeA</i> :: <i>phleoRM</i>	This study
pME4638	<i>ANmphAΔ</i> :: <i>phleoRM</i>	This study
pME4639	<i>PmphA</i> :: <i>ANmphA</i> :: <i>gfp</i> :: <i>phleoRM</i>	This study
pME4640	<i>ANmphA</i> :: <i>phleoRM</i>	This study
pME4641	<i>PnptA</i> :: <i>ANnptA</i> :: <i>gfp</i> :: <i>phleoRM</i>	This study
pME4642	<i>PrfeA</i> :: <i>ANrfeA</i> :: <i>gfp</i> :: <i>phleoRM</i>	This study
pME4643	<i>PxptB</i> :: <i>ANxptB</i> :: <i>gfp</i> :: <i>phleoRM</i>	This study
pME4645	<i>PxptC</i> :: <i>ANxptC</i> :: <i>gfp</i> :: <i>phleoRM</i>	This study
pME4646	<i>PAN8434</i> :: <i>AN8434</i> :: <i>gfp</i> :: <i>phleoRM</i>	This study
pME4647	<i>PAN8435</i> :: <i>AN8435</i> :: <i>gfp</i> :: <i>phleoRM</i>	This study

2.1.3. Primers

Oligonucleotides used in this study are listed in Table 3.

Table 3. Oligonucleotides utilized for plasmid construction.

Designation	Sequence	Basepairs
BD49	5'-ATC GAT AAG CTT GAT GTT TAA TAA ACA ACC GAG CTG GCC GTT-3'	42
BD50	5'-ACC TAT AGG CCT GAG CTT GTC TCC TTT AAC TTC TCT GC-3'	38
BD51	5'-ATA ATA TGG CCA TCT CTC ATA TCC CAA TTC TCT GAT TTT-3'	39
BD52	5'-CTG CAG GAA TTC GAT GTT TAA ACC ATC TTA ACC ATC TTG GCG-3'	42
BD61	5'-ACG GTA TCG ATA AGC TTG ATG TTT AAA CTT CTT TTG TTC CAA ACA-3'	45
BD83	5'-ATC GAT AAG CTT GAT GTT TAA ACA GAT TTG GTA GGA GCT AAC-3'	42
BD84	5'-GAC CTA TAG GCC TGA GGT TGA CGA TCT CTG AGA CGA-3'	36

Table 3. Continued, Oligonucleotides utilized for plasmid construction.

BD85	5'-ATA ATA TGG CCA TCT ATG AAC ATT GTC TTT GGA GAG TC-3'	38
BD86	5'-CTG CAG GAA TTC GAT GTT TAA ACG TGG TGA TTA TCA TCC-3'	39
BD88	5'-TGA GCA TAA TAT GGC CAT CTT TGT GAC TCT GTT GTC GGT TAT C-3'	43
BD89	5'-CCG GGC TGC AGG AAT TCG ATG TTT AAA CCC ATC ACC CAT TCG CTT-3'	45
BD63	5'-ATG GCC GAC GAC TAT CGC GAA GA-3'	23
BD64	5'-TAT TGA CCT ATA AGG CCT GAG CTA GAA CTT CGT CTC AAG TAA CTC CT-3'	47
BD70	5'-TGT GAG GTT ACC TCA GAT CTT GT-3'	23
BD71	5'-TAT TGA CCT ATA GGC CTG AGT TAT CTT AAT GGT TTC CTA GCC TG-3'	44
BD73	5'-ATA AGC TTG ATG TTT AAA CGT ACG TCT TTA TTA TAG TCG AG-3'	41
BD76	5'-ACC TAT AGG CCT GAG CGT GAA CGA ATT CGA TGT G-3'	34
BD87	5'-ATA ATA TGG CCA TCT GGC TGT GCT TCT AGA GAG ACG T-3'	37
BD90	5'-CTG CAG GAA TTC GAT GTT TAA ACA ATG CCA CAA GGA A-3'	37
BD93	5'-TAT TGA CCT ATA GGC CTG AGC TAC TCA TCA TCG CGG ATA T-3'	40
BD96	5'-TTC TCC TTT ACT CAT GTT GAC GAT CTC TGA GAC GAT C-3'	37
BD97	5'-TAC AGG CTG GTG CCA TGA GTA GCG ACA ACA CAG AGA AG-3'	38
BD98	5'-ACC ACC GCT ACC ACC CTC ATC ATC GCG GAT ATC G-3'	34
BD99	5'-GGT GGT AGC GGT GGT GTG AGC AAG GGC GAG GAG-3'	33
BD100	5'-ACC TAT AGG CCT GAG CTA CTT GTA CAG TTC GTC CAT GCC-3'	39
BD104	5'-AAC TAC TCG ACT ATA TCA ATG GA-3'	23
BD105	5'-CTC ACA CCA CCG CTA CCA CCT TTC TCT GGA CAA GGA TGA TT-3'	41
BD106	5'-GGT GGT AGC GGT GGT GTG AG-3'	20
BD107	5'-CTA CTT GTA CAG TTC GTC CAT G-3'	22
BD108	5'-TGC AGT GCC TGA TAA CTC T-3'	19
BD109	5'-AAA CGA AAC CGC CGG TGC CA-3'	20
BD111	5'-CAT ATG TGC AGG CCG CGT-3'	18
BD112	5'-CTC ACA CCA CCG CTA CCA CCG GCC GAA AAT CCA TTA GAC TC-3'	41
BD113	5'-TTC GTG CCG TCT TGG AGA-3'	18

Table 3. Continued, Oligonucleotides utilized for plasmid construction.

BD114	5'-GCT CAC ACC ACC GCT ACC ACC GTT ACC CAG CCA GCC ATG-3'	39
BD113 (<i>xptC</i>)	5'-AGG CTC AAC CTG ATA CTT ACC-3'	21
BD114 (<i>xptC</i>)	5'-GCT CAC ACC ACC GCT ACC ACC GTT ACC CAG CCA GCC ATG-3'	39
BD115	5'-ATT AGA TCT ATT AGA CCG CAG G-3'	22
BD116	5'-CAC GTG ATG TGA TAC GGT AC-3'	20
BD119 (<i>xptB</i>)	5'-AGA TCT ATT AGA CCG CAG GC-3'	20
BD120 (<i>xptB</i>)	5'-CTC ACA CCA CCG CTA CCA CCC CAC CGA TCA TCC CCC CTC C-3'	40
BD121 (<i>xptB</i>)	5'-TTC CTC TCT AGA AAC TTC TCA AA-3'	23
BD122 (<i>xptB</i>)	5'-ACA TGT ACT CGG ACC TGG TTC-3'	21
BD121	5'-TAT TTC AAG GTA ACA GTC TGG-3'	21
BD122	5'-CTC ACA CCA CCG CTA CCA CCG TTT CTG TCC GCG ATA GAC-3'	39
BD123	5'-ACA CCA AAC ATC TGT AGA GAA CA-3'	23
BD124	5'-TGT AGT CAA TTG CGG GGG TA-3'	20
BD125	5'-ATT GAC GAA TTT TGT CGC GA-3'	20
BD127	5'-CTC ACA CCA CCG CTA CCA CCG GTA CTA TGC ACT CCC AGC-3'	39
BD128	5'-TTT CGC TCC TAT AAC TGG ACT-3'	21
BD129	5'-ACT TCT TGA TAT TTA AAG CAA TTT-3'	24

2.1.4. Chemicals and equipment

Different chemicals and enzymes as well as kits were used for the results of this research.

Chemicals and the respective suppliers

The following chemicals were purchased from AppliChem GmbH (Darmstadt, Germany), the order numbers are cited in brackets. Aceton (9R006076), arginine (A3709,0250), β -glycerophosphat (A2253,0100), benzamidine (A1380,0005), bromophenol blue (A3640,0005), glucose (A3617,1000), isopropanol (A0900,2500GL), l-lysine monohydrochloride (33003468), nonident® P40 (A2239,0025), potassium chloride (A3582,1000), sodium chloride (A3597,1000),

2. Materials and methods

sodium orthovanadate (2196,0005), sucrose (A4734,1000), tween 20® (A4974,0100), xylene cyanol (A4976,0005).

Biozym Scientific GmbH (Hessisch Oldendorf, Germany) provided agarose for agarose gels (840004).

As a subsidiary company of the American multi industry group General Electric GE Healthcare GmbH (Braunschweig, Germany) provided the following chemicals. Amersham™ alkphos direct labelling reagents (11816064), amersham™ cdp-star™ detection reagents (9766233).

Merck KGaA (Darmstadt, Germany), a leading science and technology company in the field of healthcare, life science and performance materials delivered the following chemicals. Di-sodium hydrogen phosphate (1065855000), DMSO (dimethyl sulfoxide) (1029310500), formic acid (1002641000), hydrogen peroxide 30% (H₂O₂) (8.22287.2500), magnesium chloride hexahydrate (1.05833.1000), potassium acetate (1.04820.1000), potassium dihydrogen phosphate (1.04873.1000), sodium dihydrogen phosphate monohydrate (1.06346.1000).

Chemicals and suppliers, continued

Carl Roth GmbH & Co. KG (Karlsruhe, Germany) is one of the leading companies in Germany for the production of fine chemicals and provided the following chemicals. In brackets the order number is again cited. Acetonitrile (T901.1), acetic acid (3738.2), acrylamide (Rotiphorese® Gel 40 37,5:1) (3029.1), agar-agar (5210.2), ammonium persulfate (APS) (9592.3), β-mercaptoethanol (4227.1), caffeine anhydrous (N815.3), calcium chloride (CN92.1), calcium chloride dihydrate (5239.1), citric acid monohydrate (3958.1), coomassie brilliant blue G-250 (9598.1), coomassie brilliant blue R-250 (3862.1), dimethylformamide (T921.1), DTT (1,4-dithiothreitol) (A1101,0025), EDTA (ethylenediamine tetraacetic acid disodium salt dihydrate) (8043.2), formaldehyde (4979.2), glycine (0079.1), glycerol (3783.1), hydrochloric acid (4625.2), imidazole (5709.3), magnesium sulfate heptahydrate (P027.2), manganese (II) chloride tetrahydrate (T881.1), manganese(II)sulfate monohydrate (4487.1), phosphoric acid (6366.1), ponceau S (5938.2), potassium hydroxide (6751.1), rotiphorese Gel 40 (3030.2), SDS (sodium dodecyl sulfate) (4360.2), sodium acetate (6773.2), sorbitol (6213.1), TEMED (N,N,N',N'-tetramethylethylenediamine) (2367.3),

trichloroacetic acid (7875.4), tris (tris-hydroxymethyl-aminomethane) (AE15.2), tris/HCl (9090.3), urea (2317.3), yeast extract (2904.1).

Chemicals and the respective suppliers, continued

SERVA Electrophoresis GmbH (Heidelberg, Germany) acts as a privately-owned company in the field of electrophoresis and also provides a wide portfolio of fine chemicals. They provided agar-agar SERVA high gel-strength, a choice quality for *in vitro* cultures (11396.03).

Sigma-Aldrich (Schnelldorf, Germany) is a leading life science and high technology company, being a subsidiary company of Merck KGaA (Darmstadt, Germany) and provided the following chemicals. Adenine (01830-50G), ampicillin (A9518-25G), EDTA-free protease inhibitor cocktail (48998), ethidium bromide (46065), formamide (47670), maltose monohydrate (112569), PMFS (phenylmethylsulfonylfldauoride) (P-7626), triton X-114 (X114).

The global life science company Thermo Fisher Scientific (Waltham, Massachusetts, United States of America) supports scientists worldwide. Several subsidiary companies are located in Germany (Thermo Fisher Scientific GmbH, Schwerte, Germany) and provided the following chemicals and DNA as well as protein ladders. Gene ruler DNA ladder mix (Thermo Scientific, SM0331), PageRuler™ prestained protein ladder (Thermo Scientific, SM26616), x-gal (5-bromo-4-chloro-3-indolyl-beta-D-galacto-pyranoside) (R0404).

Ethanol (20821.321) and methanol (20864.320) were ordered from VWR International GmbH (Hannover, Germany).

Enzymes and suppliers

The following enzymes were purchased from different companies. Natuszym (Schliessmann, Germany, 5090), Phusion® Hot Start high-Fidelity DNA Polymerase (New England Biolabs, Frankfurt am Main, Germany, M0530S), Lysozyme (SERVA Electrophoresis GmbH, Heidelberg, Germany, 28262.03), Phospholipase C (Invitrogen life technologies, Osterode, Germany, P6466), Restriction Endonucleases (Thermo Fisher Scientific GmbH, Schwerte, Germany), RNase A (Darmstadt, Germany, 24690.0), T4 DNA ligase (Thermo Fisher Scientific GmbH, EL0011), Trypsin (SERVA Electrophoresis GmbH, 37286.01), VinoTaste® Pro (Novozymes GmbH, Bagsvaerd, Denmark, 4518)

Kits and the respective suppliers

The following different kits were used. Amersham™ Alkphos Direct Labelling Reagents Kit (GE Healthcare, 11816064), Gene Art[®] Seamless Cloning and Assembly Kit (Invitrogen life technologies, A1328), HiSpeed Plasmid Midi Kit (QIAGEN, Hilden, Germany, 12643), NucleoSpin[®]Plasmid Kit (Macherey-Nagel, 740615.250), NucleoSpin[®]Gel and PCR Clean-up Kit (Macherey-Nagel, Düren, Germany, 740609.250), QIAprep Spin Miniprep Kit (QIAGEN, 27106), QIAquick Gel Extraction Kit (QIAGEN, 28704), QIAquick PCR Purification Kit (QIAGEN, 28104).

Equipment and the respective suppliers

Further materials were provided by different companies. Standard laboratory equipment including pipets, petri dishes and other plastic consumables were purchased from Gilson, Inc., (Limburg-Offheim, Germany), Sarstedt AG & Co (Nümbrecht, Germany). In order to centrifuge samples abiofuge fresco and biofuge pico (Heraeus Instruments GmbH) were used. To grind mycelia a retsch mill MM400 (Retsch GmbH, Haan, Germany 56789.1) was applied. Measuring the concentration of DNA and proteins a nanodrop ND-1000 photospectrometer (peqlab biotechnologie GmbH, Erlangen, Germany) was used. In order to image gel pictures a gel IX20 imager (Intas Science Imaging Instruments GmbH, Göttingen, Germany) was used. Southern hybridization experiments were performed with x-ray films (Protec GmbH, Oberstenfeld, Germany) and amersham™ hyperfilm™ ECL (GE Healthcare, 28906837). For protein work the following instruments were used. Mini-protean[®]tetra cell (Bio-Rad Laboratories GmbH, Munich, Germany 1658005EDU), mini trans-blot[®]electrophoretic cell (Bio Rad, 1703930), mini-sub[®]cell GT (Bio Rad, 1704487EDU), powerpac™ 200 (Bio Rad, 1645050). For western hybridization experiments a nitrocellulose transfer membrane (protran[®] BA (Sigma-Aldrich, 10401196)) was used. Besides savant speedvac concentrator (Thermo Scientific) and sterile filters 0.45/0.2 µm (Sarstedt, 83.1826/83.1826.001) were used. A liquid chromatography (LC) coupled to an *Orbitrap Velos Pro™ Hybrid Ion Trap-Orbitrap* mass spectrometer (MS) (Thermo Fisher Scientific, Bremen, Germany) was used for the two different proteomics investigations.

2.1.5. Solutions and growth media

2.1.5.1. Solutions

Solutions regarding *Aspergillus nidulans*

The trace-element stock solution consisted of 18 μM FeSO_4 , 174 μM ETDA, 76 μM ZnSO_4 , 178 μM H_3BO_3 , 25 μM MnCl_2 , 7.1 μM , CoCl_2 , 6.4 μM CuSO_4 , 6.2 μM Na_2MoO_4 . The resulting solution was sterilized with a sterile filter.

In order to extract DNA from *Aspergillus nidulans* the following extraction buffer was used and consisted of 1 M Tris (pH 7.2), 0.5 M ETDA (Ethylenediaminetetraacetic acid), 3 g SDS and 1 ml mercaptoethanol.

In order to perform transformations in *Aspergillus nidulans* the following solutions were used.

As a citrate buffer consisting of 150 mM KCl, 580 mM NaCl, 50 mM sodium citrate, pH 5.5 was used.

Protoplast solution consisted of 20 mg/ml VinoTaste® Pro (Novozymes GmbH, 4518) and 15 mg/ml lysozyme (Serva GmbH, 28262.03).

Solutions regarding Southern hybridizations:

Alkphos direct hybridization buffer (GE Healthcare, RPN 36888) was used as a prehybridization buffer. Additionally, 0.5 mM NaCl, 4% blocking solution was added.

Gels were washed in three different washing buffers: Buffer 1: 0.25 M HCl, Buffer 2: 0.5 M NaOH, Buffer 3: 0.5 M Tris, 1.5 M NaOH.

Southern hybridization membranes were washed in two different washing buffers. Washing buffer 1: 2 M urea, 0.1% SDS, 50 mM $\text{NaH}_2\text{PO}_4 \times \text{H}_2\text{O}$ pH 7, 150 mM NaCl, 1 mM MgCl_2 , 0.2% blocking reagent.

Washing buffer 2: 1 M Tris pH 10, 2 M NaCl, 1 mM MgCl_2 .

Solutions regarding polyacrylamide gel electrophoresis:

A 10X SDS running-buffer was used consisting of 0.25 M Tris/base, 1.92 M glycine and 10 g SDS.

A 10X transfer-buffer was used consisting of 0.25 M Tris/base, 1.92 M glycine and 0.2% SDS.

A 10X TBST (Tris buffered saline with tween 20) solution was used consisting of 100 mM Tris/HCl pH 8, 1.5 M NaCl and 0.5% tween 20.

Protease inhibitor solution was used and consisted of 100 mM PMFS (phenylmethylsulfonylfluoride), 0.5 mM benzamidine, 1 M DTT (1,4-dithiothreitol) and 1 M imidazole.

A 100X phosphatase inhibitor solution was used consisting of 100 mM sodium fluoride, 50 mM sodium vanadate and 800 mM β -glycerophosphat.

A B⁺ 300 buffer for protein extraction was used and consisted of 100 mM Tris pH 7.5, 300 mM NaCl, 10% glycerol, 1 mM EDTA, 0.1% NP-40, 1 mM DTT (1,4-dithiothreitol), 0.5 M benzamidin, 100 mM PMFS (phenylmethylsulfonylfluoride) and additionally a protease inhibitor and phosphatase inhibitor were added.

Coomassie staining solution was used and consisted of 0.1% (w/v) coomassie brilliant blue G250, 2% (w/v) ortho-phosphoric acid and 10% (w/v) ammonium sulfate.

Ponceau S staining solution was used and consisted of 0.2% ponceau S and 3% trichloroacetic acid.

A destaining solution was used and consisted of 40% (v/v) ethanol and 10% (v/v) acetic acid.

2.1.5.2. Growth media

Growth medium regarding *Aspergillus nidulans*:

Minimal medium (MM) was used as a growth medium for *Aspergillus nidulans* and consisted of 1% (w/v) glucose, 1% (w/v) AspA, 2 mM MgSO₄, 2% (w/v) Agar and trace elements (added after autoclaving), pH 6.5 and 2 mM MgSO₄.

Growth media regarding *Escherichia coli*:

Escherichia coli cultures were cultivated in LB medium and consisted of 1% (w/v) tryptone/peptone, 0.5% (w/v) NaCl, pH 7.2; 0.5% (w/v) yeast extract, 1.5% (w/v) agar-agar for solid medium and ampicillin (100 µg/ml) selection.

Escherichia coli cultures were cultivated in SOB medium and consisted of 0.5% (w/v) yeast extract, 2% (w/v) tryptone/peptone, 10 mM NaCl, 2.5 KCl, 10 mM MgCl₂ and 10 mM MgSO₄.

2.2. Methods

2.2.1. Cultivation of *Aspergillus nidulans*

Spores of *A. nidulans* wild-type FGSC A4, *veA*⁺ were inoculated on solid minimal medium (1% glucose, 1% AspA, 2 mM MgSO₄, 2% Agar and trace elements (added after autoclaving), pH 6.5; 2 mM MgSO₄). Fungus was then cultivated under sexual (incubation in complete darkness and reduced oxygen conditions, therefore the petri dish was sealed with a parafilm) or under asexual conditions (incubation in light). The plates were incubated at 37 °C. The percentage of conidiophores in asexual mycelium were determined as described (Christmann et al., 2013). The diameter of cleistothecia were measured using an Olympus binocular SZX12-ILLB2-200 (Olympus GmbH, Hamburg, Germany). In order to determine the diameter of cleistothecia three biological replicates were considered. For each biological replicate the diameter of five cleistothecia were determined. In order to measure the diameter of cleistothecia Hülle cells were removed from cleistothecia using the cleistothecia-rolling technique.

2.2.1.1. Hülle cells from solid agar plate: cleistothecia-rolling technique

Hülle cells are globose multicellular cells associated with sexual tissue of *Aspergillus nidulans*. In order to perform the cleistothecia-rolling technique, fungus was cultivated on solid agar plates under sexual conditions (incubation in complete darkness and reduced oxygen conditions, therefore the petri dish was sealed with a parafilm). Three, five and seven days after inoculation Hülle cells were enriched and the sexual

2. Materials and methods

mycelium was harvested. In order to enrich Hülle cells, cleistothecium was transferred (with a fine tipped syringe) from sexual mycelium to a fresh petri dish containing 2% agar (Figure 8). This step was performed under a stereo microscope. Cleistothecium was then rolled back and forth on the solid agar plate with the fine tipped syringe and the Hülle cells adhered to the surface of the solid agar plate. In order to collect Hülle cells, they were picked with a fine tipped syringe. Hülle cells were collected into a collection tube containing 40 μl of dH_2O . Hülle cells were transferred from the solid agar petri dish to the collection tube with the fine tipped syringe. Hülle cells in the collection tube were centrifuged by 13.000 rpm for one minute and 35 μl of dH_2O was removed. In order to observe enriched Hülle cells, they were visualized under a light microscope. The residual 5 μl dH_2O was resuspended and the Hülle cells were transferred on a microscope slide.

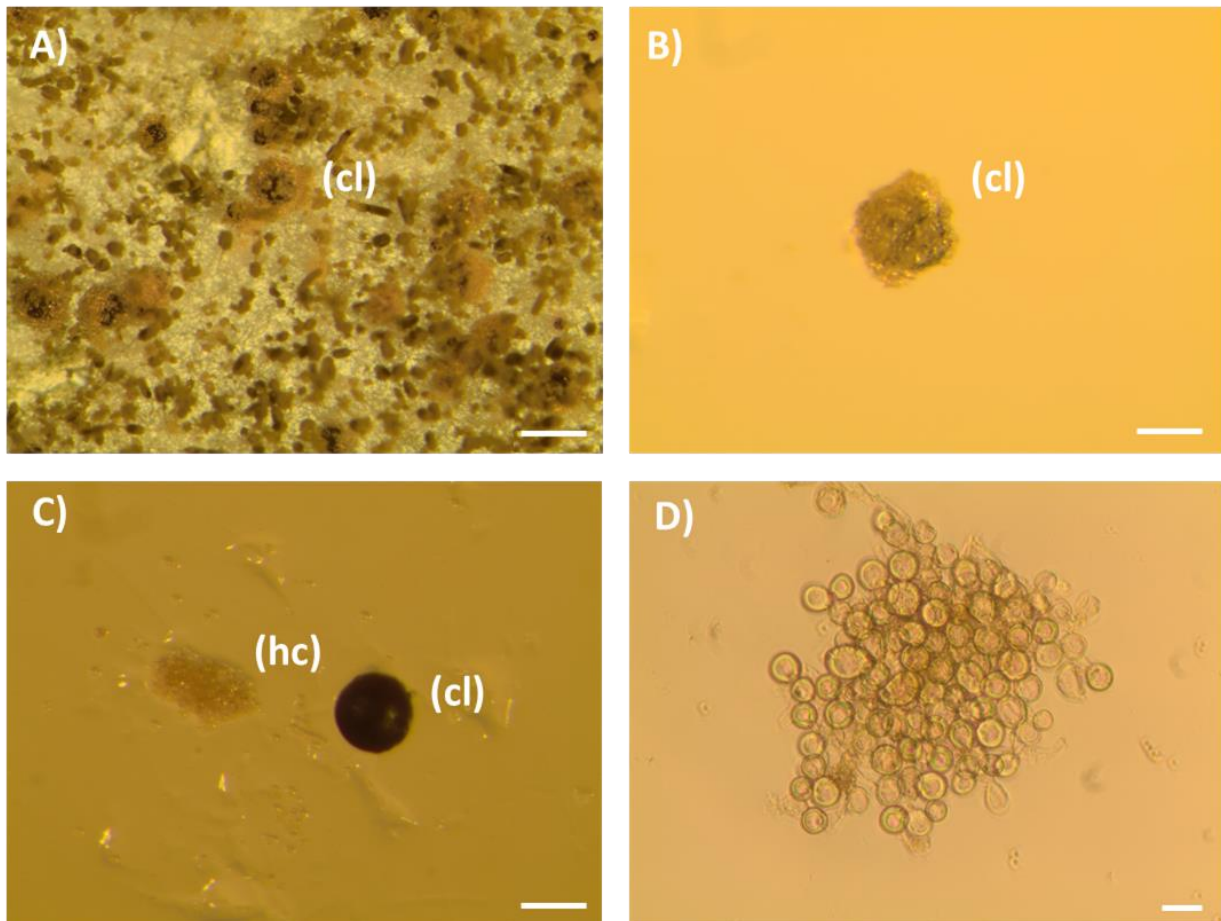


Figure 8. Illustration of enrichment of Hülle cells from solid agar plates: the cleistothecia-rolling technique.

A) Sexual mycelium of *A. nidulans* (FGSC A4 Glasgow wild-type, *veA*⁺) grown on solid minimal medium. Scale bar is 200 μm . B) The cleistothecium was transferred with a fine tipped syringe to a new petri dish containing 2% agar. Scale bar is 200 μm . C) The cleistothecium was rolled with the help of the syringe on solid agar plate and Hülle cells adhered to the surface of the solid agar plate. Hülle cells were collected into a collection tube. Scale bar is 200 μm . D) Enriched Hülle cells seen under a light microscope (cl, cleistothecium, hc Hülle cells). Scale bar is 20 μm .

2.2.1.2. Hülle cells from submerged cultures

In order to cultivate vegetative mycelium spores were inoculated in 50 ml (250 ml shake flask) minimal medium (1% glucose; 1% AspA; 2 mM MgSO₄; and trace elements; pH 6.5; 5.937 X10⁵ sp/ml) for 20 hours at 37 °C and with constant shaking. Hülle cells were observed under a light microscope. After 20 hours at 37 °C no Hülle cells were observed in wild-type FGSC A4, *veA*⁺. The minimal medium was filtered off and vegetative mycelium was washed with 0.96% NaCl. After 72 hours, vegetative mycelium was harvested and Hülle cells were observed in the hyphal ball of vegetative mycelium of the lysine prototroph *nkuA*Δ (AGB552) strain with an additional unknown mutation and lysine auxotroph *lysA*Δ (AGB1092) strains under a light microscope. The percentage of observable Hülle cells in the hyphal ball was determined within an area of 5 mm². Hülle cells were counted and their number was put into relation to the parental and the complementation strain with three biological replicates. Additionally, the dry weight of the submerged cultures was measured. Vegetative mycelia were first filtered to remove the liquid media, then they were dried for 12 hours in a drying cabinet (75 °C).

In order to perform a triple SILAC experiment the three lysine auxotroph strains were labeled with different stable isotope lysine and the labels were added from the point on where the strains were inoculated. *lysA*Δ; *nkuA*Δ (AGB1092) was labeled light (L-lysine final concentration: 0.75 mM) *lysA*Δ; *laeA*Δ; *nkuA*Δ (AGB1074) was labeled heavy (L-lysine ¹³C₆ ¹⁵N₂ HCl final concentration 0.75 mM) and *lysA*Δ; *laeA*Δ::*laeA*; *nkuA*Δ (AGB1076) was labeled medium (L-lysine D4 labeled 2 HCl final concentration 0.75 mM). For a label swap experiment strains were labeled *lysA*Δ; *nkuA*Δ was labeled heavy, *lysA*Δ; *laeA*Δ; *nkuA*Δ was labeled light and *lysA*Δ; *laeA*Δ::*laeA*; *nkuA*Δ was labeled medium. 300 mg of each mycelium was merged and grinded with a retsch™-mill for 2 min by 30 frequency 1/s.

2.2.2. DNA methods

2.2.2.1. Genetic transformation procedure

Transformations of *Escherichia coli* and *A. nidulans* cells were performed as described (Hanahan et al., 1991, Punt and van den Hondel 1992).

Escherichia coli:

For transformation 200 µl of chemo-competent cells were mixed with plasmid DNA and incubated on ice for 20 minutes, followed by an incubation for 1 minute at 42 °C. Next LB – liquid media were added to the cells and the samples were incubated for 30 minutes at 37 °C with 200 rpm. Cells were then inoculated on a solid agar plate containing LB-media with respective antibiotics.

Aspergillus nidulans:

For transformation protoplasts were used and prepared. Vegetative mycelium was used. Vegetative mycelium was harvested and washed with citrate buffer. Mycelium was transferred into a 300 ml flask and 25 ml of an enzyme mix was added (VinoTaste® Pro (Novozymes GmbH, 4518)/lysozyme (Serva GmbH, 28262.03)). The flask was incubated for 90 minutes at 30 °C by 70 rpm and protoplasts were filtered. After a washing step with 100 ml STC 1700 protoplasts were mixed with DNA cassettes. Successively 1.5 ml PEG 4000 was carefully added. Protoplasts were incubated for 30 minutes over ice to avoid crystal formation. Protoplasts were then washed with 50 ml STC 1700 buffer and inoculated on sorbitol-solid agar plates at 37 °C.

2.2.2.2. Plasmid DNA isolation from *Escherichia coli*

For the isolation of plasmids from *Escherichia coli* the following kits were used, HiSpeed Plasmid Midi Kit (QIAGEN, 12643), NucleoSpin®Plasmid Kit (Macherey-Nagel, 740615.250), QIAprep Spin Miniprep Kit (QIAGEN, 27106). Plasmid DNA isolation was performed according to the manufacturer's instructions. Therefore, *Escherichia coli* was inoculated in LB media with the respective antibiotic. Cultures were centrifuged at 13.000 rpm in a 2 ml reaction tube. The pellet was resuspended

in 250 µl buffer P1. As a next step 250 µl P2 was added and the reaction tube was inverted several times for 5 minutes. Next 350 µl of buffer N3 was added and the reaction tube was centrifuged for 10 minutes at 13.000 rpm. The supernatant was added into a DNA spin column. The DNA spin column was centrifuged for one minute at 13.000 rpm. The column was washed with a washing buffer. The DNA spin column was centrifuged at 13.000 rpm to remove the washing buffer. As a final step the plasmid DNA was eluted in 30 µl of dH₂O. The plasmid concentration was measured with a NanoDrop ND-1000 photospectrometer (peqlab biotechnologie, Erlangen, Germany).

2.2.2.3. *Aspergillus nidulans* DNA extraction

Vegetative mycelium of *A. nidulans* was used to extract genomic DNA (Lee and Taylor 1990). The mycelium was ground and 500 µl of lysis buffer (1 M Tris (pH 7.2), 0.5 M EDTA, 3 g SDS, 1 ml mercaptoethanol) was added and heated at 65 °C for 20 min. 100 µl of 8 M potassium acetate was added and tubes were inverted for 8-10 times. The samples were centrifuged for 15 min at 13000 rpm. This step was repeated. The supernatant was transferred into a new tube and 300 µl isopropanol was added. The samples were centrifuged for 15 min and the pellet was washed with 1000 µl of ethanol and dissolved in 120 µl of water/RNase A and stored at 4 °C.

2.2.2.4. Ligation of DNA fragments

Fragments were ligated into the respective vectors using the Gene Art^R Seamless Cloning and Assembly Kit (Invitrogen life technologies, A1328) or the T4 ligase (T4 DNA ligase (Thermo Scientific, EL0011)). Seamless cloning and assembly procedure was performed according to the manufacturer's instructions. The ligation procedure using the T4 ligase was performed as described by (Lehman 1974). The T4 ligase reaction was performed as following: 2-4 µl hydrolyzed vectors, 10-15 µl of the respective amplified DNA fragments and 2 µl T4 ligase buffer were mixed together. The ligation reaction was performed for 3 hours at room temperature. In order to perform the ligation, the hydrolyzed vectors were first dephosphorylated with calf intestine alkaline phosphatase (CIAP, Thermo Scientific). The dephosphorylation was performed as following: 17 µl hydrolyzed vectors, 2 µl calf intestine alkaline

phosphatase buffer, 1 μ l CIAP, were mixed together. The samples were incubated for 10 minutes at 37 °C. The enzyme reaction was then inactivated at 75 °C for 10 minutes. The amplified DNA fragments were phosphorylated as following: 15 μ l DNA, 1 μ l T4 Polynucleotide kinase (T4PNK, Thermo Scientific), 2 μ l kinase buffer, 2 μ l 10 mM adenosine triphosphate, were mixed together. The samples were incubated for 20 minutes at 37 °C. In order to inactivate the enzyme reaction, the samples were then incubated for 10 minutes at 75 °C.

2.2.2.5. PCR (Polymerase chain reactions)

Polymerase chain reactions PCR (Saiki et al., 1988) were performed using either a platinum® *Taq* polymerase (Fermentas GmbH, St. Leon Rot, Germany) or a high-fidelity DNA polymerase Phusion® (Thermo Fisher Scientific GmbH, Schwerte, Germany, 89846). The PCR program which was used in this study is illustrated in Table 4.

Table 4. PCR program used in this study.

Step	Temperature [°C]	Duration [min]	loops
1	98	00:30	
2	98	00:10	repeated 36 times
3	60	00:30	
5	72	02:00	
5	72	05:00	
6	4	pause	∞

2.2.2.6. Gelelectrophoresis of DNA

DNA was separated on a 1% agarose gel described by (Aaij and Borst 1972). DNA fragments were mixed with 1X loading dye and gelelectrophoresis was performed with 90 V using a horizontal gel chamber. The agarose gel contained ethidium bromide and DNA fragments were visualized in a DNA documentation system, Gel IX20 imager (Intas science instruments, Göttingen, Germany).

2.2.2.7. Purification of amplified DNA

For the purification of amplified DNA the following kit was used. QIAquick Gel Extraction Kit (QIAGEN, 28704) or QIAquick PCR Purification Kit (QIAGEN, 28104). This procedure was performed according to the manufacturer's instructions. Excised DNA of agarose gels were transferred into a 2 ml reaction tube. 400 µl QC buffer was added and the reaction tube was put into a 65 °C thermobloc for 10 minutes until the excised agarose gel piece melted. As a next step the melted solution was transferred into a DNA spin column. The DNA spin column was centrifuged by 13.000 rpm for one minute. The procedure was repeated for a second time. 650 µl of washing buffer was added and the DNA spinning column was centrifuged for 13.000 rpm for one minute. This procedure was repeated for a second time and the DNA spin column was centrifuged for 13.000 rpm to remove the washing buffer. As a final step the amplified DNA was eluted in 30 µl with dH₂O. The concentration of the amplified DNA was measured with a NanoDrop ND-1000 photospectrometer (peqlab biotechnologie, Erlangen, Germany).

2.2.2.8. Southern hybridization

Southern hybridization was performed with a non-radioactive probe (Amersham Bioscience, Buckinghamshire, United Kingdom) as described by (Southern 1975). Primers used for amplification of Southern probes are listed in Table 5. In order to confirm the successful integration of the mutagenesis cassette genomic DNA of the fungal mutant strains was digested with restriction enzymes for 12 hours. The DNA fragments were separated according to size by agarose gel electrophoresis. The agarose gels were washed with three different washing buffers, buffer 1 (0.25 M HCl, 10 minutes), buffer 2 (0.5 M NaOH, 25 minutes), buffer 3 (0.5 M Tris, 1.5 M NaCl, pH 7.4, 30min). All steps were performed at room temperature. DNA was transferred onto an Amersham™ Hybond-N™ Nylon membrane (GE Healthcare, 676409), by dry blotting for 150 minutes at room temperature. Membranes were dried (7 minutes, 75°C) and the transferred DNA was cross linked to the membranes using UV light ($\lambda = 254$ nm, 3 minutes per each side). Membranes were transferred into a prehybridization glass tube and 10 ml preheated prehybridization buffer was added. The membranes were incubated in a hybridization oven (60 minutes, 55 °C, rotated). After 30 minutes

2. Materials and methods

40 µl DNA southern probes were added. DNA probes were made according to the Amersham™ Alkphos Direct Labelling Reagents Kit (GE Healthcare, 11816064). Labelling of DNA probes were performed according to the manufacturer's instructions. The membrane was incubated with the DNA Southern probes for 12 hours at 55°C and rotated in the hybridization oven. The membrane was washed in 25 ml washing buffer 1 for 10 minutes. This step was performed twice at 55 °C and the membrane was rotated in the hybridization oven. 30 ml washing buffer 2 was added. The washing step was performed at room temperature for 5 minutes, shaking. For detection of DNA the Amersham™ Cdp-star™ Detection reagents (GE Healthcare, 9766233) were applied to the membrane. Finally, the labeled DNA on the membrane was detected with an Amersham™ Hyperfilm™ ECL (GE Healthcare, 28906837).

Table 5. Primers used for amplification of Southern probes.

Probe	Primer
<i>laeA</i> 5' UTR	BD45/BD46
<i>laeA</i> 3' UTR	BD47/BD48
<i>mphA</i> 3' UTR	BD85/BD86
<i>nptA</i> 3' UTR	BD108/BD109
<i>rfeA</i> 3' UTR	BD113/BD114

2.2.2.9. Sequence analysis and oligonucleotides synthesis

In order to analyze DNA sequences the software tool lasergene DNASTAR, Inc., Madison, Wisconsin, United States of America (Durfee and Schwei 2008) was used. Oligonucleotides were ordered from Eurofins MWG GmbH, Ebersberg, Germany. DNA was sequenced at SEQLAB-Sequencing Laboratories GmbH, Göttingen, Germany.

2.2.2.10. *Aspergillus nidulans* strain construction

2.2.2.10.1. Construction of *laeA*Δ, *laeA* complementation and other strains in *laeA*Δ

DNA sequence informations were obtained from AspGD (Cerqueira et al., 2014). Strains used in this study contain a recyclable marker module (Krappmann et al., 2005). In order to generate the *laeA* deletion construct the 5' UTR region was amplified from wild-type FGSC A4, *veA*⁺ genomic DNA with primers BD45/BD46 and the 3' UTR was amplified with the primers BD47/BD48. The two amplicons were fused with the recyclable *phleo* cassette (the *phleo* cassette contains a bleomycin (Bm) resistance-encoding gene *ble*) using a seamless cloning reaction (Gene Art® seamless cloning and assembly kit, Invitrogen life technologies, A13288). The deletion cassette was integrated into a *pBluescript SK (+)* vector. The linear deletion cassette was excised from the vector using a *PmeI* restriction cutting site and transformed into a *nkuA*Δ (AGBB52) and in a *lysA*Δ; *nkuA*Δ (AGB1092) parental strain. For complementation of *laeA*Δ the *laeA* genomic locus was amplified from wild-type FGSC A4, *veA*⁺ genomic DNA (primers BD45/BD76) fused together with a recyclable *phleo* marker and with the 3' UTR using a seamless cloning reaction.

In order to construct the *nptA::gfp* cassette a two-step cloning strategy was used (Mounts et al., 1989). The 5' UTR plus the sequence coding region of *nptA* was amplified with BD104/BD105 and the 3' UTR was amplified with the primers BD108/BD109. The *gfp* (green fluorescent protein) sequence was amplified using BD99 and BD100. The *gfp* sequence was fused with the coding sequence of *nptA* by fusion PCR. The fragment was integrated in the plasmid pJG229 containing a recyclable *phleo* cassette using a *SwaI* restriction cutting site. In the second step, the 3' UTR was integrated into the plasmid using an *Eco74I* restriction cutting site. In order to construct the *rfeA::gfp* cassette the 5' UTR plus the gene *rfeA* was amplified with the primers BD111/BD112. The 3' UTR was amplified with the primers BD113/BD114. The amplicons were fused using the two-step cloning strategy explained above. Linear cassettes of *nptA::gfp* and *rfeA::gfp* were transformed into a *lysA*Δ; *nkuA*Δ (AGB1092) and a *laeA*Δ; *lysA*Δ; *nkuA*Δ (AGB1074) strain. All strains were confirmed by Southern hybridization (Figure 9-13).

2. Materials and methods

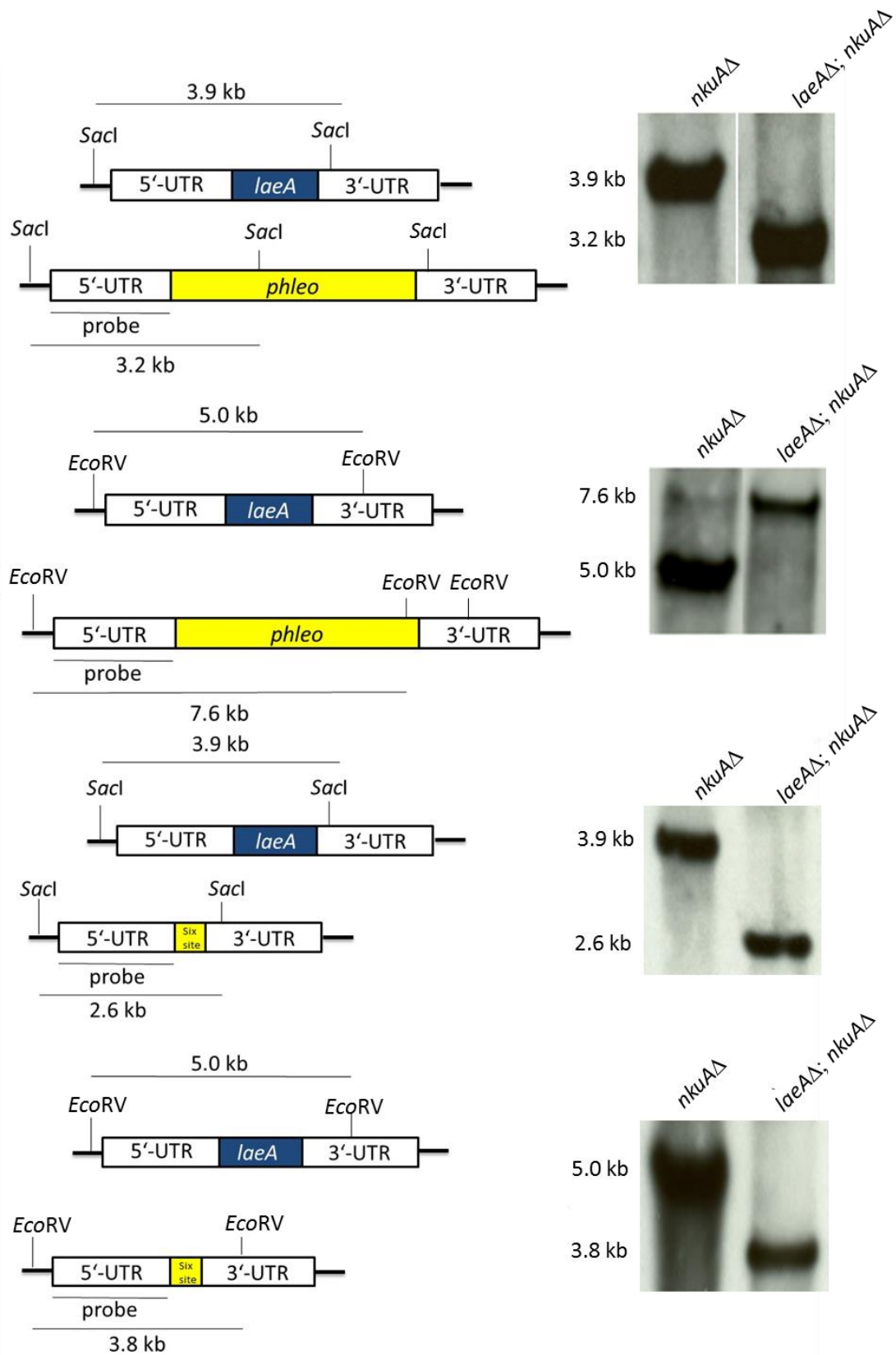


Figure 9. Restriction map and Southern hybridization before and after the marker was recycled for the deletion strain *laeAΔ; nkuAΔ* (AGB1073). The following restriction enzymes were used: *SacI* and *EcoRV*.

2. Materials and methods

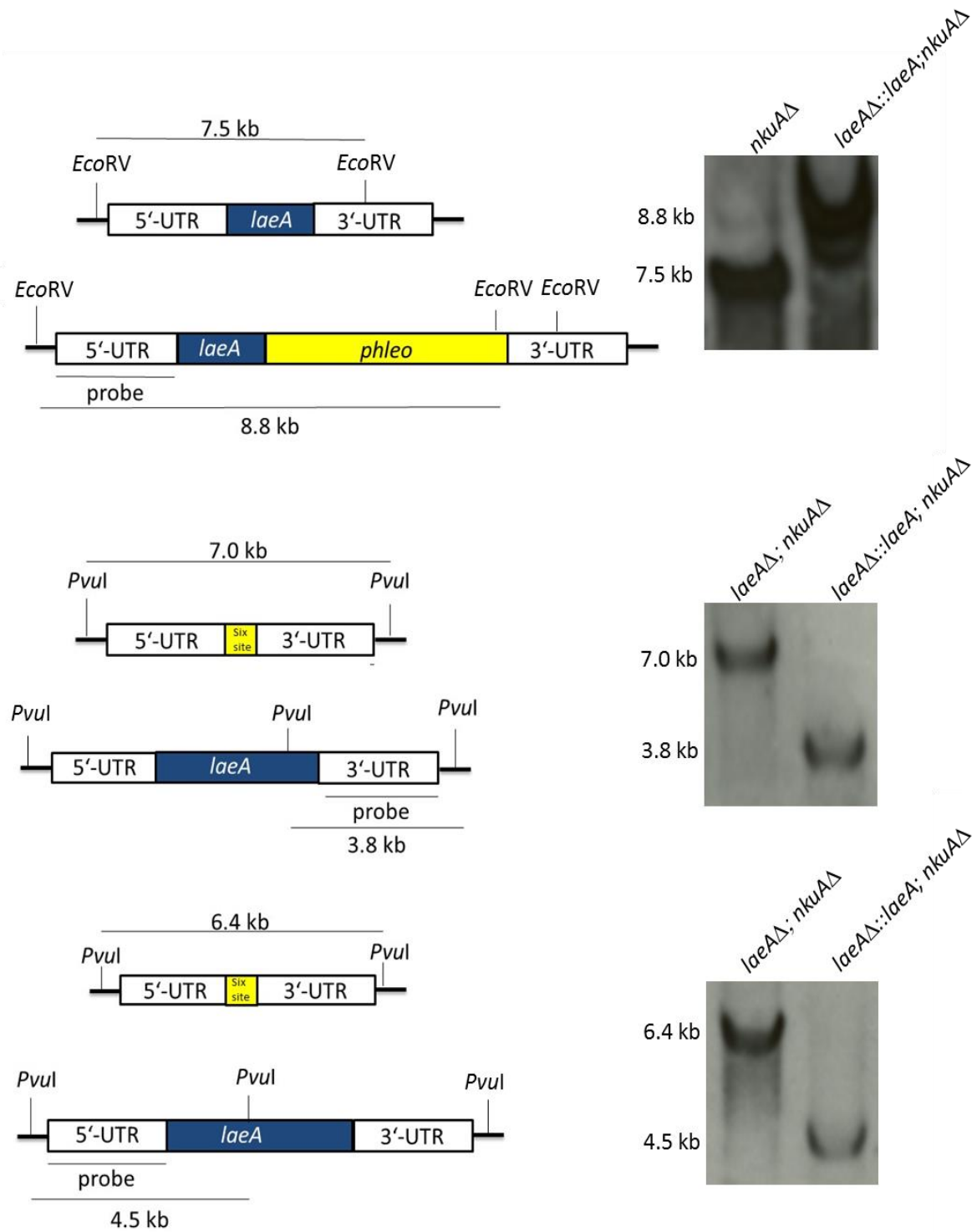


Figure 10. Restriction map and Southern hybridization before and after the marker was recycled for the complementation strain of *laeA*Δ (*laeA*Δ::*laeA*; *nkuA*Δ, AGB1075). The following restriction enzymes were used: *EcoRV* and *PvuI*.

2. Materials and methods

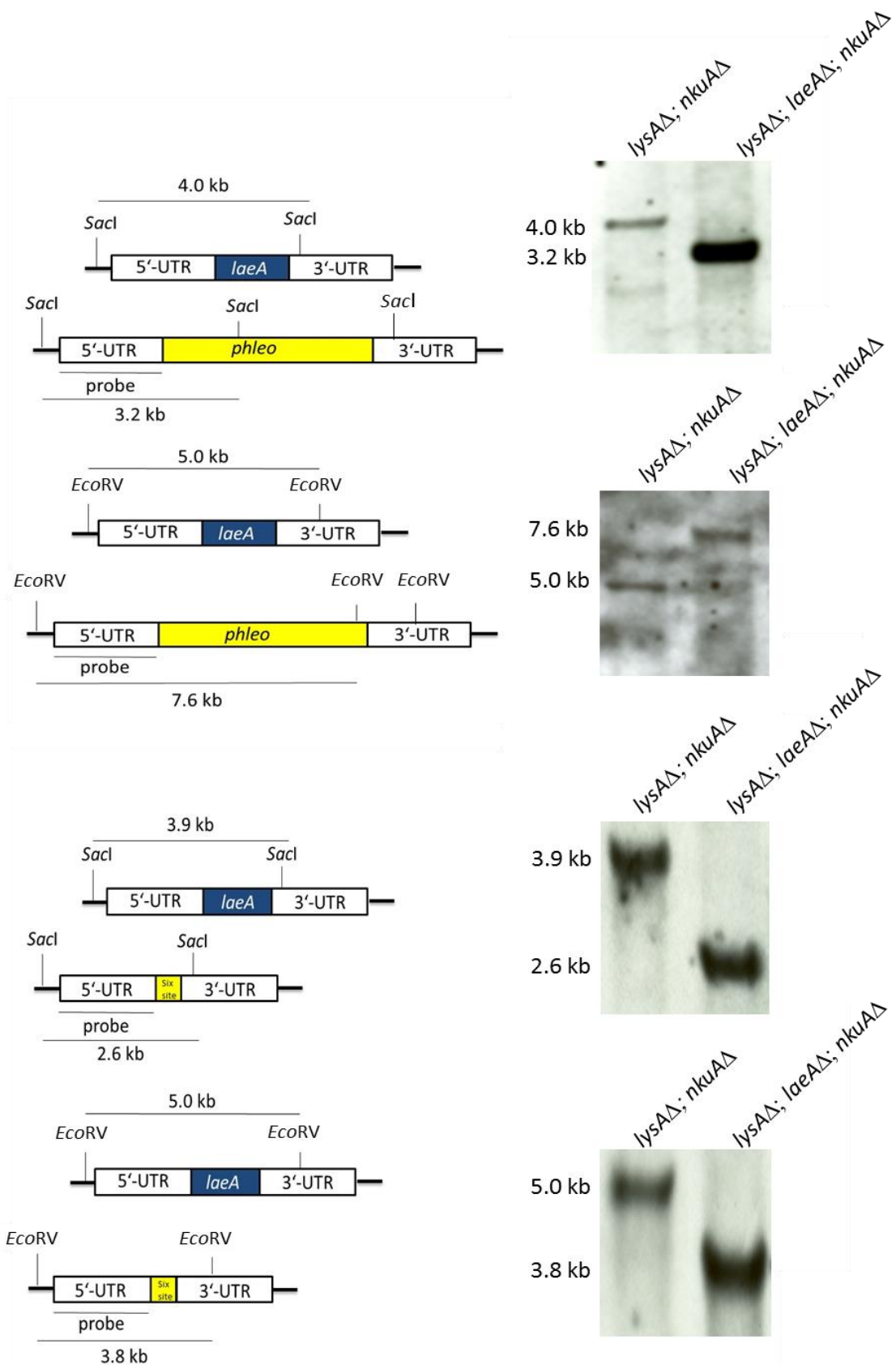


Figure 11. Restriction map and Southern hybridization before and after the marker was recycled for lysine auxotrophic *laeA*Δ strain (*lysA*Δ; *laeA*Δ; *nkuA*Δ, AGB1074). The following restriction enzymes were used: *SacI* and *EcoRV*.

2. Materials and methods

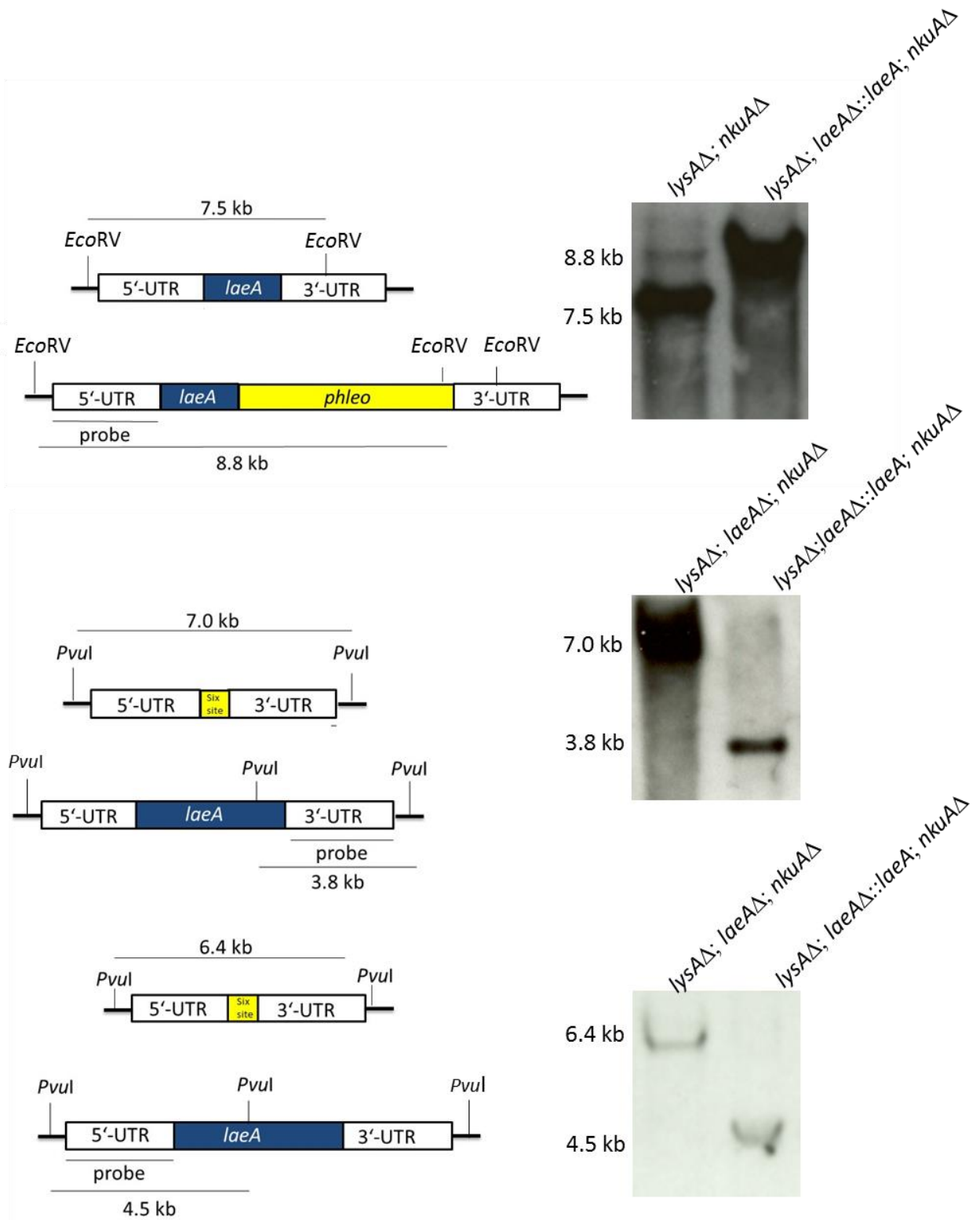


Figure 12. Restriction map and Southern hybridization before and after the marker was recycled for the complementation strain *lysA* Δ ; *laeA* Δ (*lysA* Δ ;*laeA* Δ ::*laeA*;*nkuA* Δ , AGB1076). The following restriction enzymes were used: *EcoRV* and *PvuI*.

2. Materials and methods

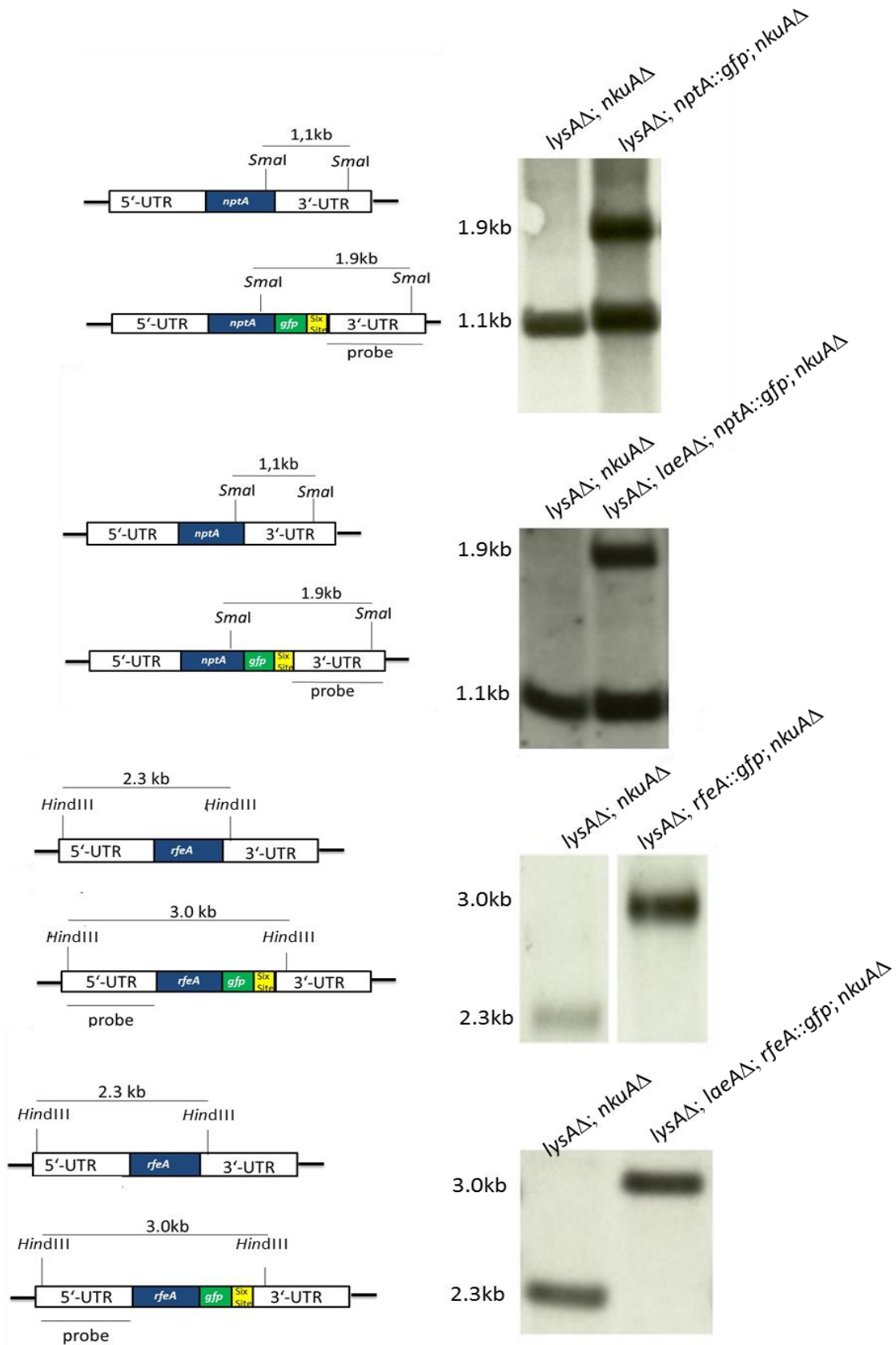


Figure 13. Restriction map and Southern hybridization to confirm *nptA::gfp* and *rfeA::gfp* strains
 Strains: *lysAΔ;nptA::gfp;nkuAΔ* (AGB1082), *lysAΔ;laeAΔ;nptA::gfp;nkuAΔ* (AGB1083). Strains: *lysAΔ;rfeA::gfp;nkuAΔ* (AGB1084), *lysAΔ;laeAΔ;nptA::gfp;nkuAΔ* (AGB1085). The following restriction enzymes were used: *SmaI* and *HindIII*. The strains contained a recyclable *phleo* cassette and were already recycled

2.2.2.10.2. Construction of *xptB::gfp* strain

The *xptB* (xanthone prenyltransferase) gene was fused with *gfp*. The *xptB::gfp* cassette was constructed using a two-step cloning strategy (Mounts et al., 1989). In order to construct the *xptB::gfp* cassette the 5' UTR plus the coding sequence of the gene *xptB* was amplified with the primers BD119/BD120(*xptB*) (Figure 14). The 5' UTR plus the coding sequence of the gene *xptB* were fused with the sequence of *gfp*. This fusion fragment was integrated into the plasmid pJG229 containing a recyclable *phleo* cassette using a *Swa*I restriction cutting site. The 3' UTR was amplified with the primers BD121(*xptB*)/BD122(*xptB*). Next the 3' UTR was integrated into the plasmid pJG299 using an *Eco*74I restriction cutting site.

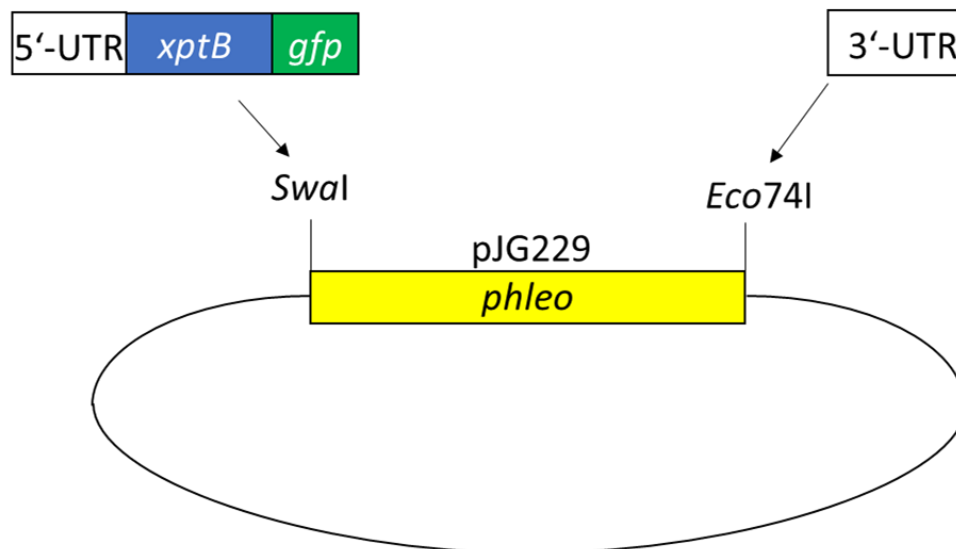


Figure 14. Schematic illustration of the two-step cloning strategy.

The sequence of the 5' UTR fused with the coding sequence of the *xptB* and with *gfp* was first integrated into the plasmid pJG229 containing a recyclable *phleo* cassette using a *Swa*I cutting site. Next the 3' UTR was integrated into the plasmid pJG229 using an *Eco*74I restriction cutting site.

The *xptB::gfp* cassette was transformed into a *lysA*Δ; *nkuA*Δ (AGB1092) parental strain and integration of the *xptB::gfp* cassette was confirmed by diagnostic PCR (Figure 15). In order to perform the diagnostic PCR to confirm the integration of the cassette the 5' UTR plus the coding sequence and the sequence of *gfp* was amplified using genomic DNA with the primers *xptB::gfp* BD119/BD107. Additionally, the *gfp* sequence was amplified with the primers BD106/BD107.

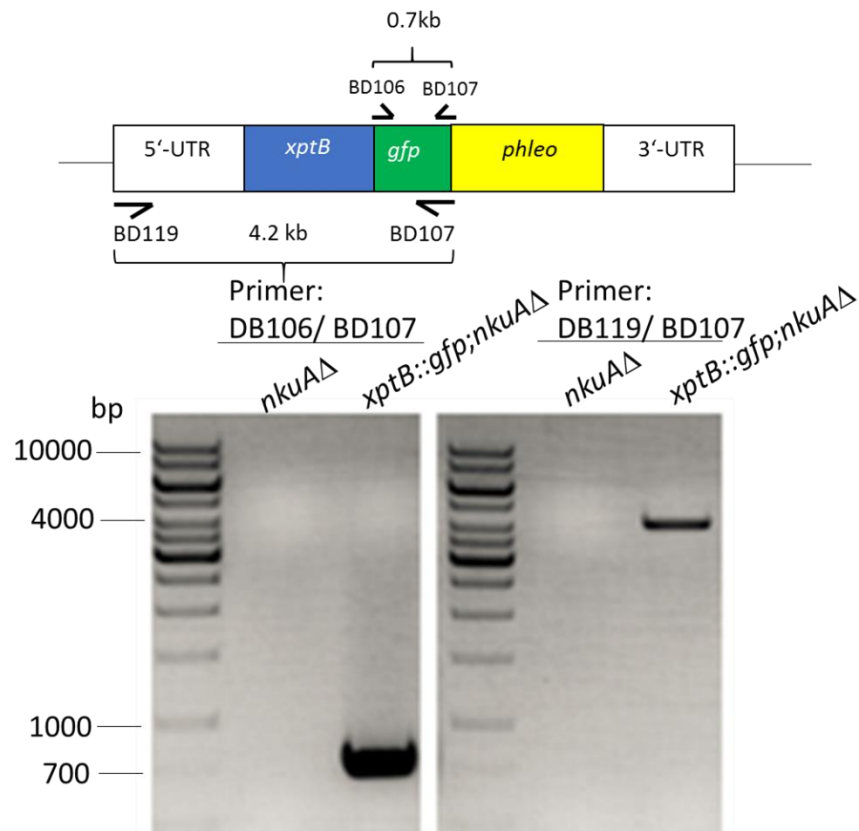


Figure 15. Diagnostic PCR to confirm the integration of the *xptB::gfp* cassette.

The 5' UTR plus the coding sequence of *xptB* and the sequence of *gfp* was amplified using genomic DNA (*xptB::gfp; nkuAΔ; lysAΔ*, AGB1086) with the primers BD119/BD107. The amplified product has a size of 4.2 kb. As negative control genomic DNA of *nkuAΔ; lysAΔ* was used. In order to amplify the *gfp* sequence the primers BD106 and BD107 were used. The amplified product has a size of 0.7 kb.

2.2.2.10.3. Construction of *xptC::gfp* strain

The *xptC* (oxidoreductase) gene was fused with *gfp*. In order to construct the *xptC::gfp* cassette the 5' UTR plus the coding sequence of the gene *xptC* was amplified with the primers BD113(*xptC*)/BD114(*xptC*). The sequence of *xptC* was fused with *gfp*. The 3' UTR was amplified with the primers BD115/BD116. The amplicons were fused using the two-step cloning strategy mentioned above. The fragments were integrated into the plasmid pJG229 using a *Swa*I and an *Eco*74I restriction cutting site. The *xptC::gfp* cassette was transformed into a *nkuAΔ* (AGB552) parental strain and integration of the *xptC::gfp* cassette was confirmed by diagnostic PCR (Figure 16). In order to perform the diagnostic PCR to confirm the integration of the cassette the 5' UTR plus the coding sequence and the sequence of *gfp* was amplified using genomic DNA with the primers BD114/BD107. Additionally, the *gfp* sequence was amplified with the primers BD106/BD107.

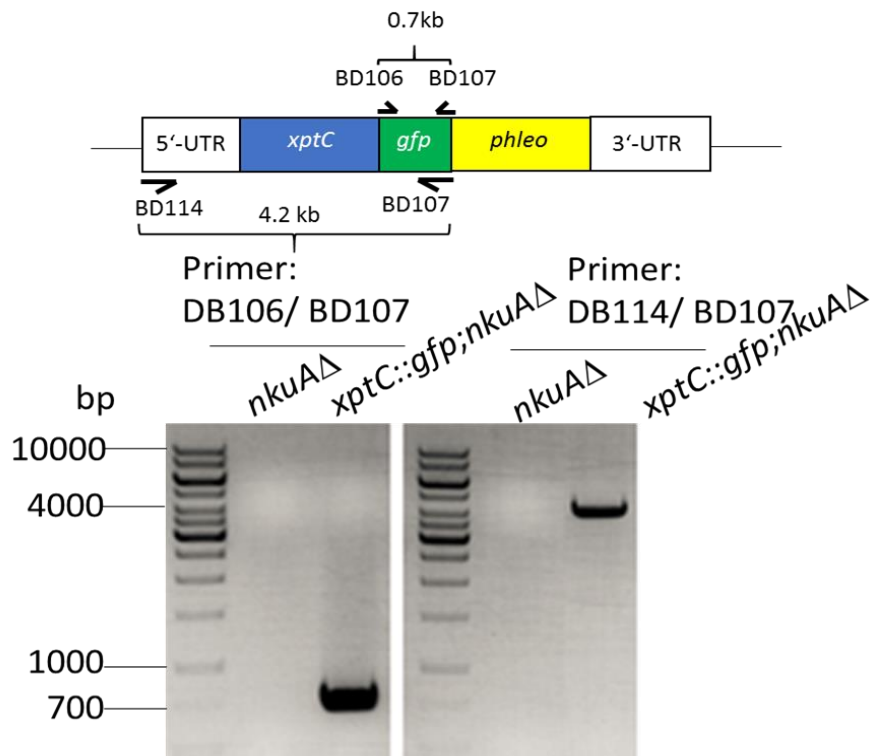


Figure 16. Diagnostic PCR to confirm the integration of *xptC::gfp* cassette.

The 5' UTR plus the coding sequence of *xptC* and the sequence of *gfp* was amplified using genomic DNA (*xptC::gfp;nkuAΔ*, AGB1088) with the primers BD114/BD107. The amplified product has a size of 4.2 kb. In order to amplify the *gfp* sequence the primers BD106 and BD107 were used. The amplified product has a size of 0.7 kb. As negative control genomic DNA of *nkuAΔ* (AGB552) was used and no amplified products were observable.

2.2.2.10.4. Construction of *AN8434::gfp* strain

In order to construct the *AN8434::gfp* cassette the 5' UTR plus the gene *AN8434* was amplified with the primers: BD121/BD122. The 3' UTR was amplified with the primers BD123/BD124. The amplicons were fused using the two-step cloning strategy mentioned above. First the 5' UTR and the coding sequence of *AN8434* was fused with the sequence of *gfp*. The fragment was integrated into the plasmid pJG229 containing a recyclable *phleo* cassette using a *SwaI* restriction cutting site. The 3' UTR was integrated into the plasmid pJG229 using an *Eco74I* restriction cutting site. The *AN8434::gfp* cassette was transformed into a *nkuAΔ* (AGB552) parental strain. Integration of the *AN8434::gfp* was confirmed by diagnostic PCR (Figure 17). In order to perform the diagnostic PCR to confirm the integration of the cassette the 5' UTR plus the coding sequence and the sequence of *gfp* was amplified using genomic DNA with the primers *AN8434::gfp* (BD121/BD107). Additionally, the *gfp* sequence was amplified with the primers BD106/BD107. As negative control genomic DNA of the parental strain *nkuAΔ* was used.

2. Materials and methods

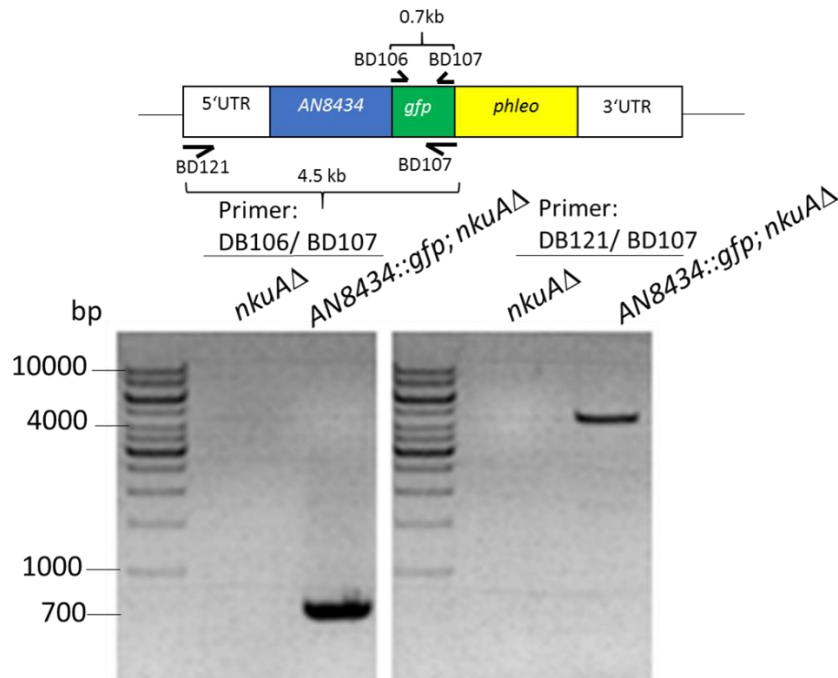


Figure 17. Diagnostic PCR to confirm the integration of the *AN8434::gfp* cassette.

The 5' UTR plus the coding sequence *AN8434* and the sequence of *gfp* was amplified using genomic DNA (*AN8434::gfp;nkuAΔ*, AGB1089) with the primers BD121/BD107. The amplified product has a size of 4.5 kb. The sequence of *gfp* was amplified using the primers BD106/BD107. The amplified product has a size of 0.7 kb. As negative control genomic DNA of *nkuAΔ* (AGB552) was used and no amplified products were observable.

2.2.2.10.5. Construction of *AN8435::gfp* strain

In order to construct the *AN8435::gfp* strain cassette the 5' UTR plus the gene *AN8435* was amplified with the primers BD125/BD127. This sequence *AN8435* was fused with the sequence of *gfp*. The 3' UTR was amplified with the primers BD128/BD129. The amplicons were fused using the two-step cloning strategy. The fragments were integrated into the plasmid pJG229 using a *Swa*I and an *Eco*74I restriction cutting site. The *AN8435::gfp* cassette was transformed into a *nkuAΔ* (AGB552) parental strain and integration of *AN8435::gfp* was confirmed by diagnostic PCR (Figure 18). In order to perform the diagnostic PCR to confirm the integration of the cassettes the 5' UTR plus the coding sequence and the sequence of *gfp* was amplified using genomic DNA with the primers *AN8435::gfp* (BD125/BD107). Additionally, the *gfp* sequence was amplified with the primers BD106/BD107. As negative control genomic DNA of the parental strain *nkuAΔ* was used.

2. Materials and methods

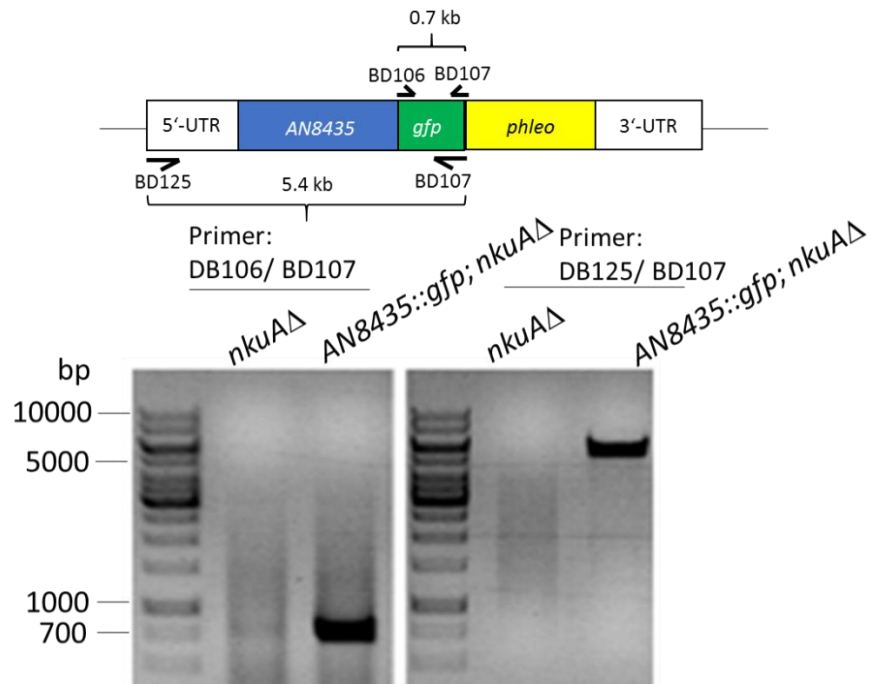


Figure 18. Diagnostic PCR to confirm the integration of the *AN8435::gfp* cassette.

The 5' UTR plus the coding sequence of *AN8435* and the sequence of *gfp* was amplified using genomic DNA (*AN8435::gfp;nkuAΔ*, AGB1090) with the primers BD125/BD107. The amplified product has a size of 5.4 kb. The sequence of *gfp* was amplified using the primers BD106/BD107. The amplified product has a size of 0.7 kb. As negative control genomic DNA of *nkuAΔ* (AGB552) was used and no amplified products were observable.

2.2.2.10.6. Construction of *mphAΔ*, *mphA* complementation and other strains in *mphAΔ*

The *mphA* (maltose permease-like protein of Hülle cells) knockout plasmid and knockout strain was constructed as mentioned above using the seamless cloning and assembly strategy. The 5' UTR and the 3' UTR region was amplified from the wild-type FGSC A4, *veA*⁺ genomic DNA using the primers BD83/BD84 and BD85/BD86. The linear deletion cassette was excised from the vector using a *PmeI* restriction cutting site and transformed into a *nkuAΔ* (AGBB52) parental strain. In order to construct the *gfp* fusion plasmids the C-terminus of *mphA* was tagged. Therefore, the 5' UTR plus the coding sequence of *mphA* was amplified with the primers BD83/BD98. The *gfp* sequence was amplified using the primers BD99/BD100. As mentioned above 3' UTR was amplified using the primers BD85/BD86. The complementation of *mphAΔ*; *nkuAΔ* was performed with and without *gfp*. The *mphA::gfp* cassette was transformed into a *laeAΔ;nkuAΔ* (AGB1073) strain. All strains were confirmed by Southern hybridization (Figure 19-21).

2. Materials and methods

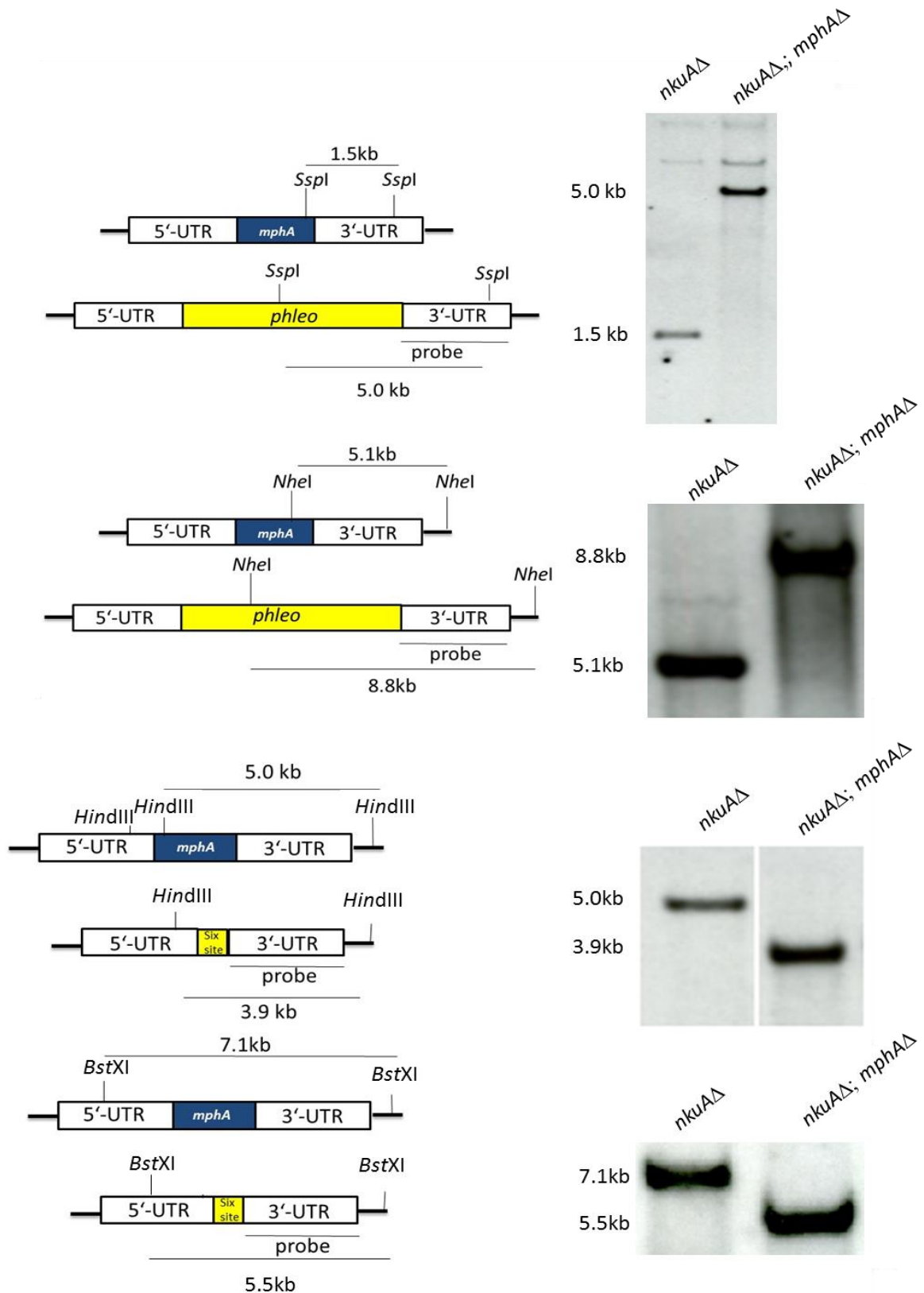


Figure 19. Restriction map and Southern hybridization before and after the marker was recycled for the *nkuA*Δ; *mphA*Δ (AGB1077) strain.

The following restriction enzymes were used: *SspI*, *NheI*, *HindIII* and *BstXI*.

2. Materials and methods

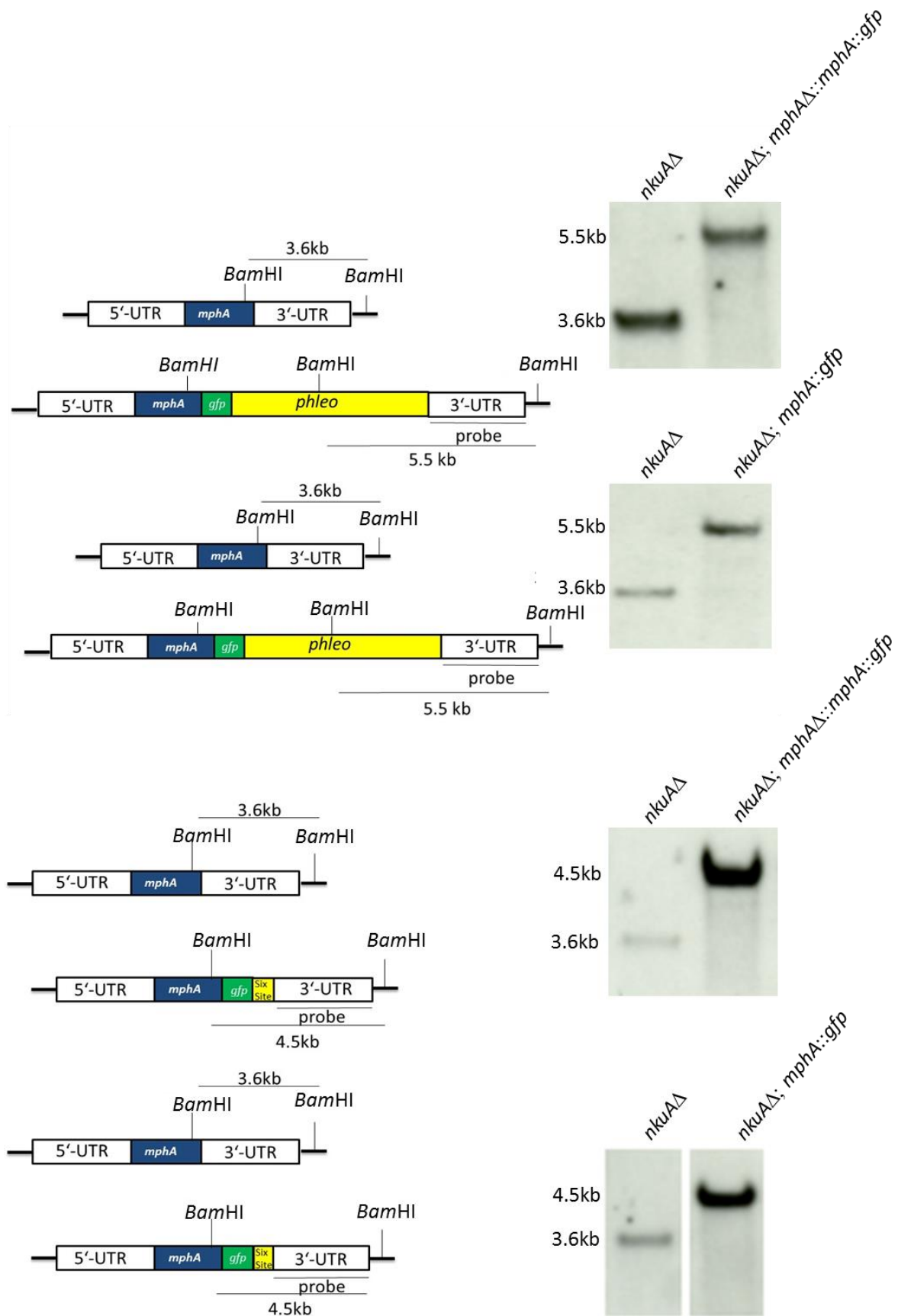


Figure 20. Restriction map and Southern hybridization before and after the marker was recycled for the complementation strain (*nkuAΔ; mphAΔ::mphA::gfp*, AGB1078) plus the *mphA::gfp;nkuAΔ* (AGB1079) strain.

*Bam*HI was used as a restriction enzyme.

2. Materials and methods

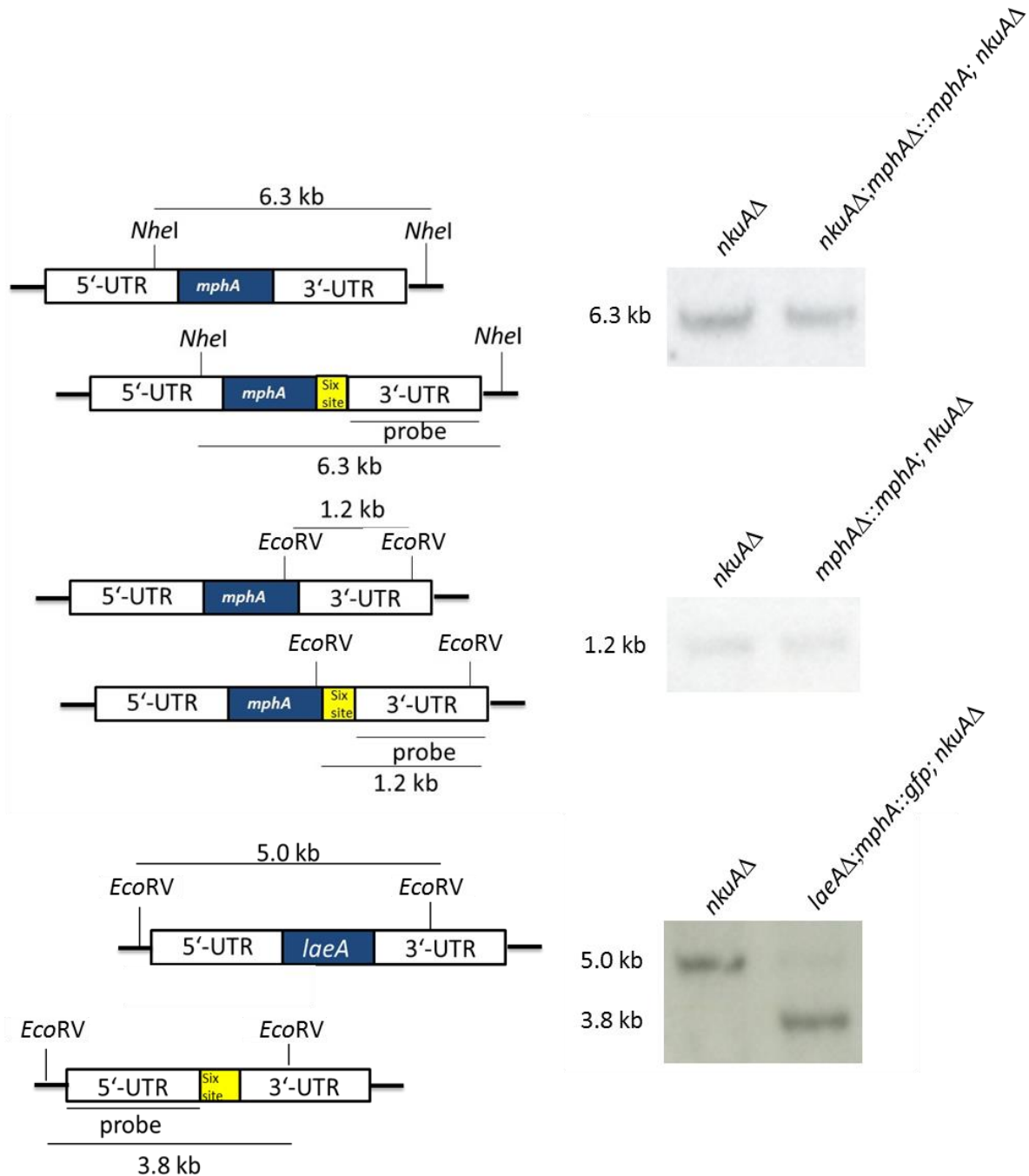


Figure 21. Restriction map and Southern hybridization to confirm the complementation strain (*mphAΔ::mphA, nkuAΔ*, AGB1080) and the *laeAΔ;mphA::gfp;nkuAΔ* (AGB1081) strain. *NheI* and *EcoRV* were used as restriction enzymes. The strains contained a recyclable *phleo* cassette and the recyclable *phleo* cassette was already recycled.

2.2.3. Protein methods

2.2.3.1. Protein extraction of Hülle cells from *Aspergillus nidulans*

In order to extract proteins from enriched Hülle cells the cleistothecia-rolling technique was used as mentioned above. Sexual mycelium of *A. nidulans* wild-type (FGSC A4 Glasgow, *veA*⁺) was grown on solid agar plate cultures. Therefore, spores were inoculated on a solid agar plate and the petri dish was sealed with a parafilm to lower the oxygen condition and was covered with an aluminium foil. After three, five and seven days the cleistothecia were transferred to a new petri dish with the help of a syringe. In order to separate Hülle cells from the cleistothecium they were rolled on the solid agar plate and Hülle cells adhered to the surface. Hülle cells were then transferred with the help of the syringe from the solid agar plate to a 1.5 ml collection tube containing 40 µl extraction buffer B + 300 (100 mM Tris pH 7.5, 300 mM NaCl, 10% glycerol, 1 mM EDTA, 0.1% NP-40, 1 mM DTT, protease inhibitor mix (Roche Pharma AG, Grenzach-Wyhlen, Germany), 0.5 M benzamidine, 100 mM PMSF) with phosphatase inhibitor (100 mM NaF, 50 mM sodium orthovanadate, 50 mM β-glycerolphosphate; sterile filtered). All further steps were performed on ice. 270 – 300 cleistothecia were rolled on the solid agar plate and the resulting Hülle cells were used for further protein extractions. Hülle cells were sonicated (60 seconds, 60% of sonoporation power, in between centrifugation steps for 30 seconds at 4°C, procedure repeated 6 times). The tube was centrifuged for 10 min by 13.000 rpm at 4°C and the supernatant was transferred into a new 1.5 ml tube. The cell disruption was verified by observation of cellular debris. Protein extract was then loaded onto 12% SDS-PAGE.

2.2.3.2. Protein extraction of sexual mycelium from *Aspergillus nidulans*

Sexual mycelium of *A. nidulans* wild-type FGSC A4, *veA*⁺ was harvested from the same plate as Hülle cells were collected to be enriched. Sexual mycelium was scraped off the solid agar plate with a spatula and transferred into a 1.5 ml tube. Sexual mycelium was frozen in liquid nitrogen and grinded in a retschTM-mill. 300 µl of

extraction buffer B⁺ 300 (100 mM Tris pH 7.5, 300 mM NaCl, 10% glycerol, 1 mM EDTA, 0.1% NP-40, 1 mM DTT, protease inhibitor mix (Roche Pharma AG, Grenzach-Wyhlen, Germany), 0.5 M benzamidine, 100 mM PMSF) with phosphatase inhibitor (100 mM NaF, 50 mM sodium orthovanadate, 50 mM β -glycerolphosphate; sterile filtered) was added and a sonication step as described before followed by centrifugation (10 min, 13.000 rpm, 4 °C) was performed. Protein extraction was performed as described (Bayram et al., 2012). 80 μ g of protein were loaded onto a 12% SDS-PAGE. All other steps were performed as mentioned above.

2.2.3.3. Protein extraction of vegetative mycelium from *Aspergillus nidulans*

In order to cultivate the vegetative mycelium spores were inoculated in 50 ml (250 ml shake flask) minimal medium (1% glucose; 1% AspA; 2 mM MgSO₄; and trace elements; pH 6.5; 5.937 X10⁵ sp/ml) for 20 hours (for Hülle cell formation 72 hours) at 37 °C with constant shaking. The vegetative mycelium was filtered to remove the media and washed twice with 0.96% NaCl. 300 mg of vegetative mycelium was transferred into a 2 ml reaction tube. The vegetative mycelium was grinded with a retschTM-mill for 2 min by 30 frequency l/s. Proteins were extracted as described (Bayram et al., 2012). 80 μ g of total protein extract was loaded onto a 12% SDS-PAGE.

2.2.3.4. Protein extraction of asexual mycelium from *Aspergillus nidulans*

Protein extraction of an asexual mycelium was performed at the same time points as a sexual mycelium. Harvesting and protein extraction was performed as mentioned above. Asexual mycelium was grown on solid agar plate cultures. Therefore, spore solution was directly inoculated on the solid agar plate. Asexual mycelium was grown in light conditions at 37 °C. The asexual mycelium was scratched off the solid agar plate and proteins were extracted as mentioned above and as described (Bayram et al., 2012).

2.2.3.5. Protein concentration measurement

In order to determine the concentration of proteins a Bradford assay was used (Bradford 1976). Additionally, the concentration of proteins was measured with an NanoDrop ND-1000 photospectrometer (peqlab biotechnologie GmbH, Erlangen, Germany).

2.2.3.6. SDS-polyacrylamide gel electrophoresis

Protein samples were mixed with 4X loading dye (50 mM Tris pH 6.8, 2% SDS, 10% glycerol, 1% β -mercaptoethanol, 12.5 mM EDTA, 0.02% bromophenol blue). The samples were heated for 5 minutes at 95 °C. The protein samples were loaded onto a 12% SDS page according to (Laemmli 1970). SDS-gels were prepared manually and consisted of a lower running gel (1 M Tris pH 8.8, 0.1% SDS, 12% acrylamide (Rotiphorese® Gel 40 37,5:1) (Roth GmbH, 3029.1), 10% ammonium persulfate (APS), 20 μ l TEMED) and an upper stacking gel (1 M Tris pH 6.8, 0.1% SDS, 12% acrylamide, 5% ammonium persulfate (APS), 10 μ l TEMED). Proteins were separated electrophoretically for 60 minutes at 180-200 V. The PageRuler™ prestained protein ladder (Thermo Scientific, SM26616) was used as size marker.

2.2.3.7. Colloidal Coomassie staining of proteins

Protein staining was performed according (Neuhoff et al., 1988). Gels were fixed in 40% (v/v) ethanol, 10% (v/v) acetic acid for 60 min, washed two times in water for 10 minutes and stained for 12 hours in coomassie solution (0.1% (w/v) coomassie brilliant blue G250, 5% (w/v) aluminum sulfate-(14-18)-hydrate, 10% (v/v) methanol, 2% (v/v) ortho-phosphoric acid). The lanes were excised from the polyacrylamide gels. The gel pieces were divided into equal lots into six 1.5 ml peptide low binding reaction tubes, destained in v (methanol):v (water) (40:60).

2.2.3.8. In-gel protein digestion with trypsin

The protein lane was excised from the gel and separated into six peptide low binding reaction tubes and tryptic digestion with trypsin was performed as described (Shevchenko et al., 1996). The gel pieces were covered with acetonitrile and shaken

2. Materials and methods

for 10 minutes at room temperature. Acetonitrile was removed and the gel pieces were dried in a speedvac (savant speedvac concentrator, Thermo Scientific). 150 μ l 10 mM DTT (in 100 mM NH_4HCO_3) was added to the gel pieces. The samples were incubated at 56 °C for 60 minutes. DTT solution was removed and 150 μ l 55 mM iodoacetamide (in 100 mM NH_4HCO_3) was added and the samples were incubated for 45 minutes at room temperature in dark. Iodoacetamide solution was removed and the gel pieces were washed in 150 μ l NH_4HCO_3 , shaken for 10 minutes at room temperature. The solution was removed and 150 μ l acetonitrile was added. The samples were shaken for 10 minutes at room temperature. The washing steps were repeated once. The gel pieces were dried in a speedvac at 50 °C and covered subsequently with trypsin (SERVA GmbH, Heidelberg, Germany, 37286.01). The trypsin buffer was prepared according to the manufacturer's instructions. The samples were incubated for 45 min on ice and the remaining digestion buffer was removed. Next 30 μ l 25 mM NH_4HCO_3 pH 8.0 was added and the samples were incubated for 12 hours at 37 °C.

The samples were centrifuged (1 minute by 13.000 rpm) and the supernatant was collected in a 1.5 ml peptide low binding reaction tube. The gel pieces were covered with 20 mM NH_4HCO_3 and shaken for 10 minutes at room temperature. The samples were centrifuged (1 minute by 13.000 rpm) and the supernatant was collected into the collection tube. Next the gel pieces were covered with 50% acetonitrile / 5% formic acid. After an incubation step of 20 minutes, shaken and at room temperature the samples were centrifuged (1 minute by 13.000 rpm) and the supernatant was collected. This step was repeated twice. The final volume of the combined supernatant was completely dried in a speedvac at 50 °C. The peptides were resuspended in 20 μ l sample buffer (2% acetonitrile, 0.1% formic acid).

After tryptic digestion peptides were desalted with the use of C18-StageTips as described (Rappsilber et al., 2007). Therefore, three C18 disks were punched out from a solid phase extraction disk (3M, Neuss, Germany, 2215) and placed into a 200 μ l tip. The C18 material was equilibrated. The C18-StageTips were placed into a 2 ml reaction tube using an adaptor. For equilibration of the C18-StageTips 100 μ l methanol 0.1% formic acid was added to the C18 material. After a centrifugation step (2 minutes, 13.000 rpm) 100 μ l 70% acetonitrile 0.1% formic acid was added. Then the C18-StageTips were centrifuged and 100 μ l 0.1% formic acid was added. This step was repeated. The peptide solution was added onto the C18 material and the C18-StageTips were centrifuged for 5 minutes by 4.000 rpm. This step was repeated. The

C18-StageTips were washed twice with 100 µl 0.1% formic acid. The peptides were eluted from the C18 material with 70% acetonitrile 0.1% formic acid. The C18-StageTips were centrifuged for 5 minutes at 4.000 rpm. The peptide samples were dried in a speedvac. For LC-MS analysis the peptide samples were resuspended in 20 µl LC-MS sample buffer.

2.2.3.9. Liquid chromatography-mass spectrometry (LC-MS) and data analysis

Peptides were analyzed on a Liquid chromatography (LC) coupled to an *Orbitrap Velos Pro™ Hybrid Ion Trap-Orbitrap* mass spectrometer (MS) (Thermo Fisher Scientific, Bremen, Germany). Peptides were dissolved in 2% (v/v) acetonitril, 0.1% (v/v) formic acid and raw data were searched with SEQUEST and Mascot algorithms present in Proteome Discoverer 1.4 (Eng et al., 1994, Koenig et al., 2008). The search parameter for SEQUEST and Mascot algorithm were: (i) precursor ion mass tolerance 10 ppm, (ii) fragment ion mass tolerance 0.6 Da, (iii) maximum of two missed cleavage sites were set, (iv) fixed cysteine static modification by carboxyamidomethylation, (v) variable modification by methionine oxidation. The MS/MS spectra were matched against the *A. nidulans* genome database (UBMG0112_Anidulans_20120325.fasta). Results filter settings of Proteome Discoverer 1.4 were set to: (a) high peptide confidence and (b) minimal number of two peptides per protein. The MS/MS data were furthermore analyzed with the Andromeda search engine operating in MaxQuant 1.5.1.0 software with the program's default parameters using the same genome database as mentioned above (Tyanova et al., 2016).

Identified proteins of enriched Hülle cells from solid agar plate cultures were analyzed within three different time points. For each time point three biological replicates were considered. The proteome of sexual mycelium was analyzed from the same solid agar plates from where Hülle cells were enriched. The proteome of sexual mycelium was also analyzed within three different time points. The same conditions were applied to analyze the proteome of asexual mycelium. For each time point three biological replicates were considered. Only proteins identified in two or more biological replicates and with two or more peptides per protein were considered for the analysis. For visualization of the analysis the accession numbers of the proteins were inserted into

a Venn diagram (Oliveros 2016). The proteome of a vegetative mycelium in submerged liquid cultures was analyzed by three biological replicates. Only proteins identified in two or more biological replicates and with two or more peptides per protein were considered for the analysis. For peptide quantification Lys4 was defined as medium peptide labels and Lys8 as heavy peptide labels. The peptide median ratio distribution was determined using Proteome Discoverer 1.4. In order to correct experimental bias, the protein median was normalized. Only peptide ratios that were determined similar in two or more biological replicates were considered for the analysis. Additionally, normalized ratios were analyzed and processed using the Perseus 1.5.0.15 software. A t-test (p value 0.05) was performed to statistically compare the log₂ SILAC ratios across three biological replicates. The log₂ SILAC ratio was determined for the strains *laeA*Δ (AGB1074) in comparison to *laeA* (AGB1092). The following thresholds were set. In the range of a log₂ SILAC ratio between - 5.0 and - 0.5 the protein quantity of identified proteins was down-regulated. In the range of a log₂ SILAC ratio between + 0.5 and + 5.0 the protein quantity of identified proteins was up-regulated. In the range between a -0.5 and + 0.5 log₂ SILAC ratio the protein quantity of identified proteins was unchanged. Workflows to process the proteomic data are illustrated in supplementary table 1 and 2.

2.2.3.10. Functional annotation of proteins

Functional annotations of identified proteins were performed using the **basic local alignment search tool** Blast2GO (<http://www.Blast2GO.com/b2ghome>). BlastP was used to blast against the NCBI nr database (NCBI: National Center for Biotechnology Information) with a blast expect value of 1×10^{-3} . The number of blast hits were set to 20 and the cutoff value for the GO terms was set to 20 (Conesa et al., 2005).

2.2.3.11. Fluorescence microscopy of fusion proteins

In order to visualize the localization of fusion proteins (fused to GFP) fluorescence microscopy was used. Hülle cells were enriched in 40 µl of dH₂O using the cleistothecia-rolling technique. After centrifugation (2 minutes at 13.000 rpm) the supernatant was removed. The cellular pellet was resuspended in 5 µl dH₂O and transferred to an object slide. The cells were observed under a reflected-light

microscope (Zeiss Axiolab - Zeiss AG, Jena, Germany) and an Olympus SZX12-ILLB2-200 binocular (Olympus GmbH, Hamburg, Germany). Fluorescence photograph pictures were taken with a confocal light microscope (Zeiss Axiolab - Zeiss AG, Jena, Germany) equipped with a QUAN-TEM: S12SC (Photometrics, Tucson, Arizona, United States of America) digital camera and the SlideBook 6 (Intelligent Imaging Innovations GmbH, Göttingen, Germany) software package. For GFP fusion protein visualization, the following parameters were used; DIC filter 200 ms; GFP filter 300 ms.

2.2.3.12. Immunoblotting

Proteins were extracted from different types of mycelia as described above. For immunoblotting experiments, proteins were first separated using a polyacrylamide gel electrophoresis and transferred onto a nitrocellulose membrane as previously described (Jöhnk et al., 2016, Schinke et al., 2016). Protein concentrations were determined as described above and as reference for equally loaded proteins amount 0.2% Ponceau S (Sigma- Aldrich, Copenhagen, Denmark), 3% TCA was used. Blocking was performed in 5% milk powder (skimmed milk powder (Sucofin, 562570765347)). Membranes were incubated for 12 hours with α -GFP antibody (dilution: 1:1000, sc-9996, Santa Cruz Biotechnology Inc., Dallas, Texas, United States of America and Heidelberg, Germany). The nitrocellulose membranes were washed three times in 150 ml 1X TBST (Tris buffered saline with tween 20) for 10 minutes at room temperature. Membranes were incubated for 60 minutes using an α -mouse secondary antibody (dilution 1:2000, G21234, Invitrogen AG, Carlsbad, California, United States of America). The nitrocellulose membranes were washed three times in 150 ml 1X TBST (Tris buffered saline with tween 20). For peroxidase reaction 100 μ l 2.5 mM luminol, 44 μ l 400 μ M paracoumarat, 100 mM Tris pH 8.5 added to 9 ml dH₂O and 6.15 μ l 30% H₂O₂ to 9 ml dH₂O. The nitrocellulose membranes were incubated with both solutions for 2 minutes, shaken and in darkness. Detection was performed on a Fusion-SL7 (Vilber Lourmat, Eberhardzell, Germany) system. Western hybridization experiments were performed with three biological replicates and samples were loaded twice on the 12% SDS-PAGE.

3. Results

3.1. Enrichment of sexual tissue and specialized Hülle cells

3.1.1. Hülle cells can be enriched from solid agar plates for comparative proteomics

Aspergillus nidulans develops closed sexual fruiting bodies during its sexual life cycle. So-called cleistothecia contain thousands of asci and are surrounded by several layers of thick-walled Hülle cells. It is assumed that Hülle cells have a protective capacity and therefore they could function e.g. in secondary metabolite formation (Alves et al., 2016, Sarikaya-Bayram et al., 2010). In order to identify and compare proteins from enriched Hülle cells from solid agar plates as well as from submerged liquid cultures, a proteome study was performed. To separate Hülle cells from cleistothecia grown on surface cultures, the cleistothecia-rolling technique was performed (Figure 22).

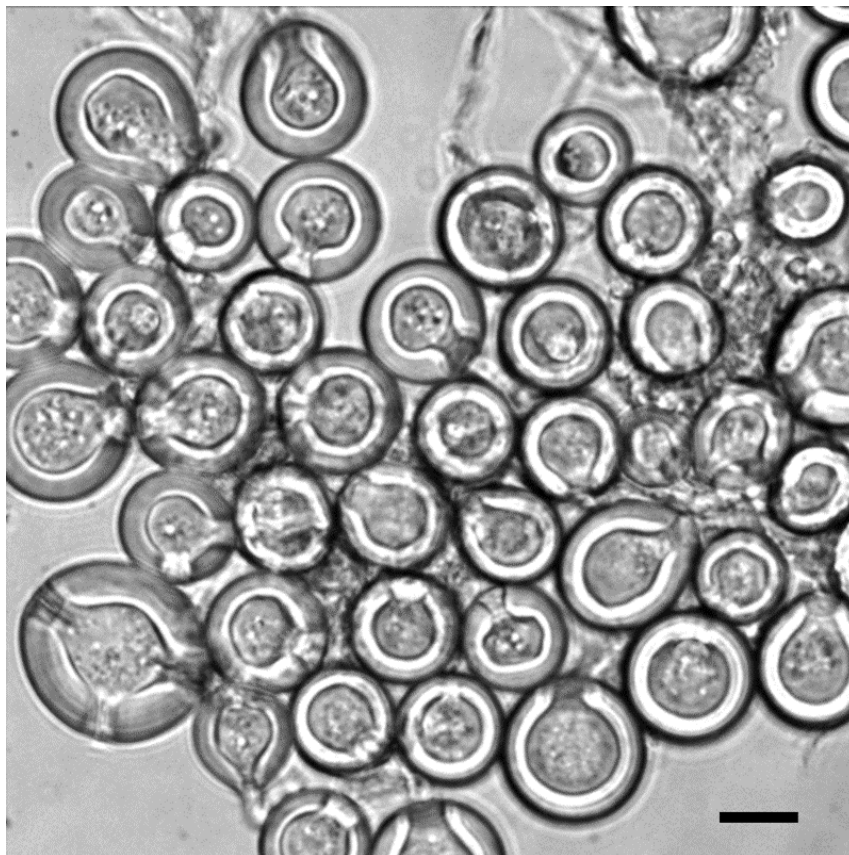


Figure 22. Enrichment of Hülle cells of cultures from solid agar plates

The cleistothecia-rolling technique was used for enrichment of Hülle cells from a single cleistothecium. Enriched surface Hülle cells from sexual mycelium using the cleistothecia-rolling technique are shown. Scale bar is 10 μm .

Hülle cells from sexual mycelium grown on solid agar plates were separated and harvested. Cleistothecia of sexual mycelium were transferred with a fine tipped syringe to a fresh solid agar plate. The cleistothecium was then rolled on the solid agar plate with a fine tipped syringe and the Hülle cells adhered to the surface of the solid agar plate. Hülle cells were collected with a fine tipped syringe and transferred into a collection tube.

3.1.2. Hülle cells can be enriched from submerged liquid cultures for comparative proteomics

In order to compare the proteome of enriched surface Hülle cells to Hülle cells grown in liquid cultures a second proteomic approach was performed. The proteomic approach from Hülle cells grown in liquid media will be discussed within the next chapter.

Hülle cells have been observed in submerged liquid cultures in different strains (Alkahyyat et al., 2015, Bayram et al., 2009, Bayram et al., 2008a, Vienken et al., 2005, Kim et al., 2002, Han et al., 2001). Vegetative mycelia under submerged liquid conditions usually form no cleistothecia and Hülle cells are, therefore, more randomly distributed throughout the mycelia ball (Bayram et al., 2009, Bayram et al., 2008a). In order to perform a quantitative proteome experiment a lysine auxotroph *lysA*Δ; *nkuA*Δ (AGB1092) strain was compared to a lysine auxotroph *laeA*Δ; *lysA*Δ; *nkuA*Δ (AGB1074) strain that causes significant reduction in formation of Hülle cells (Sarıkaya-Bayram et al., 2010). Hülle cells were observed in the lysine auxotroph and in the lysine prototroph parental *nkuA*Δ (AGB552) strain after 72 hours in submerged liquid cultures. The strain AGB552 (*pabaA1;yA;nkuA*Δ::*argB*) contains a *nkuA*Δ mutation with an additional unknown mutation which results in Hülle cell formation in submerged liquid cultures. Deletion of gene *nkuA* in *A. nidulans* leads to an improvement in gene targeting (Nayak et al., 2006). These cultures represent a version of enriched Hülle cells from submerged liquid conditions and were compared to Hülle cells enriched from solid agar plates. In the first two chapters, the results of both proteomic approaches are shown. First of all, the proteome of surface Hülle cells are compared to different mycelia types grown on surface agar plates. The proteome of surface Hülle cells is then compared to the proteome of Hülle cells grown in liquid

media. This finding emphasizes that Hülle cells can be enriched in a vegetative mycelium grown for 72 hours in submerged liquid media.

3.2. Enzymes encoded by the monodictyphenone (*mdp*) / xanthone (*xpt*) secondary metabolite gene clusters are increased during sexual differentiation: proteome comparison of *Aspergillus nidulans* development grown on surfaces

3.2.1. Enrichment of surface Hülle cells enabled to perform a comparative proteome analysis

In the first analysis (proteome experiment 1), proteome of *A. nidulans* wild-type FGSC A4, *veA*⁺ was analyzed to determine differentially expressed proteins in Hülle cells compared to other developmental stages. Vegetative mycelium without Hülle cells was compared to a sexual mycelium with Hülle cells and an asexual mycelium. Proteomes of Hülle cells, sexual and asexual mycelium were analyzed at three different time points, namely three, five and seven days after germination. At each developmental stage three biological replicates were considered. In order to analyze the proteome of surface Hülle cells, they were first enriched from sexual mycelium grown on solid agar plates using the cleistothecia-rolling technique. Therefore, a spore solution was directly inoculated on solid agar plates and the fungus was grown in darkness and reduced oxygen conditions to induce sexual development. Proteins from enriched Hülle cells were extracted, digested with trypsin and peptides were analyzed with a Liquid chromatography (LC) coupled to an *Orbitrap Velos Pro*[™] *Hybrid Ion Trap-Orbitrap* mass spectrometer (MS) (Thermo Fisher Scientific). Different mycelia types were used as controls, namely undifferentiated vegetative mycelium without Hülle cells, sexual mycelium with a high amount of Hülle cells and an asexual mycelium with a low amount of Hülle cells. The total proteome of vegetative mycelium from at least three biological replicates grown under submerged conditions for 20 hours was analyzed. Shaking cultures with submerged mycelia represent undifferentiated filaments without Hülle cells at this time point. In order to harvest vegetative mycelia a spore solution was directly inoculated in liquid media. The amount of vegetative mycelium grown for 20 hours in submerged liquid conditions is significantly higher than that of a vegetative mycelium grown on solid agar plates. Therefore, the vegetative

3. Results

mycelium of submerged liquid cultures was used for the analysis. Additionally, the proteome of sexual mycelium from where the Hülle cells were enriched was analyzed. The proteome of asexually grown mycelium was also analyzed as outlined in Figure 23.

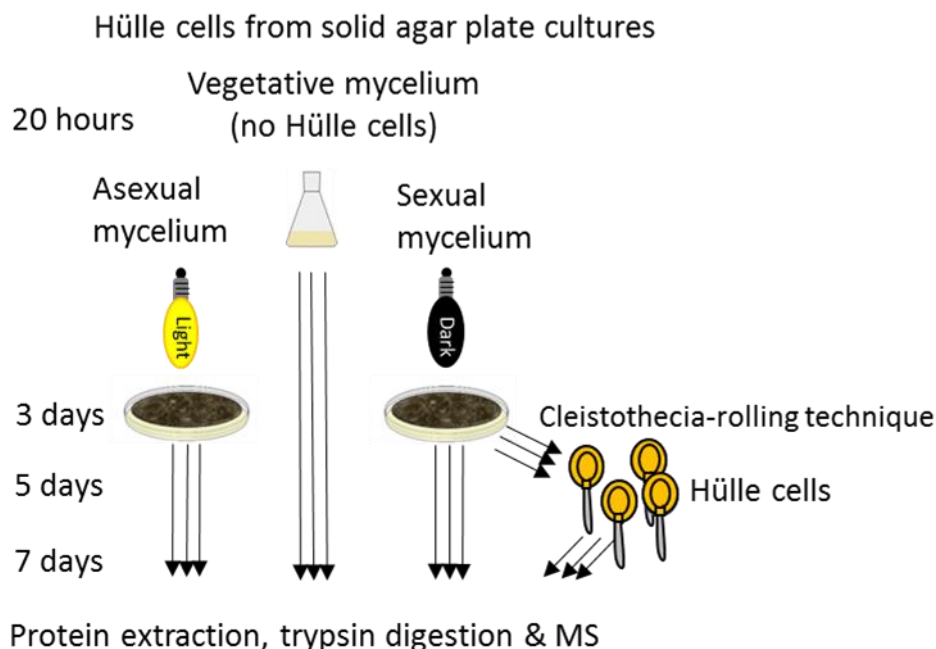


Figure 23. Proteomics workflow for analyzing enriched surface Hülle cells grown on solid agar plates and different types of mycelia.

For the first proteome analysis (**Proteome experiment 1**) *A. nidulans* wild-type (FGSC A4, *veA*⁺) was used. Hülle cells were enriched from sexual mycelium using the cleistothecia-rolling technique and from the same solid agar plates sexual mycelium was harvested (all steps were performed on day 3, 5 and 7 after germination). Sexual mycelium contained high amounts of Hülle cells. Vegetative mycelium was cultivated under submerged conditions and was harvested 20 hours after germination. At this time point no Hülle cells were observable in vegetative mycelium. Asexual mycelium was harvested from solid agar plates on day 3, 5 and 7 after germination. For each time point three biological replicates of Hülle cells as well as the other fungal tissues mentioned above were considered and are highlighted with three arrows.

3.2.2. Comparative proteomics revealed that the proteome of surface Hülle cells overlaps especially to that of sexual mycelium

Analysis of different mycelia types and Hülle cells at all three time points revealed a total number of 1.525 identified proteins (Figure 24). Detailed evaluation of all LC-MS data by using the MaxQuant, Perseus and Proteome discoverer is described in Materials and Methods. Only proteins identified in two or more biological replicates and with two or more peptides per protein were considered for analysis. In this study 401 proteins were identified from surface Hülle cells enriched from solid agar plates and they are highlighted in the red rectangle (Figure 24); (Supplementary Table 3).

3. Results

Additionally, the list of identified proteins in sexual, asexual and vegetative mycelium is listed in Supplementary Table 4.

In this study, six proteins were identified in enriched Hülle cells that were unidentified in other fungal tissues (Table 6). Proteins that were common in Hülle cells and different mycelia types were validated. 253 proteins were common in all different cell types. 24 proteins were present in sexual mycelium with high amounts of Hülle cells and overlapped to an enriched Hülle cell fraction from sexual mycelium. The list of proteins identified in surface Hülle cells and sexual mycelium is shown in Table 7. Proteins which are found in sexual mycelium and Hülle cells are potentially crucial during sexual development. The localization of several proteins found in Hülle cells and sexual mycelium, therefore, were studied in detail and functional gene studies were performed. Findings imply that identified proteins of Hülle cells overlap to other fungal tissues, especially to that of sexual mycelium.

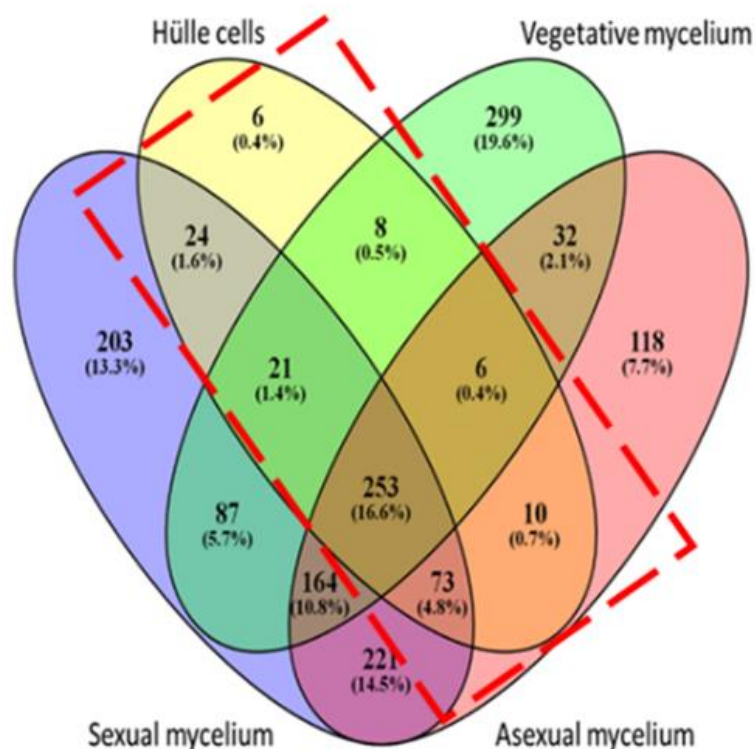


Figure 24. Comparative analysis of identified proteins from surface cultures.

A. nidulans wild-type (FGSC A4, *veA*⁺) was used for the analysis. The figure shows a Venn diagram of identified proteins of enriched surface Hülle cells, sexual mycelium, asexual mycelium and vegetative mycelium. Vegetative mycelium was grown in submerged liquid cultures and enabled to obtain the sufficient amount of mycelia for the analysis. The Venn diagram contains the 1525 proteins that were identified within the different mycelia types and surface Hülle cells from the first proteomic approach. Proteins that could be identified in two or more biological replicates and with two or more peptides per proteins were used for the analysis. The red rectangle represents the 401 proteins found in surface Hülle cells after 3, 5 and 7 days of inoculation.

3.2.3. Comparative proteomics reveal six proteins found in enriched Hülle cells from solid agar plates

Comparing the proteome of surface Hülle cells enriched from solid agar plates to the proteome of different mycelia types mentioned above revealed in this study six proteins which were identified only in surface Hülle cells enriched from solid agar plates. The specific proteins and their putative function are listed in Table 6. Two transmembrane proteins (AN2601 and AN9392) predicted to belong to the major facilitator superfamily (MSF) were identified in surface Hülle cells three, five and seven days after inoculation. A putative peptidase (AN3407) with a predicted serine-type peptidase activity was also found after five and seven days in Hülle cells. The HexA (AN4695) putative woronin body protein was also identified at the same time points. Hülle cells and the subtending hyphae are connected via two distinct types of septa. The inner one is a single perforate septum where woronin bodies often can be observed (Ellis et al., 1973). Woronin bodies were also found to be associated with septal pores of vegetative hyphae (Beck and Ebel 2013). The HexA protein was identified in one biological replicate from a vegetative mycelium and sexual mycelium. Only proteins identified in two or more biological replicates were considered for the analysis. Therefore, the HexA protein was filtered out from vegetative and sexual mycelium. In this study, a protein with an ankyrin repeat containing domain protein (AN8434) and a putative tyrosinase protein (AN8435) was observed in surface Hülle cells after five and seven days.

The biological function of the transporter protein (AN2601) was only identified in Hülle cells from solid agar plate cultures. It was studied in more detail because transporters are considered to be crucial to transport nutrition and other molecules across Hülle cells and thereby, most probably, supporting the cleistothecia (Wei et al., 2004, Pantazopoulou et al., 2007). Additionally, the cellular localization of the ankyrin repeat containing domain protein (AN8434) and the putative tyrosinase protein (AN8435) identified in Hülle cells from surface and liquid media were studied in detail as these two proteins were uniquely found in Hülle cells. This finding shows that surface Hülle cells comprise only few proteins that were not overlapping to other fungal tissues.

3. Results

Table 6. Comparative proteomics revealed six proteins that were identified in the enriched Hülle cells.

Only proteins identified in two or more biological replicates and with two or more peptides per protein were considered for the analysis. Numbers in brackets represent the average of spectral counts from three biological replicates. The yellow colour represents the six proteins found in the Venn diagram (Figure 24). The entire list of proteins identified from solid agar plate cultures is presented in Supplementary table 3.

Gene ID	Description	Found in 3 days Hülle cells	Found in 5 days Hülle cells	Found in 7 days Hülle cells	Orthologs	Phenotypes and localization in Hülle cells. Literature is cited.
Transporter						
AN2601 (MphA)	Major facilitator superfamily		X (8)	X (8)	<i>Saccharomyces cerevisiae</i> MaL31 maltose permease <i>Aspergillus fumigatus</i> putative MFS maltose transporter Afu4g00150	Knockout effects cleistothecia maturation, growth and development in <i>Aspergillus nidulans</i> . Phenotypes in other fungal species are unknown
AN9392	Major facilitator superfamily	X (7)	X (4)		<i>Saccharomyces cerevisiae</i> TnA1 nicotinic acid permease	No literature available
Cellular process						
AN3407	Protein with a predicted serine-type peptidase domain		X (25)	X (29)	<i>Neurospora crassa</i> NCU05016 predicted serine-type endopeptidase activity	No literature available
AN4695* (HexA)	Woronin body protein		X (8)	X (7)	<i>Aspergillus fumigatus</i> woronin body major protein	Ellis et al., 1973. In Hülle cells one can find woronin bodies
AN8434 (AnkG)	Ankyrin repeat domain protein		X (4)	X (4)	<i>Neurospora crassa</i> NCU5316 ankyrin-like protein	Ankyrin repeat domain protein (AN8434) is localized to the subtending hyphae of Hülle cells
AN8435	Tyrosinase domain protein		X (2)	X (3)	<i>Aspergillus oryzae</i> MelB tyrosinase associated with melanization	AN8435 is localized in Hülle cells and most probably in an unstable form

*The HexA protein was identified in one biological replicate from a vegetative mycelium and sexual mycelium.

3.2.4. Surface Hülle cells contain increased enzyme levels for the mobilization of complex sugar molecules

Whithin the next two sections 24 proteins common between Hülle cells and sexual mycelium are discussed. Six of these proteins are enzymes involved in carbohydrate metabolism (Table 7). Glucanase MutA (AN7349) was found in Hülle cells and sexual mycelium at all three time points. This protein is known to be strongly expressed in Hülle cells (Wei et al., 2001). Additionally, another glucanase AgnB (AN3790) was identified. It is thought that additional enzymes for the mobilization of different carbon sources are available during sexual development and are found in Hülle cells (Wei et al., 2001). Putative glucoamylase GlaA (AN11143) and the glucosidase AgdC (AN0941) with a predicted role in the starch and maltose metabolism were identified. This result shows that Hülle cells contain various glucanases that are involved in the mobilization of carbohydrates. Hülle cells are most probably involved in the mobilization of carbohydrates and therefore, enzymes are needed in this process.

3.2.5. Enzymes encoded by the monodictyphenone (*mdp*) / xanthone (*xpt*) gene clusters were found in Hülle cells and sexual mycelium from solid agar plates

Six enzymes out of the 24 proteins shown in Table 7 found in sexual mycelium and enriched Hülle cells are encoded by the monodictyphenone (*mdp*) as well as the xanthone (*xpt*) gene cluster (MdpL (AN10023), AN7999 (a putative oxidoreductase), XptC (AN7998), XptB (AN12402), MdpH (AN10022), MdpG (AN0150)). In a previous work it could be demonstrated that the transcripts of 10 genes within the *mdp* and *xpt* gene clusters are specifically expressed during sexual development (Bayram et al., 2016). Five enzymes encoded by the *mdp* and the *xpt* gene clusters were found again in the second approach in vegetative mycelium from submerged liquid conditions where Hülle cell formation occurred (MdpL (AN10023), XptB (AN12402), MdpG (AN0150), XptC (AN7998) and AN7999 (a putative oxidoreductase). The results of the identified proteins in submerged liquid cultures will be presented in the next chapter. This finding shows that enzymes encoded by the *mdp/xpt* gene clusters are present in Hülle cells grown on surface and liquid cultures as well as in sexual mycelium.

3. Results

Table 7. 24 proteins that were common between sexual mycelia and Hülle cells and were identified from solid agar plate cultures.

Only proteins identified in two or more biological replicates and with two or more peptides per protein were considered for the analysis. Numbers in brackets represent the average of spectral counts from three biological replicates. The grey colour represents the 24 proteins found in the Venn diagram (Figure 24). The entire list of proteins identified from solid agar plate cultures is presented in Supplementary table 3.

Gene ID	Description	3 days sex. mycelium and Hülle cells	5 days sex. mycelium and Hülle cells	7 days sex. mycelium and Hülle cells	Reference
Carbohydrate metabolism					
AN7349 (MutA)	Alpha-1,3-glucanase, specifically expressed in Hülle cells	X (3)	X (43)	X (28)	Wei et al., 2001
AN0941 (AgdE)	Alpha-glucosidase activity, predicted role in maltose metabolism	X (6)	X (32)	X (24)	Yuan et al., 2008
AN3790 (AgnB)	Putative alpha-1,3-glucanase		X (18)	X (17)	He et al., 2017
AN9443	Predicted catalytic activity and role in carbohydrate metabolic process			X (11)	Flipphi et al., 2009
AN7345 (AgdC)	Glucosidase activity, involved in degradation of glucans	X (6)	X (32)	X (24)	Yuan et al., 2008
AN11143 (GlaA)	Putative glucoamylase		X (4)		Nekiunaite et al., 2016
Secondary metabolism					
AN11049	NmrA-like; predicted secondary metabolism gene cluster member		X (35)	X (49)	Andersen et al., 2013
AN10023 (MdpL)	Member of the monodictyphenone (<i>mdp</i>) / xanthone (<i>xpt</i>) gene clusters	X (25)		X (42)	Bayram et al., 2016
AN7999	Oxidoreductase, member of the monodictyphenone (<i>mdp</i>) / xanthone (<i>xpt</i>) gene clusters		X (8)	X (47)	Bayram et al., 2016
AN7998 (XptC)	GMC oxidoreductase, member of the monodictyphenone (<i>mdp</i>) / xanthone (<i>xpt</i>) gene clusters	X (7)	X (6)		Sanchez et al., 2011
AN12402 (XptB)	Prenyltransferase, member of the monodictyphenone (<i>mdp</i>) / xanthone (<i>xpt</i>) gene clusters	X (5)		X (8)	Sanchez et al., 2011
AN10022	Member of the monodictyphenone (<i>mdp</i>) / xanthone (<i>xpt</i>) gene clusters		X (5)	X (6)	Bayram et al., 2016
AN0150 (MdpG)	Polyketide synthase, member of the monodictyphenone (<i>mdp</i>) / xanthone (<i>xpt</i>) gene clusters	X (4)	X (3)		Sanchez et al., 2011
AN7812 (StcN)	Putative versicolorin B synthase	X (3)	X (4)		Bok et al., 2009
Oxidase					
AN7641	Putative copper amine oxidase	X (22)	X (31)		Lenobel et al., 2005
AN6314	Oxidoreductase	X (5)	X (27)	X (48)	Not available
AN8203	NAD+ synthase (glutamine-hydrolyzing) activity		X (5)		Not available
AN1142	Oxidoreductase		X (4)		Not available
Cellular process					
AN11897	Ribonuclease		X (6)		Not available
AN5669	Putative succinyl-CoA:3-ketoacid-coenzyme A transferase	X (8)		X (2)	Salazar et al., 2009
AN10977	Ortholog(s) have extracellular region localization		X (6)		Not available
AN6930	Predicted transaminase activity		X (9)		Not available
Unknown					
AN5488	Protein of unknown function	X (2)	X (20)		Not available
AN1863	Protein of unknown function	X (2)		X (4)	Not available

3.2.6. Proteins encoded by the xanthone (*xpt*) gene cluster are enriched in the cytoplasm of Hülle cells

Hülle cells might produce specific secondary metabolites to protect the cleistothecia from fungivores. It is known that xanthonones are secondary metabolites with antimicrobial activities (Chen et al., 2017, Noordin et al., 2016). To gain more insight into the production of an antimicrobial agent in Hülle cells the localization of enzymes encoded by the xanthone (*xpt*) secondary metabolite gene cluster was further investigated. Monodictyphenone represents a precursor for the production of xanthonones. As an example of the 24 proteins that were common between Hülle cells and sexual mycelia the prenyltransferase XptB and the oxidoreductase XptC were found and their localization was investigated (Figure 25). The second prenyltransferase XptA was only found in a sexual mycelium and is listed in Supplementary table 4. The criteria concerning the localization investigation were the presence of the protein in both sexual mycelium and Hülle cells in the proteomics approach. Therefore, the localization of XptA is not shown.

The prenyltransferase XptB and the oxidoreductase XptC are involved in the conversion of monodictyphenone into xanthonones, which are antimicrobial agents. Localization of the prenyltransferase XptB and the oxidoreductase XptC involved in the conversion of monodictyphenone into xanthonones in Hülle cells was investigated and their presence could be confirmed (Figure 25). Hülle cells were enriched from sexual mycelium using the cleistothecia-rolling technique and the localization of XptB::GFP, XptC::GFP was observable in the cytoplasm of Hülle cells. The fusion proteins were mainly observed in the center of Hülle cells. XptB::GFP and XptC::GFP seem to be mainly equally distributed in the cytoplasm of Hülle cells. XptB::GFP and XptC::GFP was not clearly observable in the membrane. This suggests that proteins identified by the applied enrichment of Hülle cells correlate between the proteomic approach and the microscopic data in their fungal localization.

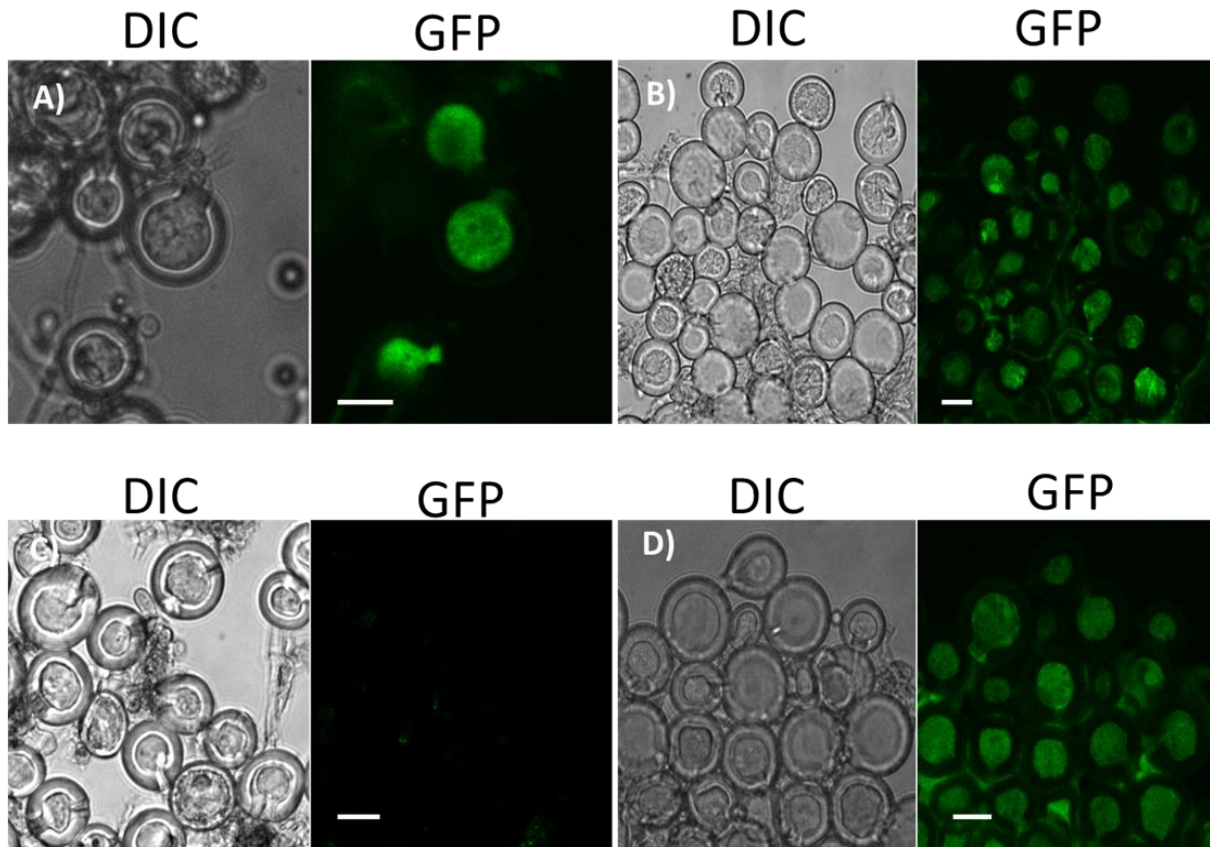


Figure 25. Enzymes encoded by the xanthone (*xpt*) gene cluster are localized in Hülle cells. XptB::GFP and XptC::GFP are observable in the cytoplasm of Hülle cells. Fluorescence microscopy of Hülle cells: A) *xptB::gfp;lysAΔ;nkuAΔ* (AGB1086) B) *xptC::gfp; nkuAΔ* (AGB1088) C) *nkuAΔ* (AGB552) parental strain D) A strain expressing GFP constitutively (AGB596). Scale bar is 10 μ m.

Additionally, the localization of XptB and XptC was apparent during initial vegetative growth. Therefore, vegetative hyphae in submerged liquid cultures were used to visualize the presence of the fusion proteins. The localization of the fusion proteins XptB::GFP and XptC::GFP could be confirmed mainly in the cytoplasm of vegetative hyphae (Figure 26). This suggests that proteins encoded by the xanthone (*xpt*) gene cluster are found not only in Hülle cells but also in vegetative hyphae suggesting that these proteins are found during initial vegetative growth.

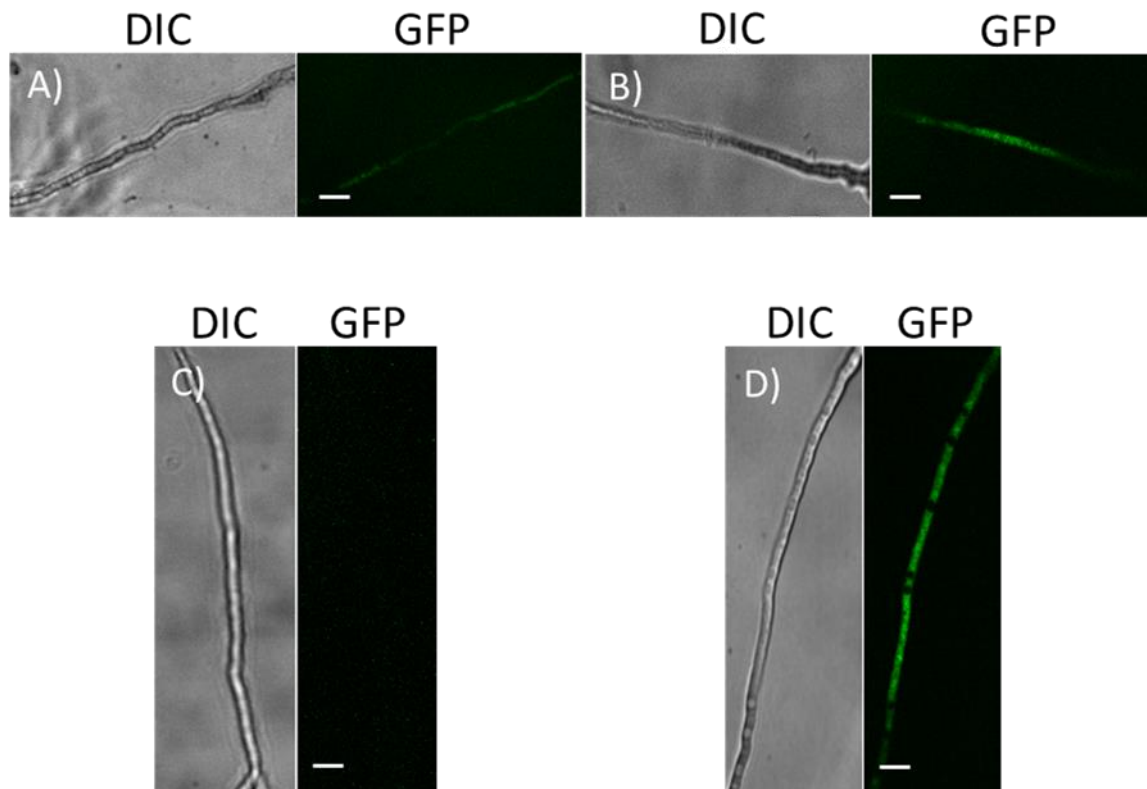


Figure 26. Enzymes encoded by the xanthone (*xpt*) gene cluster are localized in vegetative mycelium.

XptB::GFP and XptC::GFP are localized in the cytoplasm of vegetative hyphae. Fluorescence microscopy of vegetative mycelium: A) *xptB::gfp;lysAΔ;nkuAΔ* B) *xptC::gfp;nkuAΔ*. C) *nkuAΔ* E) A strain expressing GFP constitutively (AGB596). Scale bare is 20 μm

The protein sequence of green fluorescent protein (GFP) consists of 239 amino acids with a predicted molecular mass of 26.9 kDa. The XptB protein consists of 463 amino acids with a predicted molecular mass of 52.4 kDa. The XptC protein consists of 622 amino acids with a predicted molecular mass of 67.8 kDa.

Western hybridization experiments showed that XptB::GFP is detectable as expected around 79 kDa and that XptC::GFP is detectable as expected around 95 kDa in three and five day old sexual mycelium with high amounts of Hülle cells plus a three day old vegetative mycelium (Figure 27). A strain expressing GFP constitutively (AGB596) served as a positive control where GFP was detectable around 27 kDa. The parental *nkuAΔ* (ABG552) strain served as negative control where GFP was not observable. A proteolytic cleavage product of XptB::GFP was detectable around 27 kDa. This is most likely a degradation product of the full-length XptB::GFP fusion protein and represents the degraded GFP product. This result implies that the prenytransferase XptB and the oxidoreductase XptC is found in the cytoplasm of Hülle cells and that these proteins are present in vegetative and sexual mycelia.

3. Results

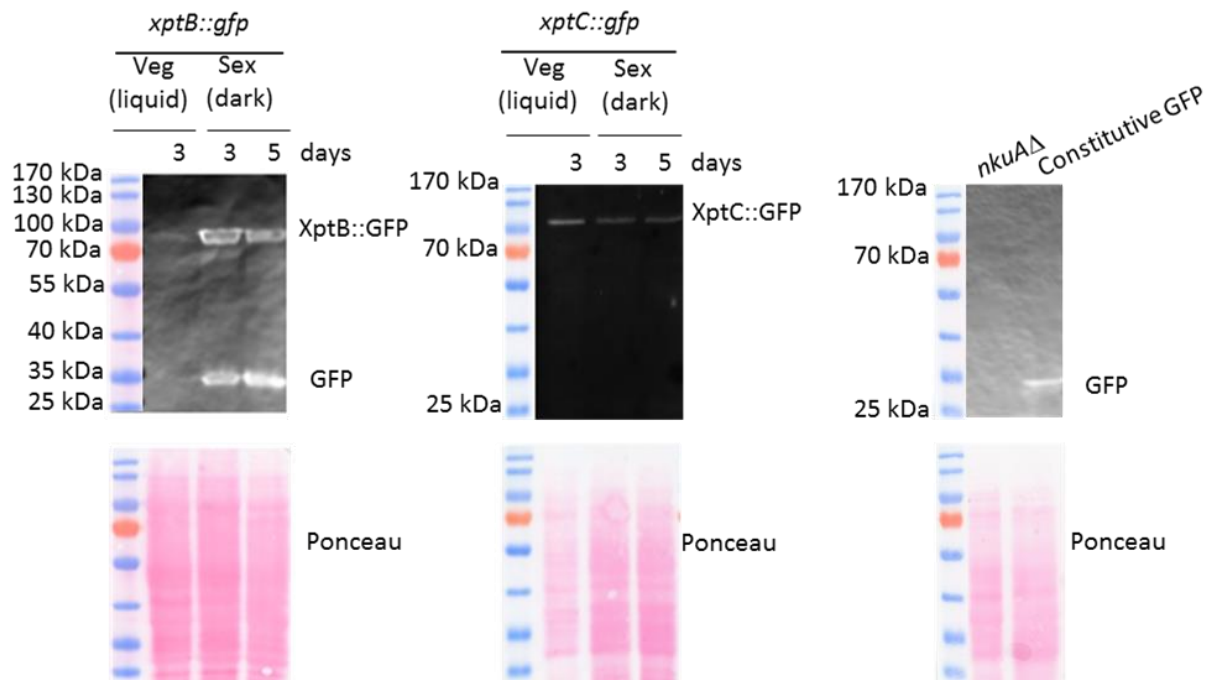


Figure 27. The fusion proteins XptB::GFP and XptC::GFP are found in sexual mycelium with high amounts of Hülle cells and a vegetative mycelium.

Western hybridization of vegetative and sexual mycelium of *xptB::gfp; lysAΔ; nkuAΔ* (AGB1086) and *xptC::gfp; nkuAΔ* (AGB1088). Vegetative mycelium was harvested after 3 days. Sexual mycelium with high amounts of Hülle cells was harvested 3 and 5 days after inoculation. The XptB protein consists of 463 amino acids with a predicted molecular mass of 52.4 kDa. The XptC protein contains 622 amino acids with a predicted molecular mass of 67.8 kDa. In order to detect XptB::GFP (*xptB::gfp; lysAΔ; nkuAΔ*, AGB1086) and XptC::GFP (*xptC::gfp; nkuAΔ*, AGB1088) a primary α -GFP antibody (sc-9996; Santa Cruz) was used followed with an incubation of an α -mouse secondary antibody (G21234, Invitrogen). The fusion protein XptB::GFP was detected as expected around 79 kDa and XptC::GFP was detected as expected around 95 kDa. A strain expressing GFP constitutively served as a control where GFP was detectable around 27 kDa. Proteolytic cleavage product of XptB::GFP was detectable around 27 kDa. This is most likely a degradation product of the full-length XptB::GFP fusion protein. The parental strain *nkuAΔ* served as a negative control where GFP and the fusion proteins were not detectable.

3.2.7. Comparative proteomics revealed that the proteome of surface Hülle cells overlaps to other fungal tissues besides of a sexual mycelium

As shown in the Venn diagram (Figure 24) the proteome of surface Hülle cells overlapped to other fungal tissues such as asexual and vegetative mycelium besides sexual mycelium. Ten proteins were identified in Hülle cells and asexual mycelium (Table 8). These proteins were unidentified in Hülle cells grown in liquid media. This suggests that these proteins are only present during surface growth. Since these proteins were unidentified in Hülle cells grown in liquid media in the second proteomic

3. Results

approach the focus was not laid on these proteins. Proteins that were common in Hülle cells and vegetative mycelium are listed in Table 8. These proteins were identified in Hülle cells grown in liquid media and are discussed in the context of core proteome of both types of Hülle cells within the next chapter. Data reveal that the proteome of surface Hülle cells overlaps to that of other fungal tissues besides sexual mycelium.

Table 8. Overlapping proteins of Hülle cells (HC), asexual (Asex.) and vegetative mycelium (Veg.). The listed proteins are found in the red rectangle of the Venn diagram of Figure 16. Only proteins identified in two or more biological replicates and with two or more peptides per protein were considered for the analysis. Six proteins are listed and represent the proteins with the highest spectral counts. Numbers in brackets represent the average of spectral counts from three biological replicates. Six proteins out of ten are listed with the highest spectral counts, that were common in Hülle cells and asexual mycelium. The orange colour represents proteins found in Hülle cells and asexual mycelium. Six proteins out of eight are listed with the highest spectral counts, that are common in Hülle cells and vegetative mycelium. The green colour represents the proteins that were found in Hülle cells and vegetative mycelium.

Hülle cells & asexual mycelium					
Gene ID	Function	3 days HC & Asex.	5 days HC & Asex.	7 days HC & Asex.	Reference
AN5324 (DlpA)	Dehydrin-like protein	X (9)	X (9)	X (6)	Wartenberg et al., 2012
AN5004	Induced in light	X (2)	X (30)	X (7)	Ruger-Herreros et al., 2011
AN6856	Up-regulated in <i>atmΔ</i>	X (5)	X (6)		Malavazi et al., 2007
AN5015 (ConJ)	Induced in light	X (2)	X (8)	X (2)	Ruger-Herreros et al., 2011
AN5971	Induced in light	X (7)	X (4)		Ruger-Herreros et al., 2011
AN1362	Cue5 ortholog		X (4)		Not available
Hülle cells & vegetative mycelium					
Gene ID	Function	3 days HC & Veg.	5 days HC & Veg.	7 days HC & Veg.	Reference
AN1182 (BenA)	Beta-tubulin	X (5)	X (4)	X (23)	Oakley et al., 2004
AN4236	Proteasome regulatory particle	X (3)		X (5)	Not available
AN6688 (AspB)	Putative Septin B	X (7)		X (2)	Hernández-Rodríguez et al., 2012
AN2918 (Cct4)	Chaperonin complex component	X (3)		X (3)	Malavazi et al., 2007
AN4159 (GlnA)	Glutamate-ammonia ligase	X (4)			Margelis et al., 2001
AN2149 (Cct1)	Chaperonin	X (2)		X (2)	Malavazi et al. 2006

3.2.8. Functional annotation reveals that surface Hülle cells are highly involved in carbohydrate and amino acid metabolism

In order to perform a gene ontology (GO) annotation based on a multiple NCBI blast search for biological functions of all 401 proteins found in surface Hülle cells the high-quality functional annotation tool Blast2GO was used (Conesa et al., 2005). The largest subsegment of the pie chart with the GO term carbohydrate metabolic process revealed that Hülle cells are highly involved in the carbohydrate metabolism (Figure 28). The presence of enzymes to degrade certain carbohydrates, such as α -1,3-glucanase and other glucanases in Hülle cells most probably represents an additional energy source to support the energy-consuming process of the development of cleistothecia. The second largest subsegment with the GO term amino acid metabolism process together with the GO terms translation plus generation of precursor metabolites and energy highlights that Hülle cells are necessary to promote growth and development. In Hülle cells one can find the laccase type II enzyme CpeA. It is presumed that laccase acts on phenolic compounds in Hülle cells, leading to the generation of reactive oxygen species (ROS), (Scherer et al., 2002). The subsegment with the GO term response to stress reveals that Hülle cells have to deal with reactive oxygen species. The subsegment with the GO term secondary metabolite process shows that Hülle cells are involved in this process. Enzymes encoded by the monodictyphenone (*mdp*) / xanthone (*xpt*) gene clusters were found in the enriched Hülle cell fraction and sexual mycelium. This points out that the proteome of surface Hülle cells comprise high amounts of proteins involved in carbohydrate and amino acid metabolism.

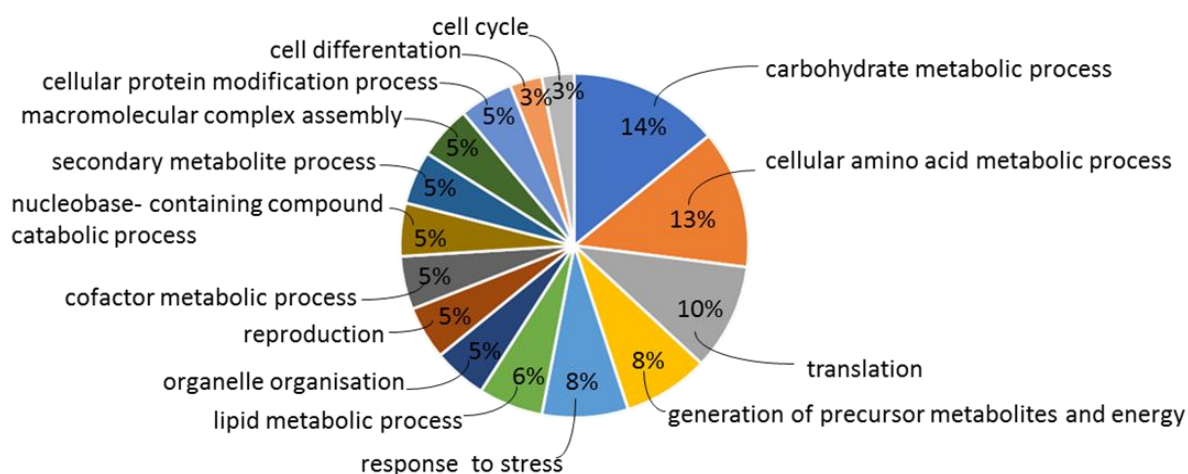


Figure 28. Functional annotation of identified proteins found in surface Hülle cells.

Blast2GO was used to perform the functional annotation of all 401 proteins that were found in surface Hülle cells. The gene ontology (GO) annotations for biological functions and the percentages of all GO terms are shown.

3.3. Hülle cells from surface growth and liquid media differ in their composition by 28% beside a shared core proteome: Proteomes of *Aspergillus nidulans* development grown on surfaces compared to liquid cultures

3.3.1. Hülle cell formation in submerged liquid cultures for comparative proteomics

A second proteomic approach (proteome experiment 2) from submerged cultures was performed to compare proteomes of Hülle cells from liquid cultures versus solid plates (Figure 29). Stable isotope labeling by amino acids in cell culture (SILAC) is a technique for the relative quantification of changes in protein abundances within complex mixtures (Schmitt et al., 2017). It was shown that the LaeA protein promotes Hülle cell formation and therefore the deletion of *laeA* leads to a significant reduction of Hülle cells (Sarıkaya-Bayram et al., 2010).

In order to gain insight into the regulation of proteins involved in secondary metabolism and Hülle cell formation the second proteome approach was performed with a *laeA*Δ strain. In order to identify and quantify proteins in a *laeA*Δ mycelium with high and low amounts of Hülle cells from submerged cultures the gene *laeA* was deleted in a lysine auxotroph strain. The deletion of the gene *lysA* that encodes a putative saccharopine dehydrogenase enabled the efficient incorporation of isotopically labeled lysines into proteins and with that a SILAC study could be performed.

In order to observe Hülle cells in submerged cultures the strains were cultivated for three days in liquid medium and labeled with isotopic lysine variants from the point on where the strains were inoculated. The parental strain *lysA*Δ; *nkuA*Δ (AGB1092) was labeled with light lysine. The knockout strain *lysA*Δ; *laeA*Δ; *nkuA*Δ (AGB1074) was labeled with heavy lysine and the complementation strain *lysA*Δ; *laeA*Δ::*laeA*; *nkuA*Δ (AGB1076) was labeled with medium lysine. For a label swap experiment, the light and the heavy labels were exchanged. This serves as a control that allows to confirm that the isotopically labeled lysines do not influence the analysis.

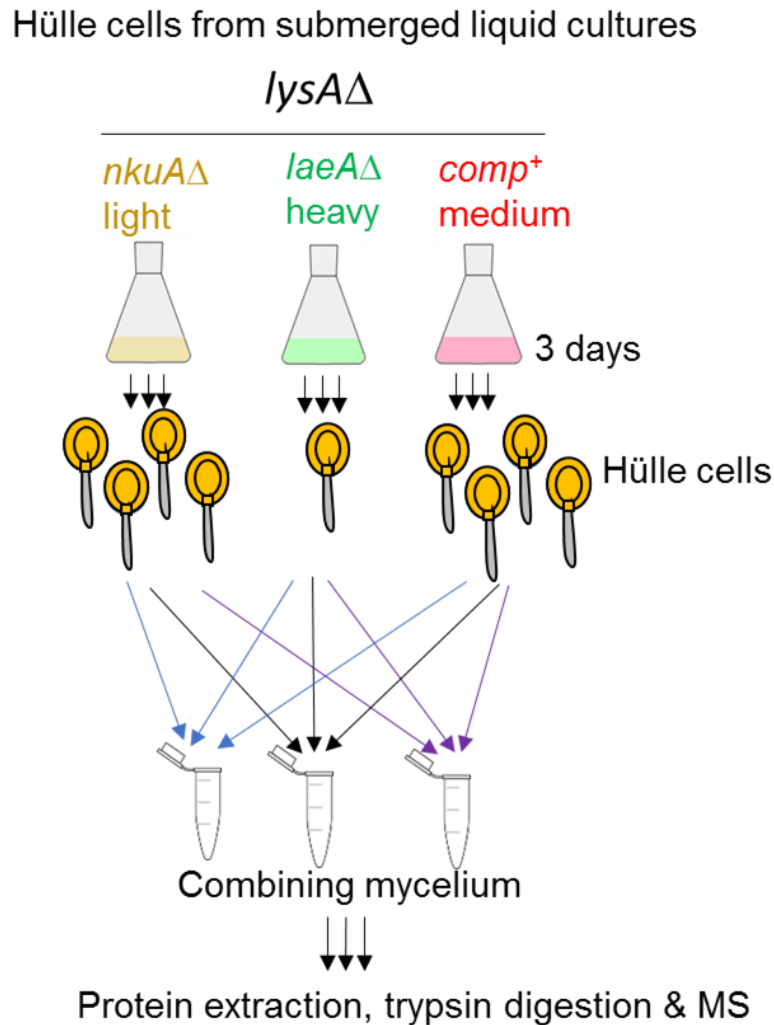


Figure 29. Proteomics workflow for analyzing enriched Hülle cells from submerged cultures.

For the second proteomic approach (**Proteome experiment 2**) three lysine auxotrophic strains were used: *nkuA* Δ (*lysA* Δ ; *nkuA* Δ , AGB1092), *laeA* Δ (*lysA* Δ ; *laeA* Δ ; *nkuA* Δ , AGB1074), *comp*⁺ (*lysA* Δ ; *laeA* Δ ::*laeA*; *nkuA* Δ , AGB1076) were inoculated in liquid medium containing light, heavy and medium labeled lysine. The strains were grown for three days and Hülle cells were observed in the hyphal balls of vegetative mycelium. The amount of 300 mg of each mycelium was pooled together and proteins were extracted and digested into peptides. The experiment was performed with three biological replicates and is highlighted with three arrows in this figure.

After growing the three strains in submerged conditions for three days 300 mg mycelia of each individual labeled strain were pooled together and proteins were extracted and digested as described (Shevchenko et al., 1996). Peptide analytics were done with a liquid chromatography (LC) coupled to an *Orbitrap Velos Pro*[™] *Hybrid Ion Trap-Orbitrap* mass spectrometer (MS). The labeled peptides of the samples allowed accurate quantification of peptide ratios relative to each other. The percentage of observable Hülle cells was determined in the hyphal balls of vegetative mycelium and almost no Hülle cells could be observed in the *laeA* Δ strains in contrast to the parental and the complementation strains (Figure 30).

3. Results

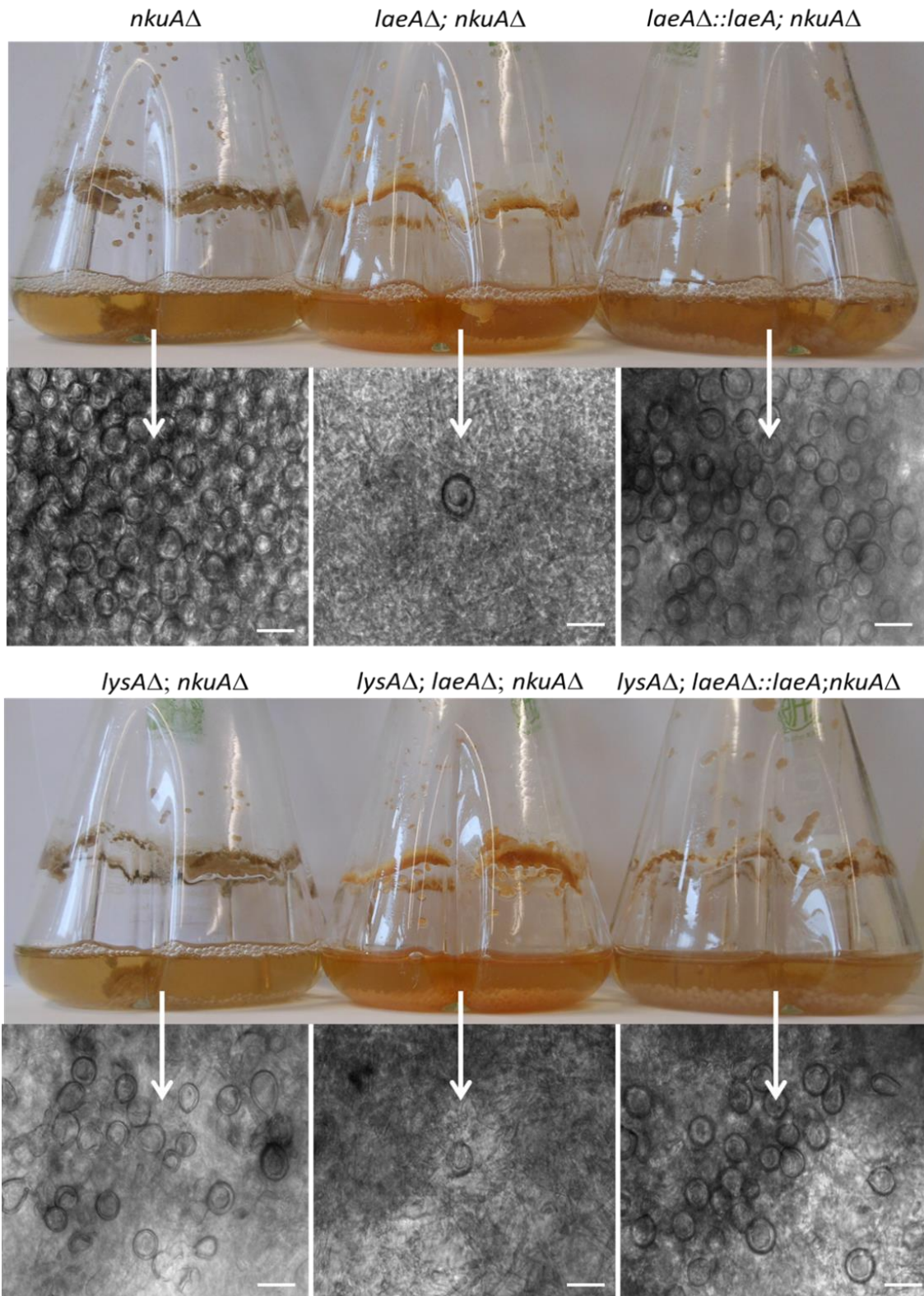


Figure 30. Lysine prototroph and auxotroph *laeAΔ* strains for the quantitative analysis of Hülle cells under submerged liquid conditions.

Hülle cells were observed in submerged cultures on day 3 after inoculation. High amounts of Hülle cells were observed in the lysine prototrophic *nkuAΔ* (AGB552) strain with an additional unknown mutation; as well as in the lysine auxotrophic *lysAΔ; nkuAΔ* (AGB1092) strain. The deletion of the gene *laeA* (AGB1073, AGB1074) in *nkuAΔ* as well as in *lysAΔ; nkuAΔ* strain resulted in a significant reduction in the amount of Hülle cells. The phenotype could be restored in the complementation strains *laeAΔ::laeA; nkuAΔ* (AGB1075) and *lysAΔ; laeAΔ::laeA; nkuAΔ* (AGB1076) where high amounts of Hülle cells were present. Scale bar is 20 μm .

3. Results

The number of observable Hülle cells, determined within an area of 5 mm² in the hyphal ball were counted and their number was put in relation to the parental and the complementation strain with three biological replicates (Figure 31A). Additionally, the dry weight of the submerged cultures was measured (Figure 31B). Vegetative mycelia were first filtered to remove the liquid media, then dried for 12 hours in a drying cabinet (75 °C). The dry weight was weighed and determined for three biological replicates. A prolongation of the drying time had no significant effect on the dry weight. The dry weight did not change in the *laeA*Δ lysine prototroph and auxotroph strain in comparison to the parental and the complementation strain.

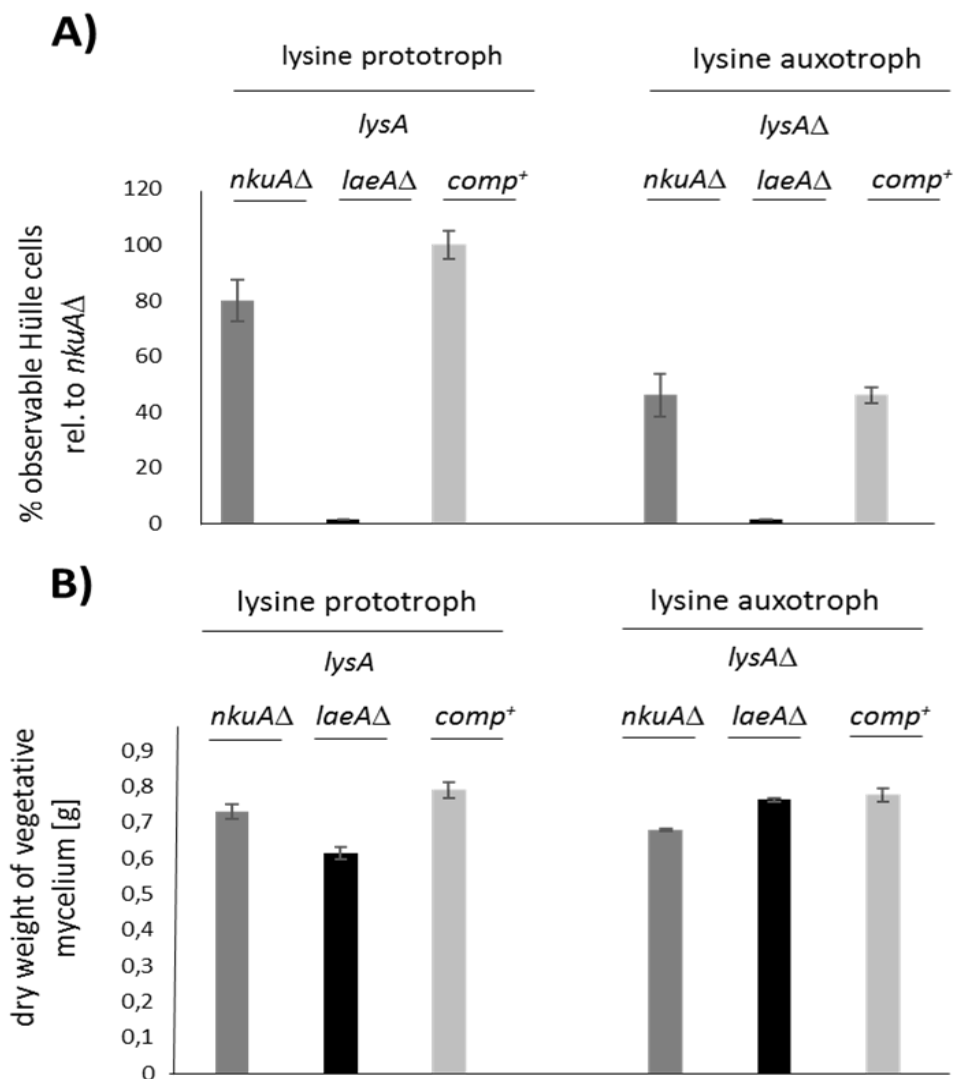


Figure 31. Determination of the number of Hülle cells in vegetative mycelia and determination of the dry weight of the vegetative mycelia.

A) The percentage of Hülle cells in the hyphal balls of vegetative mycelium of all strains were determined. The number of observable Hülle cells, determined within an area of 5 mm² in the hyphal ball were counted and their number was put in relation to the parental and the complementation strain with three biological replicates. B) The dry weight of all strains was measured. Vegetative mycelia were dried for 12 hours in a drying cabinet (75 °C). The dry weight was weighed and determined. Three biological replicates were considered.

3.3.1.1. Submerged liquid cultures revealed the proteome for comparative analysis

The proteome analysis of Hülle cells grown in submerged liquid cultures revealed a total number of 974 identified proteins (Supplementary Table 5). Three biological replicates were considered for the analysis. Only proteins identified in two or more biological replicates and with two or more peptides per protein were considered for the analysis. Comparing the proteomes of Hülle cells from solid agar plates versus submerged liquid cultures revealed a common core proteome consisting of 286 proteins that represents 72% of overlapping identified proteins. Therefore, the proteome of Hülle cells from surface growth and liquid media differ in their composition by 28% that corresponds to 115 identified proteins. Two proteins identified in the proteome of a vegetative mycelium in submerged conditions were chosen for further investigation regarding their localization. Prenyltransferase NptA (AN11080) and the serine/threonine kinase RfeA (AN2943) could be identified and quantified in the SILAC approach. These two proteins involved in the process of secondary metabolism showed a significant reduction in quantity in a *laeA* Δ strain compared to the parental strain. A substantial reduction of Hülle cells in a *laeA* Δ strain could correlate with the absence of these two proteins. NptA and RfeA, therefore, were investigated regarding the localization of these two proteins to gain more insight into the secondary metabolism in Hülle cells. 72% as a result shows a high overlapping of proteins in the core proteome of Hülle cells grown in solid agar plates and liquid media.

3.3.2. Quantification of proteins in submerged liquid cultures of a *laeA* Δ mycelium revealed two Hülle cells proteins

Protein quantities of the prenyltransferase NptA (AN11080) and the serine/threonine kinase RfeA (AN2943) were reduced in *laeA* Δ (AGB1074) mycelium. These two proteins are involved in the process of secondary metabolism (De Souza et al., 2013, Oakley et al., 2017). It is known that LaeA is a key regulator of secondary metabolism and Hülle cell formation in *A. nidulans* (Bok and Keller 2004, Sarikaya-Bayram et al., 2010).

3. Results

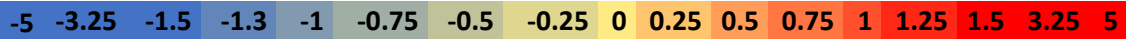
SILAC, stands for **stable isotope labeling of amino acids in cell cultures** and was applied as a technique for the relative quantification of changes in protein abundance within complex mixtures. The \log_2 SILAC ratio was determined for the strains *laeA* Δ (AGB1074) in comparison to *laeA* (AGB1092). The following thresholds were set. In the range of a \log_2 SILAC ratio between -5.0 and -0.5 identified proteins are down-regulated. In the range of a \log_2 SILAC ratio between + 0.5 and +5.0 identified proteins are up-regulated. In the range between a -0.5 and + 0.5 \log_2 SILAC ratio identified proteins were unchanged.

The protein quantity of identified proteins that is significantly down-regulated in a *laeA* Δ vegetative mycelium in submerged liquid cultures is shown in Table 9. Proteins that are down-regulated in *laeA* Δ vegetative mycelium are involved in secondary metabolism (2 proteins, NptA and RfeA), amino acid metabolism (6 proteins). In addition, the quantity of tRNA charging enzymes (16 enzymes), proteins that are required for protein folding (4), nuclear import protein (1), proteins that are involved in the carbohydrate metabolism (4) and proteins which are involved in metabolic processes (8) are reduced. The prenyltransferase NptA (AN11080) showed the most significant reduction in quantity in a *laeA* Δ mycelium (Table 9). Bok and co-workers showed that the prenyltransferase *tidB* is not expressed in a *laeA* Δ mycelium in comparison to the wild-type (Bok et al., 2006). The serine/threonine kinase RfeA (AN2943) is predicted to be involved in the regulation of secondary metabolism (De Souza et al., 2013). This kinase was significantly reduced in a *laeA* Δ mycelium (Table 9). A substantial reduction of Hülle cells in a *laeA* Δ strain could correlate with the reduction of the two proteins NptA and RfeA. These two proteins were further analyzed in more detail to gain insight into the process of secondary metabolism in Hülle cells.

Table 9. Proteins that are down-regulated in a *laeA* Δ mycelium

SILAC is applied as a technique for the relative quantification of changes in protein abundance within complex mixtures. The protein quantity of the following proteins is reduced in a *laeA* Δ vegetative mycelium. These proteins are down-regulated in *laeA* Δ mycelium. The \log_2 SILAC ratio was determined for the strains *laeA* Δ (AGB1074) in comparison to *laeA* (AGB1092). The following thresholds were set. In the range of a \log_2 SILAC ratio between -5.0 and -0.5 identified proteins are down-regulated. In the range between a -0.5 and + 0.5 \log_2 SILAC ratio identified proteins are unchanged. The \log_2 SILAC ratio for the complementation strain (*laeAcomp*⁺, AGB1076) in comparison to the parental *laeA* strain (AGB1092) is between -0.5 and + 0.5. The color scales represent \log_2 SILAC ratios. \emptyset = median of \log_2 SILAC ratio, SD = standard deviation, NaN = not a number. Biological replicates are numbered 1-3.

3. Results



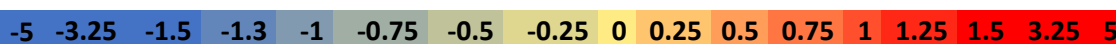
Gene ID	Description	Spectral counts			laeAΔ/laeA			∅	SD	laeAcomp+/laeA			∅	SD
		1	2	3	1	2	3			1	2	3		
Secondary metabolism														
AN11080 (NptA)	Prenyltransferase	122	79	47	-4.9	-3.9	-4.2	-4.2	0.5	-0.2	-0.5	0.4	-0.2	0.5
AN2943 (RfeA)	Kinase	19	33	63	-2.0	-1.3	-0.6	-1.3	0.7	-0.5	-0.2	-0.5	-0.5	0.2
Amino acid metabolism														
AN5591	Aminotransferase	21	63	NaN	-3.6	-3.9	NaN	-3.8	0.2	0.5	-0.1	NaN	0.2	0.3
AN2901 (AgaA)	Arginase	28	99	173	-3.0	-1.9	-2.3	-2.5	0.6	-0.5	0.2	-0.6	-0.5	0.4
AN4159 (GlnA)	Glutamate-ammonia ligase	367	384	481	-3.1	-1.0	-0.5	-2.1	1.4	-0.4	-0.2	0.5	-0.2	0.5
AN5886 (LuA)	Isomerase	46	60	218	-1.9	-1.0	-1.7	-1.5	0.5	0.0	0.0	NaN	0.0	0.0
AN0797	Role in histidine metabolism	20	41	71	-1.7	-1.1	-0.7	-1.4	0.5	0.0	-0.4	-0.1	-0.1	0.2
AN4218	Translation elongation factor	384	845	1035	-1.4	-0.6	-1.5	-1.0	0.5	0.2	0.1	-0.1	0.1	0.1
tRNA charging enzyme														
AN0046	Histidyl-tRNA ligase	46	66	100	-3.6	-1.8	-0.8	-1.8	1.4	-0.4	-0.4	0.0	-0.4	0.3
AN0705	Isoleucine-tRNA ligase	57	113	NaN	-2.2	-1.2	NaN	-1.7	0.7	-0.5	-0.1	NaN	-0.3	0.3
AN11125	Glycine-tRNA ligase	117	159	NaN	-2.1	-0.9	NaN	-1.5	0.8	-0.5	-0.3	NaN	-0.4	0.3
AN0057	Tyrosine-tRNA ligase	33	68	33	-1.9	-0.9	-1.3	-1.3	0.5	-0.5	-0.3	NaN	-0.4	0.3
AN10475	Tryptophan-tRNA ligase	36	40	NaN	-2.0	-0.7	NaN	-1.3	0.9	-0.4	-0.1	NaN	-0.3	0.2
AN10474	Tryptophan-tRNA ligase	97	113	178	-1.9	-0.7	-1.3	-1.3	0.6	-0.4	-0.3	0.4	-0.3	0.4
AN6368	tRNA charging enzyme	52	117	125	-2.0	-1.1	-0.7	-1.1	0.6	-0.4	-0.1	0.0	-0.1	0.2
AN8224	Glutamate-tRNA ligase	60	101	171	-2.0	-1.0	-1.0	-1.0	0.6	-0.5	-0.3	0.3	-0.3	0.4
AN3824	Phenylalanine-tRNA ligase	30	52	103	-2.0	-1.0	-0.9	-1.0	0.6	-0.4	-0.4	0.3	-0.4	0.4
AN8867	Serine-tRNA ligase	83	104	147	-1.2	-1.0	-1.0	-1.0	0.1	0.5	0.1	0.0	0.1	0.3
AN3702	Leucine-tRNA ligase	73	115	213	-2.3	-0.8	-0.9	-0.9	0.8	-0.4	-0.2	0.2	-0.2	0.3
AN4086	Phenylalanine-tRNA ligase	40	67	93	-2.0	-0.7	-0.9	-0.9	0.7	-0.4	-0.2	0.3	-0.2	0.4
AN9419	Alanine-tRNA ligase	149	200	374	-2.0	-0.8	-0.9	-0.9	0.7	-0.3	0.1	0.0	0.0	0.2
AN2150	Proline-tRNA ligase	149	225	329	-1.8	-0.7	-0.9	-0.9	0.6	-0.4	-0.1	0.3	-0.1	0.3
AN1380	Methionine-tRNA ligase	60	114	148	-1.8	-0.8	-0.7	-0.8	0.6	-0.3	-0.3	0.2	-0.3	0.3
AN10195	Valine-tRNA ligase	119	109	280	-1.9	-0.7	-0.6	-0.7	0.7	-0.5	-0.1	0.5	-0.1	0.5
Protein folding														
AN10202 (HscA)	Heat shock protein	89	285	NaN	-1.8	-0.7	-1.8	-1.8	0.7	-0.3	0.0	NaN	-0.2	0.2
AN1047	Heat shock protein	136	186	NaN	-1.7	-0.7	-2.1	-1.7	0.7	-0.2	-0.3	NaN	-0.2	0.1
AN2918 (Cct4)	Chaperonin complex	46	48	102	-1.6	-0.7	-1.7	-1.6	0.6	-0.1	-0.2	-0.5	-0.2	0.2
AN2062 (BipA)	Chaperonin complex	177	142	287	-1.9	-1.0	-1.4	-1.4	0.5	0.0	0.0	-0.2	0.0	0.1
Nuclear import														
AN5482 (Ran)	RAS-related nuclear protein	54	38	NaN	-1.6	-0.7	NaN	-1.1	0.7	-0.2	-0.1	0.3	-0.1	0.3
Carbohydrate metabolism														
AN6655 (GudC)	Glucose 1-dehydrogenase	15	16	7	-1.5	-1.3	-0.5	-1.3	0.5	0.4	-0.2	0.3	0.3	0.3
AN3223 (pfkA)	6-phosphofruktokinase	184	NaN	431	-1.9	-0.7	NaN	-1.3	0.9	-0.1	-0.2	NaN	-0.1	0.1
AN7459 (HxkA)	Hexokinase	53	121	146	-2.3	-1.2	-0.7	-1.2	0.8	-0.3	-0.5	-0.2	-0.3	0.2
AN0285	6-phosphogluconolactonase	91	100	119	-1.8	-0.7	-1	-1.1	0.6	-0.4	-0.4	-0.4	-0.4	0.0
Metabolic process														
AN4923	HMG-CoA synthase	7	49	212	-5.0	-2.6	-2.3	-2.6	1.5	-0.5	-0.4	0.5	-0.4	0.6
AN0565	Multifunctional enzyme	61	91	458	-2.0	-0.9	-2.2	-2.0	0.7	-0.5	-0.4	0.3	-0.4	0.4
AN3581 (TrxR)	Thioredoxin reductase	100	105	184	-2.1	-1.1	-1.7	-1.7	0.5	-0.5	-0.3	-0.4	-0.4	0.1
AN9180	Transketolase	NaN	113	133	NaN	-1.3	-1.5	-1.4	0.8	NaN	-0.2	0.5	0.2	0.4
AN10220 (Ccp1)	Cytochrome c peroxidase	25	29	57	-2.4	-1.2	-0.7	-1.2	0.9	-0.5	-0.5	-0.4	-0.5	0.1
AN0641	TCTP family protein	76	17	NaN	-1.4	-0.8	NaN	-1.1	0.7	0.5	0.3	NaN	0.4	0.2
AN0232 (UreD)	Nickel-binding protein	24	45	43	-2.2	-1.0	-0.7	-1.0	0.8	0.0	-0.3	0.5	0.0	0.4
AN7710	Halooxid dehalogenase	153	336	273	-1.4	-0.7	-0.9	-0.9	0.4	0.5	0.1	-0.3	0.1	0.4

3. Results

The proteins that are up-regulated in a *laeA*Δ vegetative mycelium are shown in Table 10. The following four proteins are up-regulated in a *laeA*Δ mycelium e.g. alcohol oxidase, two alcohol dehydrogenases (AlcA and AlcB) and a choline oxidase. These proteins are most likely not found in Hülle cells since *laeA*Δ causes significant reduction in formation of Hülle cells.

Table 10. Proteins that are up-regulated in a *laeA*Δ mycelium

The protein quantity of the following proteins is increased in a *laeA*Δ vegetative mycelium. These proteins are up-regulated in *laeA*Δ mycelium. The log₂ SILAC ratio was determined for the strains *laeA*Δ (AGB1074) in comparison to *laeA* (AGB1092). The following thresholds were set. In the range of a log₂ SILAC ratio between +5.0 and +0.5 identified proteins are up-regulated. In the range between a -0.5 and +0.5 log₂ SILAC ratio identified proteins are unchanged. The log₂ SILAC ratio for the complementation strain (*laeAcomp*⁺, AGB1076) in comparison to the parental *laeA* strain (AGB1092) is between -0.5 and +0.5. The color scales represent log₂ SILAC ratios. Ø = median of log₂ SILAC ratios, SD = standard deviation, NaN = not a number. Biological replicates are numbered 1-3. Spectral counts (PSM) for three biological replicates are shown.



Gene ID	Description	Spectral counts			<i>laeA</i> Δ/ <i>laeA</i>			Ø	SD	<i>laeAcomp</i> ⁺ / <i>laeA</i>			Ø	SD
		1	2	3	1	2	3			1	2	3		
AN0567	Alcohol oxidase	149	315	NaN	4.2	4.4	NaN	4.3	0.1	-0.5	-0.3	NaN	-0.4	0.3
AN3741 (AlcB)	Alcohol dehydrogenase II	32	44	55	4.0	4.5	NaN	4.2	0.4	0.3	0.4	NaN	0.4	0.2
AN8979 (AlcA)	Alcohol dehydrogenase	307	NaN	82	2.5	NaN	3.0	2.5	0.3	0.5	NaN	-0.4	0.5	0.6
AN1429 (CodA)	Choline oxidase	14	27	93	1.8	0.8	0.2	1.3	0.8	0.3	-0.4	0.2	-0.1	0.4

3.3.2.1. Quantitative determination of proteins in *laeA*Δ revealed that NptA is present in Hülle cells as well as in other fungal tissues

NptA (nidulanin A prenyltransferase A, AN11080) is involved in the prenylation of the secondary metabolite nidulanin A (Oakley et al., 2017). In order to verify the localization of the prenyltransferase NptA in Hülle cells, a *nptA::gfp*; *lysA*Δ; *nkuA*Δ (AGB1082) strain was used. Hülle cells were enriched from sexual mycelium using the cleistothecia-rolling technique and the localization of NptA::GFP was observable in the cytoplasm of Hülle cells (Figure 32). The parental strain *lysA*Δ; *nkuA*Δ (AGB1092) was used as a negative control. The strain *laeA*Δ; *nptA::gfp*; *lysA*Δ; *nkuA*Δ (AGB1083) was used to verify the reduced protein abundance of NptA in a *laeA*Δ mycelium. Fluorescence microscopy revealed that almost no NptA::GFP was observable in the remaining Hülle cells except for a weak autofluorescence. A strain expressing GFP constitutively served as a control where GFP was mainly observable in the cytoplasm of Hülle cells.

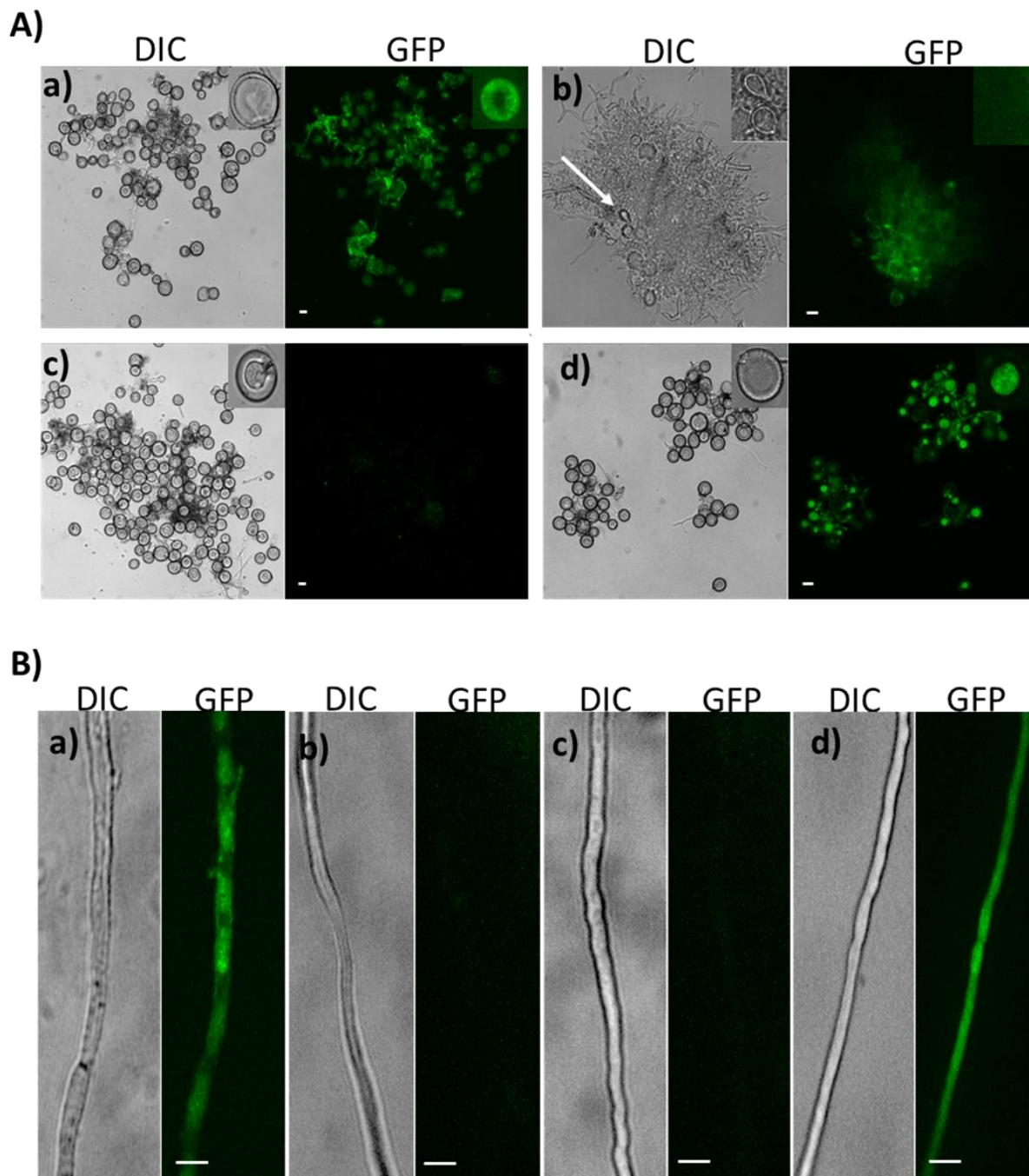


Figure 32. The prenyltransferase NptA is localized in the cytoplasm of Hülle cells.

A) Fluorescence microscopy pictures of Hülle cells: a) The picture shows the strain *nptA::gfp; lysAΔ; nkuAΔ* (AGB1082). NptA::GFP is localized to the cytoplasm of Hülle cells. b) The picture shows the strain *laeAΔ; nptA::gfp; lysAΔ; nkuAΔ* (AGB1083). Reduced NptA::GFP was observed in the remaining Hülle cells (white arrow) and in hyphae caused by *laeAΔ*. c) The picture shows the strain *lysAΔ; nkuAΔ* (AGB1092) where only autofluorescence could be detected in Hülle cells. d) A strain expressing GFP constitutively (AGB596) where GFP was mainly observable in the cytoplasm of Hülle cells. Scale bar is 10 μ m. B) Fluorescence microscopy pictures of a vegetative hypha: a) *nptA::gfp; lysAΔ; nkuAΔ* where NptA::GFP was detectable b) *laeAΔ; nptA::gfp; lysAΔ; nkuAΔ* where NptA::GFP was significantly reduced. c) *lysAΔ; nkuAΔ* where only autofluorescence could be detected. d) A strain expressing GFP constitutively where GFP was observable in the cytoplasm of the vegetative hypha. Scale bar is 20 μ m.

3. Results

The protein quantity of NptA was significantly reduced in a *laeAΔ*; *lysAΔ*; *nkuAΔ* strain. Western hybridization experiments revealed that the quantity of NptA::GFP protein is reduced in a *laeAΔ*; *nptA::gfp*; *lysAΔ*; *nkuAΔ* strain in a vegetative, sexual and asexual mycelium (Figure 33). The NptA protein consists of 434 amino acids with a predicted molecular mass of 48.9 kDa. NptA::GFP was detected as expected around 75 kDa. Additionally, degradation products of the NptA::GFP fusion protein were observable. A strain expressing GFP constitutively served as a positive control where GFP was detectable around 27 kDa. The parental *nkuAΔ* (ABG552) strain served as a negative control where GFP and the fusion protein was not observable. This finding shows that prenyltransferase NptA is reduced in a *laeAΔ* mycelium and that this prenyltransferase is localized in Hülle cells and other types of mycelia.

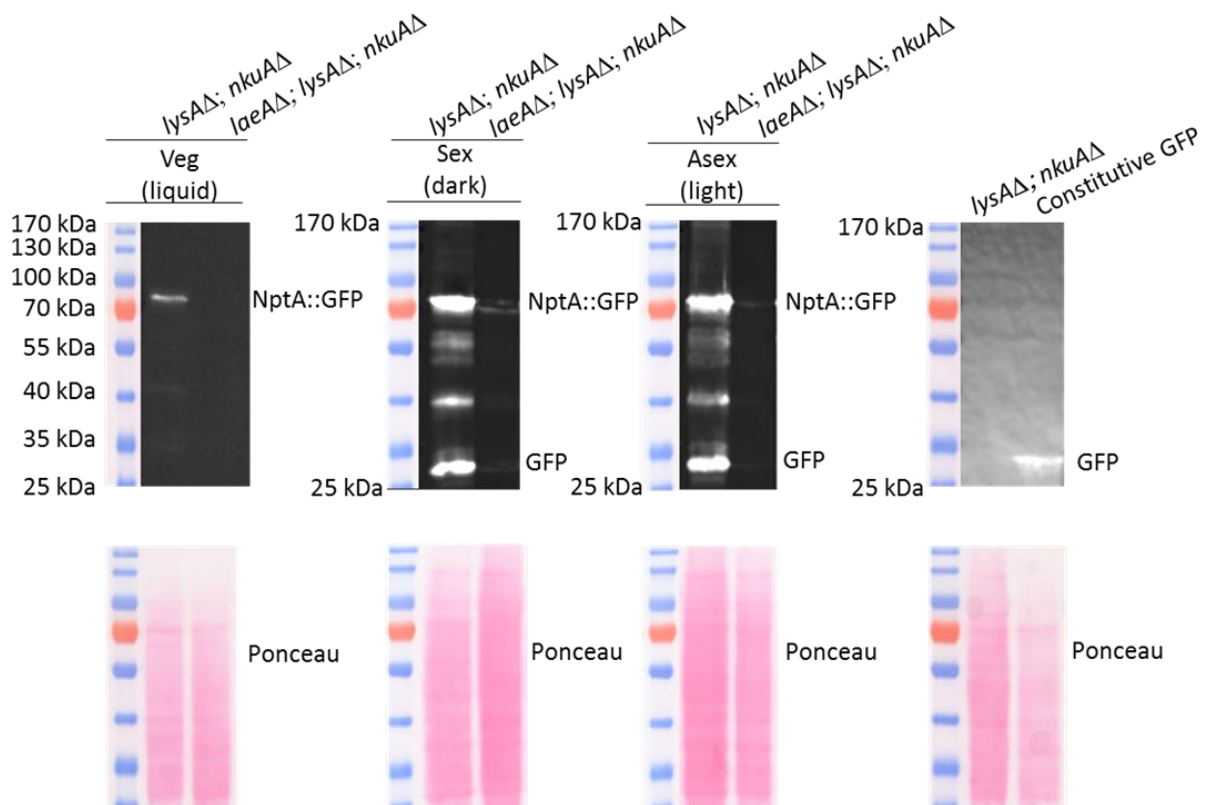


Figure 33. Reduced protein abundance of the prenyltransferase NptA in a *laeAΔ* mycelium.

Western hybridization to detect NptA::GFP in a *laeAΔ* (AGB1083) strain. NptA::GFP was detected weakly in *laeAΔ; nptA::gfp; lysAΔ; nkuAΔ* (AGB1083) strain. In order to detect NptA::GFP a primary α -GFP antibody (sc-9996; Santa Cruz) was used followed with an incubation of an α -mouse secondary antibody (G21234, Invitrogen). The NptA protein consists of 434 amino acids with a predicted molecular mass of 48.9 kDa. NptA::GFP was detected as expected around 75 kDa. Additionally, degradation products of the NptA::GFP fusion protein were observable. A strain expressing GFP constitutively served as a positive control where GFP was detectable around 27 kDa. Parental *nkuAΔ* (AGB552) strain served as a negative control where GFP and the fusion protein were not detectable.

3.3.2.2. Quantitative protein analysis revealed the kinase RfeA enriched in Hülle cells and other fungal tissues

Besides NptA, a serine/threonine kinase RfeA (AN2943) showed a significant reduction in quantity in a *laeA*Δ strain. To gain more insight into secondary metabolism in Hülle cells RfeA was further investigated. RfeA was identified and quantified in submerged liquid cultures and the localization of RfeA was further analyzed. The localization of RfeA::GFP was mainly observable in the cytoplasm of Hülle cells and vegetative hyphae (Figure 34). RfeA::GFP is possibly also located in other cellular compartments. In order to observe the localization of RfeA::GFP Hülle cells were enriched by the cleistothecia-rolling technique. A *refA::gfp;lysAΔ;nkuAΔ* (AGB1084) strain was used to observe RfeA::GFP in Hülle cells. In a *laeAΔ;rfeA::gfp;lysAΔ;nkuAΔ* (AGB1085) strain Hülle cells were observed in a reduced number. In the remaining Hülle cells, RfeA::GFP was used to verify the reduced quantity of RfeA::GFP protein in a *laeA*Δ mycelium.

Additionally, RfeA::GFP was observed in vegetative hyphae grown in submerged liquid cultures. In a *laeAΔ;rfeA::gfp;lysAΔ;nkuAΔ* strain, significantly reduced RfeA::GFP was observed in vegetative hyphae. The parental strain *lysAΔ;nkuAΔ* (AGB1092) was used as a negative control. Only autofluorescence could be detected in the *lysAΔ;nkuAΔ* strain. A strain expressing GFP constitutively served as a control where GFP was mainly observable in the cytoplasm of Hülle cells. The quantity of RfeA::GFP protein is reduced in a *laeA*Δ (AGB1085) strain.

Western hybridization experiments confirmed that without LaeA the amount of RfeA protein is reduced in vegetative, sexual and asexual mycelium (Figure 35). The RfeA protein consists of 448 amino acids with a predicted molecular mass of 50.5 kDa. The RfeA::GFP fusion protein was detected as expected around 76 kDa. A strain expressing GFP constitutively served as a positive control where GFP was detectable around 27 kDa. Parental *nkuA*Δ (ABG552) strain served as a negative control where GFP and the fusion protein were not detectable. The abundance of RfeA::GFP protein was reduced in a *laeA*Δ; *nptA::gfp;lysAΔ;nkuAΔ* strain in a vegetative, sexual and asexual mycelium. Additionally, degradation products of the RfeA::GFP fusion protein were observable. This suggests that RfeA is unstable in different fungal tissues.

3. Results

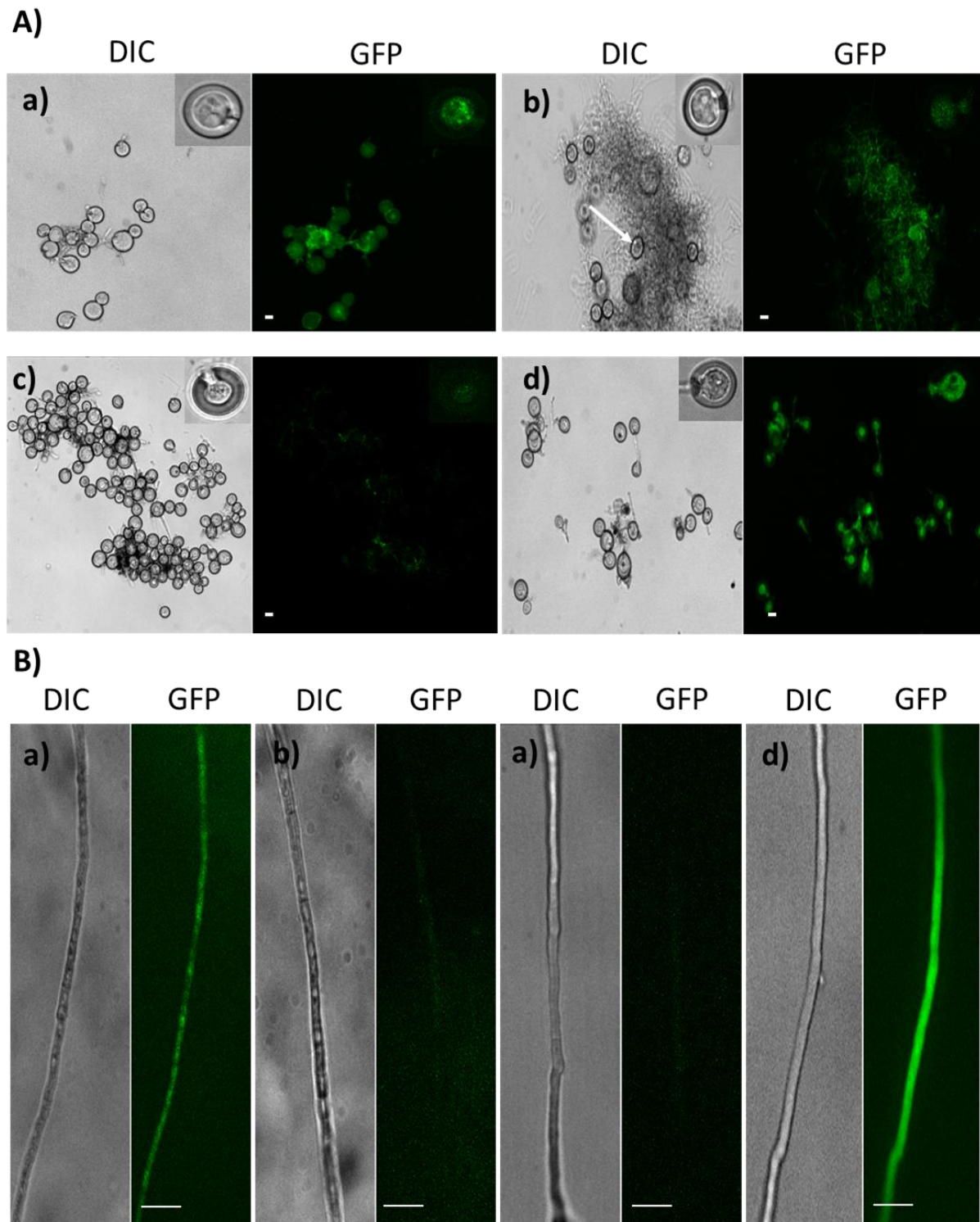


Figure 34. The serine/threonine kinase RfeA is localized in Hülle cells and is reduced in a *laeAΔ* mycelium.

A) Fluorescence microscopy pictures of Hülle cells and a vegetative hypha: a) *rfeA::gfp; lysAΔ; nkuAΔ* (AGB1084) b) *laeAΔ; rfeA::gfp; lysAΔ; nkuAΔ* (AGB1085) (white arrow points to one Hülle cell) c) *lysAΔ; nkuAΔ* (AGB1092) d) A strain expressing GFP constitutively (AGB596). Scale bar is 10 µm. B) Fluorescence microscopy pictures of a vegetative hypha: a) *rfeA::gfp; lysAΔ; nkuAΔ* (AGB1084) b) *laeAΔ; rfeA::gfp; lysAΔ; nkuAΔ* (AGB1085) c) *lysAΔ; nkuAΔ* (AGB1092) d) A strain expressing GFP constitutively (AGB596). RfeA::GFP is localized in Hülle cells and vegetative hyphae and might be in different cellular compartments. RfeA::GFP is reduced in a *laeAΔ* mycelium. Scale bar is 20 µm.

3. Results

This result indicates that the amount of RfeA is reduced in a *laeA* Δ mycelium and that this kinase is found in Hülle cells and other types of mycelia and that RfeA::GFP is most probably unstable in different fungal cell types including Hülle cells.

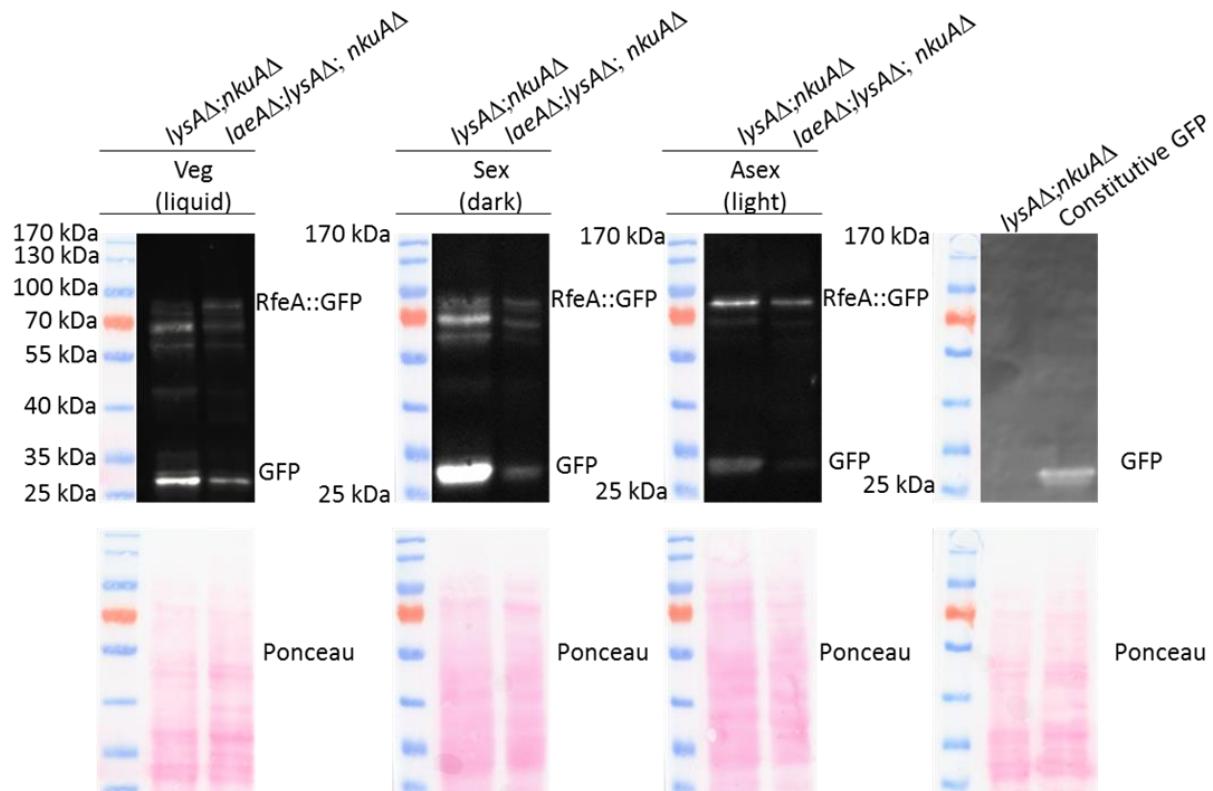


Figure 35. The serine/threonine kinase RfeA is localized in Hülle cells and the protein quantity is reduced in a *laeA* Δ mycelium.

Western hybridization of *rfeA::gfp*; *lysA* Δ ; *nkuA* Δ (AGB1084) and *laeA* Δ ; *rfeA::gfp*; *lysA* Δ ; *nkuA* Δ (AGB1085). In order to detect RfeA::GFP a primary α -GFP antibody (sc-9996; Santa Cruz) was used followed with an incubation of an α -mouse secondary antibody (G21234, Invitrogen). The RfeA protein consists of 448 amino acids with a predicted molecular mass of 50.5 kDa. RfeA::GFP was detected as expected around 76 kDa. Additionally, degradation products of the RfeA::GFP fusion protein were observable. It seems that RfeA::GFP is unstable in different fungal tissues. A strain expressing GFP constitutively served as a positive control where GFP was detectable around 27 kDa. Parental *nkuA* Δ strain (AGB552) served as negative control where GFP and the fusion proteins were not detectable.

3.3.3. The core proteome revealed a 72% overlap between the identified proteins of both types of Hülle cells

Proteomic approaches from solid agar plates and submerged cultures were compared to identify overlapping proteins found in enriched Hülle cells from solid agar plates versus submerged conditions. As such, the 401 proteins identified in Hülle cells from solid agar plates were overlaid with the proteins in submerged liquid cultures where Hülle cell formation occurred. This comparison revealed a 72% overlap between identified proteins from Hülle cells originated from solid agar plates compared to ones that were found in vegetative mycelium in submerged liquid cultures (Figure 36). The core proteome that represents the overlapping identified proteins from Hülle cells grown on solid agar plates and in liquid media consists of 286 proteins which are shortlisted in Table 11. The criterium to select proteins for the shortlist is that these proteins were identified with the highest spectral counts in Hülle cells from surface and liquid media.

The localization of the two proteins (AN8434, AN8435) uniquely found in Hülle cells from solid agar plates, were identified again in vegetative mycelium where Hülle cell formation occur, are discussed within the next chapter. The core proteome of both types of Hülle cells contain five enzymes that are encoded by the monodictyphenone (*mdp*) / xanthone (*xpt*) gene clusters (MdpG (AN0150), MdpL (AN10023), XptC (AN7998), XptB (AN12402) and AN7999 (a putative oxidoreductase). This means that five out of the six enzymes found in Hülle cells from solid agar plates were identified again in Hülle cells from submerged liquid cultures. Alves and co-workers demonstrated in a recent study that after the addition of choline Hülle cell formation occurred in a vegetative mycelium and the secondary metabolite monodictyphenone was present in these cultures (Alves et al., 2016).

These findings imply that Hülle cells from surface and liquid cultures comprise shared proteins encoded by monodictyphenone (*mdp*) / xanthone (*xpt*) gene clusters and that these enzymes are also found in a sexual mycelium with high amounts of Hülle cells.

3. Results

Table 11. List of overlapping proteins identified in Hülle cells from solid agar plates and submerged liquid cultures (Hülle cells core proteome).

Only proteins identified in two or more biological replicates and with two or more peptides per protein were considered for the analysis. 1.2.3: spectral counts of three biological replicates. * Identified proteins in two replicates and not in all three biological replicates.

Gene ID	Function	1	2	3	Reference
Uniquely found in both Hülle cell types					
AN8435	Tyrosinase domain protein	58	110	73	This study & Bayram et al., 2016
AN8434	Ankyrin repeat domain protein	36	102	62	This study & Bayram et al., 2016
Identified in both Hülle cell types & sex. mycelium					
AN10023 (MdpL)	Member of the <i>mdp/xpt</i> gene clusters	14	19	18	Bayram et al., 2016
AN12402 (XptB)	Prenyltransferase, member of the <i>mdp/xpt</i> gene clusters	9	10	17	Sanchez et al., 2011
AN0150 (MdpG)	Polyketide synthase, member of the <i>mdp/xpt</i> gene clusters	4	17	5	Sanchez et al., 2011
AN7998* (XptC)	GMC oxidoreductase, member of the <i>mdp/xpt</i> gene clusters	3	7		Sanchez et al., 2011
AN7999	Oxidoreductase, member of the <i>mdp/xpt</i> gene clusters	63	64	84	Bayram et al., 2016
AN8203	Hydrolase	10	16	35	Not available
AN6314*	Oxidoreductase		15	10	Not available
Identified in both Hülle cell types & asex. mycelium					
No overlapping proteins were identified					
In both Hülle cells types & vegetative mycelium (7 proteins were identical, 6 are listed)					
AN1182 (BenA)	Beta-tubulin	327	352	648	Oakley et al., 2004
AN6688 (AspB)	Putative septin B	180	124	8	Hernández et al., 2012
AN4159 (GlnA)	Glutamate-ammonia ligase	384	367	481	Margelis et al., 2001
AN2918 (Cct4)	Chaperonin complex component	48	46	102	Malavazi et al., 2007
AN2149 (Cct1)	Putative chaperonin complex component	27	12	86	Malavazi et al., 2006
AN4236 (RPT5)	Proteasome regulatory particle	25	32	55	Not available
In both Hülle cells types, sexual & vegetative mycelium (18 proteins were identical, 6 are listed)					
AN7570 (TubB)	Alpha-tubulin	236	192	363	Kirk et al., 1991
AN8182 (AspC)	Septin	160	139	252	Hernández et al., 2012
AN4997 (AspA)	Phosphatidylinositol transporter	44	85	110	Hernández et al., 2012
AN2142 (KapA)	Karyopherin (importin) alpha	66	43	111	Etxebeste et al., 2013
AN5895 (GdiA)	Rab GDP-dissociation inhibitor	142	112	251	Goody et al., 2017
AN4775	Cullin deneddylation	47	45	101	Dambacher et al., 2016
In both Hülle cells types, sexual & asexual mycelium (35 proteins were identical, 6 are listed)					
AN11080 (NptA)	Prenyltransferase	79	122	47	Oakley et al., 2017
AN7912* (OrsC)	Tyrosinase	14	24		Guerriero et al., 2017
AN7914	Alcohol dehydrogenase	203	159	75	Sanchez et al., 2010
AN4871 (ChiB)	Chitinase	44	66	43	Shin et al., 2009, Yamazaki et al., 2007
AN1502* (NagA)	Chitin hydrolysis	8	8		Pusztahelyi et al., 2006, Kim et al., 2002
AN2017* (AgdA)	Alpha-glucosidase	6		8	Nakamura et al., 2006
Identified in all cell types (213 proteins were identical, 6 are listed)					
AN8041 (GpdA)	Glyceraldehyde-3-phosphate dehydrogenase	971	1104	1794	Punt et al., 1988
AN7388 (CpeA)	Laccase	319	450	63	Scherer et al., 2002
AN9339 (CatB)	Catalase	637	669	575	Calera et al., 2000
AN0359 (SgdA)	Translation initiation factor 3 (eIF3)	4	13	217	Obayashi et al., 2017
AN7105	Translation initiation factor 3 (eIF3)	7	22	237	Obayashi et al., 2017
AN6542 (ActA)	Actin A	335	425	563	Upadhyay et al., 2008

3.3.4. The proteome of surface Hülle cells compared to Hülle cells from liquid media differ in composition by 28%

Identified proteins of the proteome from surface Hülle cells differ in 28% composition compared to identified proteins found in vegetative mycelium grown in submerged liquid cultures (Figure 36A). The difference between the proteomes of both types of Hülle cells revealed that surface Hülle cells contain increased numbers of glucanases as shown in Figure 36B. In a recent study it was shown that the transcripts of the α -1,3-glucanase *mutA* and *agnB* are expressed during sexual development on surface agar plates (He et al., 2017).

The MphA (AN2601) maltose permease-like protein was identified from surface Hülle cells within different developmental time points mentioned above. These results show that sexual differentiation increases α -1,3-glucanase levels and a maltose permease-like protein found in surface Hülle cells preferentially surrounding the cleistothecia. Proteins such as the α -1,3-glucanase MutA, reduced in a *laeA* Δ mycelium, are potentially found in Hülle cells (Sarıkaya-Bayram et al., 2010). Hülle cell growth in submerged liquid cultures revealed several proteins that were reduced in a *laeA* Δ ; *lysA* Δ ; *nkuA* Δ (AGB1074) mycelium. Among these proteins, several tRNA ligases were identified in this type of mycelium shown in Figure 36B. The reduction of tRNA ligases in *laeA* Δ vegetative mycelium suggests most probably that protein synthesis is reduced in this type of mycelium. This finding suggests that tRNA ligases are found in a submerged liquid mycelium where Hülle cell formation occurred and that these ligases are reduced in a *laeA* Δ mycelium.

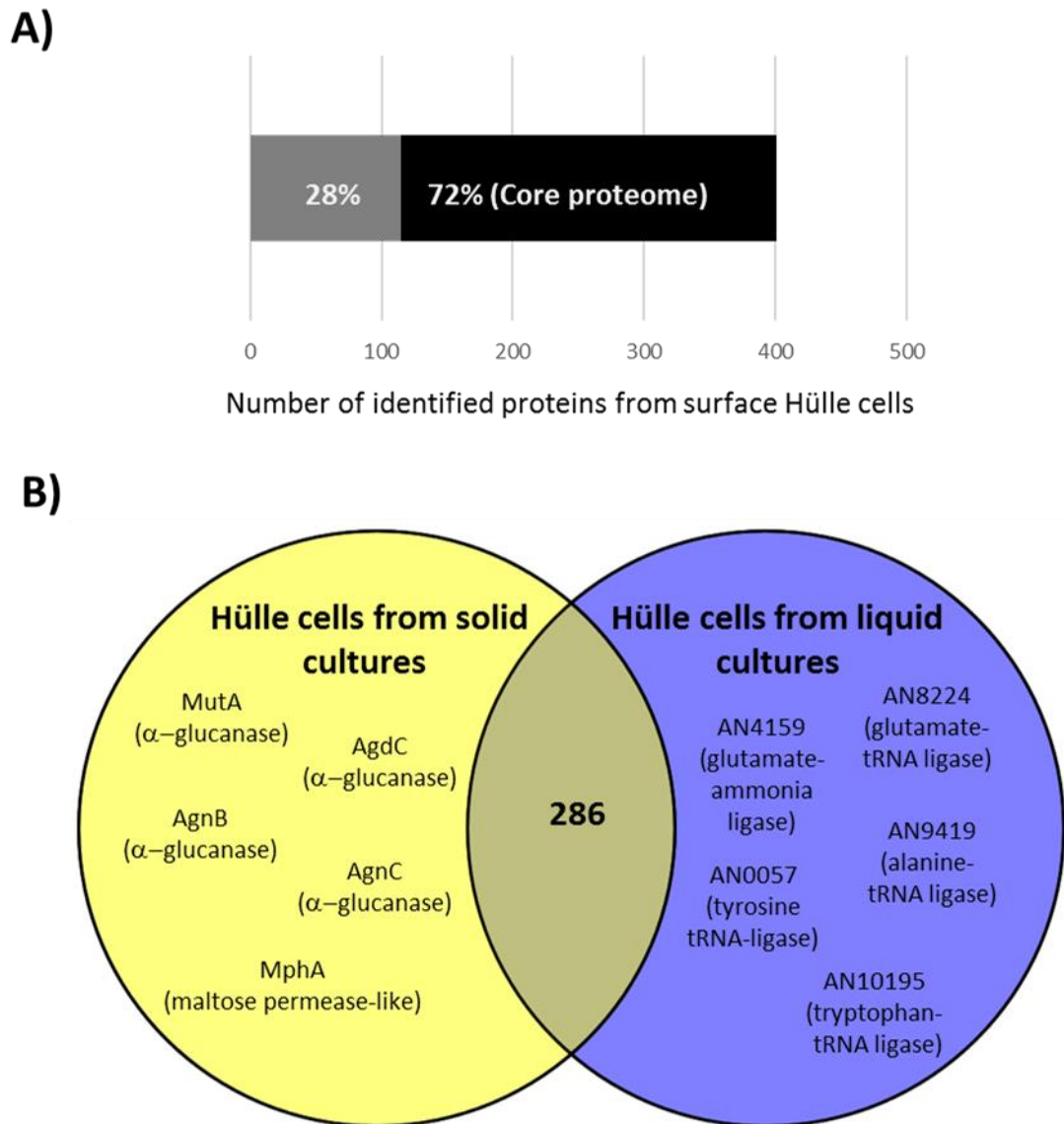


Figure 36. Hülle cells from surface growth compared to Hülle cells from liquid media differ in composition by 28% beside a shared core proteome.

A) 401 proteins shown in the graph were identified from surface Hülle cells and were overlaid with the proteins that were identified in Hülle cells grown in submerged liquid cultures. The percentages of overlapping and non-overlapping proteins are shown. The black box represents the overlapping proteins identified from Hülle cells grown on solid agar plates versus Hülle cells grown in liquid media. The grey box represents the non-overlapping proteins identified from Hülle cells grown on solid agar plates versus Hülle cells grown in liquid media. B) Comparison between proteins that were identified either from solid agar plates or from liquid cultures. The core proteome of Hülle cells that represents the identified overlapping proteins from Hülle cells grown on solid agar plates and liquid media contains 286 proteins and are shortlisted in Table 11 (page 95).

3.4. Functional analysis of genes for Hülle cell enriched proteins: A maltose permease-like protein of surface Hülle cells supports fungal growth and development

3.4.1. Comparative proteomics revealed two overlapping proteins found in Hülle cells from both approaches

Comparative proteomics revealed that two proteins were uniquely found in both types of Hülle cells and these are listed in Table 11. These two proteins encoded by the neighboring genes, *AN8434* and *AN8435*, are predicted to contain an ankyrin repeat and a tyrosinase domain. Bayram and co-workers showed that the transcripts of *AN8434* and *AN8435* are expressed in an asexual and sexual mycelium (Bayram et al., 2016).

In order to verify the localization of the ankyrin repeat domain protein (*AN8434*) and the putative tyrosinase domain protein (*AN8435*) in Hülle cells, an *AN8434::gfp* (AGB1089) and an *AN8435::gfp* (AGB1090) strain were used. Proteins with an ankyrin repeat domain are adaptor proteins bound to the membrane and are known to interact with multiple protein interaction partners for instance with the mammalian transcription factor NF- κ B (König et al., 2017). NF- κ B comprises structural similarities to the velvet domain protein VosA (Ahmed et al., 2013). It was shown that the *laeA* ortholog of *Trichoderma reesei* (*lae1*) regulates genes encoding ankyrin-proteins (Karimi-Aghcheh et al., 2013). The amino acid shared between *AN8434* and their *Homo sapiens* homologs is 36.2% to Ank3 (Cerqueira et al., 2014). The *AN8434* protein was named AnkG and stands for ankyrin repeat domain protein G.

In order to study the localization of AnkG::GFP Hülle cells were enriched from sexual mycelium using the cleistothecia-rolling technique and AnkG::GFP was detectable at the membrane of the subtending hyphae of Hülle cells as shown in Figure 37. Additionally, AnkG::GFP was observed in vegetative hyphae grown in submerged liquid cultures and was underrepresented in the membrane of vegetative hyphae and is most likely localized primarily in the endoplasmic reticulum (ER) and in the cytoplasm. The *nkuA* Δ (ABG552) parental strain was used as negative control. Only autofluorescence could be detected in the *nkuA* Δ strain. A strain expressing GFP constitutively revealed that GFP is mainly visible in the cytoplasm of vegetative hyphae.

3. Results

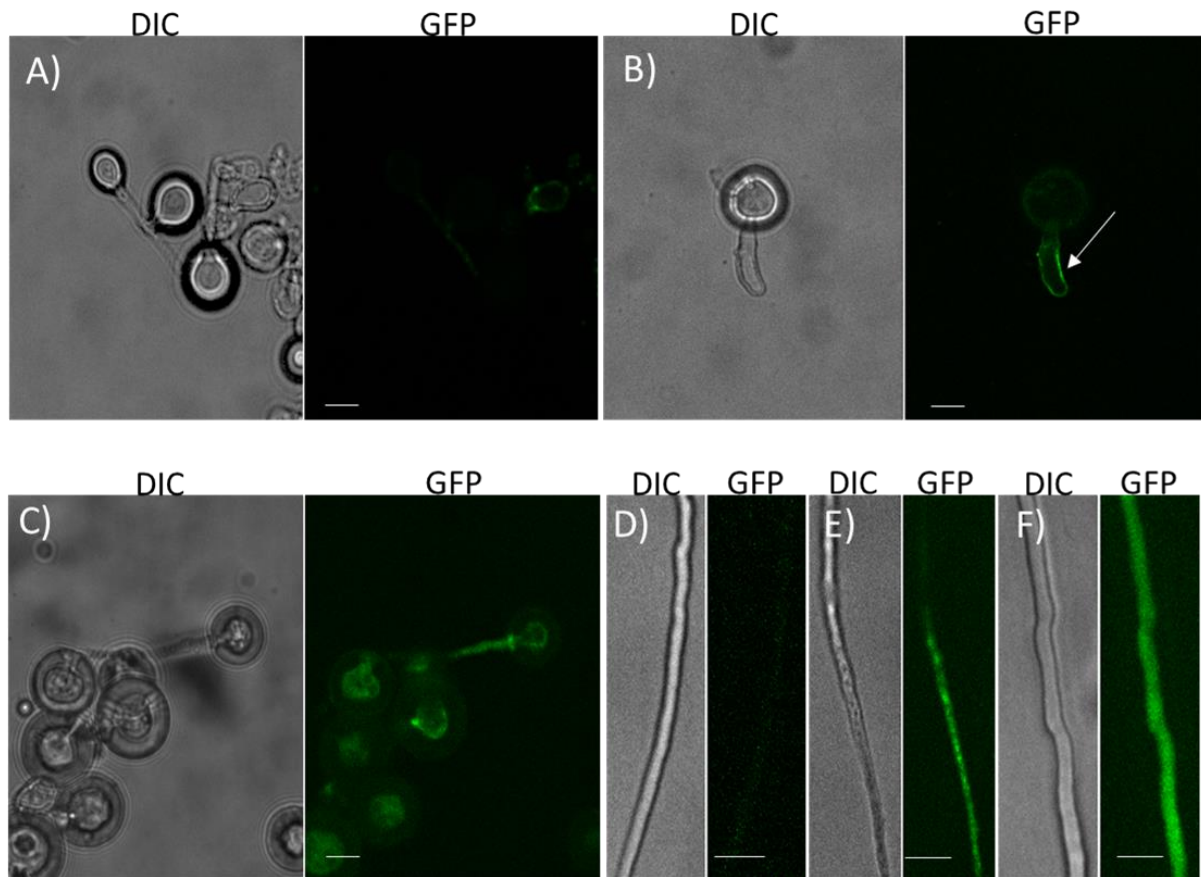


Figure 37. The AnkG (AN8434) ankyrin repeat domain protein is localized at the membrane of the subtending hyphae of Hülle cells.

Fluorescence microscopy pictures of Hülle cells A) *nkuA* Δ (ABG552) B) *ankG::gfp; nkuA* Δ (AGB1089) C) A strain expressing GFP constitutively (AGB596). AnkG::GFP is detectable at the membrane of the subtending hyphae of Hülle cells (white arrow points to one subtending hypha of Hülle cell). Scale bar is 10 μ m. Fluorescence microscopy picture of a vegetative hypha D) *nkuA* Δ E) *ankG::gfp; nkuA* Δ F) A strain expressing GFP constitutively. AnkG::GFP is detectable mainly in the cytoplasm as well as in the endoplasmic reticulum (ER) of a vegetative hypha. Scale bar is 20 μ m.

The AnkG protein consists of 477 amino acids with a predicted molecular mass of 52.0 kDa. Western hybridization experiments revealed that AnkG::GFP is detectable as expected around 79 kDa in a three and five day old sexual mycelium with high amounts of Hülle cells plus a three day old vegetative mycelium (Figure 38). Proteolytic cleavage product of AnkG::GFP fusion protein was detectable around 27 kDa. This is most likely the degradation product of the full-length AnkG::GFP fusion protein and represents the degraded GFP product. A strain expressing GFP constitutively served as a positive control where GFP was detectable around 27 kDa. Parental *nkuA* Δ (ABG552) strain served as a negative control where GFP and the fusion protein was not observable.

3. Results

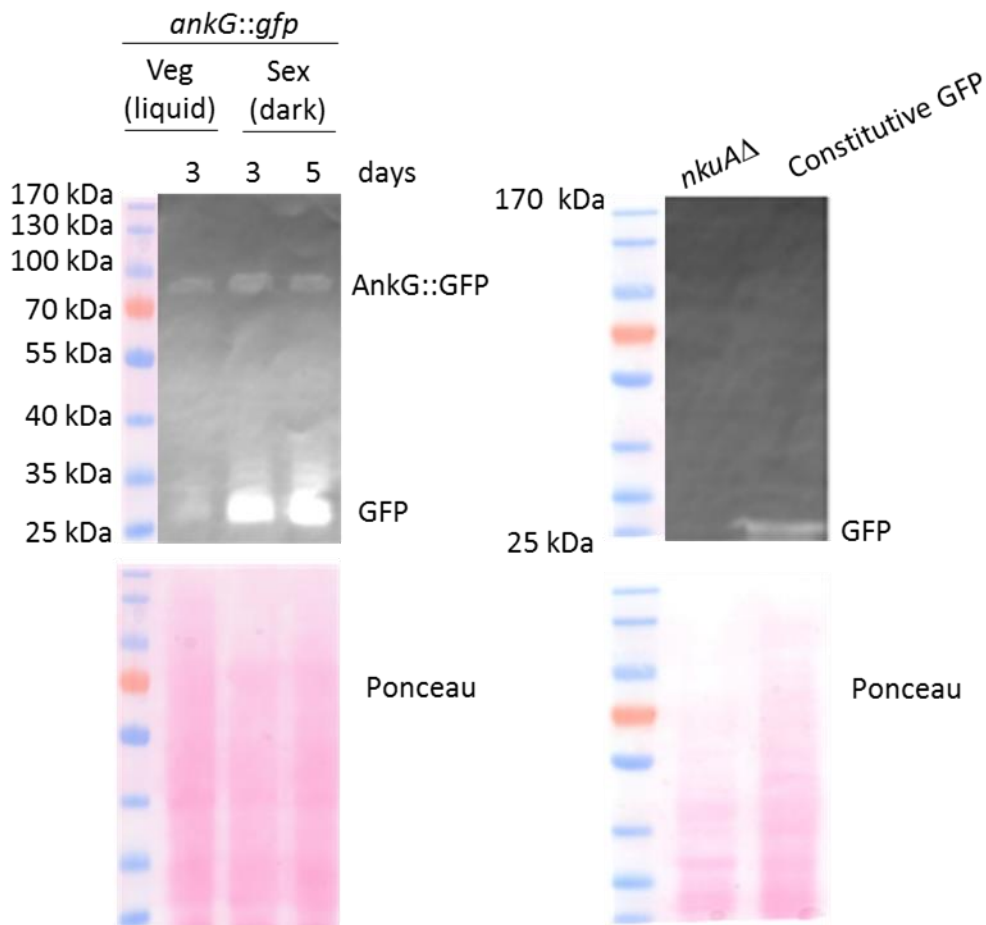


Figure 38. The AnkG::GFP fusion protein is found in sexual mycelium with high amounts of Hülle cells and a vegetative mycelium.

Western hybridization of *ankG::gfp; nkuAΔ* (AGB1089) of a vegetative and a sexual mycelium. To detect AnkG::GFP (*ankG::gfp;nkuAΔ*, AGB1089) a primary α -GFP antibody (sc-9996; Santa Cruz) was used followed with an incubation of an α -mouse secondary antibody (G21234, Invitrogen). The AnkG protein consists of 477 amino acids with a predicted molecular mass of 52.0 kDa. AnkG::GFP was detected as expected at around 79 kDa. A proteolytic cleavage product of AnkG::GFP fusion protein was detectable around 27 kDa and represents most probably the degraded GFP. A strain expressing GFP constitutively served as a positive control where GFP was detectable around 27 kDa. Parental *nkuAΔ* (AGB552) strain served as negative control where GFP and the fusion proteins were not detectable.

In order to study the localization of the putative tyrosinase domain protein (AN8435) Hülle cells were enriched from sexual mycelium using the cleistothecia-rolling technique and AN8435::GFP fusion protein was observable (Figure 39). It is possible that AN8435::GFP is situated in different cellular compartments within Hülle cells such as the cytoplasm. AN8435::GFP was also observable at the thick cell wall ringshaped structure of Hülle cells. AN8435::GFP was observable in vegetative hyphae in submerged liquid cultures. It seems that AN8435::GFP is not stable in different fungal cell types.

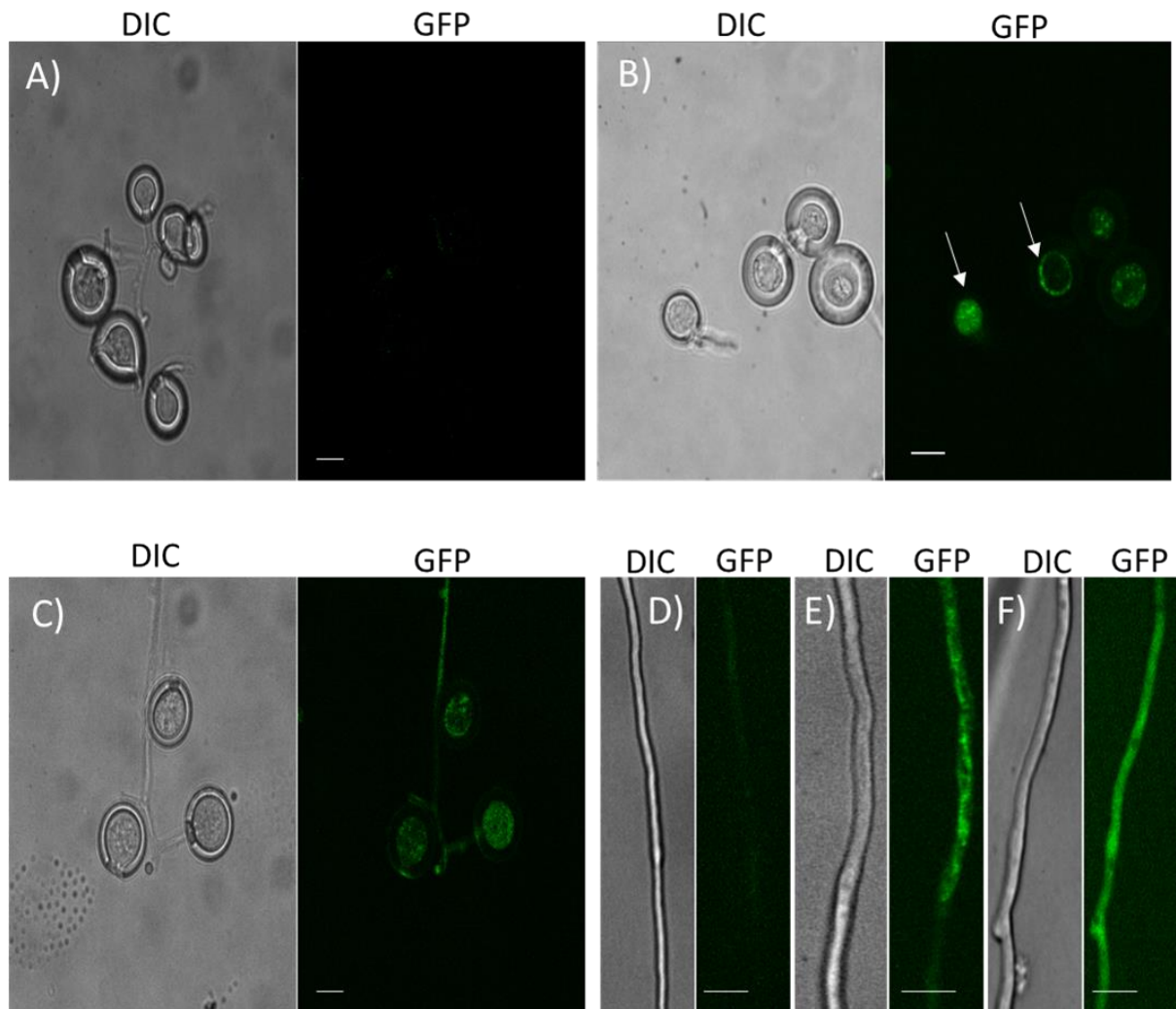


Figure 39. The localization of the tyrosinase domain protein (AN8435).

Fluorescence microscopy pictures of Hülle cells A) *nkuA* Δ (AGB552) B) *AN8435::gfp; nkuA* Δ (AGB1090) C) A strain expressing GFP constitutively (AGB596). *AN8435::GFP* was observed in different regions in Hülle cells (white arrows point to cytoplasm and ringshaped structures of Hülle cells). Scale bar is 10 μ m. Fluorescence microscopy picture of a vegetative hypha D) *nkuA* Δ E) *AN8435::gfp; nkuA* Δ F) A strain expressing GFP constitutively. *AN8435::GFP* is detectable mainly in the cytoplasm of a vegetative hypha. Scale bar is 20 μ m

The AN8435 protein consists of 846 amino acids with a predicted molecular mass of 95.7 kDa. Western hybridization experiments revealed that *AN8435::GFP* is probably detectable at the expected size of 123 kDa in a sexual mycelium with high amounts of Hülle cells and vegetative mycelium (Figure 40). Additionally, products with a higher size were observable, suggesting that the tyrosinase domain protein (AN8435) could have been modified. Degradation products of the *AN8435::GFP* fusion protein were also observable.

3. Results

A strain expressing GFP constitutively served as a positive control where GFP was detectable around 27 kDa. Parental *nkuA* Δ (ABG552) strain served as a negative control where GFP and the fusion protein were not detectable. It seems that the fusion protein AN8435::GFP is not stable.

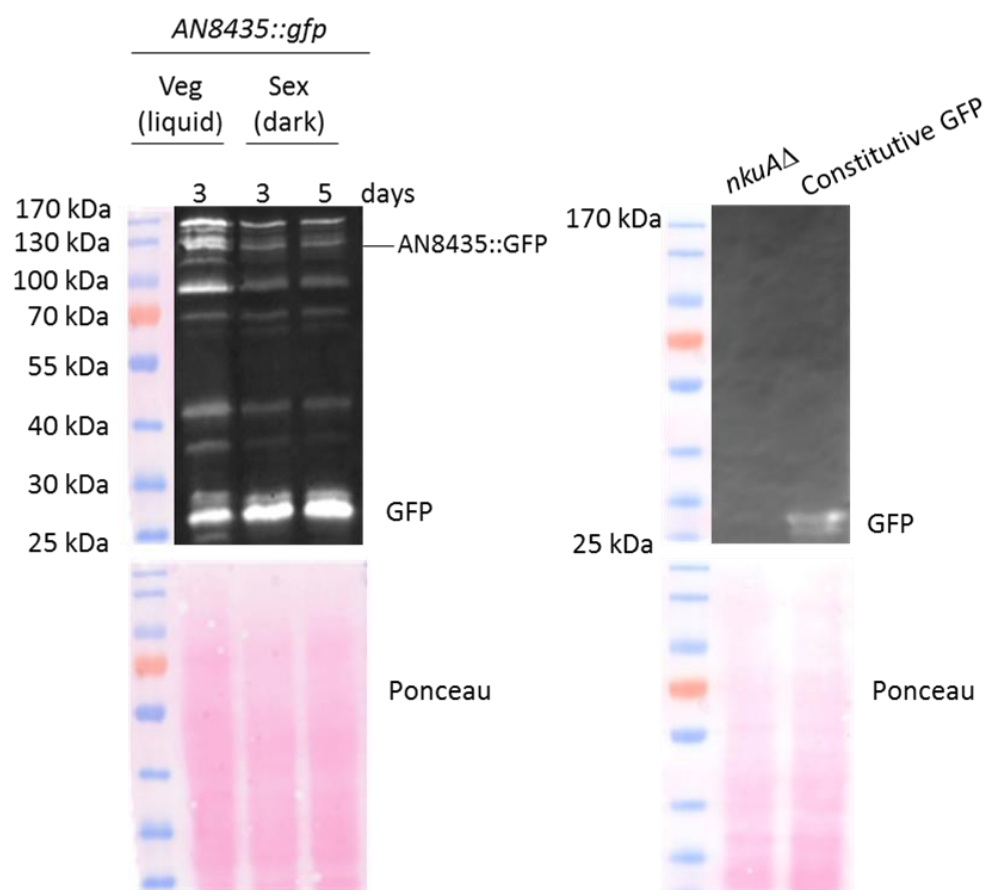


Figure 40. Western hybridization of AN8435::GFP of a vegetative and a sexual mycelium.

In order to detect AN8435::GFP (*AN8435::gfp*; *nkuA* Δ , AGB1090) a primary α -GFP antibody (sc-9996; Santa Cruz) was used followed with an incubation of an α -mouse secondary antibody (G21234, Invitrogen). The sequence of AN8435 consists of 846 amino acids with a predicted molecular mass of 95.7 kDa. AN8435::GFP was most probably detected at the expected size of 123 kDa. Additionally, products with a higher size were observable. Degradation products of the AN8435::GFP fusion protein were also observable. A strain expressing GFP constitutively served as a positive control where GFP was detectable around 27 kDa. Parental *nkuA* Δ (ABG552) strain served as a negative control where GFP and the fusion protein were not detectable.

These findings reveal that the AnkG (AN8434) ankyrin domain protein is localized to the membrane of the subtending hyphae of Hülle cells. It seems that AnkG is localized in the cytoplasm as well as in endoplasmic reticulum (ER) during vegetative growth. The localization of AN8435::GFP fusion protein was investigated. Probably AN8435 is located in different fungal tissues such as Hülle cells and vegetative mycelium. The fusion protein seems not to be stable.

3.4.2. A similar protein to a maltose transporter is enriched in surface Hülle cells and supports growth and fungal development

3.4.2.1. The sequence of MphA a maltose permease-like protein enriched in Hülle cells contains a distinctive sugar motif

The putative transmembrane transporter AN2601 was found in enriched Hülle cells of solid agar plates mentioned above. Transporters are thought to be crucial to transport nutrients and other molecules across Hülle cell membranes thereby supporting the cleistothecia (Wei et al., 2004, Pantazopoulou et al., 2007). The biological function of this putative transmembrane transporter was studied in detail. The AN2601 protein was named MphA and stands for **m**altose **p**ermease-like protein of **H**ülle cells. The best hit for an orthologous gene in an *Aspergillus* species for MphA is the putative MFS maltose transporter (Afu4g00150) of *Aspergillus fumigatus* and has a sequence identity of 88.3%. This is shown with other sequences of maltose transporters in the multiple sequence alignment in Figure 41.

The sequence of MphA contains 540 amino acids with a predicted molecular mass of 60.3 kDa. The secondary structure of MphA is predicted to contain twelve transmembrane helices which, in turn, consist of two 6-helix bundles connected by a cytoplasmic loop. The N-terminal tail of the sequence with a predicted length of 64 residues is longer than the C-terminal end with 34 residues. The sequence of MphA contains one conserved distinctive sugar motif (Horák 1997). All four sequences of the multisequence alignment (Figure 41) contain a conserved sequence region after the sixth putative transmembrane region. This region contains a sequence motif (PESP(W)L) which is specific to all sugar transporters (Horák 1997). This points out that the MphA sequence contains similarities with other sugar transporters such as the Mal31 of *Saccharomyces cerevisiae*.

3. Results

```

A.nidulans -----MSSDNTEKQTSALEVEAQPT-----SKGEPVYD
A.fumigatus -----MDNVTEKQTSALELEEQPV-----SKGGPVYD
A.niger -----MAAESV-----AEQRDEKPO-----SEKVDIHQ
S.cerevisiae MKGLSSLINRKKDRNDSHLDEIENGVNATEFNSIEMEEQGKKSDFDLSHLEYGPGSLIPN
                : : : :
A.nidulans SDEK-VD---YDRTGAINAERVEFDMTVLEAVKAYPAASWWAFVMSCTIIMESYCVFLM
A.fumigatus VNEK-VG---LDRAGAINAEDVEHKMTVVEAVKAYPAASWWAFVMSCTIIMESYCVFLM
A.niger SEVLDNP---DLMHEAFDGENYEHQMGVWEAAKQYPWACFWAFLMCFITVMSFDMFLN
S.cerevisiae DNNEEVPDLLDEAMQDAKEADESERGMPLMTALKTYPKAAAWSLLVSTTLIQEGYDTAIL
                : * : : * * : * * * * . * : : . * : * : :
A.nidulans GQFIATQKFADDFGVYSERDQAYIIIEASWQSAFQCSGPIGAFIGVFLAGPITSWIGYRWA
A.fumigatus GQFIATKRFARDYGVWSDVKQDFIIIEASWQSAFQCSGPGVAFIGVFIAGPITSWIGYRWA
A.niger TNFVALDHFVKVFGVETS-PGVYAIPTKWQSAFQSGQCGAFVGVYLAGPITNKIGYRWT
S.cerevisiae GAFYALPVFQKKYGSLSNNTGDYEISVSWQIGLCLCYMAGEIVGLQMTGPSVDYMGNRYT
                * * * * : * . . : * . * * . : . * : : : * * . : * * : :
A.nidulans TIGALMFLNAFIFIFYFGNSNGMFFASQILEGIPWGIPIANAPAYCSEIVPMRLRAPATQ
A.fumigatus TIGGLMFLNAFIFIFYFGNSQGMFLASQILEGIPWGIPIANAPAYCSEIVPMRLRAPATQ
A.niger TMLGLVLMNATIFISFFANSLTLVVGQALEGVPWGGFFIANSPAYASEVPLPLRAAVTA
S.cerevisiae LIMALFFLAAFIILYFCKSLGMIAVGQALCGMPWGCFCQCLTVSYASEICPLALRYLLTT
                : . * : : * * * * : * : * : : . * * * * * * * : : * * * * : * * * *
A.nidulans MLQMFWAIGSIIVGGITYHYQSK--QDSSAYRMPIALQWMFPTPLAILLFIAPESPWWLV
A.fumigatus MLQMFWAIGSIIVGGITYHYQSR--DDPTAYRIPIALQWMFPTPLAILLFIAPESPWWLV
A.niger TLQMSWSIGSIIVAGATYGYNSL--ETQWEWRAPLALQWIFPTPLMVLFFFAPESPWWLI
S.cerevisiae YSNLCWAFGQLFAAGIMKNSQNKYANSELGYKLPFALQWPLAVGIFFAPEPSPWWLV
                : : * : : * : : * . . : : : * : : * * * * * * * * : : * : : * * * * * : :
A.nidulans RKGRLEAEAEKSVRRLGRASANENP---ADAVAMMRRTIELE-KSEKKPSLI-ELWKGTDR
A.fumigatus RKGRLEAEKAVRRLGRASANDDP---ADAVAMMRRTIELE-KTEKKPSLV-ELWKGTDL
A.niger RRGRKEALKSIKRLGAKTEEQ-A---HQSLAMIERTVKEEETGGNPTLL-DLWKGTDR
S.cerevisiae KKGRIDQARRSLERTLSGKGPEKELLVSMELDKIKTTIEKEQKMSDEGTWDCVKDGINR
                : : * * : * : : * * . : : : : * : : * : : : * : * :
A.nidulans YRTLIVCGVYASQNLGTGNLIANQAVYFFKQAGMASNTAFALGLITSALQWIMVMSWILT
A.fumigatus YRTLIVCGVYASQNLGTGNLIANQAVYFFKQAGMADNTAFALGLITSALQWIMVMSWILT
A.niger RRTIITCLYASQNFAGNLIANQATYFFEQAGISADKSFQNLNLTTCQLQVANAVSWVLT
S.cerevisiae RRTRIALCLWIGQCSGASLIGYSTYFYEKAGVSTDTAFTFSIIQYCLGIATFISWWAS
                * * * * : * * * : . : * : : * : : : : * : : * * * * : * * :
A.nidulans TYLGRRTIYVYQGLINCAFLIALGIAASIGDPKTTAASNAQASLGLIVSVLFCGLGPAPAS
A.fumigatus TYLGRRTIYVYQGLINCVFLVALGIAASVGAASK--AASNAQASLGLIVSVLFCGLGPAPAS
A.niger SWFRRTVFLYGTATNITFLFILGIIASVPQNH--KTNYAQACLGVII SVVYAGAQQGPIS
S.cerevisiae KYCGRFDLYAFGLAFQAIMFFIIGGL--GCSDTHGAKMGSALLMVVAFFYNLGIAPVV
                . : * : : * : : : : * . . . . * : : : : . *
A.nidulans WVIIGETSSVRLRPLTTGIRGAYYVNIPIFLSSYMLNNTDKWDLGGKSGYVWAGTAFI
A.fumigatus WVIIGETSSVRLRPLTTGIRGAYYVNIPIFLASYMLNADKWNLGGKSGYVWAGTAFI
A.niger YTIISETSSVRLRALSTAVGRSAYYITEIPMIYLSRMLNNTGWNLAGKCGYVWGCTALV
S.cerevisiae FCLVSEIPSSRLRTKTIILARNAYNVIQVVVTVLIMYQLNSEKWNWGAKSGFFWGGFCLA
                : : : * * * * : : * * * : : * * * : * : * * * * * : :
A.nidulans CTAMAWVWVPEMKDRSREIDILFRRRVPARKWKQTVVDIRDDE-----
A.fumigatus CTFMSWLWIPPEMKDRSREIDILFKRRVPARKWKQTVVDINDDE-----
A.niger VWVGAYFGLPELKHRSYREADILFKRKSARKFKTTEIGVDENE-----
S.cerevisiae TLAWAVVDLPETAGRTFIEINELFRLGVPARKFKSTKVDPFAAAKAAAAEINVKDPKEDL
                : . : * * * * : : * : * * : * * * * * :
A.nidulans -----
A.fumigatus -----
A.niger -----

```

Figure 41. Multisequence alignment of four putative maltose permease-like protein sequences from MphA (*Aspergillus nidulans*), Afu4g00150 (*Aspergillus fumigatus*), Mal11 (*Aspergillus niger*), Mal31 (*Saccharomyces cerevisiae*).

The predicted twelve transmembrane regions of the transporters are underlined. The conserved distinctive sugar motif as described by (Horák 1997) is highlighted in yellow.

3.4.2.2. MphA protein supports fungal growth and development

A gene deletion of *mphA* was performed in an *nkuA* Δ (AGB552) parental strain. Hülle cells are observable in an *mphA* Δ ; *nkuA* Δ (AGB1077) strain. The dry weight of *mphA* Δ ; *nkuA* Δ was determined from submerged liquid cultures and was reduced in comparison to the *nkuA* Δ strain and the complementation strain shown in Figure 42.

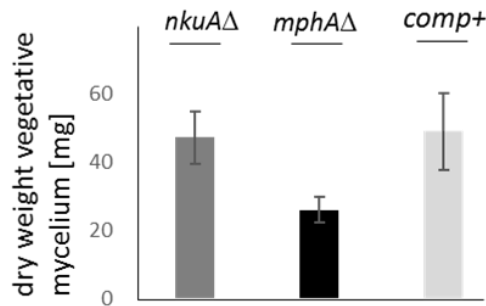


Figure 42. The MphA maltose permease-like protein supports vegetative growth.

Dry weight of vegetative mycelium concerning the parental strain (*nkuA* Δ , AGB552), the deletion strain (*mphA* Δ ; *nkuA* Δ , AGB1077) and the complementation strain *comp+* (*mphA* Δ ::*mphA*::*gfp*; *nkuA* Δ , AGB1078). Vegetative mycelium was harvested 20 hours after inoculation.

The percentage of conidiophores was determined from surface cultures and was reduced in comparison to the *nkuA* Δ strain and the complementation strain as shown at the end of this chapter. The development of cleistothecia was studied after three, five and seven days after germination (Figure 43). After three days, no cleistothecia could be observed in the *mphA* Δ ; *nkuA* Δ strain, whereas in the *nkuA* Δ and in the complementation *mphA* Δ ::*mphA*::*gfp*; *nkuA* Δ (AGB1078) strain small non-pigmented primordia could be observed. Cleistothecia of *mphA* Δ ; *nkuA* Δ were first visible after five days and at this time point, they were lightly pigmented. In the case of the *nkuA* Δ and the complementation strains, the cleistothecia were pigmented and larger in size. After seven days, the cleistothecia of *mphA* Δ ; *nkuA* Δ reached almost the size of the *nkuA* Δ strain but did not fully recover the pigmentation of cleistothecia. After 14 days, all observable cleistothecia of *mphA* Δ ; *nkuA* Δ were fully pigmented. After five days, the cleistothecia of *mphA* Δ ; *nkuA* Δ contained no dark reddish ascospores in contrast to the *nkuA* Δ and the complementation strain. Dark reddish ascospores could be observed after 14 days in the *mphA* Δ ; *nkuA* Δ strain. This finding firmly establishes that MphA supports generally growth, development and also the maturation of the cleistothecia.

3. Results

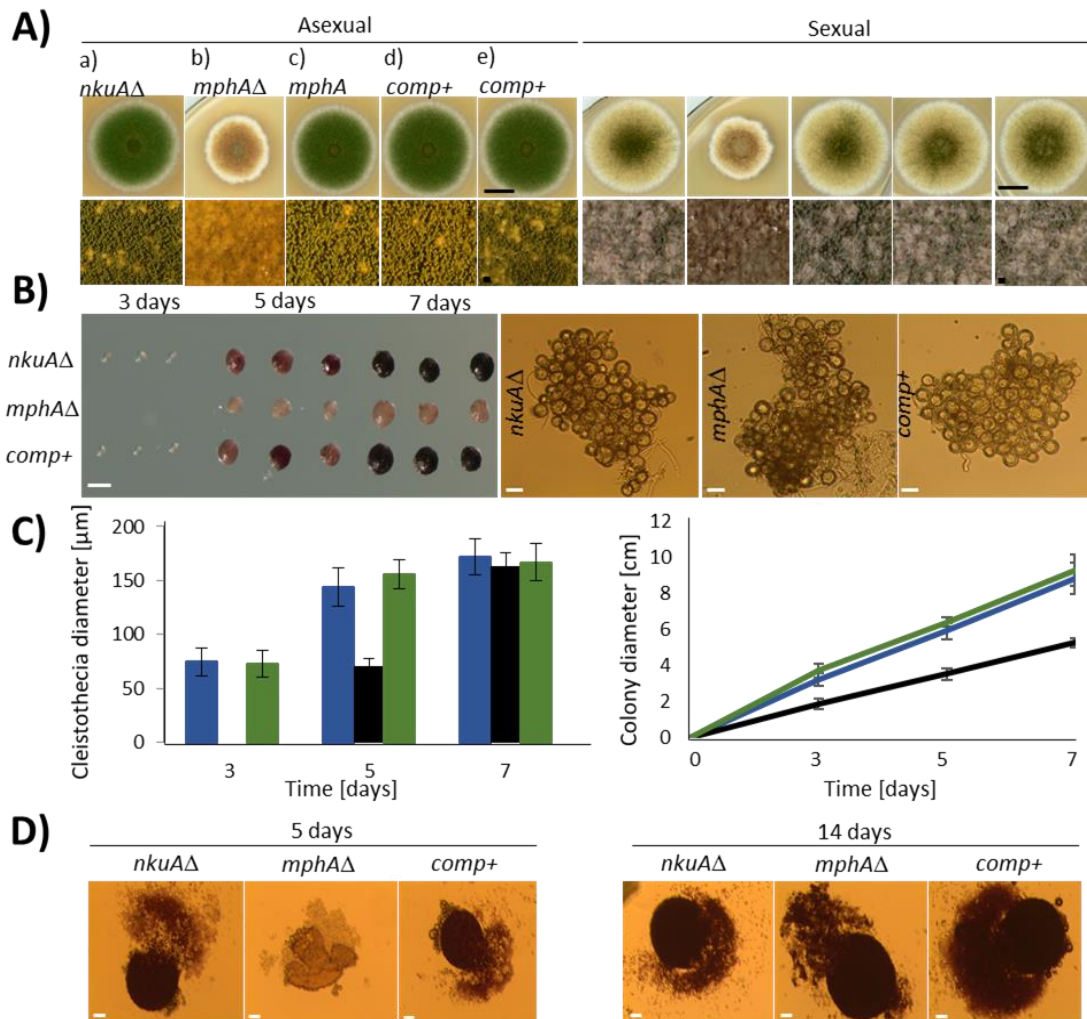


Figure 43. MphA promotes fungal growth and development.

(A) The gene *mphA* was knocked out in a a) *nkuAΔ* (AGB552) strain receiving the b) *mphAΔ; nkuAΔ* (AGB1077) strain. The phenotype could be restored in complementation strains with and without a tagged version of *gfp*: c) *mphA::gfp; nkuAΔ* (AGB1079) d) *mphAΔ::mphA::gfp; nkuAΔ* (AGB1078) and e) *mphAΔ::mphA nkuAΔ* (AGB1080). Fungal colonies scale bar is 1 cm. Fungal mycelium scale bar is 100 μm. B) Cleistothecia were observed on day 3, 5 and 7 after germination. 3 days after germination no primordia were observable in sexual mycelium of the deletion strain (*mphAΔ; nkuAΔ*). After 3 days small non-pigmented undeveloped primordia were observable in *nkuAΔ* and the complementation strain *mphAΔ::mphA::gfp; nkuAΔ* (*comp+*). 5 and 7 days after germination most of the cleistothecia of the strain *mphAΔ; nkuAΔ* were not fully pigmented. Scale bar is 200 μm. Hülle cells are shown and Hülle cells are observable in the deletion strain. Scale bar is 20 μm. C) The diameters of the cleistothecia were measured after 3, 5 and 7 days after germination. After 3 days the size of the primordia of the strains *nkuAΔ* (blue) and *mphAΔ::mphA::gfp; nkuAΔ* (green); were around 70 μm in diameter. After 5 days, the cleistothecia of the knockout strain (black) reached the size of around 70 μm. Meanwhile the strains *nkuAΔ* and *mphAΔ::mphA::gfp; nkuAΔ*; reached the size of around 150 μm. On day 7 all three strains could reach the adult cleistothecia size of around 170 μm. Colony diameter [cm] of the deletion *mphAΔ; nkuAΔ* strain (black), the parental strain and the complementation strains were measured after 3, 5 and 7 days. Growth is reduced in the deletion strain in comparison to the *nkuAΔ* strain and the complementation strain. The knockout of *mphA* shows a defect in the development of ascospores. D) The production of dark reddish ascospores were observed in the *nkuAΔ* strain, in the knockout strain *mphAΔ; nkuAΔ* and in the complementation strain *mphAΔ::mphA::gfp::nkuAΔ* on day 5 and 14 after germination. Most of the cleistothecia of the knockout strain contained no observable ascospores on day 5 after germination. Instead of dark reddish ascospores only non-pigmented spores were observable. In contrast thereto dark reddish ascospores were observable in the strains *nkuAΔ* and the complementation strain *mphAΔ::mphA::gfp::nkuAΔ*. On day 14 all three strains were able to produce dark reddish ascospores. Scale bar is 50 μm.

3.4.2.3. MphA protein is localized to the envelope of Hülle cells

The localization of MphA::GFP was studied in Hülle cells and in a vegetative mycelium. Therefore, the complementation strain *mphAΔ::mphA::gfp;nkuAΔ* (AGB1079) was used. Hülle cells were enriched from sexual mycelium using the cleistothecia-rolling technique and the localization of MphA::GFP was mainly observable in the envelope of Hülle cells as shown in Figure 44A. MphA::GFP was also observable in the center of the Hülle cells. The parental strain *nkuAΔ* (AGB552) without GFP and a strain expressing GFP constitutively (AGB596) were used as controls. Only autofluorescence could be detected in the *nkuAΔ* strain. The strain expressing GFP constitutively revealed that GFP is mainly visible in the cytoplasm of Hülle cells. Therefore, GFP was mainly observable in the center of Hülle cells and was unrepresentative in the envelope of Hülle cells. In a *laeAΔ; mphA::gfp; nkuAΔ* (AGB1081) strain almost no Hülle cells were observed. The remaining Hülle cells of a *laeAΔ* strain displayed almost no MphA::GFP. In the remaining hyphae MphA::GFP was much stronger detectable.

In order to observe MphA::GFP in vegetative hyphae the strains were grown in submerged liquid conditions for 20 hours and only autofluorescence could be detected in the *mphAΔ::mphA::gfp;nkuAΔ* and the *laeAΔ; mphA::gfp; nkuAΔ* strains (Figure 44B). This result was comparable to the observation of a *nkuAΔ* strain where only autofluorescence was detectable. The strain expressing GFP constitutively revealed that GFP is mainly visible in the cytoplasm of vegetative hyphae grown for 20 hours. These results show that MphA is most likely enriched in Hülle cells and is located mainly in the envelope of Hülle cells. Growing the complementation strain *mphAΔ::mphA::gfp;nkuAΔ* showed that MphA::GFP is not detectable in a vegetative mycelium grown within submerged cultures for 20 hours.

The sequence of MphA contains 540 amino acids with a predicted molecular mass of 60.3 kDa. Western hybridization experiments were performed without success since MphA::GFP, with an expected molecular mass around 87 kDa, was not detectable. This finding reveals that MphA is most probably enriched in sexually differentiated cells such as Hülle cells.

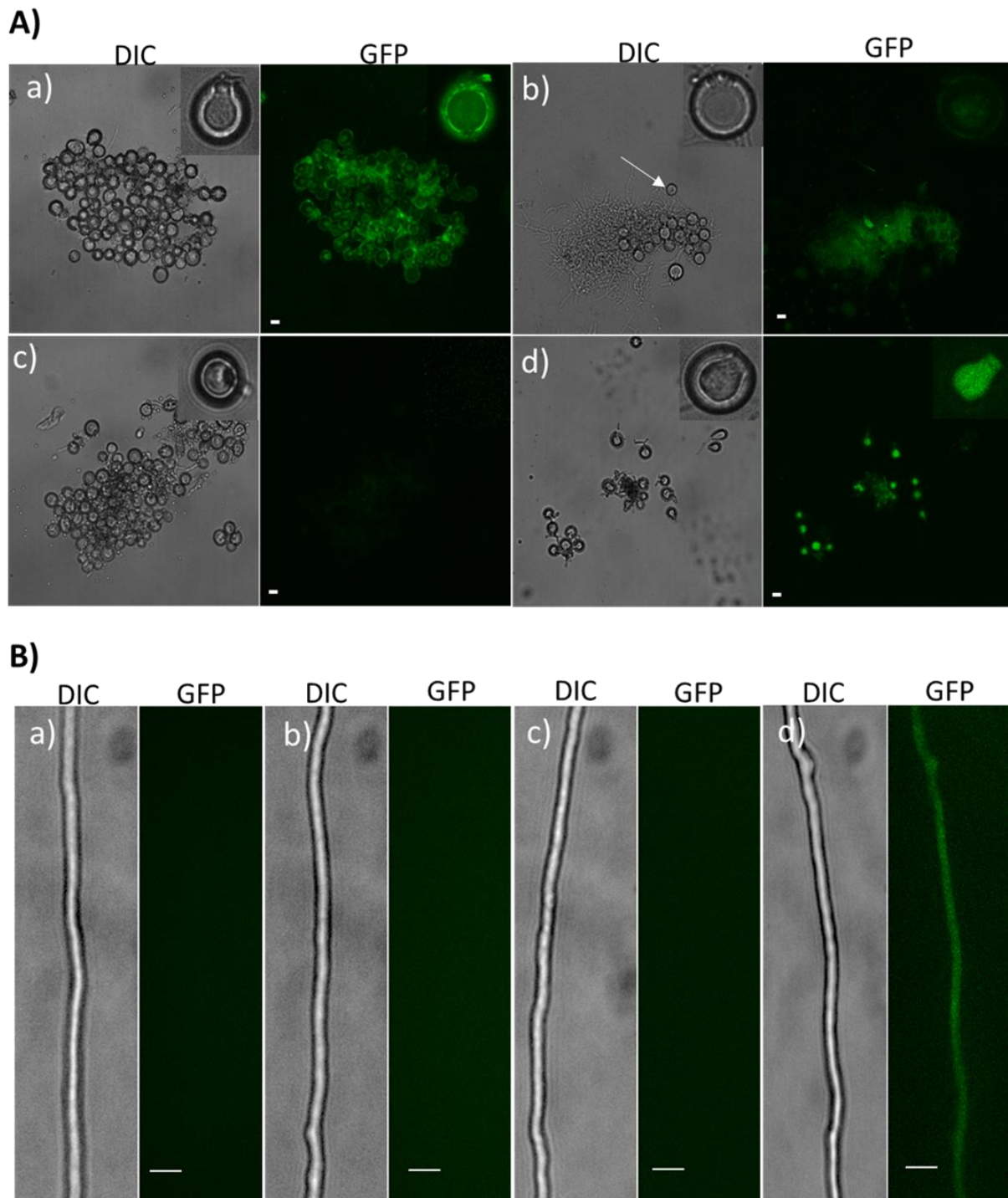


Figure 44. Localization of the maltose permease-like protein MphA.

A) Hülle cells were observed: a) The complementation strain (*mphAΔ::mphA::gfp; nkuAΔ*, AGB1078). MphA::GFP is localized mainly to the envelope of Hülle cells. MphA::GFP was also detected inside of Hülle cells. b) *laeAΔ::mphA::gfp;nkuAΔ* (AGB1081), where MphA::GFP was not clearly detectable in hyphae (white arrow points to one Hülle cell). c) *nkuAΔ* (AGB552) strain without GFP where mainly autofluorescence was detected. d) A strain expressing GFP constitutively (AGB596) where GFP was mainly detectable in the cytoplasm of Hülle cells. Scale bar is 10 μm . B) Vegetative mycelium was observed: a) In the complementation strain (*mphAΔ::mphA::gfp;nkuAΔ*), MphA::GFP was not detectable. b) In the strain *laeAΔ::mphA::gfp;nkuAΔ*, no MphA::GFP was detectable. c) *nkuAΔ* strain where mainly autofluorescence was detected in the vegetative hypha d) A strain expressing GFP constitutively where GFP was mainly detectable in the cytoplasm of the vegetative hypha. Scale bar is 20 μm .

3.4.2.4. The deletion of *mphA* prevents mycelia differentiation at higher concentration of carbohydrates in an early developmental time point

In order to investigate the influence of different carbohydrates on the phenotype of the deletion of *mphA*, different disaccharides and monosaccharide with different concentrations were added to the media. The *nkuA* Δ strain and the deletion strain *mphA* Δ ; *nkuA* Δ plus the complementation strain were inoculated on solid agar plates containing 1% or 5% of different carbohydrates. Three different carbohydrate sources were used and the influence of the different carbohydrates were observed three days after germination. The phenotype of the *mphA* deletion strain changed significantly in the case of growing the fungus on a medium containing 5% of different carbon sources such as disaccharides or monosaccharide. Hülle cells and primordia could not be observed growing the strain *mphA* Δ for three days on 5% maltose (Figure 45A).

The addition of 5% maltose to the medium influenced the development of the deletion strain negatively. Therefore, Hülle cells and conidiophores were significantly reduced and instead the fungus formed undifferentiated aerial hyphae after 3 days. The percentage of observable conidiophores in mycelia was determined (Figure 45B). The addition of 5% glucose or sucrose to the medium had a weaker effect on the phenotype of the *mphA* deletion strain in contrast to the above mentioned 5% maltose. This shows that the deletion of *mphA* Δ responds negatively to high concentrations of different carbohydrates since the transportation of carbohydrates is affected in this strain. Adding 1% maltose resulted in a differentiation of the mycelium, but with reduced development. This was also the case by adding 1% glucose or sucrose to the media. This supports the observation that with higher concentration of maltose and without the transporter MphA the fungus reacts negatively on developing complex structures such as Hülle cells or conidiophores and instead forms an undifferentiated mycelium.

The key point of this thesis is that the central observations demonstrate that sexual differentiation increases monodictyphenone (*mdp*) and xanthone (*xpt*) biosynthetic proteins localized in different sexual cell types. Genetic studies of the deletion strain *mphA* Δ illustrated that MphA protein promotes fungal growth, asexual and sexual development.

3. Results

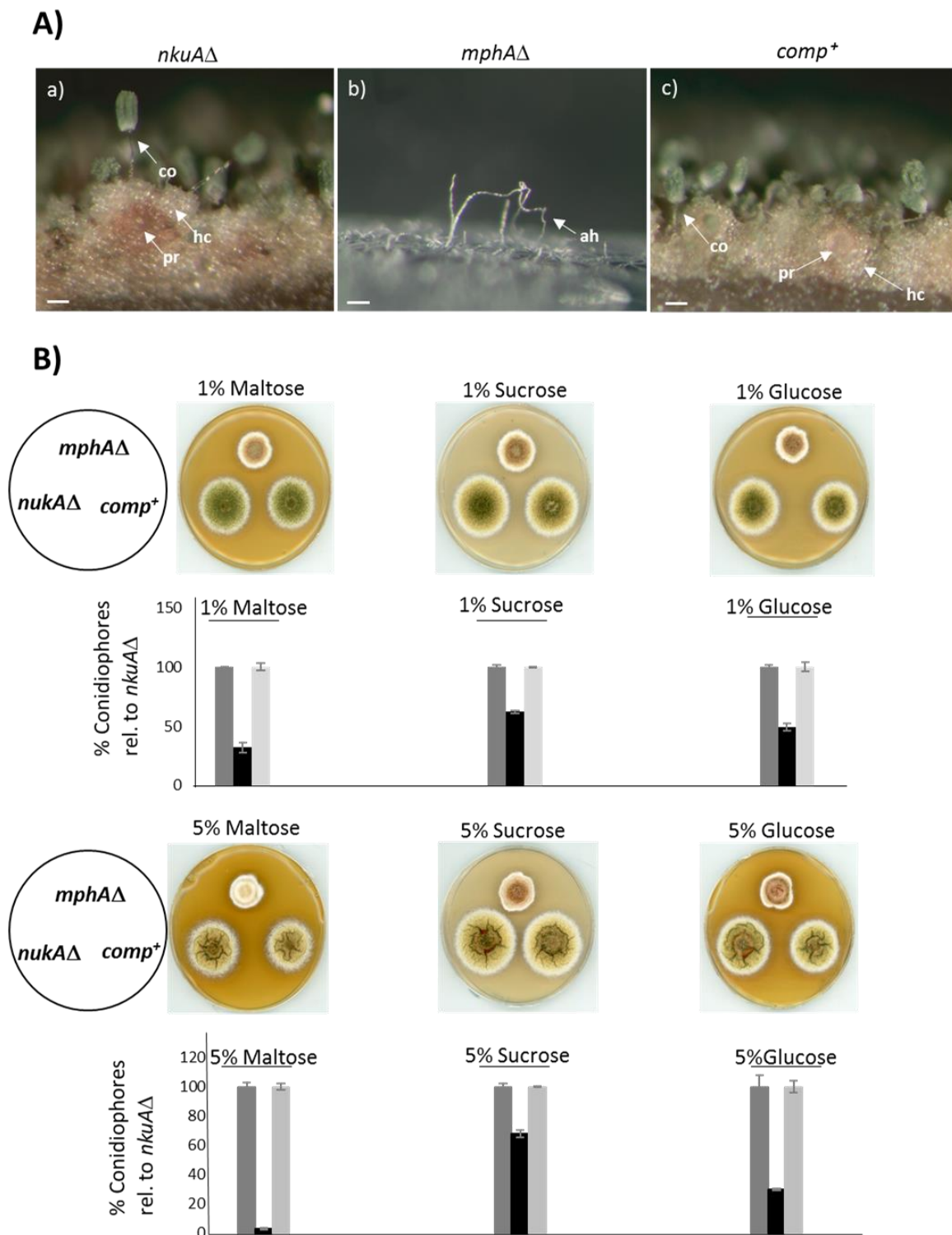


Figure 45. The maltose permease-like protein MphA prevents mycelia differentiation at higher concentration of carbohydrates.

A) Cross section of sexual mycelium three days after inoculation. a) The parental strain (*nkuAΔ*, AGB552) b) deletion strain *mphAΔ* (*mphAΔ*; *nkuAΔ*, AGB1077) and c) complementation strain *comp⁺*(*mphAΔ::mphA*; *nkuAΔ*, AGB1080) were inoculated on solid agar plates containing 5% maltose. In the case of the *nkuAΔ* (AGB552) and the complementation strain (AGB1080) sexual (pr: primordium, hc: Hülle cells) and asexual structures (co: conidiophore) were observable. Cleistothecia are surrounded by hundreds of Hülle cells. In the case of *mphAΔ*; *nkuAΔ* (AGB1077) mainly aerial hyphae (ah: aerial hyphae) were observed. Scale bar is 50 μm. B) The percentage of observable conidiophores relative to the parental strain *nkuAΔ* was determined and was significantly reduced in the *mphAΔ* (AGB1077) strain. Three different strains are shown: *nkuAΔ* (AGB552), *mphAΔ* (*mphAΔ*; *nkuAΔ*, AGB1077) and *comp⁺*(*mphAΔ::mphA*; *nkuAΔ*, AGB1080).

4. Discussion

Fungal mutant strains, which are unable to produce Hülle cells, form only small cleistothecia. This suggests that Hülle cells might have a nursing function for the cleistothecia (Sarikaya-Bayram et al., 2010, Braus et al., 2002). This thesis aimed to define specific proteins associated to sexual fungal tissue with a specific emphasis on Hülle cells. Comparative proteomic was used to determine proteins from Hülle cell fractions enriched from surface and submerged liquid cultures. Genetic methods were accomplished to investigate the function of the corresponding genes of the proteins that were identified in the comparative proteomic approach. The major finding of this thesis is that sexual differentiation increases monodictyphenone (*mdp*) and xanthone (*xpt*) biosynthetic proteins localized in different sexual cell types. Besides a maltose permease-like protein was identified in Hülle cells that supports fungal growth and development.

4.1. Hülle cells and sexual tissue grown on solid agar plates revealed the presence of proteins for the synthesis of an antimicrobial substance

One of the main findings of this thesis is that biosynthetic proteins encoded by the monodictyphenone (*mdp*) / xanthone (*xpt*) gene clusters are enriched in Hülle cells and sexual tissue, in comparison to other fungal tissue types (Figure 46). Bayram and co-workers showed that the monodictyphenone (*mdp*) / xanthone (*xpt*) gene clusters are specially expressed during sexual development (Bayram et al., 2016). This correlates with the findings of this thesis since expectedly during sexual differentiation biosynthetic proteins encoded by the monodictyphenone (*mdp*) / xanthone (*xpt*) gene clusters are present. These proteins are diminished in other fungal tissues. Furthermore, the present study shows that these proteins are localized in Hülle cells during sexual development. It seems that biosynthetic proteins for the synthesis of monodictyphenone and xanthenes are most probably present all over the sexual mycelium, especially within enriched Hülle cells.

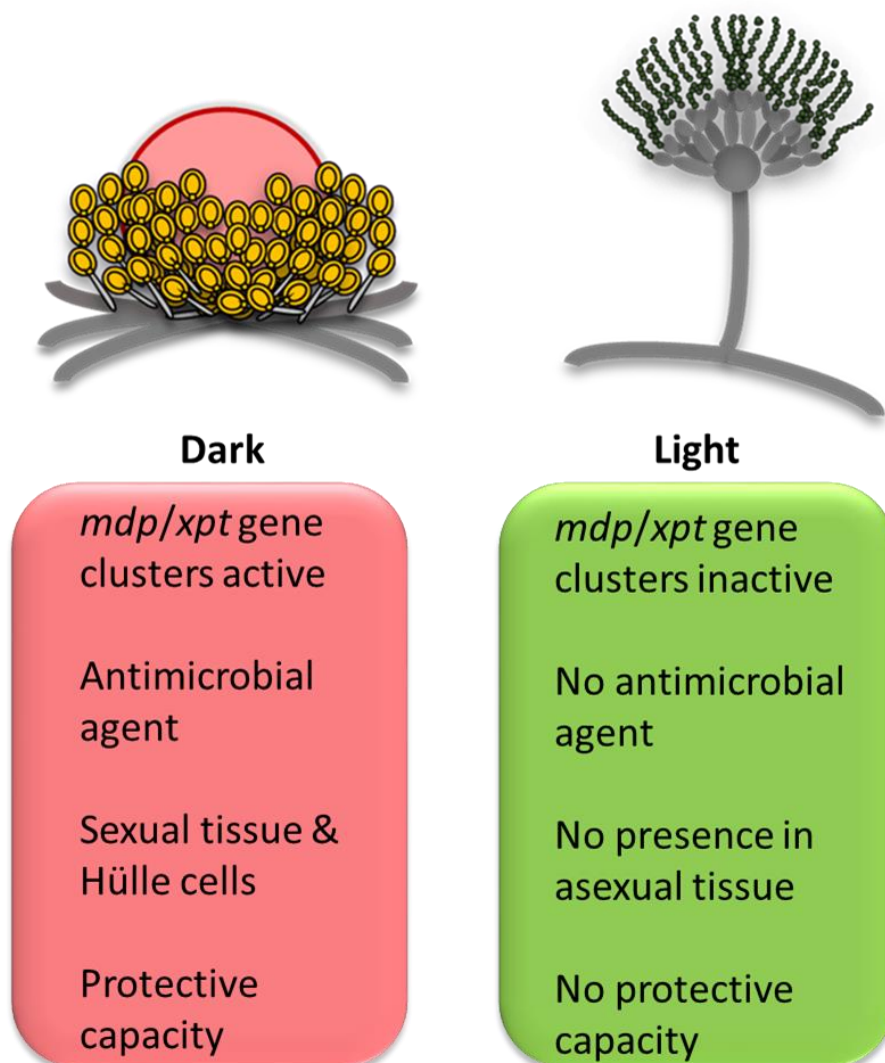


Figure 46. The monodictyphenone (*mdp*) / xanthone (*xpt*) gene clusters are active in sexual tissue including Hülle cells from surface growth.

Biosynthetic proteins encoded by the monodictyphenone (*mdp*) / xanthone (*xpt*) gene clusters are enriched during sexual development. Monodictyphenone and xanthonones are antimicrobial agents. The presence of monodictyphenone and xanthonones lead to the assumption that the cleistothecium is protected against various harsh environmental situations like fungivory. In asexual tissue the monodictyphenone (*mdp*) / xanthone (*xpt*) gene clusters are inactive. The compounds of monodictyphenone and xanthonones are consequently not present. It seems to be that monodictyphenone and xanthonones are not protecting the conidiophores (Bayram et al., 2016).

This suggests that the synthesis of an antimicrobial substance is crucial during maturation of the cleistothecia. This finding aligns to the insight that the cleistothecia of *Aspergillus nidulans* covered with Hülle cells are more resistant against fungivory when comparing to a vegetative or asexual tissue (Döll et al., 2013). Furthermore, it was shown that monodictyphenone reduces the egg laying activity of *Drosophila melanogaster* on an *A. nidulans* mycelium (Regulin and Kempken 2018). Both findings validate the assumption that Hülle cells have a protective capacity.

Limitations to the findings are that not all biosynthetic proteins encoded by the monodictyphenone (*mdp*) / xanthone (*xpt*) gene clusters were present in sexual tissue and Hülle cells. This also correlates to other studies, because not all genes of the monodictyphenone (*mdp*) / xanthone (*xpt*) gene clusters were expressed (Bayram et al., 2016). The monodictyphenone (*mdp*) gene cluster is located at the silent telomeric region of chromosome VIII. This could lead to the assumption that the expression of the monodictyphenone (*mdp*) gene cluster is generally reduced under laboratory conditions. Biosynthetic proteins encoded by the monodictyphenone (*mdp*) gene cluster are required for the production of the precursor monodictyphenone. This compound is converted into prenyl xanthenes (Sanchez et al., 2011).

Interestingly genes for the production of xanthenes are not embedded in the monodictyphenone (*mdp*) gene cluster. Biosynthetic proteins encoded by both gene clusters are present in sexual mycelium and Hülle cells. This suggests that both gene clusters collaborate, further correlating with other insights. Sanchez and co-workers showed that these two gene clusters collaborate for the synthesis of xanthenes (Sanchez et al., 2011).

The findings of this thesis indicate that Hülle cells contain biosynthetic proteins for the synthesis of antimicrobial substances such as xanthenes. This leads to the assumption that Hülle cells have a protective capacity during the maturation of cleistothecia.

4.2. Submerged liquid cultures revealed the presence of the prenyltransferase NptA and the serine/threonine kinase RfeA in Hülle cells and in other fungal tissues

Proteins from liquid cultures were analyzed and quantified. A *laeA* Δ strain with abolished Hülle cells was used for this analysis. The result was compared to the parental strain which produces Hülle cells (Figure 47). Biosynthetic proteins encoded by the monodictyphenone (*mdp*) / xanthone (*xpt*) gene cluster were present. Besides of that the prenyltransferase NptA and the serine/threonine kinase RfeA which are involved in the process of secondary metabolism are localized to Hülle cells and other fungal tissues.

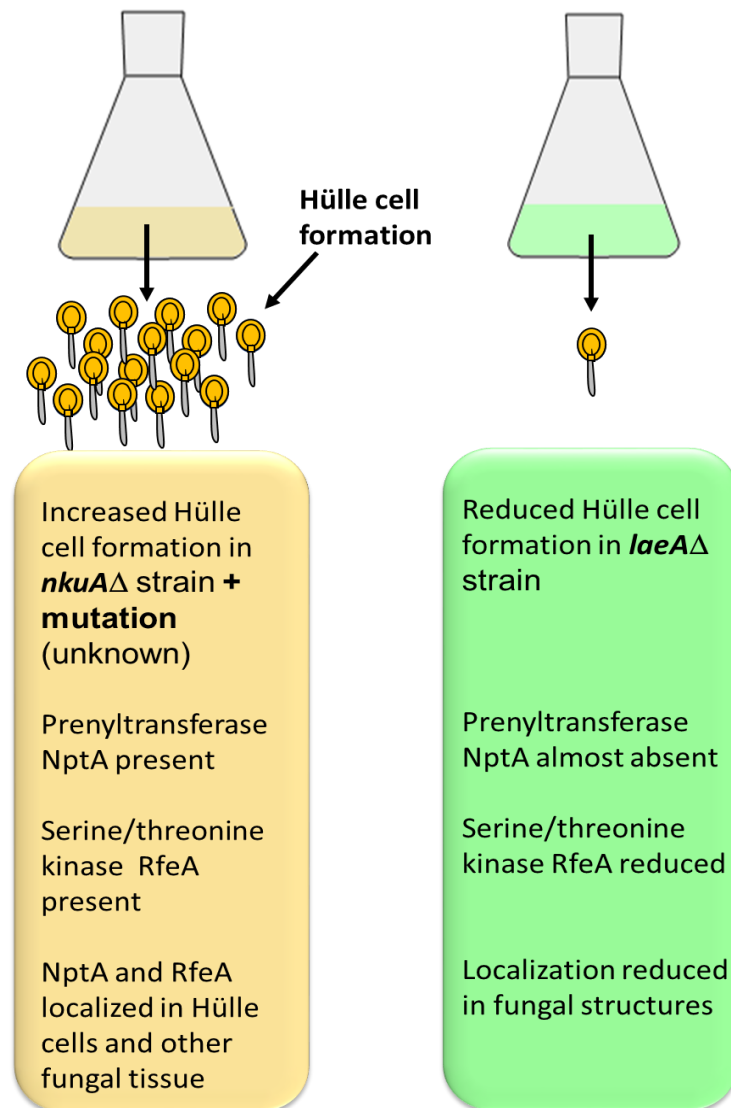


Figure 47. Hülle cell formation in submerged liquid cultures and comparison of two strains causing different results.

In a *nkuA* Δ parental strain with an unknown mutation increased Hülle cell formation is observable whereas in a *laeA* Δ strain reduced Hülle cell formation occurs. Both strains are shown under submerged liquid conditions. The protein amount of the prenyltransferase NptA and the serine/threonine kinase RfeA is significantly reduced in *laeA* Δ strain in comparison to the parental strain. The protein quantity of NptA is almost not detectable in a *laeA* Δ strain. NptA and RfeA are localized in Hülle cells and other fungal tissues. The localization of these proteins is reduced in a *laeA* Δ mycelium in different fungal structures.

Alves and co-workers showed that after the addition of the nutrient choline Hülle cell formation occurred in submerged liquid cultures and the compound monodictyphenone was present (Alves et al., 2016). This suggests that a vegetative mycelium forming Hülle cells in submerged liquid cultures has the potential to produce an antimicrobial agent. This aligns to the insights of this thesis since biosynthetic proteins for the production of monodictyphenone and xanthenes are observable in submerged liquid cultures.

This could lead to the assumption that Hülle cells, present in these submerged liquid cultures, produce also these proteins. These proteins also appear in hyphal structures. Cleistothecia are normally not formed in submerged liquid cultures. This is why the production of monodictyphenone, that has a protective capacity is noteworthy in submerged liquid cultures. The presence of proteins encoded by the monodictyphenone (*mdp*) / xanthone (*xpt*) gene clusters is unexpected in submerged liquid cultures since the production of monodictyphenone and xanthenes are linked to the sexual development of the fungus (Bayram et al., 2016).

In order to analyze proteins from submerged liquid cultures, a *laeA*Δ strain was used. In a *laeA*Δ strain, the formation of Hülle cells is abolished in comparison to a *nkuA*Δ strain with an additional unknown mutation that produce increased numbers of Hülle cells under submerged conditions. As expected, a *laeA*Δ strain correlates with abolished Hülle cells (Sarıkaya-Bayram et al., 2010). *A. nidulans* wild-type (FGSC A4 Glasgow, *veA*⁺) usually forms no Hülle cells or cleistothecia in submerged conditions. Prolonging the growth has no effect on the production of Hülle cells (Bayram et al., 2009, Bayram et al., 2008a). Unexpectedly, a *nkuA*Δ (*pabaA1;yA;nkuAΔ::argB*, AGB552) parental strain that contains an additional unknown mutation produces enlarged numbers of Hülle cells in submerged liquid cultures. Bayram and co-workers showed that after deleting the *cryA* gene that encodes a cryptochrome/photolyase Hülle cell formation occurred in submerged liquid cultures. Furthermore, it was shown that CryA has a function in DNA-repair (Bayram et al., 2008a). The gene *nkuA* encodes an ATP-dependent DNA helicase II that is involved in the repair process of double-strand breaks in DNA (Nayak et al., 2006). DNA repair activities possibly have an influence on the formation of Hülle cells in submerged liquid conditions. A variety of possible mutations in the *nkuA*Δ (AGB552) strain could most probably cause the production of Hülle cell formation in submerged liquid cultures. This mutation could be caused by single-nucleotide polymorphism (SNP) and this leads to a diverse possibility of mutations that could cause Hülle cell formation in submerged cultures.

Bok and co-workers showed that a prenyltransferase *tidB* was not expressed in a *laeA*Δ mycelium in comparison to the wild-type (Bok et al., 2006). The same applies to the insight of this study regarding the prenyltransferase NptA, since the protein quantity of NptA is significantly reduced in *laeA*Δ.

This is consensual and expected since it is known that LaeA regulates more than 50% of all secondary metabolite gene clusters in various fungi (Sarikaya-Bayram et al., 2010, Dhingra et al., 2013, Zhao et al., 2017). Andersen, Oakley and co-workers predicted that the prenyltransferase NptA is involved in the prenylation of nidulanin A (Andersen et al., 2013, Oakley et al., 2017). The addition of stable isotope labeled amino acids to *A. nidulans* cultures and the incorporation of these labels into nidulanin A, revealed that this compound is a tetracyclopeptide consisting of four different amino acids (Klitgaard et al., 2015).

The finding of this thesis is that the prenyltransferase NptA is localized in the cytoplasm of Hülle cells and other fungal tissues. Therefore, the prenylation of a cyclopeptide such as nidulanin A might also occur in Hülle cells. Besides of NptA which is reduced in a *laeA* Δ strain additional proteins such as tRNA ligases are also reduced. It was shown that cyclopeptides influence the production of chlamydospores in *Candida albicans* (Spraker et al., 2016). This supports the assumption that cyclopeptides may have an influence on Hülle cells.

A serine/threonine kinase RfeA is not yet characterized in detail and *in silico* analyses showed that it is a protein kinase with a predicted role in secondary metabolic regulation (Mogensen et al., 2006). Deletion of *rfeA* in *A. nidulans* had no effects on fungal development (De Souza et al., 2013). Findings of this thesis revealed that the serine/threonine kinase RfeA is localized in different fungal tissues such as Hülle cells and is reduced in a *laeA* Δ mycelium. This shows that beside LaeA as a key regulator in secondary metabolism RfeA might also be involved in the process of secondary metabolism. The amino acid sequence identity shared between RfeA and their *Homo sapiens* homologs is 32% to Chk1 (Stajich et al., 2012). The serine/threonine-specific protein kinase Chk1 encoded by the *chk1* gene coordinates DNA damage response (Kabeche et al., 2018). Again, possible DNA repair activities of RfeA could have an influence on Hülle cells. The finding of this thesis indicates that increased Hülle cell formation in submerged cultures is observable in a *nkuA* Δ parental strain together with an additional mutation. This is in contrast to a *laeA* Δ strain that causes a significant reduction in Hülle cell formation. Moreover, NptA and RfeA are reduced in a *laeA* Δ strain.

4.3. Hülle cells from surface and liquid cultures comprise shared proteins encoded by the monodictyphenone (*mdp*) / xanthone (*xpt*) gene clusters

In order to perform a comparative proteomic approach cultures derived from solid agar plates and submerged liquid media were analyzed. Hülle cells from solid agar plates and submerged liquid cultures were enriched and proteins found in both types of cultures were analyzed. In order to perform the investigation in submerged liquid cultures a *nkuA*Δ strain with an additional unknown mutation which forms increased numbers of Hülle cells in submerged liquid cultures was compared to a *laeA*Δ strain which under these conditions forms less Hülle cells. The comparison of Hülle cells from surface and liquid cultures shows that both cultures comprise shared proteins encoded by the monodictyphenone (*mdp*) / xanthone (*xpt*) gene clusters (Figure 48). The ankyrin repeat domain protein AnkG (AN8434) and a the tyrosinase domain protein (AN8435) are also commonly observable in both cultures. The maltose permease-like protein MphA is observable in enriched Hülle cells from surface cultures. In liquid cultures MphA seems not to be clearly present.

Findings of this thesis showed that different approaches to enrich Hülle cells led to different results. In order to increase the enrichment of Hülle cells from solid agar plate cultures the cleistothecia-rolling technique was applied. Enriched Hülle cell fractions from surface agar plate compared to a submerged liquid culture represent a small amount of starting material. In comparison homogenous material in a submerged liquid culture represents optimal conditions for proteomics. This might be the reason why only 401 solid agar plate culture proteins were identified from enriched Hülle cell fractions. From vegetative mycelia 974 proteins could be identified and differed in more than 50% compared to the 401 proteins mentioned above.

Limitation in quantification of protein abundances within the SILAC approach need to be considered. The use of only lysine auxotrophic parental strains instead of lysine in combination with arginine auxotrophic parental strains limited the quantification of a complete pattern of fungal proteins. Peptides that contain arginine residues were therefore not considered for the quantification. Peptides that only contain isotopically labeled L-lysine reduce the quantification of protein abundances in complex mixtures.

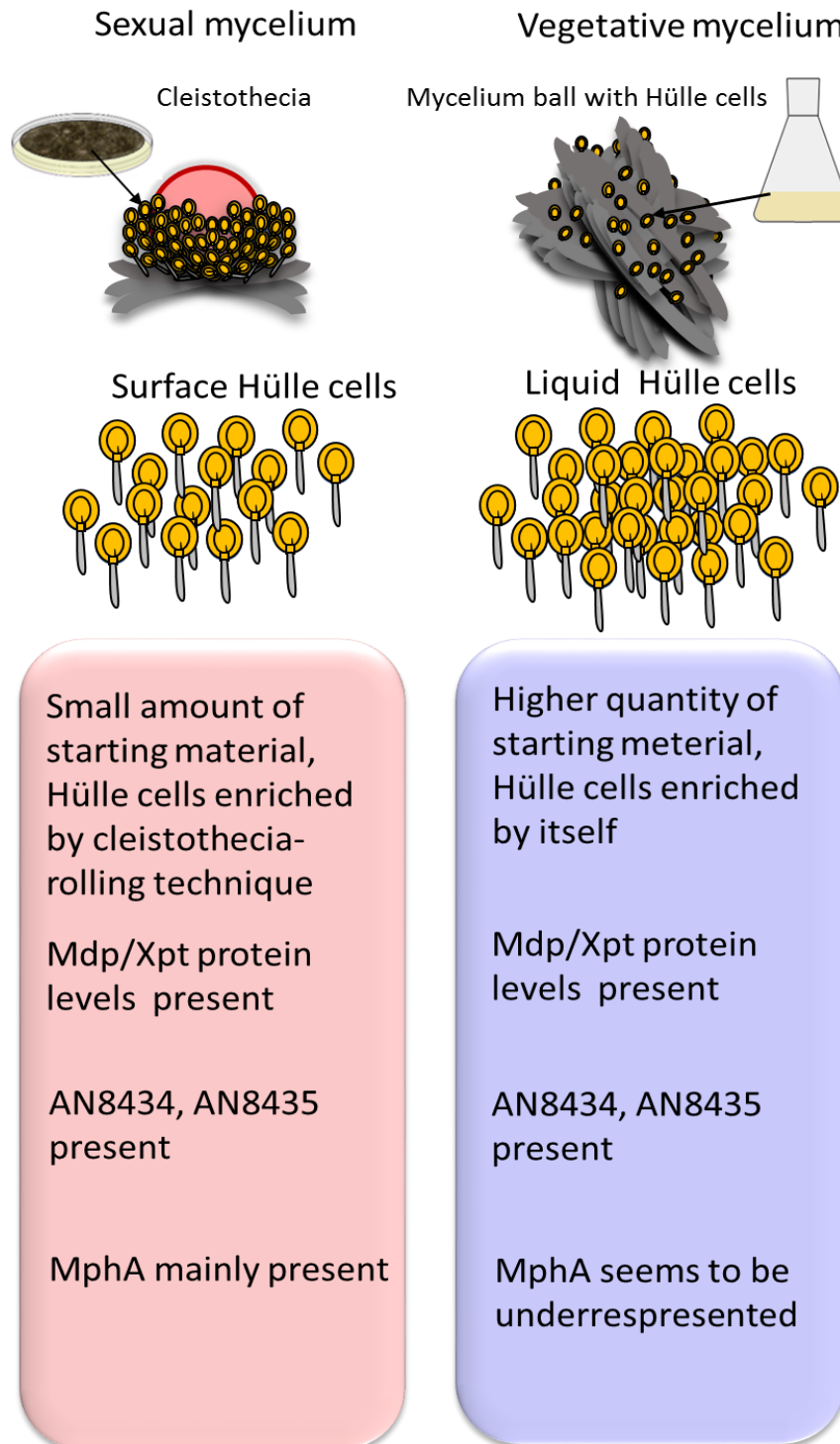


Figure 48. The comparison of the proteome of both types of Hülle cells.

The picture shows Hülle cells that are situated in a mycelium grown on surface agar plates or in submerged liquid cultures. On the left-hand side hundreds of Hülle cells surround the cleistothecium grown on solid agar plate and are enriched by the cleistothecia-rolling technique. On the right hand side Hülle cells are shown in a mycelium ball of a submerged liquid culture. This culture contains thousands of small vegetative mycelium balls with Hülle cells. After 72 hours the undifferentiated vegetative mycelium is capable to produce Hülle cells. These Hülle cells are rather randomly distributed and are not in contact with the cleistothecia since they are not produced in liquid cultures. Hülle cell enrichment is enhanced by itself. Hülle cells contain increased monodictyphenone (*mdp*) / xanthone (*xpt*) biosynthetic protein levels. The ankyrin domain protein (AN8434) and the tyrosinase domain protein (AN8435) are found in both types of Hülle cells. The maltose permease-like protein MphA (AN2601) seems to be mainly present in Hülle cells grown on solid agar plates.

Besides of technical issues, there are several biological reasons why the different approaches led to different outcomes. Hülle cells in vegetative mycelia in submerged liquid cultures are rather randomly distributed throughout the mycelia ball. In comparison Hülle cells are associated with the cleistothecia on solid agar plate cultures. The development of cleistothecia on surface cultures leads to differences in the composition of the proteome. Formation of cleistothecia on surface cultures most likely requires different carbohydrate transporters (Wei et al., 2004). This could be the reason why MphA is not clearly represented in submerged liquid cultures since cleistothecia are not usually formed under these conditions.

Interestingly biosynthetic proteins encoded by the monodictyphenone (*mdp*) / xanthone (*xpt*) gene clusters are present in both cultures. During initial vegetative growth phase, the fungus produces less secondary metabolites (Calvo et al., 2002). The production of secondary metabolites is specifically linked to the distinct developmental programs of the fungus (Bayram et al., 2016). Martins and co-workers showed in a proteomic study that after the addition of the nutrient choline, Hülle cell formation occurred in submerged liquid cultures and proteins encoded by secondary metabolite clusters were found (Martins et al., 2013). It is interesting that in a vegetative growth where Hülle cell formation occurred biosynthetic proteins encoded by the monodictyphenone (*mdp*) / xanthone (*xpt*) gene clusters are observable. It seems that the formation of Hülle cells in submerged liquid cultures goes along with the production of proteins which are required for biosynthesis of monodictyphenone and xanthenes which are antimicrobial substances.

Different outcome from cultures on solid agar plate and under liquid conditions shows that biosynthetic proteins of the monodictyphenone (*mdp*) / xanthone (*xpt*) clusters are present in both cultures. Only the MphA protein does not seem to be clearly represented in submerged liquid cultures. This could lead to the assumption that MphA has a specific function during surface growth. One of these functions could be the nursing of cleistothecia.

4.4. Hülle cells from surface growth and liquid media comprise an ankyrin and a tyrosinase protein

The AnkG (AN8434) ankyrin repeat domain protein and the tyrosinase domain protein (AN8435) were found in both approaches. The domain architecture of the AnkG (AN8434) ankyrin repeat domain protein and the tyrosinase domain protein (AN8435) is shown in Figure 49.



Figure 49. Domain architecture of the AnkG (AN8434) ankyrin repeat domain protein and the tyrosinase domain protein (AN8435).

The sequence of the AnkG ankyrin repeat domain protein of *A. nidulans* comprises 477 amino acids contains three ankyrin repeat domains and seems to have a membrane associated region (with a von Willebrand factor typ A-like domain). The sequence of the tyrosinase domain protein (AN8435) comprises 846 amino acids and a tyrosinase domain (Jones et al., 2014).

The present thesis sheds light on the localization of the ankyrin repeat domain protein AnkG to the membrane of the subtending hyphae of Hülle cells. This aligns to the findings that ankyrin proteins are localized to membranes (Islam et al., 2018). Interestingly AnkG was underrepresented in the membrane of vegetative hyphae and therefore AnkG might play a role in the outer membrane of the subtending hyphae of Hülle cells. During initial growth AnkG is most likely situated also in the endoplasmic reticulum (ER) of vegetative hyphae. AnkG is most probably transported by vesicle mediated transportation to the membrane of the subtending hyphae of Hülle cells (Figure 50). During vegetative growth the fusion protein AnkG::GFP is probably situated in the ER as well as in the cytoplasm shown in Figure 37 E). The localization of AnkG::GFP in subtending hyphae is shown in Figure 37 B).

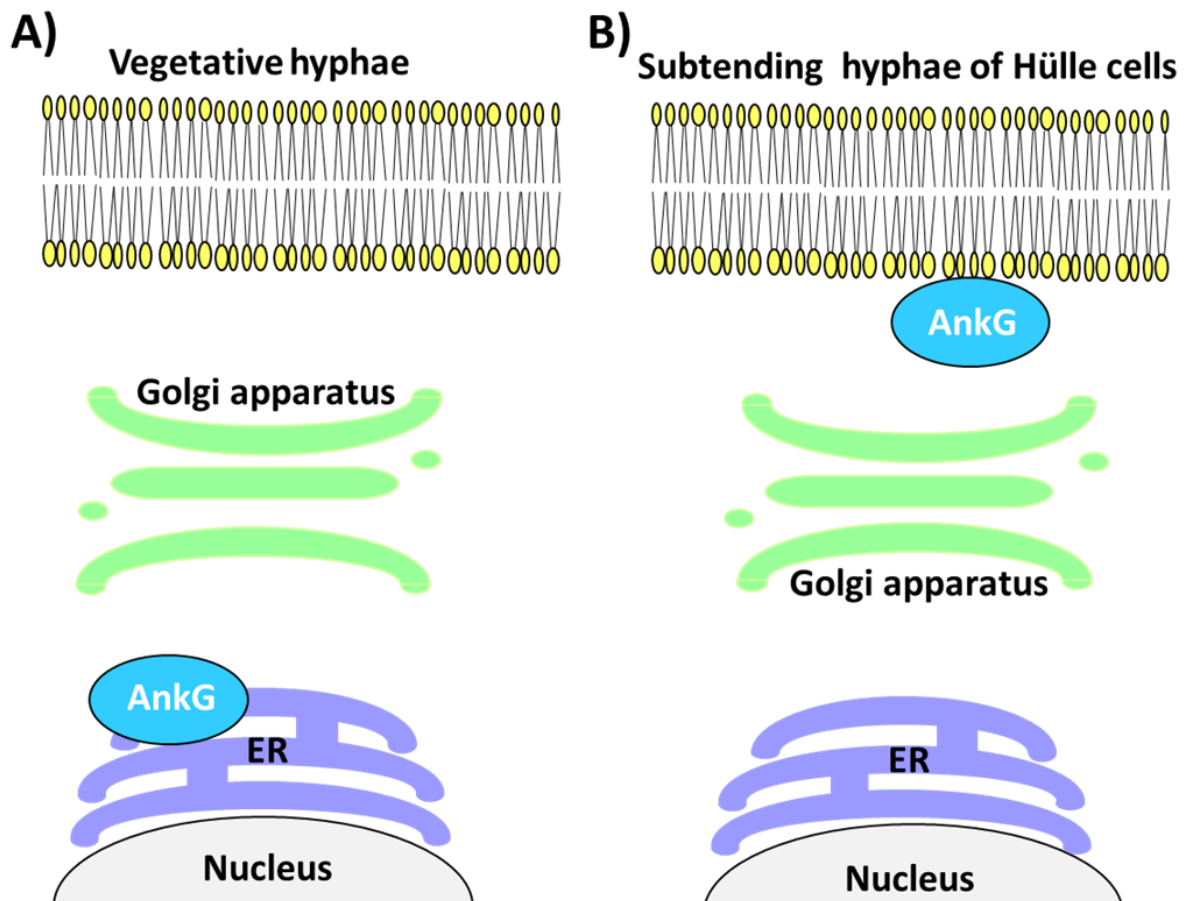


Figure 50. Protein trafficking of the AnkG ankyrin domain protein.

A) During initial vegetative growth AnkG is underrepresented in the membrane. It seems that AnkG is localized in the endoplasmic reticulum (ER) as well as in the cytoplasm during initial vegetative growth. B) Subsequently AnkG is transported to the subtending hyphae of Hülle cells.

Ankyrin repeat domain proteins are involved in the process of trafficking tyrosinase into melanocytes (Tamura et al., 2011). Melanocytes are cells which produce melanin for pigmentation. Non-pigmented cleistothecia such as those in *Aspergillus tonophilus* or *Aspergillus fisheri* are accompanied with the lack of Hülle cell formation (Hermann, et al., 1983). This goes along with the absence of the laccase II CpeA that is localized in Hülle cells (Scherer et al., 2002). Tyrosinase and laccase are known to be involved in the regulation and production of melanin pigmentation (Chai et al., 2017, Hsu et al., 2016). This supports the finding that Hülle cells have an auxiliary function in pigmentation during cleistothecia maturation. The possible localization of the tyrosinase domain protein AN8435 in Hülle cells supports the finding that Hülle cells have an auxiliary function in pigmentation of the cleistothecia. This aligns to the finding that in different *Aspergilli* without Hülle cells the cleistothecia are not pigmented.

Tyrosinases are known to undergo a complex post-translational processing before reaching melanocytes. This process includes N-glycosylation in several binding sites, movement from the endoplasmic reticulum (ER) to the golgi apparatus and copper binding (Olivares et al., 2003). As shown in Figure 39 and 40 fluorescence microscope investigation in combination with western hybridization suggest that the tyrosinase domain protein AN8435 found in different cellular compartments within fungal structures like Hülle cells is modified by a post-translational process. This corresponds to the fact that tyrosinase domains are post-translationally modified and are found in different cellular compartments (Olivares et al., 2003). The tyrosinase protein AN8435 seems to be unstable, which limited the observation of a precise localization.

Bayram and co-workers showed that the transcripts of *AN8435* and *AN8434 (ankG)* are expressed in asexual and sexual mycelia (Bayram et al., 2016). This suggests that AN8434 (AnkG) and AN8435 are found in different mycelia types. This aligns to the findings of this thesis since AN8435 and AN8434 (AnkG) is present in different mycelia types including sexual and vegetative mycelia as well as Hülle cells.

The tyrosinase domain protein (AN8435) and the AnkG (AN8434) ankyrin repeat domain protein are encoded by neighbouring genes. This could be interpreted as a co-regulation of these proteins. Bayram and co-workers also suggested that the transcripts *AN8435* and *AN8434 (ankG)* are expressed by a gene cluster which is involved in the production of an unknown pigment (Bayram et al., 2016). This supports the assumption that the proteins are co-regulated.

4.5. A maltose permease-like protein enriched in surface Hülle cells supports fungal growth and development

A so far unknown maltose permease-like protein MphA was identified and investigated. The corresponding *mphA* gene was deleted in this study. The presence of the MphA maltose permease-like protein in Hülle cells mainly grown on solid agar plates supports the insight that Hülle cells have a function in nutrient supply during fungal growth (Wei et al., 2001). MphA protein was studied in this thesis and the localization of the protein was observed in Hülle cells. The studies revealed that MphA most probably is a membrane protein with difficulties in respect of solubilization. Western hybridization was performed but without success. MphA contains a distinctive sugar motif and comprises high sequence similarities to other carbohydrate transporters (Horák 1997). This suggests that MphA might be active in the transportation of carbohydrates (Figure 51). Since MphA supports growth in general, vegetative, sexual and asexual growth, it is assumed that MphA could also function in other cell types beside Hülle cells. MphA is not essential for Hülle cell formation when Hülle cells are formed on solid agar plates. Adding a high concentration of carbohydrates reduces the formation of early Hülle cells in a *mphA*Δ strain. This is accompanied by a reduced maturation of the cleistothecia and the development of ascospores. Additionally, the development of conidiophores is stalled.

Several nutrient transporters were identified in Hülle cells. Fungal development especially the maturation of the cleistothecia was not effected by deleting the putative hexose *hxtA* and the putative purine transporters *uapA* or *azgA* (Wei et al., 2004, Dos Reis et al., 2017, Pantazopoulou et al., 2007). This suggests that additional nutrient transporters are needed during maturation of the cleistothecia. Cleistothecia formation requires high amounts of energy in the form of carbohydrate initially stored in vegetative hyphae. This fact indicates an existence of effective transportation systems for nutrient uptake into the cells of developing cleistothecia (Pöggeler et al., 2006). As expected, alternative possible nutrient transporters were observed in Hülle cells in this study.

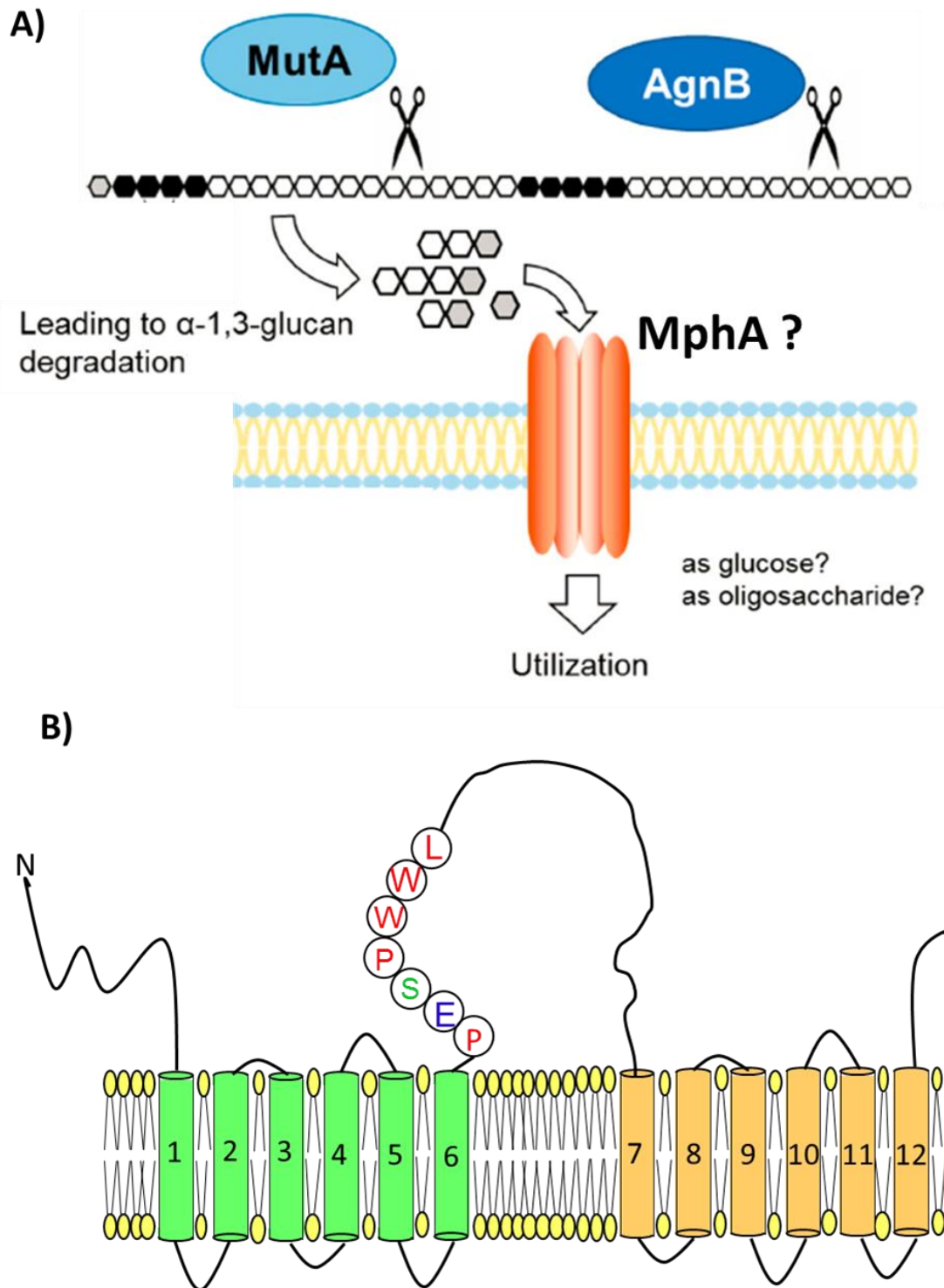


Figure 51. Model for the maltose permease-like protein MphA in the transportation of α -1,3 glucans in *Aspergillus nidulans*.

A) In Hülle cells the α -1,3 glucanases MutA and AgnB are required in the processes of degrading of α -1,3 glucans. MphA might be involved in the transportation of carbohydrates. This could lead to a supporting function during nutrient supply for the growth of the fungus, especially the cleistothecium. Image modified (Yoshimi et al., 2017). B) Model for a possible structure of MphA. The sequence of MphA consists of 540 amino acids and contains twelve transmembrane helices which, in turn consist of two 6-helix bundles connected by a cytoplasmic loop. This loop contains a sequence motif (PESP(W)L) which is specific for all sugar transporters (Horák 1997). MphA might have a central role regarding transportation of carbohydrates.

MphA effects the maturation of cleistothecia and ascospores. Interestingly MphA also influences other developmental processes such as the development of asexual structures like conidiophores. This finding differs to previous studies (Wei et al., 2004, Dos reis et al., 2017, Pantazopoulou et al., 2007). The deletion of the gene *mphA* has an unexpected negative effect on supporting fungal growth, asexual and sexual development. MphA has a central role in supporting fungal structures especially during surface growth. Hülle cells are associated with cleistothecia which need the growth on surfaces. In submerged liquid cultures where cleistothecia are not normally formed, the activity of MphA seems to be reduced.

During vegetative growth α -1,3 glucans are stored in the cell wall and α -1,3-glucanase like MutA found mainly in Hülle cells during surface growth are required for the degradation of these glucans (Zonneveld 1973, Wei et al., 2001, He et al., 2017, Yoshimi et al., 2017). This finding aligns to the observation of this thesis since α -1,3-glucanase MutA is unrepresentative during initial vegetative growth and was found in Hülle cells as well as in sexual mycelium.

Hülle cells are known to nurse the cleistothecia during maturation since abolished Hülle cells correlate with a reduced size of the cleistothecia (Sarikaya-Bayram et al., 2010). The deletion of *mphA* appears to correlate with a stalled development of cleistothecia. The addition of higher concentrations of carbohydrates to the *mphA* Δ strain effects the development of the fungus negatively. This suggests that MphA could be crucial for the transportation of carbohydrates since the deletion of gene *mphA* causes a significant reduction of the development regarding cleistothecia and other fungal structures. This finding could support the existence of effective transport systems during development (Pöggeler et al., 2006). The development of thick spherical cells called chlamyospores are produced at the very end of the hyphae in *Candida albicans* and are reduced in higher concentration of carbohydrates (Böttcher et al., 2016). This supports the suggestion and aligns to the observation of this thesis that spore-like structures like chlamyospores and Hülle cells are influenced by carbohydrate metabolism.

Taken together, this study shows that sexual differentiation increases monodictyphenone (*mdp*) / xanthone (*xpt*) biosynthetic protein levels localized in differentiated sexual cell types. Hülle cells formed in surface and liquid cultures contain shared proteins encoded by the monodictyphenone (*mdp*) / xanthone (*xpt*) gene

clusters. Proteins encoded by these gene clusters are found in a sexual mycelium with high amounts of Hülle cells grown on surface agar plate cultures. Monodictyphenone and xanthones are antimicrobial substances against fungivory and other environmental threats and thereby protecting the fungus (Regulin and Kempken 2018, Chen et al., 2017, Bok et al., 2009). This suggests that Hülle cells and sexual mycelium are involved in the production of an antimicrobial agent.

Studies of the deletion strain *mphA* Δ demonstrate that MphA protein promotes fungal growth, asexual and sexual development. MphA was identified in enriched Hülle cells from surface growth and was underrepresented in submerged liquid cultures. This points out that Hülle cells are supporting fungal growth (Figure 52).

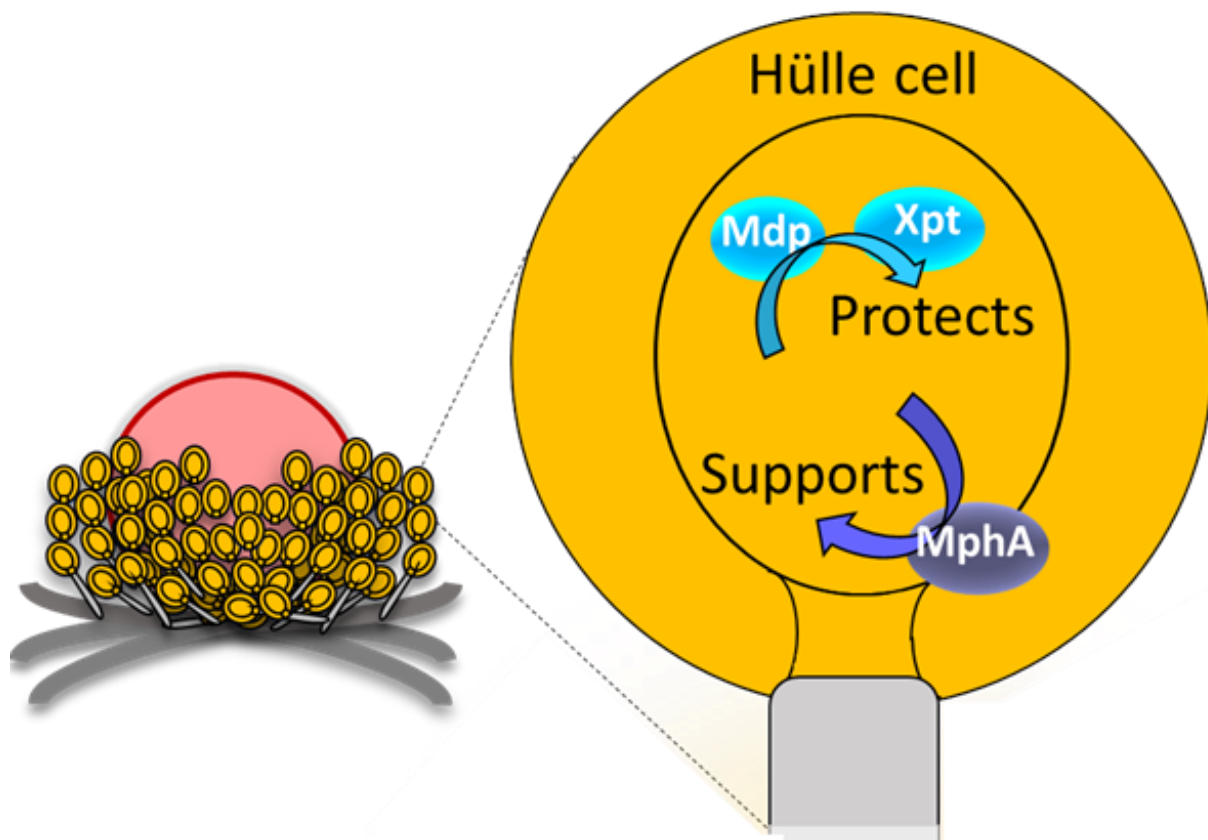


Figure 52. Hülle cells protect and support the cleistothecia.

The picture shows left a cleistothecium surrounded by Hülle cells. On the right a single enlarged Hülle cell is shown. Sexual differentiation of *A. nidulans* increases monodictyphenone (*mdp*) / xanthone (*xpt*) biosynthetic protein levels. Enzymes encoded by the monodictyphenone (*mdp*) / xanthone (*xpt*) gene clusters are found in Hülle cells. Monodictyphenone and xanthones are antimicrobial substances. This suggests that the synthesis of an antimicrobial substance is crucial during maturation of the cleistothecia. The MphA maltose permease-like protein was found in Hülle cells. MphA promotes fungal growth and development.

4.6. Conclusion

The central findings of this thesis lead to the conclusion that sexual differentiation of *Aspergillus nidulans* increases biosynthetic proteins encoded by the monodictyphenone (*mdp*) / xanthone (*xpt*) secondary metabolite gene clusters. These proteins are present in a sexual mycelium with high amounts of Hülle cells from solid agar plate cultures. Proteins encoded by the monodictyphenone (*mdp*) / xanthone (*xpt*) secondary metabolite gene clusters are present in Hülle cells and in other fungal cell types. Bayram and co-workers showed that the transcripts of the monodictyphenone (*mdp*) / xanthone (*xpt*) clusters are specifically expressed during sexual development (Bayram et al., 2016). The presence of the prenyltransferase XptB and the oxidoreductase XptC encoded by the xanthone (*xpt*) secondary metabolite gene cluster was studied in this thesis and their localization in Hülle cells and other fungal tissues could be confirmed. Monodictyphenone and xanthonones are antimicrobial agents that protect most probably the fungus especially sexual structures against fungivory and other environmental threats (Regulin and Kempken 2018, Chen et. al., 2017, Bok et al., 2009) The cleistothecia of *A. nidulans* covered with Hülle cells are more resistant against fungivory when comparing to vegetative or asexual tissue (Döll et. al, 2013). In this study it was shown that proteins required for the synthesis of antimicrobial substances such as monodictyphenone and xanthonones, are present in Hülle cells. This confirms the assumption that Hülle cells have a capacity to protect the cleistothecia.

Secondly, this thesis shows that protein quantities of prenyltransferase NptA and the serine/threonine kinase RfeA are reduced in a *laeA*Δ strain. These proteins are localized in Hülle cells and in other fungal tissues. For this analysis a parental *nkuA*Δ strain with an additional unknown mutation that leads to increased numbers of Hülle cells was compared to a *laeA*Δ strain that forms reduced numbers of Hülle cells both under submerged liquid conditions. Overall, this thesis provides insights that demonstrate that prenyltransferases NptA and serine/threonine kinase RfeA are localized in different fungal cell types including Hülle cells and the protein quantity is reduced in strains lacking *LaeA*. This aligns to the findings that other prenyltransferases such as *tidB* are not expressed in a *laeA*Δ strain (Bok et al., 2006). *RefA* is mainly uncharacterized in *A. nidulans* (De Souza et. al., 2013).

Furthermore, the AnkG (AN8434) ankyrin repeat domain protein and the tyrosine domain protein (AN8435) are found in enriched Hülle cells from solid agar plate as well as in submerged liquid cultures. Ankyrin repeat domain proteins are adaptor proteins associated with membranes (Islam et al., 2017). Additionally, observations in this study aligned to the findings that AnkG (AN8434) ankyrin repeat domain protein is associated to the membrane and furthermore, is localized to the membrane of the subtending hyphae of Hülle cells. Beyond that, in this thesis the localization of tyrosinase domain protein (AN8435) was studied. Probably AN8435 is localized to Hülle cells and other fungal tissues. Tyrosinases are known to be involved in the process of pigmentation (Chai et al., 2017, Hsu et al., 2016). The absence of Hülle cells in *Aspergillus tonophilus* and *Aspergillus fisheri* correlates with non-pigmented cleistothecia (Hermann et al., 1983). This indicates that Hülle cells are potentially important for pigmentation and, therefore, tyrosinases are most probably required during the maturation process of the cleistothecia.

Lastly the findings of this thesis reveal that the MphA protein supports fungal growth and development and that MphA protein is specially enriched in Hülle cells. During the thesis research the corresponding gene of MphA was deleted and observation demonstrated that MphA promotes fungal development and growth. MphA protein supports also the maturation of the cleistothecium. Abolished Hülle cell formation correlates with a significantly reduced size of the cleistothecia (Sarıkaya-Bayram et al., 2010). This supports the view that Hülle cells have a nursing function to nourish the growing cleistothecia.

Taken together the biological function of Hülle cells is highly likely to have a protective and a nursing function especially during sexual development. Further research is hence needed to determine the biological function of Hülle cells during sexual development in more detail.

References

- Aaij, C., & Borst, P. 1972. The gel electrophoresis of DNA. *Biochimica et Biophysica Acta (BBA) – Nucleic Acids and Protein Synthesis* **269**:192-200.
- Abraham, W. R. 2018. Fumitremorgins and relatives - from tremorgenic compounds to valuable anti-cancer drugs. *Current Medicinal Chemistry* **25**:123-140.
- Ahmed, Y. L., Gerke, J., Park, H. S., Bayram, Ö., Neumann, P., Ni, M., Dickmanns, A., Kim, S. C., Yu, J. H., Braus, G. H., & Ficner, R. 2013. The velvet family of fungal regulators contains a DNA-binding domain structurally similar to NF- κ B. *PLoS Biology* **11**: e1001750.
- Alam, S., & Khan, F. 2018. Virtual screening, docking, ADMET and system pharmacology studies on *Garcinia* caged xanthone derivatives for anticancer activity. *Scientific Report* **8**: 5524.
- Alkahyyat, F., Ni, M., Kim, S. C., & Yu, J. H. 2015. The WOPR domain protein OsaA orchestrates development in *Aspergillus nidulans*. *PLoS One* **10**: e0137554.
- Alves, P. C., Hartmann, D. O., Núñez, O., Martins, I., Gomes, T. L., Garcia, H., Galceran, M. T., Hampson, R., Becker, J. D., & Silva-Pereira, C. 2016. Transcriptomic and metabolomic profiling of ionic liquid stimuli unveils enhanced secondary metabolism in *Aspergillus nidulans*. *BMC Genomics* **17**: 284.
- Andersen, M. R., Nielsen, J. B., Klitgaard, A., Petersen, L. M., Zachariassen, M., Hansen, T. J., Blicher, L. H., Gottfredsen, C. H., Larsen, T. O., Nielsen, K. F., & Mortensen, U. H. 2013. Accurate prediction of secondary metabolite gene clusters in filamentous fungi. *Proceedings of the National Academy of Sciences of the United States of America* **110**: E99-E107.
- Bayram, Ö., Feussner, K., Dumkow, M., Herrfurth, C., Feussner, I., & Braus, G. H. 2016. Changes of global gene expression and secondary metabolite accumulation during light-dependent *Aspergillus nidulans* development. *Fungal Genetics and Biology* **87**: 30-53.
- Bayram, Ö., & Braus, G. H. 2012. Coordination of secondary metabolism & development in fungi: the velvet family of regulatory proteins. *FEMS Microbiology Reviews* **36**: 1-24.
- Bayram, Ö., Sarikaya-Bayram, Ö., Valerius, O., Jöhnk, B., & Braus, G. H. 2012. Identification of protein complexes from filamentous fungi with tandem affinity purification. *Methods in Molecular Biology* **944**: 191-205.
- Bayram, Ö., Sari, F., Braus, G. H., & Irniger, S. 2009. The protein kinase ImeB is required for light-mediated inhibition of sexual development and for mycotoxin production in *Aspergillus nidulans*. *Molecular Microbiology* **71**: 1278-1295.
- Bayram, Ö., Biesemann, C., Krappmann, S., Galland, P., & Braus, G. H. 2008a. More than a repair enzyme: *Aspergillus nidulans* photolyase-like CryA is a regulator of sexual development. *Molecular Biology of the Cell* **19**: 3254-3262.
- Bayram, Ö., Krappmann, S., Ni, M., Bok, J. W., Helmstaedt, K., Valerius, O., Braus-Stromeyer, S., Kwon, N. J., Keller, N. P., & Braus, G. H. 2008b. VelB / VeA / LaeA complex coordinates light signal with fungal development and secondary metabolism. *Science* **320**: 1504-1506.

- Beck, J., & Ebel, F. 2013. Characterization of the major woronin body protein HexA of the human pathogenic mold *Aspergillus fumigatus*. *International Journal of Medical Microbiology* **303**: 90-97.
- Bennett, R. J., & Turgeon, B. G. 2017. Fungal sex: the Ascomycota. In: *The fungal kingdom*. Heitman, J., James, T., Gow, N. (eds.), Washington, D.C., United States of America, ASM Press, pp. 117-145.
- Böttcher, B., Pöllath, C., Staib, P., Hube, B., & Brunke, S. 2016. *Candida* species rewired hyphae developmental programs for chlamydospore formation. *Frontiers in Microbiology* **7**: 1697.
- Bok, J. W., & Keller, N. P. 2016. 2 Insight into fungal secondary metabolism from ten years of LaeA research. In: *Biochemistry and molecular biology. The mycota III, a comprehensive treatise on fungi as experimental systems for basic and applied research*. Hoffmeister, D. (ed.), Springer International Publishing, pp 21-29.
- Bok, J. W., Chiang, Y. M., Szewczyk, E., Reyes-Dominguez, Y., Davidson, A. D., Sanchez, J. F., Lo, H. C., Watanabe, K., Strauss, J., Oakley, B. R., Wang, C. C., & Keller, N. P. 2009. Chromatin-level regulation of biosynthetic gene clusters. *Nature Chemical Biology* **5**: 462-464.
- Bok, J. W., Hoffmeister, D., Maggio-Hall, L. A., Murillo, R., Glasner, J. D., & Keller, N. P. 2006. Genomic mining for *Aspergillus* natural products. *Chemistry & Biology*. **13**: 31-37.
- Bok, J. W., & Keller, N. P. 2004. LaeA, a regulator of secondary metabolism in *Aspergillus* spp. *Eukaryotic Cell* **3**: 527-535.
- Bouhired, S., Weber, M., Kempf-Sontag, A., Keller, N. P., & Hoffmeister, D. 2007. Accurate prediction of the *Aspergillus nidulans* terrequinone gene cluster boundaries using the transcriptional regulator LaeA. *Fungal Genetics and Biology* **44**: 1134-1145.
- Bradford, M. M. 1976. A rapid and sensitive method for the quantitation of microgram quantities of protein utilizing the principle of protein-dye binding. *Analytical biochemistry* **72**: 248-254.
- Brakhage, A. A. 2013. Regulation of fungal secondary metabolism. *Nature Reviews Microbiology* **11** : 21-32.
- Braus, G. H., Krappmann, S., & Eckert, S. E. 2002. Sexual development in ascomycetes: fruit body formation of *Aspergillus nidulans*. In: *Molecular biology of Fungal Development*. Osiewacz, H. D. (ed.), New York, United States of America, Marcel Dekker, Inc., pp. 215-244.
- Busch, S., & Braus, G. H. 2007. How to build a fungal fruit body: from uniform cells to specialized tissue. *Molecular Microbiology* **64**: 873-876.
- Caballero-Ortiz, S., Trienens, M., & Rohlfs, M. 2013. Induced fungal resistance to insect grazing: reciprocal fitness consequences and fungal gene expression in the *Drosophila-Aspergillus* model system. *PLoS One* **8**: e74951.
- Calera, J. A., Sanchez-Weatherby, J., Lopez-Medrano, R., & Leal, F. 2000. Distinctive properties of the catalase B of *Aspergillus nidulans*. *FEBS letter* **475**: 117-120.
- Calvo, A. M., Wilson, R. A., Bok, J. W., & Keller, N. P. 2002. Relationship between secondary metabolism and fungal development. *Microbiology and Molecular Biology Reviews* **66**: 447-459.

- Carvalho, M. D. F., Baracho, M. S., & Baracho, I. R. 2002. An investigation of the nuclei of Hülle cells of *Aspergillus nidulans*. *Genetics and Molecular Biology* **25**: 485-488.
- Cary, J. W., Harris-Coward, P., Scharfenstein, L., Mack, B. M., Chang, P. K., Wei, Q., Lebar, M., Carter-Wientjes, C., Majumdar, R., Mitra, C., Banerjee, S., & Chanda, A. 2017. The *Aspergillus flavus* homeobox, *hbx1*, is required for development and aflatoxin production. *Toxins* **9**: 315.
- Cerqueira, G. C., Arnaud, M. B., Inglis, D. O., Skrzypek, M. S., Binkley, G., Simison, M., Miyasato, S. R., Binkley, J., Orvis, J., Shah, P., Wymore, F., Sherlock, G., & Wortman, J. R. 2014. The *Aspergillus* Genome Database: multispecies curation and incorporation of RNA-Seq data to improve structural gene annotations. *Nucleic Acids Research* **42**: D705–D710.
- Chai, B., Qiao, Y., Wang, H., Zhang, X., Wang, J., Wang, C., Zhou, P., & Chen, X. 2017. Identification of YfiH and the catalase CatA as polyphenol oxidases of *Aeromonas media* and CatA as a regulator of pigmentation by its peroxy radical scavenging capacity. *Frontiers in Microbiology* **8**: 1939.
- Champe, S. P., & Simon, L. D. 1992. Cellular differentiation and tissue formation in the fungus *Aspergillus nidulans*. In: *An analysis of the development of biological structure*. Rossomando, E. F., Alexander, S. (eds.), New York, United States of America, Marcel Dekker Inc., pp. 63-91.
- Chang, P. K., Scharfenstein, L. L., Li, R. W., Arroyo-Manzanares, N., De Saeger, S., & Diana Di Mavungu, J. 2017. *Aspergillus flavus* *aswA*, a gene homolog of *Aspergillus nidulans* *oefC*, regulates sclerotial development and biosynthesis of sclerotium-associated secondary metabolites. *Fungal Genetics and Biology* **104**: 29-37.
- Chen, A. J., Frisvad, J. C., Sun, B. D., Varga, J., Kocsubé, S., Dijksterhuis, J., Kim, D. H., Hong, S. B., Houbraken, J., & Samson, R. A. 2016. *Aspergillus* Section *Nidulantes* (Formerly *Emericella*): polyphasic taxonomy, chemistry and biology. *Studies in Mycology* **84**: 1-118.
- Chen, X., Leng, J., Rakesh, K. P., Darshini, N., Shubhavathi, T., Vivek, H. K., Mallesha, N., & Qin, H. L. 2017. Synthesis and molecular docking studies of xanthone attached amino acids as potential antimicrobial and anti-inflammatory agents. *MedChemComm* **8**: 1706-1719.
- Chiang, Y. M., Szewczyk, E., Davidson, A. D., Entwistle, R., Keller, N. P., Wang, C. C., & Oakley, B. R. 2010. Characterization of the *Aspergillus nidulans* monodictyphenone gene cluster. *Applied and Environmental Microbiology* **76**: 2067-2074.
- Chiang, Y. M., Szewczyk, E., Nayak, T., Davidson, A. D., Sanchez, J. F., Lo, H. C., Ho, W. Y., Simityan, H., Kuo, E., Praseuth, A., Watanabe, K., Oakley, B. R., & Wang, C. C. 2008. Molecular genetic mining of the *Aspergillus* secondary metabolome: discovery of the emericellamide biosynthetic pathway. *Chemistry & Biology* **15**: 527-532.
- Christmann, M., Schmalzer, T., Gordon, C., Huang, X., Bayram, Ö., Schinke, J., Stumpf, S., Dubiel, W., & Braus, G. H. 2013. Control of multicellular development by the physically interacting deneddylases DEN1/DenA and COP9 signalosome. *PLoS Genetics* **9**: e1003275.

- Clevenger, K. D., Bok, J. W., Ye, R., Miley, G. P., Verdan, M. H., Velk, T., Chen, C., Yang, K., Robey, M. T., Gao, P., Lamprecht, M., Thomas, P. M., Islam, M. N., Palmer, J. M., Wu, C. C., Keller, N., P. & Kelleher, N. L. 2017. A scalable platform to identify fungal secondary metabolites and their gene clusters. *Nature Chemical Biology* **13**: 895-901.
- Conesa, A., Götz, S., García-Gómez, J. M., Terol, J., Talón, M., & Robles, M. 2005. Blast2GO: a universal tool for annotation, visualization and analysis in functional genomics research. *Bioinformatics* **21**: 3674-3676.
- Dambacher, C. M., Worden, E. J., Herzik, M. A., Martin, A., & Lander, G. C. 2016. Atomic structure of the 26S proteasome lid reveals the mechanism of deubiquitinase inhibition. *eLife* **5**: e13027.
- Dasgupta, A., Fuller, K. K., Dunlap, J. C., & Loros, J. J. 2016. Seeing the World differently: variability in the photosensory mechanisms of two model fungi. *Environmental Microbiology*. **18**: 5-20.
- De Groot, P. W., Brandt, B. W., Horiuchi, H., Ram, A. F., de Koster, C. G., & Klis, F. M. 2009. Comprehensive genomic analysis of cell wall genes in *Aspergillus nidulans*. *Fungal Genetics and Biology* **46**: S72-S81.
- Demain, A. L., & Fang, A. 2000. The natural functions of secondary metabolites. *Advances in Biochemical Engineering/Biotechnology* **69**: 1-39.
- De Souza, C. P., Hashmi, S. B., Osmani, A. H., Andrews, P., Ringelberg, C. S., Dunlap, J. C., & Osmani, S. A. 2013. Functional analysis of the *Aspergillus nidulans* kinome. *PLoS One* **8**: e58008.
- De Vries, R. P., Riley, R., Wiebenga, A., Aguilar-Osorio, G., Amillis, S., Uchima, C. A., Anderluh, G., & Asadollahi, M. 2017. Comparative genomics reveals high biological diversity and specific adaptations in the industrially and important fungal genus *Aspergillus*. *Genome Biology* **18**: 28.
- Dhingra, S., Lind, A. L., Lin, H. C., Tang Y., Rokas, A., & Calvo, A. M. 2013. The fumagillin gene cluster, an example of hundreds of genes under *veA* control in *Aspergillus fumigatus*. *PLoS One* **8**: e77147.
- Döll, K., Chatterjee, S., Scheu, S., Karlovsky, P., & Rohlfs, M. 2013. Fungal metabolic plasticity and sexual development mediate induced resistance to arthropod fungivory. *Proceedings of the Royal Society B: Biological Science* **280**: 20131219.
- Dos Reis, T. F., Nitsche, B. M., de Lima, P. B., de Assis, L. J., Mellado, L., Harris, S. D., Meyer, V., Dos Santos, R. A., Riaño-Pachón, D. M., Ries, L. N., & Goldman, G. H. 2017. The low affinity glucose transporter HxtB is also involved in glucose signalling and metabolism in *Aspergillus nidulans*. *Scientific Reports* **7**: 45073.
- Drott, M. T., Lazzaro, B. P., Brown, D. L., Carbone, I., & Milgroom, M. G. 2017. Balancing selection for aflatoxin in *Aspergillus flavus* is maintained through interference competition with and fungivory by insects. *Proceedings of the Royal Society B: Biological Science* **284**: 20172408.
- Durfee, T., & Schwei, T. 2008. DNASTAR's next-generation software. In: *Next generation genome sequencing: towards personalized medicine*. Janitz, M. (ed.), Weinheim, Germany, Wiley-VCH Verlag, pp. 89-94.

- Dyer, P. S., & O' Gorman, C. M. 2012. Sexual development and cryptic sexuality in fungi: insights from *Aspergillus* species. *FEMS Microbiology Reviews* **36**: 165-192.
- Dyer, P. S., Ingram, D. S., & Johnstone, K. 1993. Evidence for the involvement of linoleic acid and other endogenous lipid factors in perithecial development of *Nectria haematococca* mating population VI. *Mycological Research* **97**: 485-496.
- Eckert, S. E., Hoffmann, B., Wanke, C., & Braus, G. H. 1999. Sexual development of *Aspergillus nidulans* in tryptophan auxotrophic strains. *Archives of Microbiology* **172**: 157-166.
- Eidam, E. 1883. Zur Kenntnis der Entwicklung bei den Ascomyceten. III. *Sterigmatocystis nidulans* n. sp. In: *Beiträge zur Biologie der Pflanzen*. Laibach, F. (ed.), Berlin, Germany, Dunker & Humblot, pp. 377-433.
- Elbein, A. D., Pan, Y. T., Pastuszak, I., & Carroll, D. 2003. New insights on trehalose: a multifunctional molecule. *Glycobiology* **13**: 17-27.
- Ellis, T. T., Reynolds, D. R., & Alexopoulos, C. J. 1973. Hülle cell development in *Emericella nidulans*. *Mycologia* **65**: 1028-1035.
- Eng, J. K., McCormack, A. L., & Yates, J. R. 1994. An approach to correlate tandem mass spectral data of peptides with amino acid sequences in a protein database. *American Society for Mass Spectrometry* **5**: 976-989.
- Engl, I., Nowrousian, M., & Kück, U. 2007. Regulation of melanin biosynthesis via the dihydroxynaphthalene pathway is dependent on sexual development in the ascomycete *Sordaria macrospora*. *FEMS Microbiology Letters* **275**: 62-70.
- Etxebeste, O., Villarino, M., Markina-Iñarrairaegui, A., Araújo-Bazán, L., & Espeso, E. 2013. Cytoplasmic dynamics of general nuclear import machinery in apically growing syncytial cells. *PLoS One* **8**: e85076.
- Flipphi, M., Sun, J., Robellet, X., Karaffa, L., Fekete, E., Zeng, A. P., & Kubiecek, C. P. 2009. Biodiversity and evolution of primary carbon metabolism in *Aspergillus nidulans* and other *Aspergillus* spp. *Fungal Genetics and Biology* **1**: S19-S44.
- Flores-Gallegos, A. C., Veana-Hernandez, F., Michel-Michel, M., Lara-Victoriano, F., & Rodriguez-Herrera R. 2016. Molecular evolution of *Aspergillus*. In: *New and future developments in microbial biotechnology and bioengineering – Aspergillus system properties and applications*. Gupta, V. K. (ed.), Amsterdam, Netherlands, Elsevier, pp. 41-51.
- Gacek, A., & Strauss, J. 2012. The chromatin code of fungal secondary metabolite gene clusters. *Applied Microbiology and Biotechnology* **95**: 1389-1404.
- Galagan, J. E., Calvo, S. E., Cuomo, C., Ma, L. J., Wortman, J. R., Batzoglou, S., Lee, S. I. Basturkmen, M., et al. 2005. Sequencing of *Aspergillus nidulans* and comparative analysis with *A. fumigatus* and *A. oryzae*. *Nature* **438**: 1105-1115.
- Gerke, J., & Braus, G. H. 2014. Manipulation of fungal development as source of novel secondary metabolites for biotechnology. *Applied Microbiology and Biotechnology*. **98**: 8443-8455.
- Goodrich-Tanrikulu, M., Jacobson, D. J., Stafford, A. E., Lin, J. T., & McKeon, T. A. 1999. Characterization of *Neurospora crassa* mutants isolated following repeat-induced point mutation of the beta subunit of fatty acid. *Current Genetics* **36**: 147-152.

- Goody, R. S., Müller, M. P., & Wu, Y. W. 2017. Mechanisms of action of Rab proteins, key regulators of intracellular vesicular transport. *Biological Chemistry* **398**: 565-575.
- Guerrero, G., Silvestrini, L., Legay, S., Maixner, F., Sulyok, M., Hausman, J. F., & Strauss, J. 2017. Deletion of the *celA* gene in *Aspergillus nidulans* triggers overexpression of secondary metabolite biosynthetic genes. *Scientific Reports* **7**: 5978.
- Han, K. H., Lee, D. B., Kim, J. H., Kim, M. S., Han, K. Y., Kim, W. S., Park, Y. S., Kim, H. B., & Han, D. M. 2003. Environmental factors affecting development of *Aspergillus nidulans*. *The Journal of Microbiology* **41**: 34-40.
- Han, K. H., Han, K. Y., Yu, J. H., Chae, K. S., Jahng, K. Y., & Han, D. M. 2001. The *nsdD* gene encodes a putative GATA-Type transcription factor necessary for sexual development of *Aspergillus nidulans*. *Molecular Microbiology* **41**: 299-309.
- Hanahan, D., Jessee, J., & Bloom, F. R. 1991. Plasmid transformation of *Escherichia coli* and other bacteria. *Methods in Enzymology* **204**: 63-113.
- He, X., Li, S., & Kaminskyj, S. 2017. An amylase-like protein, AmyD is the major negative regulator for α -glucan synthesis in *Aspergillus nidulans* during the asexual life cycle. *International Journal of Molecular Sciences* **18**: 695.
- Heckman, D. S., Geiser, D. M., Eidell, B. R., Stauffer, R. L., Kardos, N. L., & Hedges, S. B. 2001. Molecular evidence for the early colonization of land by fungi and plants. *Science* **293**: 1129-1133.
- Hermann, T. E., Kurtz, M., & Champe, S. P. 1983. Laccase localized in Hulle cells and cleistothecial primordia of *Aspergillus nidulans*. *Journal of Bacteriology* **154**: 955-964.
- Hernández-Rodríguez, Y., Hastings, S., & Momany, M. 2012. The septin AspB in *Aspergillus nidulans* forms bars and filaments and plays roles in growth emergence and conidiation. *Eukaryotic Cell* **11**: 311-323.
- Horák, J. 1997. Yeast nutrient transporters. *Biochimica et Biophysica Acta (BBA)-Reviews on Biomembranes* **1**: 41-79.
- Hou, B., Lin, Y., Wu, H., Guo, M., Petkovic, H., Tao, L., Zhu, X., Ye, J., & Zhang, H. 2017. The novel transcriptional regulator LmBU promotes lincomycin biosynthesis through regulating expression of its target genes in *Streptomyces lincolnensis*. *Journal of Bacteriology* **200**: e00447-17.
- Hsu, K. D., Chen, H. J., Wang, C. S., Lum, C. C., Wu, S. P., Lin, S. P., & Cheng, K. C. 2016. Extract of *Ganoderma formosanum* mycelium as a highly potent tyrosinase inhibitor. *Scientific Reports* **6**: 32854.
- Islam, Z., Nagampalli, R. S. K., Fatima, M. T., & Ashraf, G. M. 2018. New paradigm in ankyrin repeats: beyond protein-protein interaction module. *International Journal of Biological Macromolecules* **109**: 1164-1173.
- Itoh, E., Shigemoto, R., Oinuma, K. I., Shimizu, M., Masuo, S., & Takaya, N. 2017. Sirtuin A regulates secondary metabolite production by *Aspergillus nidulans*. *The Journal of General and Applied Microbiology* **63**: 228-235.

- Jiang, P., Wei, W. F., Zhong, G. W., Zhou, X. G., Qiao, W. R., Fischer, R., & Lu, L. 2017. The function of the three phosphoribosyl pyrophosphate synthetase (Prs) genes in hyphal growth and conidiation in *Aspergillus nidulans*. *Microbiology* **163**: 218-232.
- Jöhnk, B., Bayram, Ö., Abelmann, A., Heinekamp, T., Mattern, D. J., Brakhage, A. A., Jacobsen, I. D., Valerius, O., & Braus, G. H. 2016. SCF ubiquitin ligase F-box controls nuclear co-repressor localization, stress response and virulence of the human pathogen *Aspergillus fumigatus*. *PLoS Pathogens* **12**: e1005899.
- Jones, P., Binns, D., Chang, H. Y., Fraser, M., Li, W., McAnulla, C., McWilliam, H., Maslen, J., Mitchell, A., Nuka, G., Pesseat, S., Quinn, A. F., Sangrador-Vegas, A., Scheremetjew, M., Yong, S. Y., Lopez, R., & Hunter, S. 2014. InterProScan 5: genome-scale protein function classification. *Bioinformatics* **30**: 1236-1240.
- Kabeche, L., Nguyen, H. D., Buisson, R., & Zou, L. 2018. A mitosis-specific and R loop-driven ATR pathway promotes faithful chromosome segregation. *Science* **359**: 108-114.
- Kale, S. P., Milde, L., Trapp, M. K., Frisvad, J. C., Keller, N. P., & Bok, J. W. 2008. Requirement of LaeA for secondary metabolism and sclerotial production in *Aspergillus flavus*. *Fungal Genetics and Biology* **45**: 1422-1429.
- Karimi-Aghcheh, R., Bok, J. W., Phatale, P. A., Smith, K. M., Baker, S. E., Lichius, A., Omann, M., Zeilinger, S., Seiboth, B., Rhee, C., Keller, N. P., Freitag, M., & Kubicek, C. P. 2013. Functional analyses of *Trichoderma reesei* LAE1 reveal conserved and contrasting roles of this regulator. *G3 (Bethesda)* **3**: 369-378.
- Keller, N. P., Turner, G., & Bennett, J. W. 2005. Fungal secondary metabolism - from biochemistry to genomics. *Nature Reviews Microbiology* **3**: 937-947.
- Kim, H., Han, K., Kim, K., Han, D., Jahng, K., & Chae, K. 2002. The *veA* gene activates sexual development in *Aspergillus nidulans*. *Fungal Genetics and Biology* **37**: 72-80.
- Kim, H. Y., Han, K. H., Lee, M., Oh, M., Kim, H. S., Zhixiong, X., Han, D. M., Jahng, K. Y., Kim, J. H., & Chae, K. S. 2009. The *veA* gene is necessary for the negative regulation of the *veA* expression in *Aspergillus nidulans*. *Current Genetics* **55**: 391-407.
- Kim, S., Matsuo, I., Ajisaka, K., Nakajima, H., & Kitamoto, K. 2002. Cloning and characterization of the *nagA* gene that encodes beta-n-acetylglucosaminidase from *Aspergillus nidulans* and its expression in *Aspergillus oryzae*. *Bioscience, Biotechnology, and Biochemistry* **66**: 2168-2175.
- Kim, Y. J., Yu, Y. M., & Maeng, P. J. 2017. Differential control of asexual development and sterigmatocystin biosynthesis by a novel regulator in *Aspergillus nidulans*. *Scientific reports* **7**: e46340.
- Kirk, K. E., & Morris, N. R. 1991. The *tubB* alpha-tubulin gene is essential for sexual development in *Aspergillus nidulans*. *Genes & Development* **5**: 2014-2023.
- Kirkwood, M., Todd, J. D., Rypien, K. L., & Johnston, A. W. 2010. The opportunistic coral pathogen *Aspergillus sydowii* contains *dddP* and makes dimethyl sulfide from dimethylsulfoniopropionate. *The ISME Journal* **4**: 147-150.

References

- Kleijnstrup, M. L., Frandsen, R. J. N., Holm, D. K., Nielsen, M. T., Mortensen, U. H., Larsen, T. O., & Nielsen, J. B. 2012. Genetics of polyketide metabolism in *Aspergillus nidulans*. *Metabolites* **2**: 100-133.
- Klitgaard, A., Nielsen, J. B., Frandsen, R. J., Andersen, M. R., & Nielsen, K. F. 2015. Combining stable isotope labeling and molecular networking for biosynthetic pathway characterization. *Analytical Chemistry* **87**: 6520-6526.
- Knox, B. P., Blachowicz, A., Palmer, J. M., Romsdahl, J., Huttenlocher, A., Wang, C. C., Keller, N. P., Venkateswaran, K. 2016. Characterization of *Aspergillus fumigatus* isolates from air and surfaces of the international space station. *mSphere* **1**: e00227-16.
- Koenig, T., Menze, B. H., Kirchner, M., Monigatti, F., Parker, K. C., Patterson, T., Steen, J. J., Hamprecht, F. A., & Steen, H. 2008. Robust prediction of the MASCOT score for an improved quality assessment in mass spectrometric proteomics. *Journal of Proteome Research* **7**: 3708-3717.
- König, H. G., Schwamborn, R., Andresen, S., Kinsella, S., Watters, O., Fenner, B., & Prehn, J. H. 2017. NF- κ B regulates neuronal ankyrin-G via a negative feedback loop. *Scientific Reports* **7**: e42006.
- Krappmann, S., Bayram, Ö., & Braus, G. H. 2005. Deletion and allelic exchange of the *Aspergillus fumigatus* *veA* locus via a novel recyclable marker module. *Eukaryotic Cell* **4**: 1298-1307.
- Laemmli, U. K. 1970. Cleavage of structural proteins during the assembly of the head of bacteriophage T4. *Nature* **227**: 680-685.
- Lee, S. B. & Taylor, J. W. 1990. Isolation of DNA from fungal mycelia and single spores. In: *PCR protocols: a guide to methods and applications*. Innis, N., Gelfand, D., Sninsky, D., & White, T. (eds.), New York, United States of America, Academic Press, pp 282-287.
- Lehman, I. R. 1974. DNA ligase: structure, mechanism, and function. *Science* **186**: 790-797.
- Lenobel, R., Sebela, M., & Frebort, I. 2005. Mapping the primary structure of copper/topaquinone containing methylamine oxidase from *Aspergillus niger*. *Folia Microbiology* **50**: 401-408.
- Malavazi, I., Savoldi, M., da Silva Ferreira, M. E., Soriani, F. M., Bonato, P. S., de Souza Goldman, M. H., & Goldman, G. H. 2007. Transcriptome analysis of the *Aspergillus nidulans* *AtmA* (*ATM*, Ataxia-Telangiectasia mutated) null mutant. *Molecular Microbiology* **66**: 74-99.
- Malavazi, I., Savoldi, M., Di Mauro, S. M., Menck, C. F., Harris, S. D., Goldman, M. H., & Goldman, G. H. 2006. Transcriptome analysis of *Aspergillus nidulans* exposed to camptothecin-induced DNA damage. *Eukaryotic Cell* **5**: 1688-1704.
- Margelis, S., D'Souza, C., Small, A. J., Hynes, M. J., Adams, T. H., & Davis, M. A. 2001. Role of glutamine synthetase in nitrogen metabolite repression in *Aspergillus nidulans*. *Journal of Bacteriology* **183**: 5826-5833.
- Martins, I., Hartmann, D., Alves, P. C., Planchon, S., Renaut, J., Leitão, M. C., Rebelo, L. P. N., & Pereira, C., S. 2013. Proteomic alterations induced by ionic liquids in *Aspergillus nidulans* and *Neurospora crassa*. *Journal of Proteomics* **94**: 262-278.

- Mendoza-Martínez, A. E., Lara-Rojas, F., Sánchez, O., & Aguirre, J. 2017. NapA mediates a redox regulation of the antioxidant response, carbon utilization and development in *Aspergillus nidulans*. *Frontiers in Microbiology* **8**: 516.
- Mounts, P., Wu, T. C., & Peden, K. 1989. Method for cloning single-stranded oligonucleotides in a plasmid vector. *BioTechniques* **7**: 356-359.
- Muntanjola-Cvetkovic, M., & Vukic, V. V. 1972. Influence of light on Hülle cell and aleuriospore formation in *Aspergillus*. *Transactions of British Mycological Society* **58**: 67-72.
- Nakamura, T., Maeda, Y., Tanoue, N., Makita, T., Kato, M., & Kobayashi, T. 2006. Expression profile of amyolytic genes in *Aspergillus nidulans*. *Bioscience, Biotechnology, and Biochemistry* **70**: 2363-2370.
- Navarathna, D. H., Pathirana, R. U., Lionakis, M. S., Nickerson, K. W., & Roberts, D. D. 2016. *Candida albicans* ISW2 regulates chlamydospore suspensor cell formation and virulence *in vivo* in a mouse model of disseminated candidiasis. *PLoS One*. **11**: e0164449.
- Nayak, T., Szewczyk, E., Oakley, C. E., Osmani, A., Ukil, L., Murray, S. L., Hynes, M. J., Osmani, S. A., & Oakley, B. R. 2006. A versatile and efficient gene-targeting system for *Aspergillus nidulans*. *Genetics* **172**: 1557-1566.
- Nekiunaite, L., Arntzen, M., Svensson, B., Vaaje-Kolstad, G., & Abou Hachem, M. 2016. Lytic polysaccharide monooxygenases and other oxidative enzymes are abundantly secreted by *Aspergillus nidulans* grown on different starches. *Biotechnology for Biofuels* **9**: 187.
- Neuhoff, V., Arold, N., Taube, D., & Ehrhardt, W. 1988. Improved staining of proteins in polyacrylamide gels including isoelectric focusing gels with clear background at nanogram sensitivity using coomassie brilliant blue G-250 and R-250. *Electrophoresis* **9**: 255-262.
- Nishimura, I., Shinohara, Y., Oguma, T., & Koyama, Y. 2018. Survival strategy of the salt-tolerant lactic acid bacterium, *Tetragenococcus halophilus*, to counteract koji mold, *Aspergillus oryzae*, in soy sauce brewing. *Bioscience, Biotechnology and Biochemistry* **8**: 1-7.
- Noble, L. M., & Andrianopoulos, A. 2013. Reproductive competence: a recurrent logic module in eukaryotic development. *Proceedings of the Royal Society B: Biological Science* **280**: 20130819.
- Noordin, M. A. M., Noor, M. M., Kamaruddin, W. M. A. W., Lazim, A. M., & Fazry, S. 2016. Toxicity test of xanthone from mangosteen on zebrafish embryos. *AIP Conference Proceedings* **1784**: 020014.
- Oakley, B. R. 2004. Tubulins in *Aspergillus nidulans*. *Fungal Genetics and Biology* **41**: 420-427.
- Oakley, C. E., Ahuja, M., Sun, W. W., Entwistle, R., Akashi, T., Yaegashi, J., Guo, C. J., Cerqueira, G. C., Russo Wortman, J., Wang, C. C., Chiang, Y. M., & Oakley, B. R. 2017. Discovery of *mcrA*, a master regulator of *Aspergillus* secondary metabolism. *Molecular Microbiology* **103**: 347-365.

- Obayashi, E., Luna, R. E., Nagata, T., Martin-Marcos, P., Hiraishi, H., Singh, C. R., Erzberger, J. P., Zhang, F., et al. 2017. Molecular landscape of the ribosome pre-initiation complex during mRNA scanning: structural role for eIF3c and its control by eIF5. *Cell Reports* **18**: 2651-2663.
- Olivares, C., Solano, F., & Garcia-Borron, J. C. 2003. Conformation-dependent post-translational glycosylation of tyrosinase. Requirement of a specific interaction involving the CuB metal binding site. *Journal of Biological Chemistry* **278**: 15735-15743.
- Oliveros, J. C. 2007. VENNY an interactive tool for comparing lists with Venn diagrams. <http://bioinfogp.cnb.csic.es/tools/venny/index.html>.
- Pan, L. L., Song, L. F., Miao, Y., Yang, Y., & Merz, K. M. Jr. 2017. Mechanism of formation of the nonstandard product in the prenyltransferase reaction of the G115T mutant of FtmPT1: a case of reaction dynamics calling the shots? *Biochemistry* **56**: 2995-3007.
- Pantazopoulou, A., Lemuh, N. D., Hatzinikolaou, D. G., Drevet, C., Cecchetto, G., Scazzocchio, C., & Diallinas, G. 2007. Differential physiological and developmental expression of the UapA and AzgA purine transporters in *Aspergillus nidulans*. *Fungal Genetics and Biology* **44**: 627-640.
- Patananan, A. N., Palmer, J. M., Garvey, G. S., Keller, N. P., & Clarke, S. G. 2013. A novel automethylation reaction in the *Aspergillus nidulans* LaeA protein generates S-methylmethionine. *Journal of Biological Chemistry* **288**: 14032-14045.
- Park, H. S., Lee, M. K., Kim, S. C., & Yu, J. H. 2017. The role of VosA/VelB-activated developmental gene *vadA* in *Aspergillus nidulans*. *PLoS One* **12**: e0177099.
- Petersen, L. M., Hoeck, C., Frisvad, J. C., Gottfredsen, C. H., & Larsen, T. O. 2014. Dereplication guided discovery of secondary metabolites of mixed biosynthetic origin from *Aspergillus aculeatus*. *Molecules* **19**: 10898-10921.
- Pitt, J. I., Samson, R. A., & Frisvad, J. C. 2000. List of accepted species and their synonyms in the family Trichocomaceae. In: *Integration of modern taxonomic methods for Penicillium and Aspergillus classification*. Samson R. A., & Pitt, J. (eds.), Amsterdam, Netherlands, Harwood Academic Publishers, pp. 9-49.
- Pockrandt, D., Ludwig, L., Fan, A., König, G. M., & Li, S. M. 2012. New insights into the biosynthesis of prenylated xanthenes: XptB from *Aspergillus nidulans* catalyses an O-prenylation of xanthenes. *Chembiochem* **13**: 2764-2771.
- Pöggeler, S., Nowrousian, M., Teichert, I., Beier, A., & Kück, U. 2018. Fruiting-body development in ascomycetes. In: *The mycota XV, physiology and genetics 2nd edition*. Anke, T., Schöffler, A. (eds.), Springer International Publishing, pp 1-56.
- Pöggeler, S., Nowrousian, M., & Kück, U. 2006. Fruiting-body development in ascomycetes. In: *The mycota I, growth, differentiation and sexuality, 2nd edition*. Kues, U., & Fischer, R.(eds.), Berlin, Germany, Springer Verlag, pp 325-355.
- Punt, P. J., & van den Hondel, C. A. 1992. Transformation of filamentous fungi based on hygromycin B and phleomycin resistance markers. *Methods in Enzymology* **216**: 447-457.
- Punt, P. J., Dingemanse, M. A., Jacobs-Meijsing, B. J., Pouwels, P.H., & van den Hondel, C. A. 1988. Isolation and characterization of the glyceraldehyde-3-phosphate dehydrogenase gene of *Aspergillus nidulans*. *Gene* **69**: 49-57.

- Pusztahelyi, T., Molnár, Z., Emri, T., Klement, E., Miskei, M., Kerékgyártó, J., Balla, J., & Pócsi, I. 2006. Comparative studies of differential expression of chitinolytic enzymes encoded by *chiA*, *chiB*, *chiC* and *nagA* genes in *Aspergillus nidulans*. *Folia Microbiologica* **51**: 547-554.
- Rajasekaran, K., Sayler, R. J., Sickler, C. M., Majumdar, R., Jaynes, J. M., & Cary, J. W. 2018. Control of *Aspergillus flavus* growth and aflatoxin production in transgenic maize kernels expressing a tachyplesin-derived synthetic peptide, AGM182. *Plant Science* **270**: 150-156.
- Raper, K. B., & Fennell, I. 1965. The genus *Aspergillus*. In: The genus *Aspergillus*. Austwick, P. K. C. (ed.), Baltimore, Maryland, United States of America, Williams and Wilkins pp. 1-686.
- Rappsilber, J., Mann, M., & Ishihama, Y. 2007. Protocol for micro-purification, enrichment, pre-fractionation and storage of peptides for proteomics using StageTips. *Nature Protocols* **2**: 1896-1906.
- Regulin, A., & Kempken, F. 2018. Fungal genotype determines survival of *Drosophila melanogaster* when competing with *Aspergillus nidulans*. *PLoS One* **13**: e0190543.
- Reyes-Dominguez, Y., Bok, J. W., Berger, H., Shwab, E. K., Basheer, A., Gallmetzer, A., Scazzocchio, C., Keller, N. P., & Strauss, J. 2010. Heterochromatic marks are associated with the repression of secondary metabolism clusters in *Aspergillus nidulans*. *Molecular Microbiology* **76**: 1376-1386.
- Röhrig, J., Yu, Z., Chae, K. S., Kim, J. H., Han, K. H., & Fischer, R. 2017. The *Aspergillus nidulans* velvet-interacting protein, VipA, is involved in light-stimulated heme biosynthesis. *Molecular Microbiology* **105**: 825-838.
- Ruger-Herreros, C., Rodríguez-Romero, J., Fernández-Barranco, R., Olmedo, M., Fischer, R., Corrochano, L. M., & Canovas, D. 2011. Regulation of conidiation by light in *Aspergillus nidulans*. *Genetics* **188**: 809-822.
- Rypien, K. L., Andras, J. P., & Harvell, C. D. 2008. Globally panmictic population structure in the opportunistic fungal pathogen *Aspergillus sydowii*. *Molecular Ecology* **17**: 4068-4078.
- Saiki, R. K., Gelfand, D. H., Stoffel, S., Scharf, S. J., Higuchi, R., Horn, G. T., Mullis, K. B., & Erlich, H. A. 1988. Primer-directed enzymatic amplification of DNA with a thermostable DNA polymerase. *Science* **239**: 487-491.
- Salazar, M., Vongsangnak, W., Panagiotou, G., Andersen, R., & Nielsen, J. 2009. Uncovering transcriptional regulation of glycerol metabolism in *Aspergilli* through genome-wide gene expression data analysis. *Molecular Genetics and Genomics* **282**: 571-586.
- Samson, R. A., Visagie, C. M., Houbraken, J., Hong, S. B., Hubka, V., Klaassen, C. H., Perrone, G., Seifert, K. A., Susca, A., Tanney, J. B., Varga, J., Kocsube, S., Szigeti, G., Yaguchi, T., & Frisvad, J. C. 2014. Phylogeny, identification and nomenclature of the genus *Aspergillus*. *Studies in Mycology* **78**: 141-173.
- Sanchez, J. F., Chiang, Y. M., Szewczyk, E., Davidson, A. D., Ahuja, M., Elizabeth Oakley, C., Bok, W. J., Keller, N. P., Oakley, B. R., & Wang, C. C. 2010. Molecular genetic analysis of the orsellinic acid/F9775 gene cluster *Aspergillus nidulans*. *Molecular Biosystems* **6**: 587-593.

- Sanchez, J. F., Entwistle, R., Hung, J. H., Yaegashi, J., Jain, S., Chiang, Y. M., Wang, C. C., & Oakley, B. R. 2011. Genome-based deletion analysis reveals the prenyl xanthone biosynthesis pathway in *Aspergillus nidulans*. *Journal of the American Chemical Society* **133**: 4010-4017.
- Sarikaya-Bayram, Ö., Bayram, Ö., Feussner, K., Kim, J. H., Kaeffer, A., Feussner, I., Chae, K., S., Han, D. M., Han, K. H., & Braus, G. H. 2014. Membrane-bound methyltransferase complex VapA-VipC-VapB guides epigenetic control of fungal development. *Developmental Cell* **29**: 406-420.
- Sarikaya-Bayram, Ö., Bayram, Ö., Valerius, O., Park, H. S., Irniger, S., Gerke, J., Ni, M., Han, K. H., Yu, J. H., & Braus, G. H. 2010. LaeA control of velvet family regulatory proteins for light-dependent development and fungal cell-type specificity. *PLoS Genetics* **6**: e1001226.
- Satterlee, T., Cary, J. W., & Calvo, A. M. 2016. RmtA, a putative arginine methyltransferase regulates secondary metabolism and development in *Aspergillus flavus*. *PLoS One* **11**: e0155575.
- Scherer, M., Wei, H., Liese, R., & Fischer, R. 2002. *Aspergillus nidulans* catalase peroxidase gene (*cpeA*) is transcriptionally induced during sexual development through the transcription factor *stuA*. *Eukaryotic Cell* **1**: 725-735.
- Schinke, J., Kolog Gulko, M., Christmann, M., Valerius, O., Stumpf, S. K., Stirz, M., & Braus, G. H. 2016. The DenA/DEN1 interacting phosphatase DipA controls septa positioning and phosphorylation-dependent stability of cytoplasmic DenA/DEN1 during fungal development. *PLoS Genetics* **12**: e1005949.
- Schmitt, K., Smolinski, N., Neumann, P., Schmaul, S., Hofer-Pretz, V., Braus, G. H., & Valerius, O. 2017. Asc1p/RACK1 connects ribosomes to eukaryotic phosphosignaling. *Molecular and Cellular Biology* **37**: e00279-16.
- Serlupi-Crescenzi, O., Kurtz, M. B., & Champe, S. P. 1983. Developmental defects resulting from arginine auxotrophy in *Aspergillus nidulans*. *Microbiology* **129**: 3535-3544.
- Shevchenko, A., Wilm, M., Vorm, O., & Mann, M. 1996. Mass spectrometric sequencing of proteins from silver-stained polyacrylamide gels. *Analytical chemistry* **68**: 850-858.
- Shin, K. S., Kwon, N. J., Kim, Y. H., Park, H. S., Kwon, G. S., & Yu, J. H. 2009. Differential roles of the ChiB chitinase in autolysis and cell death of *Aspergillus nidulans*. *Eukaryotic Cell* **8**: 738-746.
- Shlezinger, N., Irmer, H., Dhingra, S., Beattie, S. R., Cramer, R. A., Braus, G. H., Sharon, A., & Hohl, T. M. 2017. Sterilizing immunity in the lung relies on targeting fungal apoptosis-like programmed cell death. *Science* **357**: 1037-1041.
- Simpson, T. J. 2012. Genetic and biosynthetic studies of the fungal prenylated xanthone shamixanthone and related metabolites in *Aspergillus* spp. revisited. *Chembiochem* **13**: 1680-1688.
- Sohn, K. T., & Yoon, K. S. 2002. Ultrastructural study on the cleistothecium development in *Aspergillus nidulans*. *Mycobiology* **30**: 117-127.

- Southern, E. M. 1975. Detection of specific sequences among DNA fragments separated by gel electrophoresis. *Journal of Molecular Biology* **98**: 503-517.
- Soukup, A. A., Fischer, G. J., Luo, J., & Keller, N. P. 2017. The *Aspergillus nidulans* Pbp1 homolog is required for normal sexual development and secondary metabolism. *Fungal Genetics and Biology* **100**: 13-21.
- Spraker, J. E., Sanchez, L. M., Lowe, T. M., Dorrestein, P. C., & Keller, N. P. 2016. *Ralstonia solanacearum* lipopeptide induces chlamydospore development in fungi and facilitates bacterial entry into fungal tissues. *ISME Journal* **10**: 2317-2330.
- Stajich, J. E., Harris, T., Brunk, B. P., Brestelli, J., Fischer, S., Harb, O. S., Kissinger, J. C., Li, W., Nayak, V., Pinney, D. F., Stoeckert, C. J. Jr., & Roos, D. S. 2012. FungiDB: an integrated functional genomics database for fungi. *Nucleic Acids Research*. **40**: 675-681.
- Tamura, K., Ohbayashi, N., Ishibashi, K., & Fukuda, M. 2011. Structure function analysis of VPS9-ankyrin-repeat protein (Varp) in the trafficking of tyrosinase-related protein 1 in melanocytes. *Journal of Biological Chemistry* **286**: 7507- 7521.
- Tian, Y. Q., Lin, X. P., Wang, Z., Zhou, X. F., Qin, X. C., Kaliyaperumal, K., Zhang, T. Y., Tu, Z. C., & Liu, Y. 2015. Asteltoxins with antiviral activities from the marine sponge-derived fungus *Aspergillus sp.* SCSIO XWS02F40. *Molecules* **21**: e34.
- Tsitsigiannis, D. I., & Keller, N. P. 2004a. Oxylipins as developmental and host–fungal communication signals. *Trends in Microbiology* **15**: 109-118.
- Tsitsigiannis, D. I., Zarnowski, R., & Keller, N. P. 2004b. The lipid body protein, PpoA, coordinates sexual and asexual sporulation in *Aspergillus nidulans*. *Journal of Biological Chemistry* **279**: 11344-11353.
- Tyanova, S., Temu, T., & Cox, J. 2016. The MaxQuant Computational platform for mass spectrometry-based shotgun proteomics. *Nature Protocols*. **11**: 2301-2319.
- Upadhyay, S., & Shaw, B. D. 2008. The role of actin, fimbrin and endocytosis in growth of hyphae in *Aspergillus nidulans*. *Molecular Microbiology* **68**: 690-705.
- Upadhyay, S., Torres, G., & Lin, X. 2013. Laccases involved in 1,8-dihydroxynaphthalene melanin biosynthesis in *Aspergillus fumigatus* are regulated by developmental factors and copper homeostasis. *Eukaryotic Cell* **12**: 1641-1652.
- Veraldi, S., Chiaratti, A., & Harak, H. 2010. Onychomycosis caused by *Aspergillus versicolor*. *Mycoses* **53**: 363-365.
- Vienken, K., Scherer, M., & Fischer, R. 2005. The Zn(II)2Cys6 putative *Aspergillus nidulans* transcription factor repressor of sexual development inhibits sexual development under low-carbon conditions and in submerged culture. *Genetics* **169**: 619-630.
- Wartenberg, D., Vödisch, M., Kniemeyer, O., Albrecht-Eckardt, D., Scherlach, K., Winkler, R., Weide, M., & Brakhage, A. A. 2012. Proteome analysis of the farnesol-induced stress response in *Aspergillus nidulans* the role of a putative dehydrin. *Journal of Proteomics* **75**: 4038-4049.

- Wei, H., Vienken, K., Weber, R., Bunting, S., Requena, N., & Fischer, R. 2004. A putative high affinity hexose transporter, HxtA, of *Aspergillus nidulans* is induced in vegetative hyphae upon starvation and in ascogenous hyphae during cleistothecium formation. *Fungal Genetics and Biology* **41**: 148-156.
- Wei, H., Scherer, M., Singh, A., Liese, R. & Fischer, R. 2001. *Aspergillus nidulans* alpha-1,3 glucanase (mutanase), MutA, is expressed during sexual development and mobilizes mutan. *Fungal Genetics and Biology* **34**: 217-227.
- Yamazaki, H., Yamazaki, D., Takaya, N., Takagi, M., Ohta, A., & Horiuchi, H. 2007. A chitinase gene, *chiB*, involved in the autolytic process of *Aspergillus nidulans*. *Current Genetics* **51**: 89-98.
- Yoshimi, A., Miyazawa, K., & Abe, K. 2017. Function and biosynthesis of cell wall α -1,3-glucan in fungi. *Journal of Fungi* **3**: 63.
- Yuan, X. L., van der Kaaij R, M., van den Hondel, C. A., Punt, P. J., van der Maarel, M. J., Dijkhuizen, L., & Ram, A. F. 2008. *Aspergillus niger* genome-wide analysis reveals a large number of novel alpha-glucan acting enzymes with unexpected expression profiles. *Molecular Genetics and Genomics* **279**: 545-561.
- Yu, B., Zhang, X., Sun, W., Xi, X., Zhao, N., Huang, Z., Ying, Z., Liu, L., Liu, D., Niu, H., Wu, J., Zhuang, W., Zhu, C., Chen, Y., & Ying, H. 2018. Continuous citric acid production in repeated-fed batch fermentation by *Aspergillus niger* immobilized on a new porous foam. *Journal of Biotechnology* **24**: 276-277.
- Zaho, X., Spraker, J. E., Bok, J. W., Velk, T., He, Z. M., & Keller, N. P. 2017. A cellular fusion cascade regulated by LaeA is required for sclerotial development in *Aspergillus flavus*. *Frontiers in Microbiology* **8**: 1925.
- Zonneveld, B. J. 1973. Inhibitory effect of 2-Deoxyglucose on cell wall alpha-1,3-glucan synthesis and cleistothecium development in *Aspergillus nidulans*. *Developmental Biology* **34**: 1-8.

Abbreviations

°C.....celsius

Δ..... deletion

μ..... micro

Σ..... sum

aa.....amino acid

Blast.....Basic local alignment search tool

bp.....base pairs

cm.....centimeter

comp⁺.....complementation

C-terminus..... carboxy terminus

Da.....dalton

DIC..... differential interference contrast

DNA.....deoxyribonucleic acid

et al.,.....et alii, and others

e.g..... exempli gratia, for example

ER..... endoplasmic reticulum

FGSCFungal Genetics Stock Center

PSM.....peptide spectral match

g..... gram

gDNA..... genomic DNA

Abbreviations

GFP.....	green fluorescent protein
ID.....	identification
LC-MS.....	liquid chromatography–mass spectrometry
l.....	liter
log ₂	logarithm to the base 2
kDa.....	kilodalton
MS.....	mass spectrometry
ms.....	millisecond
min.....	minute(s)
mg.....	milligram
ml.....	milliliter
mm.....	millimeter
mM.....	millimolar
M.....	molar
N-terminus	amino-terminus
µg.....	microgram
µl.....	microliter
µm.....	micrometer
PAGE	polyacrylamide gelelectrophoresis
PCR.....	polymerase chain reaction
pH.....	power of hydrogen
sp.....	spore
RNA.....	ribonucleic acid

Abbreviations

rpm..... revolutions per minute
tRNA.....transfer ribonucleic acid
Tris..... tris(hydroxymethyl)aminomethane
UTR..... untranslated region
UV..... ultraviolet
V..... Volt
v..... volume
v/v..... volume per volume
w..... weight
wt.....wildtype
w/v..... weight per volume

List of Figures

Figure 1. Adult Hülle cells and the subtending hyphae of Hülle cells.	8
Figure 2. Electron microscope images of the content and septa found in Hülle cells of <i>Aspergillus nidulans</i>	10
Figure 3. Asexual and sexual differentiation.	12
Figure 4. Secondary metabolite gene clusters which are involved in the production of monodictyphenone and xanthones.	18
Figure 5. Biosynthesis of monodictyphenone and xanthones.	20
Figure 6. Domain architecture of the methyltransferase LaeA.	22
Figure 7. LaeA methyltransferase promotes Hülle cell formation.	23
Figure 8. Illustration of enrichment of Hülle cells from solid agar plates: the cleistothecia-rolling technique.	38
Figure 9. Restriction map and Southern hybridization before and after the marker was recycled for the deletion strain <i>laeAΔ; nkuAΔ</i> (AGB1073).	46
Figure 10. Restriction map and Southern hybridization before and after the marker was recycled for the complementation strain of <i>laeAΔ</i> (<i>laeAΔ::laeA; nkuAΔ</i> , AGB1075).	47
Figure 11. Restriction map and Southern hybridization before and after the marker was recycled for lysine auxotrophic <i>laeAΔ</i> strain (<i>lysAΔ; laeAΔ; nkuAΔ</i> , AGB1074).	48
Figure 12. Restriction map and Southern hybridization before and after the marker was recycled for the complementation strain <i>lysAΔ; laeAΔ</i> (<i>lysAΔ; laeAΔ::laeA; nkuAΔ</i> , AGB1076).	49
Figure 13. Restriction map and Southern hybridization to confirm <i>nptA::gfp</i> and <i>rfeA::gfp</i> strains 50	50
Figure 14. Schematic illustration of the two-step cloning strategy.	51
Figure 15. Diagnostic PCR to confirm the integration of the <i>xptB::gfp</i> cassette.	52
Figure 16. Diagnostic PCR to confirm the integration of <i>xptC::gfp</i> cassette.	53
Figure 17. Diagnostic PCR to confirm the integration of the <i>AN8434::gfp</i> cassette.	54
Figure 18. Diagnostic PCR to confirm the integration of the <i>AN8435::gfp</i> cassette.	55
Figure 19. Restriction map and Southern hybridization before and after the marker was recycled for the <i>nkuAΔ; mphAΔ</i> (AGB1077) strain.	56
Figure 20. Restriction map and Southern hybridization before and after the marker was recycled for the complementation strain (<i>nkuAΔ; mphAΔ::mphA::gfp</i> , AGB1078) plus the <i>mphA::gfp;nkuAΔ</i> (AGB1079) strain.	57
Figure 21. Restriction map and Southern hybridization to confirm the complementation strain (<i>mphAΔ::mphA, nkuAΔ</i> , AGB1080) and the <i>laeAΔ; mphA::gfp;nkuAΔ</i> (AGB1081) strain.	58
Figure 22. Enrichment of Hülle cells of cultures from solid agar plates.	66
Figure 23. Proteomics workflow for analyzing enriched surface Hülle cells grown on solid agar plates and different types of mycelia.	69
Figure 24. Comparative analysis of identified proteins from surface cultures.	70
Figure 25. Enzymes encoded by the xanthone (<i>xpt</i>) gene cluster are localized in Hülle cells.	76
Figure 26. Enzymes encoded by the xanthone (<i>xpt</i>) gene cluster are localized in vegetative mycelium.	77
Figure 27. The fusion proteins XptB::GFP and XptC::GFP are found in sexual mycelium with high amounts of Hülle cells and a vegetative mycelium.	78
Figure 28. Functional annotation of identified proteins found in surface Hülle cells.	80
Figure 29. Proteomics workflow for analyzing enriched Hülle cells from submerged cultures.	82
Figure 30. Lysine prototroph and auxotroph <i>laeAΔ</i> strains for the quantitative analysis of Hülle cells under submerged liquid conditions.	83
Figure 31. Determination of the number of Hülle cells in vegetative mycelia and determination of the dry weight of the vegetative mycelia.	84
Figure 32. The prenyltransferase NptA is localized in the cytoplasm of Hülle cells.	89
Figure 33. Reduced protein abundance of the prenyltransferase NptA in a <i>laeAΔ</i> mycelium.	90

List of Tables

Figure 34. The serine/threonine kinase RfeA is localized in Hülle cells and is reduced in a <i>laeA</i> Δ mycelium.	92
Figure 35. The serine/threonine kinase RfeA is localized in Hülle cells and the protein quantity is reduced in a <i>laeA</i> Δ mycelium.	93
Figure 36. Hülle cells from surface growth compared to Hülle cells from liquid media differ in composition by 28% beside a shared core proteome.	97
Figure 37. The AnkG (AN8434) ankyrin repeat domain protein is localized at the membrane of the subtending hyphae of Hülle cells.	99
Figure 38. The AnkG::GFP fusion protein is found in sexual mycelium with high amounts of Hülle cells and a vegetative mycelium.	100
Figure 39. The localization of the tyrosinase domain protein (AN8435).	101
Figure 40. Western hybridization of AN8435::GFP of a vegetative and a sexual mycelium.	102
Figure 41. Multisequence alignment of four putative maltose permease-like protein sequences from MphA (<i>Aspergillus nidulans</i>), Afu4g00150 (<i>Aspergillus fumigatus</i>), Mal11 (<i>Aspergillus niger</i>), Mal31 (<i>Saccharomyces cerevisiae</i>).	104
Figure 42. The MphA maltose permease-like protein supports vegetative growth.	105
Figure 43. MphA promotes fungal growth and development.	106
Figure 44. Localization of the maltose permease-like protein MphA.	108
Figure 45. The maltose permease-like protein MphA prevents mycelia differentiation at higher concentration of carbohydrates.	110
Figure 46. The monodictyphenone (<i>mdp</i>) / xanthone (<i>xpt</i>) gene clusters are active in sexual tissue including Hülle cells from surface growth.	112
Figure 47. Hülle cell formation in submerged liquid cultures and comparison of two strains causing different results.	114
Figure 48. The comparison of the proteome of both types of Hülle cells.	118
Figure 49. Domain architecture of the AnkG (AN8434) ankyrin repeat domain protein and the tyrosinase domain protein (AN8435).	120
Figure 50. Protein trafficking of the AnkG ankyrin domain protein.	121
Figure 51. Model for the maltose permease-like protein MphA in the transportation of α -1,3 glucans in <i>Aspergillus nidulans</i>	124
Figure 52. Hülle cells protect and support the cleistothecia.	126

List of Tables

Table 1. Strains used in this study.	28
Table 2. Plasmids used in this study.	29
Table 3. Oligonucleotides utilized for plasmid construction.	29
Table 4. PCR program used in this study.	42
Table 5. Primers used for amplification of Southern probes.	44
Table 6. Comparative proteomics revealed six proteins that were identified in the enriched Hülle cells.	72
Table 7. 24 proteins that were common between sexual mycelia and Hülle cells and were identified from solid agar plate cultures.	74
Table 8. Overlapping proteins of Hülle cells (HC), asexual (Asex.) and vegetative mycelium (Veg.). .	79
Table 9. Proteins that are down-regulated in a <i>laeA</i> Δ mycelium.	86
Table 10. Proteins that are up-regulated in a <i>laeA</i> Δ mycelium.	88
Table 11. List of overlapping proteins identified in Hülle cells from solid agar plates and submerged liquid cultures (Hülle cells core proteome).	95

Acknowledgements

I would like to thank Professor Dr. Gerhard H. Braus for lots of advice and assistance for my research during my doctoral work. Many thanks also to Professor Dr. Stefanie Pöggeler and Dr. Oliver Valerius to patronize my work as members of the doctoral thesis committee. I appreciated very much the possibility to discuss different results and aspects with Stefanie Pöggeler and Oliver Valerius beyond the thesis committee meetings. I am grateful to my examination board: Professor Dr. Heike Krebber, Professor Dr. Kai Heimel, Privatdozent Dr. Michael Hoppert. I would like to thank Dr. Abishek Kumar who performed with me the functional annotation of the surface Hülle cells proteome during a QuantFung course at the University of Kiel. I would like to thank Dr. Oliver Valerius and Dr. Kerstin Schmitt for helping me to identify proteins by mass spectrometry. I am very grateful to Marie Skłodowska-Curie actions and the Göttingen Graduate School for Neuroscience, Biophysics and Molecular Biosciences for financial support and giving me the opportunity to be part of the QuantFung consortium. I enjoyed very much the networking opportunities within the QuantFung community and also the courses provided during the three years of the project. Many thanks to Dr. Oliver Valerius, Dr. Christoph Sasse, Dr. Jenny Gerke and Dr. Danielle Troppens for helping me in the lab and challenging me in many discussions. Cindy Meister for the construction of the lysine auxotrophic strain. Enikő Fekete-Szücs, for in gel digestion. For proof – reading I am grateful to Oliver, Christoph, Jenny. Moreover, I am grateful to Cindy Meister, Dr. Mirit Gluko, Dr. Razieh Aghcheh Karimi and Liu Li for proof-reading of my doctoral thesis. Special thanks goes to my lab 102, Dr. Razieh Aghcheh Karimi, Dr. Karl Thieme, Sabine Thieme, Anja Abelmann, Verena Große. I am grateful for the moral support of my mum, Franz, my Sister Maria and Toby Boyce, her kids Henry and Elsa. For english proofreading I am grateful to Toby Boyce. I enjoyed the time in Hannover, Celle, Stuttgart and Goettingen very much. The research leading to these results has received funding from the European Union's Seventh Framework Programme FP7/2007-2013, under grant agreement n° 607332. This work was partly supported by the Göttingen Graduate School for Neuroscience, Biophysics and Molecular Biosciences (DFG GSC 226/2).

Curriculum vitae

Private data

Name: Benedict Dirnberger
Data of birth: 22. April 1984
Birthplace: Vienna
Civil status: unmarried

Academic achievements

02/2014 – ongoing **PhD student / Doctor rerum naturalium in Biochemistry and Microbiology**

Place of education: Georg August University of Goettingen,
Institute: Department for Molecular Microbiology and Genetics
Title of the thesis: Proteomics of *Aspergillus nidulans* sexually differentiated cells
Supervisor: Prof. Dr. Gerhard H. Braus

11/2010 – 01/2013 **Diploma (corresponding to M.Sc.) in Biology, Major in Genetics and Microbiology**

Place of education: University of Vienna
Institute: Department for Molecular Systems Biology
Title of the thesis: A subcellular fractionation that allows the measurement of the proteome and the metabolome
Supervisor: Prof. Dr. Wolfram Weckwerth & Ass. Prof. Dr. Stefanie Wienkoop

10/2004 - 11/2010 **Prediploma in Biology**

Place of education: University of Vienna

International experience

2/2013- ongoing	University of Goettingen (Ger)
07/2009 - 08/2009	University of Cambridge (UK)
07/2007	University of Bristol (UK)

Publications in peer reviewed international journals

Büttel, Z., Díaz, R., Dirnberger, B., Flak, M., Grijseels, S., Kwon, M. J., Nielsen, J. C. F., Nygård, Y., Phule, P., Pohl, C., Prigent, S., Randelovic, M., Schütze, T., Troppens, D., & Viggiano, A. 2015. Unlocking the potential of fungi: the QuantFung project. *Fungal Biology and Biotechnology* 2: 6.

Presentations in scientific meetings (talks and posters)

[1] **Benedict Dirnberger**, Oliver Valerius, Enikő Fekete-Szücs, Cindy Meister, Ines Teichert, Jennifer Gerke, Danielle Troppens, Gerhard H. Braus (2017). A quantitative comparative proteomic approach to investigate Hülle cells from the filamentous fungus *Aspergillus nidulans*. **16th Human Proteome Organization World Congress (HUPO2017), Dublin, Ireland (poster A-016)**.

[2] **Benedict Dirnberger**, Oliver Valerius, Enikő Fekete-Szücs, Cindy Meister, Ines Teichert, Jennifer Gerke, Danielle Troppens, Gerhard H. Braus (2016). A comparative proteomic approach to investigate secondary metabolite gene cluster expression in various *Aspergillus nidulans* cell types. **13th European Conference on Fungal Genetics, Paris, France, p 567 (poster CS7W41)**.

[3] Danielle Troppens, **Benedict Dirnberger**, Gerhard Braus (2016). Investigating the potential of Hülle cells in *Aspergillus nidulans*. **13th European Conference on Fungal Genetics, Paris, France, p 134 (poster CS1M28)**.

[4] **Benedict Dirnberger**, Oliver Valerius, Enikő Fekete-Szücs, Cindy Meister, Ines Teichert, Jennifer Gerke, Danielle Troppens, Gerhard H. Braus (2016). A comparative proteomic approach to investigate secondary metabolite gene cluster expression in various *Aspergillus nidulans* cell types. **The Thirteenth International Aspergillus Meeting, Paris, France, p 17 (poster 23)**.

[5] **Benedict Dirnberger et al., (2015)**. Investigation of Hülle cells from the filamentous fungus *Aspergillus nidulans*. **Proteomics Forum 2015, Berlin, Germany, p48 (poster 091)**.

[6] Danielle Troppens, Özgür Bayram, **Benedict Dirnberger**, Gerhard Braus (2015). Investigating the potential of Hülle cells in *Aspergillus nidulans*. **Annual Conference of the Association for General and Applied Microbiology, Marburg, Germany p 218 (poster SMaP07)**.

[7] **Benedict Dirnberger et al., (2015)**. Investigation of Hülle cells from the filamentous fungus *Aspergillus nidulans*. **Annual Conference 2015 of the Association for General and Applied Microbiology, Marburg, Germany p 228 (poster SCP01)**.

[8] **Benedict Dirnberger (2015)**. Investigation and quantification of secondary metabolite gene cluster expression in *Aspergillus nidulans*. **Annual Conference 2015 of the Association for General and Applied Microbiology, Marburg, Germany (oral presentation)**.

[9] **Benedict Dirnberger**, Oliver Valerius, Ines Teichert, Holm Frauendorf, Danielle Troppens, Bastian Jöhnk, Gerhard H. Braus (2014). Investigation of Hülle cells from the filamentous fungus *Aspergillus nidulans*. **ESF-EMBO Symposium Synthetic biology of antibiotic production II, Sant Feliu de Guixols, Spain, p14 (poster013)**.

[10] Benedict Dirnberger & Gerhard H. Braus (2014). Exploration of molecular switches from filamentous growth to single Hülle cells as tool for synthetic biology. **Proceeding of the 12th European Conference of Fungal Genetics (ECFG), Seville, Spain, p78 (poster 018).**

Fellowships, scholarships and awards

- | | |
|---------|---|
| 03/2018 | TOP scholarship foreign countries, Lower Austria, awarded for Doctoral thesis |
| 11/2017 | Travel award, 16 th Human Proteome Organization World Congress (HUPO2017) 17.09-21.09.2017, awarded by European proteomics association (EUPA) |
| 08/2017 | Travel award, 16 th Human Proteome Organization World Congress (HUPO2017), 17.09-21.09.2017, awarded by German society for proteomics |
| 11/2016 | GGNB scholarship (DFG Grant GSC 226/2), awarded for Doctoral thesis |
| 04/2016 | Award for best poster presentation, The Thirteenth International <i>Aspergillus</i> Meeting, Paris, France, p 17 (poster 23), awarded by Novozymes |
| 07/2015 | Travel award (offered), 9 th European Summer School – Advanced Proteomics, 02.08-08.08. 2015 Kloster Neustift Brixen, awarded by German society for proteomics |
| 02/2015 | Travel award, Proteomics Forum 2015, 22.03-25.03.2015 Berlin Germany, awarded by Austrian society for proteomics |
| 02/2014 | Marie Skłodowska-Curie Fellowship (ITN), awarded for Doctoral thesis (University of Goettingen) |
| 08/2013 | Leonardo da Vinci scholarship, awarded for research in the Mass Spectrometry – Yeast Group (University of Goettingen) |
| 01/2013 | University of Goettingen scholarship, awarded for research in the Department of Plant Biochemistry |

Supplements

Supplementary Table 1:

Overview of the proteome data evaluation using Proteome Discoverer 1.4.

Proteome experiment 1	
No.	Description
1	Vegetative mycelium: 20 hours after germination in liquid shake flasks Three biological replicates
2	Filter: proteins identified in two or more biological replicates and with more than two peptides per proteins
3	Asexual mycelium: 3 days after germination on solid agar plate cultures Three biological replicates
4	Filter: proteins identified in two or more biological replicates and with more than two peptides per proteins
5	Asexual mycelium: 5 days after germination on solid agar plate cultures Three biological replicates
6	Filter: proteins identified in two or more biological replicates and with more than two peptides per proteins
7	Asexual mycelium 7 days after germination on solid agar plate cultures Three biological replicates
8	Filter: proteins identified in two or more biological replicates and with more than two peptides per proteins
9	Sexual mycelium: 3 days after germination on solid agar plate cultures Three biological replicates
10	Filter: proteins identified in two or more biological replicates and with more than two peptides per proteins
11	Sexual mycelium: 5 days after germination on solid agar plate cultures Three biological replicates
12	Filter: proteins identified in two or more biological replicates and with more than two peptides per proteins
13	Sexual mycelium: 7 days after germination on solid agar plate cultures Three biological replicates
14	Filter: proteins identified in two or more biological replicates and with more than two peptides per proteins
15	Hülle cells: 3 days after germination on solid agar plate cultures Three biological replicates
16	Filter: proteins identified in two or more biological replicates and with more than two peptides per proteins
17	Hülle cells: 5 days after germination on solid agar plate cultures Three biological replicates
18	Filter: proteins identified in two or more biological replicates and with more than two peptides per proteins
19	Hülle cells: 7 days after germination on solid agar plate cultures Three biological replicates
20	Filter: proteins identified in two or more biological replicates and with more than two peptides per proteins
21	Insert lists into a Venn diagram
22	Additional steps were performed

Supplementary Table 2:

Overview of the proteome data evaluation using Perseus 1.5.0.15.

Proteome experiment 2		
No.	Command	Description
1	Generic matrix upload	ProteinGroup.txt normalized ratio
2.1	Filter rows based on categorical columns	Remove rows with + in reverse column
2.2	Filter rows based on categorical columns	Remove rows with + in only identified by site
3	Select rows manually	Remove rows with contaminants
4	Transform	Inverse ratio (1/x) when <i>lysA</i> Δ; <i>nkuA</i> Δ is not in the denominator
5	Transform	Log ₂ (X)
6	Categorical annotation rows	Group biological replicates
7	Normalization	Subtract column median of ratio
8	Average groups	Calculate median of each group
9	Sample t-test	One - sample t-test, side both, p value 0.05
10	Select rows manually	Selected proteins with t-test significant (+)
11	Select rows manually	Filter protein ratio for values outside -0.5 to +0.5
12	Additional steps and analyses were performed beside using Perseus 1.5.0.15.	

Supplementary Table 3.

The list of the 401 proteins found in enriched Hülle cells. Hülle cells enriched from solid agar plate cultures were analyzed within three different time points. Proteins were sorted according to the criteria of the Venn diagram shown in Figure 24. For each time point three biological replicates were considered. Only proteins identified in two or more biological replicates and with two or more peptides per protein were considered for the analysis. Numbers represent the average of spectral counts from three biological replicates. Spectral counts were obtained from enriched Hülle cells and are listed. Proteins that were common between Hülle cells and different type of mycelia are also listed. Putative function or role proteins are listed under Description. Different sources were used, mainly AspGD (Cerqueira et al., 2014).

Found only in Hülle cells (6 proteins)				
		Spectral counts, found in Hülle cells		
Gene ID	Description	3 day	5 day	7 day
AN2601 (MphA)	Major facilitator superfamily		8	8
AN9392	Major facilitator superfamily	7	4	
AN3407	Protein with a predicted serine-type peptidase domain		25	29
AN4695 (HexA)	Woronin body protein		8	7
AN8434 (AnkG)	Ankyrin repeat domain protein		4	4
AN8435	Tyrosinase domain protein		2	3
Shared in Hülle cells & sexual mycelium (24 proteins)				
		Spectral counts, found in Hülle cells		
Gene ID	Description	3 day	5 day	7 day
AN7349 (MutA)	Alpha-1,3-glucanase, specifically expressed in Hülle cells	3	43	28
AN0941 (AgdE)	Alpha-glucosidase activity, predicted role in maltose metabolism	6	32	24
AN3790 (AgnB)	Putative alpha-1,3-glucanase		18	
AN9443	Predicted catalytic activity and role in carbohydrate metabolic process			11
AN7345 (AgdC)	Glucosidase activity, involved in degradation of glucans	6	32	24
AN11143 (GlaA)	Putative Glucoamylase		4	
AN11049	NmrA-like, predicted secondary metabolite member		35	49
AN10023 (MdpL)	Member of the monodictyphenone (<i>mdp</i>) / xanthone (<i>xpt</i>) gene clusters	25		42
AN7999	Oxoreductase, member of the monodictyphenone (<i>mdp</i>) / xanthone (<i>xpt</i>) gene clusters		8	47
AN7998 (XptC)	GMC oxoreductase, member of the monodictyphenone (<i>mdp</i>) / xanthone (<i>xpt</i>) gene clusters	7	6	
AN12402 (XptB)	Prenyltransferase, member of the monodictyphenone (<i>mdp</i>) / xanthone (<i>xpt</i>) gene clusters	5		8
AN10022	Member of the monodictyphenone (<i>mdp</i>) / xanthone (<i>xpt</i>) gene clusters		5	6
AN0150 (MdpG)	Polyketide synthase, member of the monodictyphenone (<i>mdp</i>) / xanthone (<i>xpt</i>) gene clusters	4	3	
AN7812 (StcN)	Putative versicolorin B synthase	3	4	
AN7641	Putative copper amine oxidase	22	31	
AN6314	Oxidoreductase	5	27	48
AN8203	Hydrolase		5	
AN1142	Oxidoreductase		4	
AN11897	Ribonuclease		6	
AN5669	Putative succinyl-CoA:3-ketoacid-coenzyme A transferase	8		2
AN10977	Ortholog(s) have extracellular region localization		6	
AN6930	Predicted transaminase activity		9	
AN5488	Protein of unknown function	2	20	
AN1863	Protein of unknown function	2		4

Supplementary Table 3.

Continued.

Shared in Hülle cells & asexual mycelium (10 proteins)		Spectral counts, found in Hülle cells		
Gene ID	Description	3 day	5 day	7 day
AN5324 (DlpA)	Dehydrin-like protein	9	9	6
AN5004	Induced in light	2	30	7
AN6856	Upregulated in <i>atmΔ</i>	5	6	
AN5015 (ConJ)	Induced in light	2	8	2
AN5971	Induced in light	7	4	
AN1362	Cue5 ortholog		4	
AN0635	Intracellular localization	8	4	8
AN0691	Protein of unknown function	6	16	
AN4646	Protein of unknown function		13	
AN5764	Induced by light	2		
Shared in Hülle cells & vegetative mycelium (8 proteins)		Spectral counts, found in Hülle cells		
Gene ID	Description	3 day	5 day	7 day
AN1182 (BenA)	Beta-tubulin	5	4	23
AN4236	Proteasome regulatory particle	3		5
AN6688 (AspB)	Putative Septin B	7		2
AN2918 (Cct4)	Chaperonin complex component	3		3
AN4159 (GlnA)	Glutamate-ammonia ligase	4		
AN2149 (Cct1)	Chaperonin	2		2
AN10476	Dehydrogenase	7	9	10
AN4281 (SrgB)	GTPase		2	3
Shared in Hülle cells, sexual mycelium & asexual mycelium (73 proteins)		Spectral counts, found in Hülle cells		
Gene ID	Description	3 day	5 day	7 day
AN0045	Induced by light	15	55	
AN0158	2-alkenal reductase [NAD(P)] activity,	21		4
AN0472 (EngA)	1,3-beta-glucosidase	33	9	5
AN0567	Alcohol oxidase	10		6
AN0693	Induced by light		23	7
AN0694	Intracellular localization		66	
AN0779	Glucan 1,3-beta-glucosidase	6	22	
AN0787	Mannosyl-oligosaccharide 1,2-alpha-mannosidase	6		8
AN0950	Protein of unknown proteins	4	36	9
AN10040	Oxidoreductase	59		10
AN10281	Serine/threonine phosphatase	2	20	12
AN10499	Intracellular localization	6	9	
AN10563 (Pho8)	Vacuolar alkaline phosphatase	4		8
AN10631	Protein of unknown function	5	10	
AN10930	UDP-N-acetylmuramate dehydrogenase activity	16	66	
AN11080 (NptA)	Prenyltransferase	11		26

Supplementary Table 3.

Continued.

Shared in Hülle cells, sexual mycelium & asexual mycelium (73 proteins)		Spectral counts, found in Hülle cells		
Gene ID	Description	3 day	5 day	7 day
AN12027	Protein of unknown function	6		
AN1502 (NagA)	Chitin hydrolysis	6		7
AN1616	Oxidoreductase	7	15	
AN1675	Lysophospholipase	2	17	
AN1733 (PrnC)	Delta-1-pyrroline-5-carboxylate dehydrogenase	13		
AN1918 (AcuF)	Phosphoenolpyruvate carboxykinase	25	44	
AN2000 (Ubi4)	Polyubiquitin	15	9	
AN2017 (AgdA)	Alpha-glucosidase	2	2	
AN2092	Prolyl aminopeptidase	3	4	
AN2314	1,4-alpha-glucane-branching enzyme	6		
AN2383	Protein of unknown function		8	25
AN2395	Beta-glucuronidase		4	2
AN2572	Dipeptidyl-peptidase	6		
AN2828 (BglL)	Beta-glucosidase	28		10
AN2860	Protein of unknown function	4		5
AN2866	Oxidoreductase	2		8
AN2936	Alpha-mannosidase	17	2	
AN3121	Protein of unknown function		8	4
AN3402 (AmyB)	Alpha-amylase	6	5	
AN3416 (SsoA)	Syntaxin protein	2	15	
AN3512	Protein of unknown function	5	4	
AN3983	Protein of unknown function		9	21
AN4058	Dihydroxy acid dehydratase	2		10
AN4102 (BglA)	Beta-glucosidase	16	2	
AN4577 (fmdS)	Kynurenine formamidase		2	
AN4825	Glucan 1,3-beta-glucosidase	2		8
AN4871 (ChiB)	Chitinase	78	111	16
AN4940	Meiotic recombination	13	64	12
AN4988	Intracellular localization	16	55	2
AN5217 (PilA)	Protein similarity to sphingolipid	8	65	
AN5281	Pyranose oxidase	8	44	
AN5422	Beta-lactamase family protein	11	8	7
AN5442	Carboxypeptidase Y	7		
AN5446	Protein of unknown function	14	62	
AN5634 (AcuB)	Isocitrate lyase	39		
AN6024 (GstB)	Glutathione S-transferase	6	10	4
AN6273	Intracellular localization		4	8
AN6279 (AcuJ)	Carnitine acetyltransferase	16		8
AN6398	Intracellular localization	4	8	
AN6796	Intracellular localization	2	22	

Supplementary Table 3.

Continued.

Shared in Hülle cells, sexual mycelium & asexual mycelium (73 proteins)		Spectral counts, found in Hülle cells		
Gene ID	Description	3 day	5 day	7 day
AN6844	3-hydroxyisobutyryl-CoA hydrolase activity	6		10
AN6963	Oxidoreductase	4	36	
AN7269	UDP-N-acetylmuramate dehydrogenase		7	
AN7307	Catalytic activity	5	5	
AN7836	Protein of unknown function	2	13	4
AN7912 (OrsC)	Tyrosinase	2	2	
AN7914	Alcohol dehydrogenase	19	10	2
AN7962 (PepJ)	Extracellular deuterolysin-type metallo-proteinase		8	
AN8007 (AbnC)	Arabinan endo-1,5-alpha-L-arabinosidase activity	2	12	8
AN8330	Oxidoreductase	7		14
AN8553	Catalase	29	69	10
AN8829	Protein of unknown function		17	
AN9002	Monoxygenase, secondary metabolite enzyme	13	54	
AN9094	UDP-N-acetylglucosamine pyrophosphorylase	17		10
AN9180	Transketolase	20	34	
AN9194 (CetL)	Transcript enriched in dormant conidia	20	20	
AN9340 (TreA)	Alpha-trehalase	4	5	20
Shared in Hülle cells, sexual mycelium & vegetative mycelium (21 proteins)		Spectral counts, found in Hülle cells		
Gene ID	Description	3 day	5 day	7 day
AN10276	Nucleic acid binding	2		4
AN10614	G-quadruplex DNA binding	4	3	
AN10946	Protein of unknown function	7	9	
AN1222	S-adenosylmethionine synthetase	18	6	4
AN1358	Serine/threonine phosphatase activity	2	4	4
AN1990	Homocitrate synthase	5		5
AN2142 (kapA)	Karyopherin (importin) alpha	4		2
AN2455	Zinc ion binding activity	6		2
AN2980	Ribosome activity	6	15	2
AN4575	Protein of unknown function	6	9	8
AN4667 (AspA)	Septin	11		
AN4727	Involved in galactose metabolism	2	30	
AN4775	Cullin deneddylation	10		9
AN5134 (GltA)	Glutamate synthase	12	2	
AN5601	Saccharopine dehydrogenase	16		
AN5602	Chaperone	6	66	
AN5740	Rho family GTPase	6		2
AN5895	Rab GDP-dissociation inhibitor	16	19	19
AN7570 (tubB)	Alpha-tubulin	2		8
AN8182 (AspC)	Septin	12		
AN8863	Nap/SET family protein	4		9

Supplementary Table 3.

Continued.

Shared in Hülle cells, asexual mycelium & vegetative mycelium (6 proteins)					
		Spectral counts, found in Hülle cells			
Gene ID	Description	3 day	5 day	7 day	
AN0316 (tubA)	Alpha-tubulin	19		16	
AN1126	ADP ribosylation factor	6	2	2	
AN1971	ATP-dependent 3'-5' DNA helicase	2	3	6	
AN2012	Protein of unknown function	2	4	3	
AN6631	F1F0-ATPase complex subunit	8	8		
AN7350	Nucleic acid binding	8	9	3	
Shared in Hülle cells, sexual mycelium, asexual mycelium & vegetative mycelium (253 proteins)					
		Spectral counts, found in Hülle cells			
Gene ID	Description	3 day	5 day	7 day	
AN0046	Protein of unknown function	13		19	
AN0084	Ran GTPase binding activity	8	11		
AN0170 (TrxA)	Thioredoxin		6	6	
AN0240 (PppA)	Transaldolase	64	25	30	
AN0241 (SodA)	Cu/Zn-superoxide dismutase	5	50	11	
AN0252	F1F0-ATPase complex gamma	9	12	2	
AN0262	Ribosomal large subunit assembly	4	16	6	
AN0285	6-phosphogluconolactonase	8	16	3	
AN0297	Protoplast secreted protein 2	8	6	9	
AN0359 (SgdA)	Translation initiation factor 3 (eIF3)	8	3		
AN0432	Cytochrome-b5 reductase activity	4	3		
AN0433	Ribosome activity		4	10	
AN0443	Alcohol dehydrogenase	6	7	21	
AN0465	Protein of unknown function	9	10	4	
AN0554 (AldA)	Aldehyde dehydrogenase	57	43	89	
AN0579	Isopentenyl-diphosphate delta-isomerase	6		9	
AN0641	Osmoadaptation	11	8	8	
AN0687 (SpdA)	Spermidine synthase		4	4	
AN0688	Transketolase	52	57	63	
AN0734	Histone H4	5		6	
AN0747	Ubiquinol-cytochrome-c reductase	10	10	3	
AN0776	Ribosome activity	4	8	10	
AN0843	Ribosome activity		8	3	
AN0870	Transporter	6	6	14	
AN0893	Adenylosuccinate synthase	16	5	3	
AN0932 (GlrA)	Glutathione oxidoreductase	3	4	7	
AN1003	Isocitrate dehydrogenase (NAD ⁺)	12	2		
AN10030	Serine protease	4	18	5	
AN1013	60S ribosomal protein L5	29	7	25	
AN1015	Phosphorylase	7	10	8	
AN10170	ATPase activity and cytoplasm localization	28			
AN10202	ATP binding activity	20	5	7	
AN10223	Peroxiredoxin	6	7	2	

Supplementary Table 3.

Continued.

Shared in Hülle cells, sexual mycelium, asexual mycelium & vegetative mycelium (253 proteins)				
		Spectral counts, found in Hülle cells		
Gene ID	Description	3 day	5 day	7 day
AN10266	Ubiquitin-activating enzyme	7	3	
AN10273 (Gst3)	Glutathione S-transferase	16		
AN10279	Nucleic acid binding	5	2	11
AN10311 (MnpA)	Mannoprotein	4	6	2
AN10351	Aminopeptidase activity	19	3	23
AN10416	60s ribosomal protein similar to subunits L15 and L27	10		6
AN1047	Heat shock protein	33	32	5
AN10474	Protein of unknown function	6		
AN10540	Dipeptidyl-peptidase activity	14	12	4
AN10675	Mitochondrion localization	5	3	
AN10709 (GfaA)	Glutamine-fructose-6-phosphate transaminase	13		6
AN10745	Glycine hydroxymethyltransferase activity	10	10	9
AN1084	Elongation factor EF-Tu	8	9	
AN11005	Metalloexopeptidase activity	5	5	
AN11045	D-lactate dehydrogenase (cytochrome) activity	2		5
AN11125	Protein of unknown function	8	6	
AN1122	Ribosome activity	3	7	
AN11227	70 kilodalton heat shock protein	26	15	20
AN1152	Protein of unknown function		7	
AN1162	Guanyl-nucleotide exchange factor	26	20	3
AN1166	Ribosome activity	10	9	9
AN11898	Protein of unknown function	2		10
AN1228	Maturation of rRNA	2	8	10
AN1246 (PgfA)	Phosphoglycerate kinase	53	10	16
AN12465	Intracellular localization	35	18	33
AN1263	Adenosylhomocysteinase	31	3	7
AN1342	Alanine-glyoxylate transaminase	9	6	4
AN1378	Protein of unknown function		10	
AN1380	tRNA ligase	4		
AN1409	Acetyl-CoA C-acetyltransferase	30	7	14
AN1430	Oxidoreductase	2		4
AN1523	F1F0-ATPase complex	62	35	77
AN1543	Succinate dehydrogenase	13	7	7
AN1547	Carboxylate CoA-transferase	27	13	4
AN1638	Metalloaminopeptidase	21	24	3
AN1689	Oxidoreductase	4	10	2
AN1757 (ssfA)	20s core proteosome		8	
AN1810	Ornithine transaminase	19	2	

Supplementary Table 3.

Continued.

Shared in Hülle cells, sexual mycelium, asexual mycelium & vegetative mycelium (253 proteins)				
		Spectral counts found in Hülle cells		
Gene ID	Description	3 day	5 day	7 day
AN1883	Argininosuccinate synthase	19	10	
AN1923	Alanine transaminase	12	35	26
AN1964	Protein of unknown function	8	4	
AN1993	Aspartate transaminase	24	10	12
AN2062 (BipA)	Chaperone	14	15	14
AN2150	Protein of unknown function	5	2	
AN2208	Galactose 1-dehydrogenase	9	2	6
AN2225	Role in cytoplasmic translation	7	4	
AN2248 (GatA)	4-aminobutyrate transaminase	23	16	
AN2272	Protein of unknown function	10		4
AN2275	Ribosome activity	8		
AN2286 (AlcC)	Alcohol dehydrogenase III	11	2	8
AN2295	Succinate-CoA ligase	4	6	6
AN2304	Protein of unknown function	8	9	
AN2315	DNA-directed RNA polymerase activity	120	33	
AN2435 (AlcA)	Citrate synthase	49		40
AN2436 (AclB)	ATP citrate synthase	64	3	13
AN2526	Ketol-acid reductoisomerase	44	5	2
AN2734	rRNA binding activity	3	8	10
AN2867 (PgmB)	Phosphoglucomutase	24	29	39
AN2875 (FbaA)	Fructose-bisphosphate aldolase	80	36	26
AN2903 (PepE)	Aspartic protease	22	9	22
AN2914	Argininosuccinate lyase	14		3
AN2916	Succinate dehydrogenase	19	14	3
AN2932	Eukaryotic initiation factor 4A	17		4
AN2954	Protein of unknown function	4		4
AN2968 (IppA)	Inorganic diphosphatase	20	24	25
AN2981 (GsdA)	Glucose 6-phosphate 1-dehydrogenase	18		12
AN2999 (IldpA)	Isocitrate dehydrogenase	22	7	7
AN3031	Threonine synthase	7		2
AN3058	Glycine hydroxymethyltransferase	23		23
AN3059 (PgmA)	Phosphoglycerate mutase	24	2	7
AN3112 (UgmA)	UDP-galactopyranose mutase	19		14
AN3172	Protein of unknown function	11	11	7
AN3413	Ribosomal protein S2 and S5	3	2	
AN3459	Metalloprotease activity	7	2	
AN3466 (KgdB)	Dihydrolipoamide S-succinyl transferase	21		10
AN3592 (ClxA)	Calnexin		5	15
AN3674	Protein of unknown function	40	22	43

Supplementary Table 3.

Continued.

Shared in Hülle cells, sexual mycelium, asexual mycelium & vegetative mycelium (253 proteins)				
		Spectral counts, found in Hülle cells		
Gene ID	Description	3 day	5 day	7 day
AN3814 (CypA)	Peptidyl-prolyl cis-trans isomerase	6	6	2
AN3829	Succinate-semialdehyde dehydrogenase	7		15
AN3873	Oxidoreductase	15	8	
AN3918	Aminopeptidase activity	3	9	
AN3928 (ThiF)	Thiazole synthase	26	10	6
AN3954	Phosphogluconate dehydrogenase	102	20	46
AN4000 (FabM)	Poly(A)-binding proteins	9	10	5
AN4064	ADP/ATP carrier protein	5	8	17
AN4087	40S ribosomal protein subunit	30	29	17
AN4163 (CpcB)	Response to amino acid starvation	18	15	17
AN4218	Translation elongation factor activity	58	41	33
AN4259	Protein of unknown function	10		12
AN4282	Intracellular localization	16	19	4
AN4288	Protein of unknown function	27	3	
AN4323	Aminotransferase	4	4	4
AN4376	NADP-linked glutamate dehydrogenase	42	9	37
AN4390 (EcmA)	GPI-anchored protein,role in cell wall biosynthesis	3	5	
AN4409 (ArgB)	Ornithine carbamoyltransferase	11		3
AN4414	Diphosphomevalonate decarboxylase	17		
AN4443 (MetH)	Methionine synthase	95	64	115
AN4462 (PycA)	Pyruvate carboxylase	46	16	16
AN4464 (PurH)	Bifunctional enzyme	19		9
AN4470	Role in positive regulation of translaion	6		10
AN4475	Ribosomal large subunit assembly	2	9	4
AN4501 (ArtA)	14-3-3 protein	24	24	56
AN4594	Maturation of rRNA		5	5
AN4616	Protein of unknown function	5		4
AN4769	ATP sulfurylase	18	5	9
AN4793	Aspartate semialdehyde dehydrogenase	6	4	8
AN4794	Ribosomal protein		11	9
AN4802	60S ribosomal protein L21	3	7	2
AN4862	Ran GTPase activating	4		
AN4888 (PdcA)	Decarboxylase	16		9
AN4905 (GstA)	Glutathione S-transferase		6	6
AN4916	Ribosome biogenesis	10	6	9
AN5014	Ribosome activity		4	2
AN5129	Heat shock protein	104		75
AN5162 (PdhB)	Pyruvate dehydrogenase	17		2
AN5210 (PkiA)	Pyruvate kinase	15	5	6
AN5441	Endonucleolytic cleavage		21	3

Supplementary Table 3.

Continued.

Shared in Hülle cells, sexual mycelium, asexual mycelium & vegetative mycelium (253 proteins)				
		Spectral counts, found in Hülle cells		
Gene ID	Description	3 day	5 day	7 day
AN5520	Ribosome biogenesis	8	15	5
AN5523	Alpha-trehalose-phosphate synthase	6		5
AN5525 (AcoA)	Aconitate hydratase	52	49	9
AN5563	Dehydrogenase	22		19
AN5564	Phosphatidyl synthase	10	2	
AN5566	Protein of unknown function	10		11
AN5571 (KgdA)	Oxoglutarate dehydrogenase	18		2
AN5626	Acetyl-CoA synthase	22	31	4
AN5686 (TpmA)	Tropomyosin		10	3
AN5701 (AroF)	3-deoxy-D-arabino-heptulosonate 7-phosphate synthase	7		3
AN5715	40s ribosomal protein S26		5	2
AN5719	Ribosome activity	2	3	14
AN5744	14-3-3-like protein	19	17	19
AN5746 (AcuN)	Phosphopyruvate hydratase	91	29	59
AN5800	Ribosome activity	6	20	7
AN5810 (PepP)	Prolidase	7		10
AN5872	Proteasom		6	8
AN5907	Ribose-5-phosphate isomerase			7
AN5960	Ribosomal small subunit assembly		9	4
AN5975	Mannitol-1-phosphate 5-dehydrogenase	45	24	64
AN5996	Ribosome activity		9	6
AN5997	Role in rRNA export from nucleus	5		5
AN5999	Arginine or pyrimidine metabolism	16	5	
AN6004	Protein of unknown function	6	6	2
AN6010 (SgdE)	Hsp70-family protein	73	21	22
AN6037 (SwoB)	Glucose-6-phosphate isomerase	37	10	71
AN6048	Aspartate transaminase	17	9	4
AN6089	Heat shock protein	48	10	5
AN6202	Ribosomal protein L3	20	7	8
AN6209	5'-phosphoribosyl-4-(N-succinocarboxamide)-5-aminoimidazole lyase	5	7	10
AN6232 (VmaB)	F1F0-ATPase complex subunit	15		9
AN6330	Elongation factor 2	98	28	9
AN6341	Similarity to <i>Saccharomyces cerevisiae</i> Crn1p	15		6
AN6346	Dihydroxy-acid dehydratase	10	8	5
AN6499 (MdhC)	Malate dehydrogenase	35	27	86
AN6500	Ribosome activity	35	8	2
AN6525 (AciA)	Formate dehydrogenase	41	23	29
AN6542 (ActA)	Actin A	41	25	29
AN6547	Proteasom		25	5
AN6563	Translation elongation factor EF-1 gamma	50	6	73

Supplementary Table 3.

Continued.

Shared in Hülle cells, sexual mycelium, asexual mycelium & vegetative mycelium (253 proteins)				
		Spectral counts, found in Hülle cells		
Gene ID	Description	3 day	5 day	7 day
AN6629	Ribosomal protein L14	12	23	10
AN6630	Polypeptide-associated complex	6	12	7
AN6639 (McdB)	2-methylcitrate dehydratase	28	9	27
AN6653 (AcuE)	Malate synthase	28	7	10
AN6679	DNA binding activity and nucleus localization		10	
AN6699	Electron carrier activity		4	19
AN6700	ATPase activity	23	2	
AN6708 (PdhA)	Dihydrolipoamide S-acetyltransferase	8	2	2
AN6717 (MdhA)	Mitochondrial malate dehydrogenase	76	87	72
AN6840	Hydroxyacylglutathione hydrolase		11	10
AN6900 (TpiA)	Triose-phosphate isomerase	13	24	7
AN6921	Chaperone	3	2	5
AN7003	Ribosome activity		5	2
AN7105	Translation initiation factor 3 (eIF3)	8	9	
AN7107	Ribosome activity		9	10
AN7141	NAD-dependent aldehyde dehydrogenase	4	4	11
AN7193	NADPH-dependent glycerol dehydrogenase	8		4
AN7254	Cell division protein	44		
AN7262	Protein of unknown function	2	11	2
AN7299	Role in cellular process		7	4
AN7354	Ribosome activity	2	6	10
AN7388 (CpeA)	Laccase	24	40	89
AN7436 (PdiA)	Protein disulfide isomerase	19	16	
AN7451	NAD-glutamate dehydrogenase	9	23	
AN7459 (hxA)	Hexokinase	15	10	27
AN7590	Reductase	4	6	2
AN7600	Iron-sulfur cluster binding	4	8	
AN7625	Myo-inositol-1-phosphate synthase	32	22	
AN7632	Dehydrogenase	15	12	
AN7657	1,3-beta-transglycosidase	6	10	2
AN7708	NADP+ 1-oxidoreductase activity	2	3	3
AN7710	Intracellular localization	3	19	13
AN7725 (PyroA)	Protein required for biosynthesis of pyridoxine	3	5	
AN7950 (EgIC)	Glucan endo-1,3-beta-D-glucosidase	3	17	
AN8009 (Nmt1)	Protein of unknown function	21	20	29
AN8041 (GpdA)	Glyceraldehyde-3-phosphate dehydrogenase	106	58	47
AN8054	20S core proteasome		5	10
AN8170 (NapB)	Nap/SET family member	7		4
AN8176	Ribosome activity	63	22	30
AN8187	Protein of unknown function	4		3

Supplementary Table 3.

Continued.

Shared in Hülle cells, sexual mycelium, asexual mycelium & vegetative mycelium (253 proteins)				
		Spectral counts, found in Hülle cells		
Gene ID	Description	3 day	5 day	7 day
AN8216 (SwoH)	Nucleoside diphosphate kinase	10	19	19
AN8218 (TrxB)	Thioredoxin reductase	10	16	3
AN8269 (Hsp90)	Heat shock protein	47	22	55
AN8273	Ubiquinol-cytochrome-c reductase	19	10	10
AN8275	Mitochondrial citrate synthase	69	24	17
AN8277 (CysD)	Bifunctional enzyme		13	4
AN8605 (Cyp1)	Peptidyl-prolyl cis-trans isomerase	5		11
AN8637 (CatA)	Catalase	8		6
AN8689 (GikA)	Glucokinase	15	10	16
AN8692	Thioredoxin-dependent peroxidase	11	8	7
AN8704	Ribosomal protein	4	6	6
AN8707	Fumarate hydratase	20	8	9
AN8770	Bifunctional enzyme	3		4
AN8856	RNA binding activity	9	5	6
AN8866	Phosphoglycerate dehydrogenase	7	6	9
AN8867	Serine-tRNA ligase activity	17	3	9
AN8953 (AgdB)	Alpha-glucosidase	21	17	2
AN9042 (AgnC)	Alpha-1,3-glucanase		21	6
AN9103 (AifA)	Oxidoreductase	14	5	6
AN9148	UTP-glucose-1-phosphate uridylyltransferase	32	16	31
AN9339 (CatB)	Catalase	18	34	10
AN9403 (PdhC)	Pyruvate dehydrogenase (lipoamide)	7	5	7
AN9465	Ribosome activity	2	14	4

Supplementary Table 4.

The list of protein found in sexual, asexual and vegetative mycelium from solid agar plates (Figure 24). Sexual and asexual mycelium from solid agar plate cultures were analyzed within three different time points. Vegetative mycelium was analyzed 20 hours after inoculation (submerged liquid cultures). For each time points three biological replicates were considered for the different mycelia types. Only proteins identified in two or more biological replicates and with two or more peptides per protein were considered for the analysis. Proteins that were common between the different mycelia types are also listed. Numbers represent the average of spectral counts from three biological replicates. Putative function or role proteins are listed under Description. Different sources were used, mainly AspGD (Cerqueira et al., 2014).

Found in sexual mycelium (203 proteins)				
Gene ID	Description	Spectral counts found in sex. mycelium		
		3 day	5 day	7 day
AN6000 (AptA)	Polyketide synthase	153	60	127
AN7806 (StcU)	Versicolorin reductase	13	43	22
AN8162	Oxidoreductase activity	20	63	58
AN8466	Cell wall macromolecule catabolic process	20	21	2
AN5348	Nucleotide binding activity	17	5	40
AN5558	Protease	63	10	3
AN10965	Protein of unknown function	18	25	15
AN6002 (AptC)	Monooxygenase	3	22	21
AN4105	Erythromycin esterase	16	22	5
AN8514 (TdiB)	Prenyltransferase	14	16	7
AN12267	UDP-N-acetylmuramate dehydrogenase	15	10	33
AN6784 (XptA)	Prenyltransferase	5		3
AN0146 (MdpC)	Monodictyphenone secondary metabolite cluster	4	10	
AN2704	Aryl-alcohol oxidase-related	9	8	4
AN3206	Aryl-alcohol oxidase-related	10	35	
AN10952	Monooxygenase activity	6	31	6
AN0052	Oxidoreductase activity	16	26	
AN3573	Oxidoreductase activity	2	12	34
AN4016	60S ribosomal protein L40	30	42	
AN6082	Ribosome activity	15	31	22
AN3432	Aldose 1-epimerase	21	24	
AN3601	Catalytic activity	15	21	5
AN5698	Fatty acid metabolism		37	33
AN8004	Cytochrome P450	2	4	30
AN8086	Protein of unknown function	18	12	2
AN8106	Protein of unknown function	9	19	3
AN9322	Nucleotide binding activity	7	17	10
AN0034	Glycerone kinase	5	2	2
AN0212	Oxidoreductase	8	8	
AN0221	Chitinase	12	8	8
AN0270	Kinase	4		6
AN0380 (Cyp10)	Peptidyl-prolyl cis-trans isomerase	4		8
AN0385	Aminotransferase	4	7	
AN0558 (GelB)	1,3-beta-transglycosidase	7		8
AN0593	Dehydrogenase	2	17	
AN0596 (DdbA)	DNA damage binding protein	11		5
AN0602	Protein of unknown function	5		5
AN0628	D-lactate dehydrogenase	2	3	
AN0788	Protein of unknown function	8	5	
AN0806	Protein of unknown function	14	2	
AN0839	oxidoreductase	4	2	
AN0875	Protein of unknown function		9	8
AN0887 (LamA)	Urea amidolyase	5		5
AN10130	Ribosome activity	2	4	
AN10214	Protein of unknown function	6	19	
AN10290	Pyridoxamine-phosphate oxidase	7		2
AN10326	Protein of unknown function	4		4
AN10358	Oxidoreductase activity	2	3	9
AN10370	Oxidoreductase	4		6
AN10379	Glutathione transferase	17	8	4
AN10429	Phosphatase	8	6	
AN10444	Involved in sexual development, gamma glutamyl transpeptidase	9	3	

Supplementary Table 4.

Continued.

Found in sexual mycelium (203 proteins)		Spectral counts, found in sex. mycelium		
Gene ID	Description	3 day	5 day	7 day
AN10863	Oxidoreductase	4	9	
AN10973	Citrate synthase		4	8
AN11035	Monoxygenase activity	10	5	
AN11097	Dioxygenase activity	10	33	
AN11115	Purine nucleosidase	3		9
AN11246	Protein of unknown function	16	15	4
AN11419	Ribosome activity	2	8	4
AN11917	Methyltransferase activity	4	4	
AN1204	Protein of unknown function	8	2	
AN12050	Nucleotide binding activity	3	3	
AN12090	Methyltransferase activity	5	14	
AN12335 (AcdA)	Acyl-CoA dehydrogenase domain	3	6	
AN12369	Protein of unknown function		6	6
AN12446	Protein of unknown function	14	5	
AN1271	Arylformamidase activity	6	5	
AN1277 (AdfC)	Alpha-arabinofuranosidase activity	2	4	
AN1291	Carbon-sulfur lyase activity	2	4	
AN1446 (MecB)	Cystathionine gamma-lyase	9	6	
AN1477	Beta-1,4-xylosidase	4	2	
AN1611	Flavin adenine dinucleotide binding	2	8	
AN1639	Oxidoreductase	14	2	
AN1688	Protein of unknown function		5	5
AN1699	Acyl-coA dehydrogenase	2	7	9
AN1763	Oxidoreductase	6	12	5
AN1837	Hydrophobin	12		2
AN1849	Protein of unknown function	12	2	
AN1979	Protein of unknown function	3	4	
AN2161 (Ngn1)	GNAT-type acetyltransferase	13	2	
AN2166	Protein of unknown function	4	7	8
AN2180 (XprF)	Hexokinase-like protein	13	13	
AN2311	Phosphomevalonate kinase		5	6
AN2351	Alcohol dehydrogenase		9	7
AN2359 (XlnD)	Beta-xylosidase	6	8	
AN2366	Trypsin-like protease	14	8	5
AN2405	Protein of unknown function	5	7	
AN2416	Ubiquitin-activating enzyme	7		4
AN2426	Protein of unknown function	13	11	
AN2439 (SldB)	Spindle assembly checkpoint protein	4	19	
AN2441	Nucleotide binding activity	6	5	
AN2463 (LacF)	Beta-galactosidase	5	5	
AN2469	Oxidoreductase	2	13	4
AN2493	Alkaline phosphatase	17	5	3
AN2577	Oxidoreductase		5	5
AN2622 (IpnA)	Isopenicillin-N synthase	6	5	
AN2762	Acyl-coA dehydrogenase	8	2	
AN2801	Oxidoreductase activity	2	8	
AN2853	Protein of unknown function	8	3	
AN2859	Lyase activity	5	21	4
AN2878	Protein of unknown function	17	2	
AN2921	Protein of unknown function		13	2
AN3135	Protein of unknown function		2	3
AN3184	Aldose 1-epimerase	6		2
AN3191	Hydrolase activity	3	2	3
AN3201 (LacD)	Beta-galactosidase	17	14	
AN3312	L-xylulose reductase	2	2	
AN3375	Heat shock protein binding	8	8	
AN3419	Acetyltransferase activity	6	4	
AN3488	Flavin adenine dinucleotide binding	4		8
AN3499	Phosphotransferase activity	4	4	
AN3565	Hydrolase activity	2	2	6
AN10723	Acetyltransferase activity	2	2	
AN10581	Protein of unknown function	2	10	4
AN1059 (FacC)	Carnitine acetyltransferase	6	3	
AN10673	Serine-type peptidase activity	10	5	

Supplementary Table 4.

Continued.

Found in sexual mycelium (203 proteins)		Spectral counts in sex. mycelium		
Gene ID	Description	3 day	5 day	7 day
AN3577	Citrate lyase	2	10	
AN3590	Protein of unknown function	12	6	
AN3598 (FprA)	Peptidyl-prolyl cis-trans isomerase	2	6	
AN3706	Role in rRNA export from nucleus	4	6	2
AN3708	Hydrolase activity	25		4
AN3741 (AlcB)	Alcohol dehydrogenase	2	18	8
AN3779	Exopolyphosphatase activity	7	2	
AN3789	Protein of unknown function	19	12	
AN3805	Oxaloacetase		22	23
AN3867	Pheromone precursor processing	6	2	
AN3916	Glycerol kinase	3	5	
AN3972	Cytosol localization	15	20	
AN4011	5'-phosphoribosyl-4-(N-succinocarboxamide)-5-aminoimidazole lyase	2	2	
AN4041	Protein of unknown function	2	3	
AN4177	Catalytic activity	14	6	
AN4231	Protein required for riboflavin biosynthesis	4	5	6
AN4290	S-methyl-5-thioribose-1-phosphate isomerase	4	31	
AN4299	Protein of unknown function	4	5	7
AN4317	Nuclear pore complex protein	8	6	
AN4353	3-oxoacyl-[acyl-carrier-protein] synthase	4	26	
AN4396	Ras guanine nucleotide exchange factor	2	2	
AN4458	Ubiquitin thiolesterase activity	5	4	
AN4494	Ribosome activity	2	22	4
AN4504 (DfgG)	Endo-mannanase	10	23	
AN4522	Ribosome activity	6	7	3
AN4532	Catechol oxygenase	12	12	20
AN4687 (MccB)	3-methylcrotonyl-CoA carboxylase	13	4	
AN4691	Oxidoreductase	24		10
AN4777	Ribosome activity	11	5	4
AN4822	Tartrate dehydrogenase	11	5	
AN4830	Coenzyme A biosynthetic process	4	4	
AN4901	Glutaminase A	11	21	
AN4967	Protein of unknown function	2	8	
AN5019	5-methyltetrahydropteroyltriglutamate-homocysteine S-methyltransferase	2	16	5
AN5109	Oxidoreductase activity		10	13
AN5144 (PfkZ)	6-phosphofructo-2-kinase	2	4	
AN5178	Glycerol dehydrogenase	2	2	
AN5193	1-aminocyclopropane-1-carboxylate synthase	7		9
AN5373	Oxidoreductase activity	8	21	
AN5421	Protein of unknown function			
AN5480	RNA binding protein	9	15	2
AN5556	Oxidoreductase activity	3	13	
AN5718	Fumarate hydratase	22		13
AN5737	Oxidoreductase	21	3	
AN5777	Triglyceride lipase activity	26	4	
AN5830	Hydrolase activity	2	11	5
AN5937	Manganese ion binding	2	2	6
AN5977	Carbonyl reductase (NADPH) activity	5	2	2
AN5986	Reductase	6	6	4
AN6031	Monooxygenase activity	4	6	7
AN6035	Catalytic activity	4	5	
AN6197	Nuclear migration protein		8	23
AN6329	Protein of unknown function	4	9	
AN6362	Arsenate reductase activity	4	4	
AN6394	Acyl-coA dehydrogenase	9	8	
AN6423	Protein of unknown function	11		13
AN6470	Carbohydrate catabolism	12		6
AN6535	Protein of unknown function	21	4	8
AN6632	40S ribosomal protein S28	2		8
AN6687	DNA binding activity	11		6
AN6933 (MaeB)	Malate dehydrogenase	7	9	
AN7044	Histidinol-phosphatase	6	4	
AN7128	Oxidoreductase activity	2	4	

Supplementary Table 4.

Continued.

Found in sexual mycelium (203 proteins)		Spectral counts found in sex. mycelium		
Gene ID	Description	3 day	5 day	7 day
AN7259 (DcnA)	NEDD8 ligase activity, ubiquitin bindin	4	3	
AN7274	Fumiquinazoline C biosynthetic protein	5	15	
AN7367	Hydrolase activity	2	18	17
AN7564	Threonine aldolase	7		8
AN7704	Catabolic process	16		6
AN7705	Protein of unknown function	3	3	
AN7711	ADP-ribose diphosphatase		8	5
AN8016	ATP-dependent RNA helicase		4	22
AN8045	Protein of unknown function	8	5	
AN8163	Short-chain dehydrogenase/reductase	12	18	
AN8415 (ApdG)	Acyl-coA dehydrogenase	7	2	
AN8592	Monoxygenase activity	6	3	4
AN8606 (GudA)	Glucose 1-dehydrogenase	2	2	3
AN8654	Aminomethyltransferase	4	3	4
AN8657	Oxidoreductase	12		8
AN8797	Protein of unknown function	20		14
AN8808	Phosphoric diester hydrolase	9	18	
AN8899	1-aminocyclopropane-1-carboxylate deaminase	2	2	
AN8988	oxidoreductase		9	10
AN9116	Phosphoribosyltransferase	3	6	22
AN9227	Dioxygenase	12	12	
AN9285	Glucose repressible		4	22
AN9323	Protein of unknown function	4	3	13
AN10762	Protein of unknown function	8	4	

Found in asexual mycelium (118 proteins)		Spectral counts found in asex. mycelium		
Gene ID	Description	3 day	5 day	7 day
AN7558	Transcript induced by light in developmentally competent mycelia		3	37
AN8339	Transcript induced by light in developmentally competent mycelia		29	29
AN1553	Role in fruiting body development	29	29	
AN10378	bZIP transcription factor	4	8	
AN2946	Pheromone precursor processing	41	41	
AN7734	Transcription factor	4		5
AN9171	Protein of unknown function		10	15
AN4852	Glucan 1,3-beta-glucosidase	68	20	
AN1754	Protein of unknown function	3	8	3
AN1035 (AfoF)	Asperfuranone biosynthesis		9	10
AN4742	Translation initiation factor	4	6	
AN3239	Oxidoreductase	26		26
AN0357	Ubiquinol-cytochrome-c reductase subunit	5		5
AN0483	Protein of unknown function		6	8
AN0941 (AgdE)	Alpha-glucosidase activity	13	13	
AN10113	Protein of unknown function	8	8	
AN10174	Protein of unknown function	3		3
AN10219	Transcript induced in response to calcium dichloride in a CrzA-dependent	4	4	
AN10308	Protein of unknown function	5	15	
AN10510	Protein of unknown function	3		3
AN10522	Peptidase	4	4	4
AN1063	NADH dehydrogenase	8	2	8
AN11149	Arylsulfatase activity	2	10	2
AN11533	Protein of unknown function	3	5	3
AN11698	Exopeptidase activity		33	22
AN11718	Mitochondrial intermembrane spce localization		11	11
AN11764	Binding activity	2	4	2
AN11946	Protein of unknown function	2	4	2
AN12376	Nucleotide binding	4	6	2
AN1396	Role in glycerol metabolism	9		9
AN1403	Protein of unknown function	14	15	10
AN1426	Serine-type carboxypeptidase activity	5	5	

Supplementary Table 4.

Continued.

Found in asexual mycelium (118 proteins)		Spectral counts found in asex. mycelium		
Gene ID	Description	3 day	5 day	7 day
AN1433	Protein of unknown function		9	8
AN1532	Protein of unknown function	3	4	
AN1683	Oligosaccharyltransferase delta	2		10
AN1778 (PantoB)	Ketopentolate hydroxymethyl transferase		2	10
AN1857	Kynureninase	4	4	
AN1986	Ferroxidase activity	6	2	6
AN2005 (YpdA)	Histidine-containing phosphotransfer	2	6	2
AN2047	Calmodulin	3	5	3
AN2050	Cell wall organization and Golgi apparatus		10	10
AN2069	Cytochrome b5	2	2	8
AN2070	Protein of unknown function	4	10	
AN2110	Oxidoreductase activity	3	3	3
AN2119	Sphingolipid transporter activity	5	2	5
AN2140	Endoplasmic reticulum localization	2	5	2
AN2185	Protein of unknown function		3	10
AN2237	Carboxypeptidase		4	8
AN2325	Carbohydrate binding	4	23	
AN2431 (Nup49)	Nuclear pore complex		2	
AN2472	Serine/threonine phosphatase activity	2		2
AN2576	Monooxygenase activity	14	2	14
AN2662	Carbon-nitrogen ligase activity		13	15
AN2776	Protein of unknown function		4	6
AN3022	Protein of unknown function		6	8
AN3163 (StoA)	Stomatin ortholog	2		2
AN3367	Sequence-specific DNA binding activity	2	5	2
AN3388 (AmyF)	Alpha-amylase	5	16	
AN3687	Protein of unknown function		18	10
AN3783	Protein of unknown function	2	10	
AN3931 (PilB)	Conserved eisosome protein		2	10
AN4034 (HapC)	Component of AnCP/AnCF CCAAT-binding complex	4	6	
AN4081	Cysteine dioxygenase activity	2	4	2
AN4277	Glucose transmembrane transporter activity	12		10
AN4292	Possible pseudogene	3	3	6
AN4305	Catalytic activity	3		3
AN4499	Nuclear transport protein	5		8
AN4515 (CrhB)	Transglycosidase	4	4	5
AN4525	Transglycosidase		10	5
AN4553	Mitochondrial outer membrane	5	6	8
AN4615	Transmembrane domain-containing protein	5	6	11
AN4636	Lipid particle localization	5	10	5
AN4911	Protein of unknown function	4	4	
AN4927	F1F0-ATPase complex	5		5
AN4946	Protein of unknown function	6	5	
AN5485	Nuclear pore complex	6	4	3
AN5624	DNA binding activity	9		10
AN5670	Protein transporter activity	8		8
AN5671	Protein of unknown function	2	5	2
AN6078 (NadA)	Adenine deaminase	3		3
AN6203	Protein of unknown function	2	5	
AN6228	Cytosol localization		13	6
AN6256	Nucleotide binding activity		6	8
AN6337	Protein of unknown function	2	2	3
AN6382	Phospholipase C activity		4	8
AN6445	Paryl-alcohol oxidase-related protein	22	36	
AN6450	Oxidoreductase	5		5
AN6473	Protein of unknown function	2	6	2
AN6518	Hydrolase activity	2		2
AN6847	Sulfuric ester hydrolase		9	10
AN7102	Protein of unknown function	5	2	11
AN7153	UDP-N-acetylmuramate dehydrogenase	12	12	
AN7201	Role in proteolysis	8	7	
AN7214	Oxidoreductase activity	9	29	
AN7488	Endoplasmic reticulum, fungal-type vacuole localization	2	2	5

Supplementary Table 4.

Continued.

Found in asexual mycelium (118 proteins)				
Gene ID	Description	Spectral counts found in asex. mycelium		
		3 day	5 day	7 day
AN7567	Role in actin cytoskeleton organization	4		4
AN7579	K48-linked polyubiquitin binding		4	5
AN7595	Protein of unknown function		4	8
AN7669	Hydrolase activity	6	4	
AN7680	Protein of unknown function		11	8
AN7864 (BxID)	Beta-1,4-xylosidase	7	7	9
AN7960	Protein of unknown function	8	2	
AN7990	Protein of unknown function	4	4	5
AN7992	Protein of unknown function	5	5	
AN8043	Protein of unknown function	8	10	
AN8234	Protein phosphatase inhibitor activity		8	6
AN8242	Lipase		8	5
AN8546	Phospholipase C	8	10	
AN8607	Protein of unknown function	2	10	10
AN8690	Protein expressed at increased levels during osmoadaptation	5		3
AN8805	Unfolded protein binding activity		5	8
AN8974	Protein of unknown function		4	8
AN9004	Oxidoreductase activity	13	4	13
AN9027	Hydrolase activity	3		3
AN9037	Oxidoreductase		2	10
AN9163	Protein of unknown function	2	2	2
AN9235	Catalytic activity		2	12
AN0328	Nucleus localisation	3	4	

Found in vegetative mycelium (299 proteins)							
Gene ID	Description	Spectral counts found in veg. mycelium		Gene ID	Description	Spectral counts found in veg. mycelium	
			20h				20h
AN0117	Cellular response to oxidative stress		32	AN10480	Protein of unknown function		19
AN0133	RNA helicase		30	AN10489	Peptidyl-prolyl cis-trans isomerase		25
AN0183	Molybdopterin binding domain protein		13	AN10519	Binding activity		50
AN0242	Hydrolase activity		68	AN10535	Translation initiation factor		4
AN0327	Role in ribosomal small subunit		41	AN1055	Formation of translation preinitiation complex		12
AN0381	Unfolded protein binding activity		71	AN10557	ATP-dependent RNA helicase		91
AN0411	Role in ER to Golgi transport		36	AN10595 (AspE)	Septin		23
AN0490	CTP synthase		10	AN10734	Role in regulation of translational elongation		87
AN0565	Multifunctional enzyme		422	AN10743	Establishment or maintenance of actin cytoskeleton		19
AN0692	Cytoplasm localization		13	AN10765	Nucleic acid binding		11
AN0707	5'-3' exoribonuclease activity		5	AN10837	Amidophosphoribosyltransferase activity		25
AN0708	Polypeptide		86	AN10848	Nucleic acid binding		26
AN0717	Histidinol-phosphate aminotransferase		47	AN11008	Squalene monooxygenase activity		18
AN0753	Intracellular localization		106	AN11052	5'-3' exonuclease activity		35
AN0757	tRNA (cytosine-5-)-methyltransferase		54	AN11128	Binding activity		19
AN0809	DNA binding		25	AN11168	Nucleus localization		13
AN0840	Alpha-isopropylmalate synthase		131	AN11238	IMP dehydrogenase/GMP reductase		23
AN0879	Protein of unknown function		29	AN1158	mRNA 5'-UTR binding		128
AN0917	Nucleotide binding activity		7	AN1163	Chaperone		22

Supplementary Table 4.

Continued.

Found in vegetative mycelium (299 proteins)							
Gene ID	Description	Spectral counts found in veg. mycelium		Gene ID	Description	Spectral counts found in veg. mycelium	
			20h				20h
AN1558 (MyoA)	Myosin I, required for secretion and polarized growth		17	AN2523 (ChsB)	Class III chitin synthase		6
AN1606	Calcium ion binding		31	AN2682	Oxidoreductase activity		35
AN1636	Protein of unknown function		7	AN2731	ATPase activator activity		46
AN1667	Protein of unknown function		19	AN2751	topoisomerase II-associated protein		15
AN1700	26S proteasome regulatory		53	AN2756 (SalB)	Actin binding protein		126
AN1709	Mitochondrial tyrosyl-tRNA synthetase		5	AN2765	Localized to chromosomes		14
AN1752	Sulfite reductase		210	AN2862	CAP-Gly domain protein		41
AN1851	Unfolded protein binding activity		90	AN2871 (McnC)	CUE-domain containing phosphoprotein		22
AN1873	Protein of unknown function		9	AN2904	26S proteasome regulatory subunit		64
AN1901 (PdmA)	Sterol 14 alpha-demethylase		3	AN2907	Protein of unknown function		135
AN1904	Chaperonin-containing T-complex		55	AN2909	ATP binding		16
AN1911	Mannose-1-phosphate guanylyltransferase		60	AN2917	Role in positive regulation of RNA polymerase II		37
AN1922	Proteasome regulatory particle		31	AN2954	Protein of unknown function		8
AN1929	DNA-dependent ATPase activity		9	AN2967	tRNA dihydrouridine synthase		4
AN1949	RNA helicase activity		12	AN2976	Intracellular localization		6
AN1954	Protein of unknown function		13	AN2992	Eukaryotic translation initiation factor 2 complex		15
AN1965	Ribose-phosphate pyrophosphokinase		11	AN3019	Ubiquitin-dependent protein		56
AN1966 (HulE)	HECT ubiquitin ligase		37	AN3029	Protein transporter activity		23
AN2014	7S RNA binding activity		12	AN3055	Ribosome binding		23
AN2042	Oxidoreductase		23	AN3070	ATP binding, unfolded protein		45
AN2068	RNA binding activity		124	AN3080	Role in ER to Golgi vesicle-mediated transport		38
AN2080	Intracellular localization		58	AN3122	Transcript levels increase during the unfolded-protein		42
AN2120 (KapJ)	Karyopherin (importin) beta 3		181	AN3134	ATP binding, unfolded protein		65
AN2126	Actin capping protein		32	AN3147	Intracellular localization		28
AN2147	Ribosomal RNA processing protein		37	AN3156	Eukaryotic translation initiation factor 2 complex		47
AN2164	Protein transporter activity		90	AN3169	Ribose-phosphate pyrophosphokinase		22
AN2210	ABC-transporter		80	AN3188	Phosphatidylserine decarboxylase		21
AN2213	ATPase activity		25	AN3344 (Ngn27)	PGNAT-type acetyltransferase		10
AN2226	Protein of unknown function		6	AN3628	Peptide alpha-N-acetyltransferase		34
AN2278	Helicase activity		30	AN3709	Protein of unknown function		20
AN2284 (HemA)	5-aminolevulinic acid synthase		46	AN3716	Protein of unknown function		34
AN2412	NADH dehydrogenase		11	AN3719	Protein of unknown function		6
AN2458	Protein of unknown function		56	AN3720	Putative dehydrogenase		61
AN2516 (AmpA)	Localized to peripheral patches and to hyphal tips		11	AN3739	Intracellular localization		45
AN2518	Involved in exocytosis		16	AN3744	Ribosome activity		35

Supplementary Table 4.

Continued.

Found in vegetative mycelium (299 proteins)							
Gene ID	Description	Spectral counts found in veg. mycelium		Gene ID	Description	Spectral counts found in veg. mycelium	
			20h				20h
AN3804	IgE binding activity		25	AN4865	Nucleic acid binding		35
AN3807	Lipid binding activity		7	AN4890	Role in Golgi to plasma membrane transport		13
AN3824	Phenylalanine-tRNA ligase activity		65	AN4891	Histone binding activity		10
AN3827	Role in cell proliferation		17	AN4892	Role in mRNA processing		13
AN3830 (IleA)	L-threonine dehydratase		38	AN4908	Eukaryotic translation initiation factor subunit		184
AN3832	Mitochondrial translation		11	AN4923	3-hydroxy-3-methylglutaryl coenzyme A synthase		147
AN3839 (SwoF)	Control of polar growth		25	AN4947	Protein of unknown function		5
AN3933	DNA-directed RNA polymerase activity		42	AN5068	Aryl formamidase activity		16
AN4025	Tubulin-tyrosine ligase		10	AN5141	Protein of unknown function		28
AN4038	Translation initiation factor		133	AN5186	Ubiquitin thiolesterase activity		20
AN4051	Heme binding		36	AN5318	Non-ribosomal peptide synthetase		68
AN4094	Role in sterol metabolism		5	AN5521 (AlpA)	Microtubule stabilizing		15
AN4187	Helicase activity		21	AN5529 (CotA)	Protein involved in cell polarity		24
AN4192	Heat shock protein binding		16	AN5629	NADH dehydrogenase		7
AN4207	Protein transporter activity		34	AN5635 (TreB)	Trehalase		23
AN4258	Role in phospholipid metabolism		24	AN5652	Hydantoinase/oxoprolinase		29
AN4300	Protein of unknown function		5	AN5666 (MpkA)	Mitogen-activated protein kinase (MAP kinase)		25
AN4346	Nucleotide binding activity		10	AN5688	Role in lipid biosynthetic process		11
AN4380	Ribonucleotide reductase		77	AN5702	Role in ribosomal large subunit biogenesis		11
AN4412	Nuclear exosomal DEAD-box family RNA helicase		10	AN5705	Protein of unknown function		12
AN4430	Acetolactate synthase		34	AN5713	chaperonin complex component		65
AN4431	RNA binding activity		5	AN5716	Inosine-5'-monophosphate dehydrogenase		17
AN4453	Protein of unknown function		22	AN5717 (Kapl)	Required for normal hyphal growth		117
AN4460	18S rRNA processing complex subunit		4	AN5743	Potassium-transporting ATPase		8
AN4483	Serine/threonine kinase activity		6	AN5747	Protein domain specific binding		20
AN4492	Ubiquitin-specific protease activity		25	AN5775	DNA binding transcription factor		4
AN4523	Spliceosome involved in pre-mRNA splicing		37	AN5823	Protein of unknown function		38
AN4546	RNA binding activity		33	AN5865	GTP-binding protein		20
AN4547	Role in establishment or maintenance of cell polarity		90	AN5883 (MetF)	Methylenetetrahydrofolate reductase		59
AN4563	Protein serine/threonine kinase activity		30	AN5894	RNA polymerase II core binding		11
AN4564 (TeaA)	Cell-end marker protein		11	AN5918 (CatC)	Catalase with a role in gluconic acid		6
AN4602	Tubulin binding activity		9	AN5931	ATP-dependent RNA helicase		13
AN4717 (PkaB)	Cyclic AMP-dependent protein kinase A (PKA)		9	AN5957	Amino acid aminotransferase		78
AN4762	Protein of unknown function		11	AN5970	Disulfide isomerase, ER localization		13
AN4774	Uroporphyrin-III C-methyltransferase		48	AN5972	Ubiquitin binding activity		24

Supplementary Table 4.

Continued.

Found in vegetative mycelium (229 proteins)							
Gene ID	Description	Spectral counts found in veg. mycelium		Gene ID	Description	Spectral counts found in veg. mycelium	
			20h				20h
AN5973 (PkcB)	Similarity to protein kinase C		26	AN6980	Component of the nuclear pore complex		10
AN5992	ATP binding		9	AN6993	Phosphoribosyltransferase		27
AN6006 (KapD)	Karyopherin and nuclear receptor		75	AN7005	Protein of unknown function		7
AN6014 (FaaA)	Long-chain-fatty-acid-CoA ligase		12	AN7028	Thymidylate synthase		6
AN6033	Role in ER to Golgi vesicle-mediated transport		28	AN7146	Role in sterol metabolism		24
AN6058	Menadione stress-induced protein		20	AN7169 (FhbA)	NirA-dependent flavohemoprotein		167
AN6067	GTPase activator activity		43	AN7199	Cytoplasm localization		29
AN6126 (AccA)	Acetyl-CoA carboxylase		377	AN7208	Protein of unknown function		19
AN6168 (MaeA)	Malate dehydrogenase		40	AN7297	Role in chromatin remodeling		4
AN6193	ATP-dependent peptidase activity		37	AN7422	ubiquitin carboxyl-terminal hydrolase		12
AN6207	ATP binding		14	AN7441	ATP-dependent 3'-5' DNA helicase activity		25
AN6231 (TrpB)	Tryptophan synthase		149	AN7474	RNA binding		8
AN6266	Ribosome biogenesis and nucleus localization		6	AN7498	Deoxyhypusine monooxygenase activity		26
AN6267	Nucleotide binding activity		11	AN7540	Translation initiation factor		93
AN6366	Oxidoreductase activity		8	AN7544	Zinc ion binding		7
AN6489	Ribosome activity, role in translation		19	AN7659	RNA helicase activity		60
AN6508	Protein kinase		52	AN7687	Membrane translocase complex		31
AN6510	Translocase of outer mitochondrial membrane complex		12	AN7699	Protein of unknown function		4
AN6515	Protein targeting to endoplasmic reticulum membrane		35	AN7706	Nucleic acid binding		8
AN6521 (LysF)	Homoaconitate hydratase		65	AN7752	Ferrochelatase activity		5
AN6643 (BioB)	Biotin synthase		48	AN7928	Possible pseudogene		4
AN6651	Ribosomal small subunit biogenesis		33	AN7995	Role in ribose metabolism		9
AN6676	Nucleic acid binding		9	AN8023 (VpsA)	Required for vacuole biogenesis		85
AN6705	DNA-dependent ATPase activity		35	AN8038	Nucleic acid binding		10
AN6712 (PldA)	Phospholipase D		7	AN8072	Protein of unknown function		9
AN6731 (SdeA)	Delta-9-stearic acid desaturase		22	AN8073	RNA binding, S-adenosylmethionine-dependent		7
AN6734 (KapF)	Karyopherin		73	AN8102 (PepAc)	Pepsin-like aspartic protease		4
AN6753	NADH-dependent flavin oxidoreductase		35	AN8118	cytochrome c oxidase		4
AN6838 (TubC)	Beta-tubulin		149	AN8225	Ribosomal protein L1		6
AN6853	Phosphatidylinositol transporter activity		25	AN8233	Role in phospholipid transport		51
AN6865	Protein of unknown function		7	AN8268	RasGAP SH3 binding protein		47
AN6866 (AroC)	Role in aromatic amino acid biosynthesis		12	AN8346	Oxidoreductase activity		49
AN6903	Nucleic acid binding		13	AN8488	Palmitoyltransferase activity		13
AN6922	Role in cytoplasmic translation		11	AN8706 (GnaA)	Glucosamine-phosphate N-acetyltransferase		13
AN6978	Nucleotide exchange factor		17	AN8709	Aspartate transaminase		34

Supplementary Table 4.

Continued.

Found in vegetative mycelium (229 proteins)							
Gene ID	Description	Spectral counts found in veg. mycelium		Gene ID	Description	Spectral counts found in veg. mycelium	
			20h				20h
AN8722	ATP-dependent RNA helicase		39	AN1177	Structural molecule activity		75
AN8748	Palmitoyl-(protein) hydrolase activity		12	AN1194	Adenylyl phosphosulfate kinase		18
AN8794	RNA binding		6	AN12101	NADPH dehydrogenase		21
AN8815	Isoflavone reductase family protein		40	AN12272	Protein of unknown function		5
AN8819	Dehydrogenase		7	AN12419	DNA-directed RNA polymerase activity		9
AN8836	PAK (p21-activated kinase) family protein		14	AN1270	Translation initiation factor 3		40
AN8843	Homoserine kinase		54	AN1281	Chaperone binding, protein binding		27
AN8853 (SnpA)	Eukaryotic polypeptide releasing		33	AN1287 (StoB)	Stomatin-like protein		4
AN8859	Aspartate kinase		32	AN1288	Protein of unknown function		77
AN8862 (MyoA)	Involved in the movement of vesicles to the hyphal tip		30	AN0922	Golgi to ER and COPI vesicle coat localization		37
AN8869	Uracil phosphoribosyltransferase		10	AN0999 (CapA)	Adenylate cyclase-associated protein		31
AN8874	GTPase activity		38	AN1006 (NiaD)	Nitrate reductase		38
AN9067 (TinC)	NIMA-interacting protein		37	AN10088	Protein of unknown function		9
AN9090 (RrmA)	RNA binding protein		50	AN10103	DNA binding activity		19
AN9149	Protein of unknown function		14	AN10156	Phosphotransferase activity		27
AN9304 (ElfA)	Glutathione S-transferase		31	AN10173	RNA binding activity		24
AN9357	Cytoplasm localization		9	AN1023 (SagA)	Sensitivity to DNA-damaging agents		12
AN9467	Serine/threonine phosphatase activity		13	AN10257	mRNA binding activity		42
AN9497	Hydrolase activity		5	AN1306	Role in actin filament severing		18
AN10301	Nucleotide binding activity		10	AN1328 (NnaA)	GNAT-type acetyltransferase		6
AN10337	Enzyme regulator activity		28	AN1401 (KapK)	Essential exportin 1		62
AN10350	Phosphatidylinositol binding activity		55	AN1405	Protein of unknown function		4
AN10352	rRNA processing		26	AN1408	U5 snRNP-specific protein		42
AN10396	Farnesyl-diphosphate farnesyltransferase		5	AN1466	Nucleus localization		25
AN1045	RNA binding		30	AN1524	Methylenetetrahydrofolate dehydrogenase		21
AN10475	Tryptophan-tRNA ligase		41				

Supplementary Table 4.

Continued.

Shared in sexual and asexual mycelium (221 proteins)				
Gene ID	Description	Spectral counts found in sex. mycelium		
		3 day	5 day	7 day
AN0050	Picolinic acid decarboxylase	29	28	
AN0076	Role in interspecies interaction	11	2	4
AN0089 (AvaA)	Small GTPase	4		10
AN0131	Cytoplasm localization	2	6	
AN0184	Role in actin filament	6	2	
AN0193	Hydrolase activity	11	12	10
AN0224	Dipeptidase activity	15	18	18
AN0231 (IvoB)	Conidiophore-specific phenol oxidase	15	9	15
AN0248 (PdiB)	Disulfide isomerase	13	2	
AN0391	Protein of unknown function	58	69	
AN0400	Protein of unknown function		10	10
AN0447	Iron ion binding	11		12
AN0733 (HhtA)	Histone H3; core histone protein	2		2
AN0768	Protein of unknown function	31	60	26
AN0774	Nucleotide binding	7	10	
AN0775	Oxidoreductase activity	5	20	
AN0783	Carbon-nitrogen ligase		32	4
AN0824 (ScdA)	Short-chain fatty acid beta-oxidation	15	54	8
AN0880	Peroxisomal targeting signal 2	21	21	
AN0886	Role in nitrogen metabolism		16	14
AN0895	Oxidoreductase	41	87	19
AN0933 (CrhC)	Transglycosidase	10	10	4
AN0942 (LadA)	L-arabinitol 4-dehydrogenase	15	43	14
AN10054	Phosphotransferase activity	8	9	
AN10060	Alpha-amylase	41	116	11
AN10109	Protein of unknown function	19	32	
AN10131 (PyrD)	Dihydroorotase	4	16	
AN10146	Protein of unknown function	8	20	
AN10197	Role in coenzyme M biosynthetic	12	4	
AN10217	Oxidoreductase activity	3	4	
AN10233	Phosphogluconate dehydrogenase	8	119	
AN10260	Menadione stress-induced protein	14	61	
AN10335	Nucleotide binding	6	9	
AN10421	Protein of unknown function	3	13	
AN10437	Mitochondrion localization	22	21	
AN10482	Beta-glucosidase		5	4
AN10494	Nucleotide binding	12	13	5
AN1050	3-ketoacyl-CoA thiolase	23	91	
AN10507	Unfolded protein binding activity		6	10
AN10520	Alpha/beta hydrolase	3	32	
AN10626 (RmtA)	Arginine methyltransferase	3	146	18
AN10695 (AspE)	Septin	4	3	4
AN10700	Protein of unknown function	7	10	
AN10708	Role in proteasomal ubiquitin	15	42	6
AN1074	Glycine dehydrogenase	9	6	
AN10797	Catalytic activity	8	10	4
AN10839	Role in retrograde transport	8	16	
AN11039	Carbon-sulfur lyase activity	4	20	4
AN11062	Protein of unknown function	11	9	8
AN11161	Phosphatidylserine decarboxylase	14	14	4
AN11187	Monooxygenase activity	17	10	
AN11233	Chitinase activity	23	3	
AN11778	Exoinulinase	13	29	
AN1184	Ribosome localization	13		8
AN11862	TRC complex localization	11	9	
AN11908	Hydrolase activity	4	7	
AN1191 (SumO)	Small ubiquitin-like modifier (SUMO) protein		2	5
AN11945	Protein of unknown function	2	18	4
AN1197	Catalytic activity	16	5	4
AN11985	Protein of unknown function		4	13
AN12004	Protein of unknown function	7	7	
AN12070	Carbon-nitrogen ligase activity	3	5	
AN12198	Protein of unknown function		4	8
AN12221	Deoxyribose-phosphate aldolase activity	9	19	4

Supplementary Table 4.

Continued.

Shared in sexual and asexual mycelium (221 proteins)				
Gene ID	Description	Spectral counts found in sex. mycelium		
		3 day	5 day	7 day
AN12229	Zinc ion binding activity	13		14
AN12466	Glutathione synthase activity	7	11	
AN1418	Glucosamine-6-phosphate deaminase activity	22	4	
AN1427	Role in transmembrane transport	8	10	2
AN1428	N-acetylglucosamine-6-phosphate deacetylase	42	47	2
AN1503	Dihydrodipicolinate synthase	10	19	
AN1659	Amino acid transporter		10	5
AN1715	Mannose-6-phosphate isomerase	31	87	30
AN1734	Protein of unknown function	5	45	
AN1742	Fumarylacetoacetase activity	38	4	
AN1809	Fumarylacetoacetase		34	66
AN1868	Glycerol dehydrogenase	15	12	
AN1882	Role in cell redox homeostasis		58	7
AN1896 (FahA)	Fumarylacetoacetate hydrolase	41	79	27
AN1897 (HmgA)	Homogentisate 1,2-dioxygenase	41		16
AN1899 (HpdA)	Role in aromatic amino acid biosynthesis	24	7	4
AN1947	Hydrolase activity	5	12	
AN2085	Endopeptidase activity	3		5
AN2091	Carboxy-lyase activity	9	4	
AN2133	Uracil phosphoribosyltransferase	7	45	8
AN2332	Succinate dehydrogenase	5	49	
AN2393	Nucleotide binding	10	25	
AN2404	Protein of unknown function	5	6	
AN2470	Nucleotide binding	32	45	4
AN2471	Protein of unknown function	15	8	
AN2479 (Ngn16)	GNAT-type acetyltransferase	4	4	
AN2532	Copper ion binding	11	12	
AN2548 (EasC)	Required for emericellamide biosynthesis	4	2	4
AN2720	Catalytic activity	8	30	4
AN2815	Mannitol 2-dehydrogenase	11	81	3
AN2847	DNA binding activity	15	13	
AN2879	Carbon-nitrogen ligase activity	10		15
AN2896	Catalytic activity	10	20	10
AN2977	Role in small molecule transport	2	4	
AN3017	Epoxide hydrolase	25	11	
AN3091	Metalloendopeptidase	44	12	9
AN3104	Allantoicase	10	12	
AN3200	Beta-glucuronidase	4	16	
AN3222	IMP 5'-nucleotidase activity	22	2	
AN3299	Protein of unknown function	11	7	
AN3305	Nucleotide binding activity	18	47	
AN3334	Nucleotide binding activity	37	145	19
AN3351	UDP-N-acetylmuramate dehydrogenase activity	28	18	9
AN3361 (NopA)	Rhodopsin family G-protein coupled receptor-like	8	19	9
AN3431	Nicotinate-nucleotide diphosphorylase	9	21	
AN3605	Oxidoreductase activity	7	7	9
AN3627	Intracellular localization	47	2	2
AN3634	Phosphoribosyltransferase	11	25	7
AN3679	Nucleotide binding	6	44	
AN3756	Endopeptidase activity	9	2	2
AN3869	Role in sterol metabolism	44	10	6
AN3987	Tetratricopeptide	7	4	
AN4018	Role in protein targeting to vacuole	28	13	19
AN4048	Endodeoxyribonuclease activity	4		19
AN4052 (ExgC)	Glucan 1,3-beta-glucosidase	9		29
AN4245	Ceramidase	18	10	
AN4268	Monooxygenase activity	2	28	
AN4397	Protein of unknown functionp	9	15	
AN4421	Oxidoreductase activity	46	123	11
AN4452	Ribosome activity	2	3	2
AN4467 (CypB)	Cyclophilin B	4	5	
AN4531	Protein of unknown function	10	7	
AN4688 (IvdA)	Acyl-coA dehydrogenase	17	23	4
AN4690 (MccA)	Alpha subunit of 3-methylcrotonyl-CoA carboxylase	19	10	

Supplementary Table 4.

Continued.

Shared in sexual and asexual mycelium (221 proteins)				
Gene ID	Description	Spectral counts found in sex. mycelium		
		3 day	5 day	7 day
AN4807	Protein of unknown function	6	3	4
AN4809 (GtaA)	Glutaminase A	61	33	27
AN4843	Alpha-glucosidase		6	
AN4913 (PhK)	Phosphoketolase	5	25	2
AN4914	Acetate kinase	22	34	
AN4957 (GalE)	Galactokinase	11	22	4
AN4979	Dihydroneopterin aldolase activity	8	10	
AN4987 (PkaR)	Protein kinase A	30	47	
AN5021	Role in biosynthetic process	19	21	2
AN5110	Protein of unknown function	4	32	2
AN5194	ATPase activity	7	2	3
AN5354	Oxidoreductase activity	7	12	
AN5387	Protein of unknown function	7	27	
AN5411	Metal ion binding, phosphoric diester hydrolase	9	28	2
AN5452	Splicing factor 3b	25	28	
AN5524	Hydrolase activity	8	5	
AN5607	Role in proteasome assembly	26	2	
AN5613 (HxA)	Xanthine dehydrogenase	29	2	
AN5658	Gamma-glutamyltransferase activity	35	16	
AN5704	Type II fatty acid synthase	10	9	
AN5831	Chorismate synthase	8	16	
AN5879	Ribosomal small subunit assembly	5	32	5
AN5916	Mitochondrial enoyl-CoA hydratase		55	6
AN5942	Protein of unknown function		7	2
AN5989	Epimerase/dehydratase		36	15
AN5994	ATP-dependent NAD(P)H-hydrate dehydratase	56	36	2
AN6066	Catalytic activity	19	20	
AN6111	Exosome		6	11
AN6169	Rho guanyl-nucleotide exchange factor	7	9	10
AN6274	Oxidoreductase activity	50	41	5
AN6438	Aromatic-amino-acid transaminase	20	18	24
AN6512	ATPase activity	6	6	
AN6536 (HisB)	Imidazole glycerol-phosphate dehydratase	7	2	
AN6606	Role in post-translational protein modification	8	10	
AN6635 (YA)	Conidial laccase (p-diphenol oxidase)	30	62	22
AN6654	Glutamate-ammonia ligase activity	10		
AN6655 (GudC)	Glucose 1-dehydrogenase	11	44	8
AN6723 (DhbD)	2,3-dihydroxybenzoate carboxylase	6	13	5
AN6792 (GfdB)	Dehydrogenase	5	91	
AN6804	Transporter of the major facilitator superfamily (MFS)	7	9	12
AN6862	Protein of unknown function	10		
AN6918	Oxidoreductase	2		26
AN6923 (HxtA)	High-affinity hexose transporter	5	9	2
AN6985	Ribulokinase	48	60	37
AN7008 (HadA)	Mitochondrial hydroxyacyl-CoA dehydrogenase	10	10	
AN7011	Protein of unknown function	13	6	
AN7035	Peptidase activity		8	4
AN7140	Protein of unknown function	34		
AN7181	Protein of unknown function	38	46	20
AN7231	Serine-type peptidase	15	27	4
AN7278	Glutamate decarboxylase	12	15	
AN7298	Starvation-induced autophagy	17	15	16
AN7331	Cyanate hydratase activity	12	31	5
AN7471	Hydrolase activity	4	3	
AN7517	Protein of unknown function	22	4	6
AN7691 (PlcB)	Phospholipase	14	7	
AN7742	Single-stranded DNA binding activity	14	8	2
AN7805 (StcV)	Role in sterigmatocystin/aflatoxin biosynthesis	13	21	24
AN7907	Glyoxylate-bleomycin resistance protein	15	6	
AN7911 (OrsB)	Member of the F9775 SM gene cluster	35	71	9
AN7959	Protein of unknown function	4		15
AN8010	Glycogen (starch) synthase	14	16	
AN8046	Triacylglycerol lipase	6	25	2
AN8050	Protein of unknown function	7	8	

Supplementary Table 4.

Continued.

Shared in sexual and asexual mycelium (221 proteins)				
Gene ID	Description	Spectral counts found in sex. mycelium		
		3 day	5 day	7 day
AN8219	Plasma membrane ATPase	25	9	
AN8335	Protein of unknown function	12	51	
AN8396 (PdcB)	Pyruvate decarboxylase	36	34	4
AN8445	Aminopeptidase Y	26	35	31
AN8496	Metal ion binding activity	23	16	16
AN8561	Nucleotide binding	2		15
AN8566	Catechol 1,2-dioxygenase activity		33	4
AN8628	Cofactor binding	5	64	4
AN8638 (cetJ)	Transcript enriched in dormant conidia induced by light	37	24	
AN8639	Alpha-trehalose-phosphate synthase	19	82	2
AN8737 (MstA)	Sugar transporter	3	2	9
AN8744	Oxidoreductase activity	2	5	
AN8755 (MclA)	Methylisocitrate lyase	24	43	6
AN8777 (amdS)	Acetamidase	13	3	6
AN8782	S-formylglutathione hydrolase	13	44	10
AN8803 (RodA)	Hydrophobin	26	9	11
AN8908	Phosphoric diester hydrolase	9	53	14
AN8932	TIM-barrel enzyme family protein	10	9	
AN8968	Isoflavone reductase	5	38	
AN8977 (AlcP)	Gluconolactonase	18	6	4
AN9011	Aryl-alcohol oxidase-related	15	23	4
AN9054	Protein of unknown function	5	53	26
AN9064	Xylitol dehydrogenase	25	30	2
AN9130 (AifA)	Apoptosis-inducing factor (AIF)-like	53	17	10
AN9183 (BglR)	Beta-glucosidase	3	4	4
AN9348	Aryl-alcohol oxidase-related protein	13	16	
AN9380	Chitin deacetylase	13	17	4
AN9425	Carbon-carbon lyase	6	6	22
AN9434	Nucleus localization		10	10

Shared in sexual, asexual and vegetative mycelium (164 proteins)				
Gene ID	Description	Spectral counts found in sex. mycelium		
		3 day	5 day	7 day
AN0121 (HemC)	Porphobilinogen deaminase	7		9
AN0140	Role in actin assembly	24	15	5
AN0163	Rho GDP-dissociation inhibitor activity		12	
AN0182 (RasA)	Small monomeric GTPase	5		
AN0261 (Sec23)	COPII coat component	13	5	
AN0271	dUTP pyrophosphatase	15	3	10
AN0306	Role in regulation of actin filament polymerization	29	23	4
AN0317	Ubiquitin binding activity	20	8	12
AN0410 (BimG)	Required for the completion of anaphase	22	8	
AN0445	Ribosome activity	16	79	10
AN0570	RNA binding	6	11	22
AN0648 (TrpC)	Involved in tryptophan biosynthesis	41	41	21
AN0667 (ManA)	Mannose-6-phosphate isomerase	22	28	8
AN0705	Isoleucine-tRNA ligase activity	10	26	3
AN0797	Multifunctional enzyme	65	29	57
AN0847	Chaperone	3	8	19
AN0858 (Hsp104)	Chaperone	4	2	
AN0906 (KapB)	Essential nuclear transport protein	12		7
AN0912	Beta-isopropylmalate dehydrogenase	11	23	17
AN0952	Acid phosphatase activity	7		13
AN10020	Regulator activity	25	13	6
AN10079 (UreB)	Urease	7	7	13
AN10087	Similar to proliferating cell nuclear antigen (PCNA)	24	46	8
AN10188	Protein of unknown function	2		
AN10194	Helicase activity	9		2
AN10195	Valine-tRNA ligase activity	13	15	9
AN10220 (Ccp1)	Cytochrome c peroxidase	14		8

Supplementary Table 4.

Continued.

Shared in sexual, asexual and vegetative mycelium (164 proteins)				
Gene ID	Description	Spectral counts found in sex. mycelium		
		3 day	5 day	7 day
AN10222	Glucose-6-phosphate 1-epimerase activity	31	31	
AN10230	S-methyl-5-thioadenosine phosphorylase activity	20	14	9
AN10284	Glutathione synthase	12	8	7
AN10296	Fumarate reductase (NADH) activity	32	10	14
AN10298	3-phosphoserine aminotransferase	37	160	5
AN10512 (MthA)	Mitochondrial ketoacyl-CoA thiolase	26	92	5
AN10533	Trehalose-6-phosphate synthase		2	2
AN10681	Ribosome activity	5	10	2
AN10710	Rhosphomannomutase activity	13	19	
AN10718 (RiboG)	6,7-mimethyl-8-ribityl-lumazine synthase	23	46	5
AN10740	Ribosome activity, role in translati	14	75	25
AN10783	Coenzyme binding	15	44	
AN10901	Glycine dehydrogenase	11	51	37
AN10942	Actin depolymerizing	15	35	13
AN10981	Bifunctional GTP cyclohydrolase II	16	10	2
AN11054	Alpha-1,4-glucosidase	12	6	10
AN11070	Metalloaminopeptidase activity	45	163	7
AN11094	Zinc-binding oxidoreductase	4	67	
AN1198	Aminomethyltransferase	12	38	11
AN12237 (AbpA)	Actin-binding protein	8	13	5
AN1274	NADP+ 1-oxidoreductase activity	33	79	
AN1345	Structural constituent of ribosome activity	6	17	10
AN1429 (CodA)	Choline oxidase	26	46	
AN1485	Serine/threonine kinase activity	27	6	3
AN1534	Succinate dehydrogenase	46	90	10
AN1677	Short-chain dehydrogenase	10	90	10
AN1805 (CanB)	Carbonic anhydrase	19		21
AN1913	Lysyl-tRNA synthetase		78	8
AN2306	Ubiquinol-cytochrome-c reductase	4	2	
AN2317	Actin depolymerizing protein	5	3	
AN2414	NADH dehydrogenase (ubiquinone)	11	24	2
AN2440	Ribose-5-phosphate isomerase	18	16	
AN2873 (LysA)	Saccharopine dehydrogenase	22	81	3
AN2882	Homoserine dehydrogenase	59	129	9
AN2930	Mitochondrion localization	9	14	2
AN2964 (PdhX)	Dehydrogenase complex component	19	7	
AN2970	Phosphatase activity	10	9	
AN2998	Multifunctional enzyme	18	133	5
AN3034 (SuAprgA1)	Regulation of penicillin biosynthesis	7	31	2
AN3223 (PfkA)	6-phosphofructokinase	36	171	19
AN3469 (H2B)	Histone H2B	3	5	2
AN3581 (TrxR)	Thioredoxin reductase	34	58	4
AN3591	Propionyl-CoA-yielding methylmalonate semialdehyde	74	77	
AN3593	Aldolase/adducin domain protein	9	27	
AN3626	Phosphoribosylamino-imidazole-carboxylase	18	30	10
AN3695	Anthranilate synthase	8	9	11
AN3702	Leucine-tRNA ligase activity	2	14	5
AN3712	Dienelactone hydrolase	25	79	
AN3748	Phosphoribosyltransferase	44	39	14
AN3853	Metalloendopeptidase activity	22	13	19
AN3932	Proteasome beta-5 subunit	19	46	13
AN3973	Peroxisome protein	15	27	
AN4015	Translation elongation factor activity		41	15
AN4060 (Rps16)	Ribosomal protein S16	16	40	
AN4073	Cytosolic small ribosomal subunit protein S12	7	18	2
AN4085	Intracellular localization	14		4
AN4127	Intracellular localization	4	6	
AN4174	Lactoylglutathione lyase	39	68	18
AN4178 (Myg1)	UPF0160 domain-containing protein	15	26	12
AN4202 (Rpl16A)	Ribosomal protein of the large (60S) ribosomal subunit	8	46	38

Supplementary Table 4.

Continued.

Shared in sexual, asexual and vegetative mycelium (164 proteins)					
Gene ID	Description	Spectral counts found in sex. mycelium			
		3 day	5 day	7 day	
AN4222	Ribosome activity	29	54	16	
AN4234 (PcmA)	Phosphoacetylglucosamine mutase	22	54	48	
AN4402	Voltage-gated anion channel activity	9	7	9	
AN4449	Endopeptidase activator activity	21	8	3	
AN4457	Endopeptidase activator activity	4	13	7	
AN4550 (Cyp7)	Peptidyl-prolyl cis-trans isomerase D	29		4	
AN4583	Peptidyl-prolyl cis-trans isomerase D		53	7	
AN4591	Phosphopentomutase activity		50	16	
AN4803	rRNA binding	12	101	49	
AN4859 (PmaA)	Plasma membrane ATPase	10			
AN4869	20S proteasome component	19	59	13	
AN5028 (PpoC)	Fatty acid oxygenase	69		10	
AN5121	Protein similar to proteasome regulatory	5	11	13	
AN5122	Kinase	5		10	
AN5222	Ribosome activity	12	52		
AN5226 (AcpA)	Acetate permease	5	7	8	
AN5376	Protein of unknown function	7	10	10	
AN5482	Ran GTPase	27	4	2	
AN5547	Oxidoreductase		8	2	
AN5577	Manganese-superoxide dismutase		36	10	
AN5586	Mannose-1-phosphate guanylyltransferase		5		
AN5604 (AcuG)	Fructose-bisphosphatase	45		28	
AN5610	L-aminoadipate-semialdehyde dehydrogenase	12	62	11	
AN5616	Pyridoxal phosphate binding	9	23	5	
AN5646	Role in fatty acid degradation	15	42	13	
AN5662	Threonine-tRNA ligase activity	24	59	23	
AN5749	Metallopeptidase activity	27	32	11	
AN5784	Role in proteasomal ubiquitin-dependent protein	17	51	14	
AN5790	Isocitrate dehydrogenase (NAD+)	3	18		
AN5793	20S proteasome beta-type subunit	22	51	22	
AN5799	Gamma-glutamyl phosphate reductase	18	9	22	
AN5803 (FimA)	Fimbrin protein	22	8	10	
AN5812	Epoxide hydrolase activity	39	48	24	
AN5884 (PyrF)	Orotate phosphoribosyltransferase	16			
AN5886 (LuA)	Alpha-isopropylmalate isomerase	10		10	
AN5979	Role in ribosomal small subunit	5	34	2	
AN6083	Role in ribosomal large subunit assembly	15	70	11	
AN6157 (PyrG)	Orotidine-5'-phosphate decarboxylase	15	36	14	
AN6182 (GalD)	Hexose-1-phosphate uridylyltransferase	8	9	2	
AN6214 (Nha1)	Hat1 acetyltransferase	4		7	
AN6227	Catalytic activity	29	10	19	
AN6248	Adenyl-nucleotide exchange factor activity		22	5	
AN6257	Protein of unknown function	12	15	4	
AN6368	Arginyl-tRNA synthetase	19	6		
AN6490	Phosphorylase	14	27	4	
AN6650 (McsA)	Methylcitrate synthase	85	141	69	
AN6726	Role in proteasomal ubiquitin-dependent protein	42	91	13	
AN7000	Succinate-CoA ligase	11	3	2	
AN7111 (FoxA)	Peroxisomal multifunctional enzyme	23	4		
AN7194	Nucleotide binding	25	25	3	
AN7484	Increased levels during osmoadaptation	13	7	4	
AN7511 (GelE)	1,3-beta-transglycosidase	8		66	
AN7554	Poly(A) RNA binding activity	2	10	10	
AN7594	Protein of unknown function		6		
AN7721	Translocon	4		5	
AN8012 (StcN)	Versicolorin B synthase	32	11	6	
AN8021 (VmaA)	Vacuolar ATPase (V-ATPase)	32	30	20	
AN8022	Protein of unknown function	4		9	
AN8032	C-3 sterol dehydrogenase	9	22		
AN8044	Metalloendopeptidase activity	34	3	35	

Supplementary Table 4.

Continued.

Shared in sexual, asexual and vegetative mycelium (164 proteins)				
Gene ID	Description	Spectral counts found in sex. mycelium		
		3 day	5 day	7 day
AN8057 (CysB)	Cysteine synthase	16	32	
AN8065	Role in actin filament organization	5		6
AN8080	Thioredoxin peroxidase activity	17	80	2
AN8204 (NdxC)	Undix hydrolase	9	2	6
AN8664	Hydrolase activity	19	79	5
AN8674	Vacuolar proton-transporting V-type ATPase	12	2	
AN8698	Role in actin cortical patch assembly	8	41	
AN8870	Expression increased in salt-adapted strains	30	140	27
AN8979 (AlcA)	Alcohol dehydrogenase	52		24
AN9085	Protein of unknown function	10	6	2
AN9097	Ribosomal protein	14	20	3
AN9124	Hsp90 protein binding	18	9	10
AN9308	UDP-N-acetylmuramate dehydrogenase activity	3	2	2
AN9401	Mitochondrial localization	50	69	
AN9407 (FasA)	Fatty acid synthase	16	14	2
AN9468	Maturation of SSU-rRNA	9	45	3
AN9470 (UaZ)	5-hydroxy-isourate	15	10	2

Shared in asexual and vegetative mycelium (32 proteins)				
Gene ID	Description	Spectral counts found in asex. mycelium		
		3 day	5 day	7 day
AN0075 (TigA)	Disulfide isomerase		11	
AN0162	Sequence-specific DNA binding	2	5	2
AN0745	Nucleolar protein		2	4
AN0943	Mitochondrial F1F0-ATP synthase	2	5	2
AN10229	NADH dehydrogenase		13	12
AN11055	Phosphatase	4		2
AN1195	Hydrolase		2	2
AN1282	Role in posttranslational protein targeting to membrane		14	
AN2086	Nuclear pore complex protein	2		
AN2279	Endoplasmic reticulum organization	3		2
AN2316	Cytochrome c oxidase		10	6
AN2420	U2 snRNP localization	2		10
AN2743	Regulation of translation in response		6	
AN2885	Role in sequence-specific DNA binding		6	2
AN3843	Role in cristae formation	2		2
AN3906	Protein of unknown function	27		
AN4080	Role in cytoplasmic translation, polysomal ribosome		2	2
AN4270	Role in actin cortical patch assembly		2	
AN4919	Role in actin cortical patch assembly		3	3
AN4929	Protein of unknown function		43	
AN5181 (NudC)	Protein involved in nuclear migration		11	2
AN5499	Nuclear pore complex; Spindle-assembly checkpoint		12	
AN5606	Proton-transporting ATPase activity	9	24	7
AN5745	Eukaryotic translation initiation factor 3	4	12	
AN6060	Binding activity and role in RNA metabolic process	5	4	
AN6077	NADH dehydrogenase	10	4	3
AN6287	F1F0-ATPase complex subunit	3	11	6
AN6591	Essential nuclear export receptor	3	2	2
AN7051 (MetG)	Cystathionine beta-lyase	4		
AN7159	Tripeptidyl-peptidase activity	20		
AN7177	Protein of unknown function		8	
AN8274	DNA binding activity		4	2

Supplementary Table 4.

Continued.

Shared in sexual and vegetative mycelium (87 proteins)				
Gene ID	Description	Spectral counts found in sex. mycelium		
		3 day	5 day	7 day
AN0057	Tyrosine-tRNA ligase activity		4	5
AN0179	Oxidoreductase	2		2
AN0351 (GfdA)	Glycerol-3-phosphate dehydrogenase		16	
AN0354 (GroG)	3-deoxy-D-arabino-heptulosonate 7-phosphate synthase	10		
AN0495	Formyltetrahydrofolate deformylase		11	3
AN0651 (FadA)	Heterotrimeric G protein		4	5
AN0665	Involved in vesicle transport	10	7	7
AN0673	Role in actin assembly	5	6	
AN0907	Ribosome activity	2	11	23
AN0997	Ribosome activity		2	5
AN10148 (ChpA)	Cysteine- and histidine-rich-domain [CHORD]-containing protein		6	3
AN10182	Translation initiation factor 3	8	7	
AN10278	Cytosol, mitochondrion, nucleus localization	5	6	
AN10282	Nucleus localization		11	5
AN10418	Protein of unknown function	2	9	
AN10472	Hydroxyethylthiazole kinase activity	2	5	
AN10526 (RmtA)	Arginine methyltransferase	2	3	
AN11058	Intracellular localization	7	7	
AN1150	Role in arginine metabolism	10	7	
AN12246	Ribosome activity		2	9
AN1256	ATPase activity	10	24	4
AN1379	Role in cysteine metabolism	3	18	
AN1394 (AspD)	Septin	6	8	
AN1769	Role in cysteine metabolism	3	19	7
AN2051	Hsp90p co-chaperone		3	8
AN2243	Carbamoyl-phosphate synthase	10	2	
AN2343	Protein of unknown function	2	10	5
AN2733	Uroporphyrinogen decarboxylase activity	4	2	
AN2775	Protein of unknown function		11	5
AN2997	Protein of unknown function	2	7	
AN3026 (CopA)	Alpha-COP coatamer-related protein	7	6	
AN3456	Cystathionine gamma-synthase	2	4	4
AN3823	Ribosome activity	9	4	
AN3894	Aconitate hydratase		10	7
AN3901	Lactic acid dehydrogenase		3	5
AN4086	Phenylalanine-tRNA ligase	9	6	
AN4401	Asparagine synthase		10	2
AN4404	Aminopeptidase activity		2	10
AN4463	Vesicle-mediated transport and clathrin coat of coated pit	2	2	
AN4647	Protein of unknown function	2	4	4
AN4739	Phosphoribosyl amino imidazolesuccinocarboxamide synthetase		5	8
AN4820	Succinate-semialdehyde dehydrogenase	5	16	
AN4872	Protein of unknown function		94	5
AN4956	Acetolactate synthase		2	4
AN4997	Phosphatidylinositol transporter	8	12	
AN5123	Oxidoreductase		7	12
AN5130	Coproporphyrinogen oxidase	2	8	
AN5206 (LysB)	Homoisocitrate dehydrogenase	9	10	
AN5534	Glyoxylate reductase activity		2	4
AN5589	Glycerol kinase	10	5	5
AN5591	Aminotransferase	10	8	10
AN5731	Chorismate synthase	3	8	
AN5741	Ribosome activity		5	10
AN5778	Actin binding activity		9	18
AN5782	Catalytic activity		12	19
AN5820 (MecA)	Cystathionine beta-synthase		13	11
AN5904	Beta-ketoacyl-[acyl-carrier-protein] synthase		12	6
AN5954	Eukaryotic translation initiation factor 3		11	8
AN6338	Aromatic-amino-acid transaminase		20	5
AN6354	Ubiquitin C-terminal hydrolase	3		4
AN6391 (PphA)	Phosphatase	2	3	4
AN6505 (RcoA)	WD40 repeat protein	10	19	3
AN6541	Ligase with a role in purine metabolism	2	8	4
AN6644 (BiA)	Dethiobiotin synthetase	7	6	

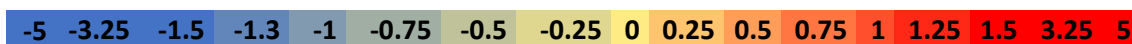
Supplementary Table 4.

Continued.

Shared in sexual and vegetative mycelium (87 proteins)				
Gene ID	Description	Spectral counts found in sex. mycelium		
		3 day	5 day	7 day
AN7010	Role in biosynthetic process		10	10
AN7143	Cytosol localization	14	10	
AN7289	Actin monomer binding activity		2	11
AN7387 (PcrA)	Pyrroline-5-carboxylate reductase	2		
AN7430 (HisHF)	Glutamine amidotransferase	3	8	4
AN7479	Asparaginyl-tRNA synthetase	8	3	
AN7587	Protein of unknown function		9	12
AN7636	Oxidoreductase	5	9	
AN7722	Role in arginine metabolism	9	2	
AN7895 (CipB)	Oxidoreductase		37	
AN8121	5'-phosphoribosylformyl glycinamide synthetase		9	
AN8224	Glutamate-tRNA ligase		15	7
AN8406	Menadione stress-induced		10	11
AN8547	Glucose-methanol-choline (GMC) oxidoreductase		5	6
AN8790	D-xylulokinase	3	6	
AN8800 (SgdC)	CysteinyI tRNA synthase		4	8
AN8820 (CnaA)	Calmodulin-dependent protein phosphatase		13	9
AN8824	Ribosomal large subunit binding activity	2	18	16
AN9080	Nucleus localization		8	5
AN9157	Glutamine-tRNA ligase	6	5	6
AN9408 (FasB)	Fatty acid synthase		32	8
AN9419	Alanine-tRNA ligase		23	11
AN6906	Ubiquitin ligase E3	10	5	

Supplementary Table 5. Proteins that were unchanged in *laeAΔ* vegetative mycelium

The protein quantity of the following proteins is unchanged in a *laeAΔ* vegetative mycelium. The log₂ SILAC ratio was determined for the strains *laeAΔ* (AGB1074) in comparison to *laeA* (AGB1092). The following thresholds were set. In the range of a log₂ SILAC ratio between -0.5 and + 0.5 the protein quantity is unchanged. The log₂ SILAC ratio for the complementation strain (*laeAcomp⁺*, AGB1076) in comparison to the parental *laeA* strain (AGB1092) is also listed. Ø = median of log₂ SILAC ratios, SD = standard deviation, NaN = not a number. Biological replicates are numbered 1-3. Spectral counts (PSM) for three biological replicates are shown (Spectral counts were obtained by Proteome Discoverer 1.4.). The color scales represent log₂ SILAC ratios

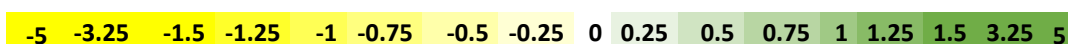


Gene ID	Description	Spectral counts			<i>laeAΔ/laeA</i>			Ø	SD	<i>laeAcomp⁺/laeA</i>			Ø	SD
		1	2	3	1	2	3			1	2	3		
Actin														
AN0306	Actin filament	80	79	105	-0.5	0	-0.5	-0.5	0.3	0.2	-0.1	0.5	0.2	0.3
AN6542 (ActA)	Actin A	335	425	563	-0.4	0	0.0	0.0	0.2	0.2	-0.1	0.5	0.2	0.3
AN0140	Actin assembly	53	68	91	-0.3	0.1	-0.1	-0.1	0.2	0.2	-0.1	0.5	0.2	0.3
AN2756 (SlaB)	Actin binding protein	117	100	191	-0.5	0	-0.5	-0.5	0.3	0	-0.4	0.3	0.0	0.4
AN2862	Cytoskeleton protein	69	55	84	-0.5	-0.1	-0.5	-0.5	0.2	0.5	0	0.4	0.4	0.3
Cellular processes														
AN3720	Coat protein complex II	21	43	56	-0.5	0.3	0.5	0.3	0.5	-0.1	0.2	0.4	0.2	0.2
AN0117	Response to oxidative stress		6	26	NaN	-0.5	-0.5	-0.5	0.3	NaN	0	-0.5	-0.3	0.3
AN1757 (SsfA)	Proteasome subunit	13	20	29	-0.5	0.4	-0.2	-0.2	0.5	0.4	0.1	0.5	0.4	0.2
AN0084	GTPase-activating protein	118	135	164	-0.2	0.2	-0.5	-0.2	0.4	0.4	0.1	0.3	0.3	0.2
AN0999 (capA)	Adenylate cyclase	13	32	54	-0.4	0.1	-0.5	-0.4	0.3	0.5	0.1	0.3	0.3	0.2
Metabolic process														
AN8041 (GpdA)	Glyceraldehyde-3-phosphate dehydrogenase	1104	971	1794	0	0	-0.3	0.0	0.2	-0.3	-0.1	0.3	-0.1	0.3
AN0932 (GlrA)	Oxidoreductase	15	42	52	-0.4	-0.1	-0.4	-0.4	0.2	0.3	0.1	0.4	0.3	0.1
AN10526 (RmtA)	Arginine methyltransferase	4	15	NaN	NaN	0	0.2	0.1	0.1	0	0	0.2	0.0	0.1
AN1430	Oxidoreductase		3	14	NaN	0.2	-0.5	-0.2	0.4	NaN	0	0.4	0.2	0.2
AN7451	NAD-glutamate dehydrogenase	244	229		-0.4	0	NaN	-0.2	0.2	0.2	-0.4	NaN	-0.1	0.3
AN2999 (IdpA)	Isocitrate dehydrogenase	99	69	205	-0.2	0.5	-0.2	-0.2	0.4	-0.1	-0.4	0.2	-0.1	0.3
AN8012	Farnesyl-pyrophosphate synthase	28	41	80	-0.4	-0.2	-0.3	-0.3	0.1	0.4	-0.2	0.4	0.4	0.3
AN7632	Dehydrogenase	93	83	99	-0.4	0.4	0.2	0.2	0.4	0.5	-0.3	0.2	0.2	0.4
AN1342	Alanine-glyoxylate transaminase	42	47	27	-0.3	0.5	-0.5	-0.3	0.5	0.1	-0.3	0.3	0.1	0.3
AN0254	Catalytic activity		29	4	NaN	-0.5	-0.4	-0.5	0.3	NaN	-0.5	-0.5	-0.5	0.3
Catabolic process														
AN2903 (PepE)	Aspartic protease	167	184	164	-0.5	0.1	0.0	0.0	0.3	0.1	-0.5	0.6	0.1	0.5
AN5442 (CpyA)	Carboxypeptidase Y	16	39	94	-0.5	0	0.1	0.0	0.3	0.2	-0.3	-0.5	-0.3	0.4
AN5810 (PepP)	Prolidase	11	67	67	-0.3	0.4	0.5	0.4	0.4	0.3	0.4	0.3	0.3	0.1
Vacuole function														
AN1195	V-ATP synthase subunit C	28	22	28	-0.3	0.3	-0.2	-0.2	0.3	0.5	-0.1	0.4	0.4	0.3
AN10563 (Pho8)	Vacuolar alkaline phosphatase	38	10	12	-0.5	0.5	0.5	0.5	0.6	0.5	-0.1	0.2	0.2	0.3

Supplementary Table 5, continued. Protein quantity of the following proteins was unchanged or unquantifiable in *laeAΔ* vegetative mycelium.

The log₂ SILAC ratio was determined for the strains *laeAΔ* (AGB1074) in comparison to *laeA* (AGB1092). Additionally, the log₂ ratio for the complementation strain (*laeAcomp⁺*, AGB1076) in comparison to the parental *laeA* strain (AGB1092) is listed. The range between these two ratios are unchanged or unquantifiable. Proteins without a log₂ SILAC ratio are listed (marked with NaN). These proteins are unquantifiable. It cannot be ruled out that protein quantities of some of the following identified proteins are quantifiable.

∅ = median of log₂ SILAC ratios, SD = standard deviation, NaN = not a number. Biological replicates are numbered 1-3. Spectral counts (PSM) for three biological replicates are shown (Spectral counts were obtained by Proteome Discoverer 1.4.). The color scales represent log₂ SILAC ratios.



Gene ID	Description	Spectral counts			<i>laeAΔ/laeA</i>			∅	SD	<i>laeAcomp⁺/laeA</i>			∅	SD
		1	2	3	1	2	3			1	2	3		
AN6700	ATPase binding activity	77	237	638	-4.2	-4.4	-1.5	-2.9	1.7	-2.4	0.5	-1.6	-1.6	1.5
AN5028 (PpoC)	Fatty acid oxygenase	124	99	86	1.4	-3.3	-1.8	-2.6	2.4	1.2	-0.2	3.9	1.2	2.1
AN8777 (AmdS)	Acetamidase	17	44	51	-2.3	-2.7	-1.7	-2.2	0.5	-0.2	-1.0	1.8	-0.2	1.5
AN3017	Epoxide hydrolase	83	73	88	-3.1	-2.2	-1.5	-2.2	0.8	-1.8	-1.1	1.5	-1.1	1.8
AN0870	Small molecule transport	74	33	129	-2.1	-0.3	-2.8	-2.1	1.3	-0.8	-0.2	-1.3	-0.8	0.6
AN0354 (AroG)	DAHP synthase	78	91	124	-2.6	-1.6	-1.7	-2.1	0.5	-1.7	-0.8	-0.4	-0.8	0.7
AN1913	Lysyl-tRNA synthetase	62	95	139	-2.6	-1.4	-2.0	-2.0	0.6	-1.1	-0.4	-0.7	-0.7	0.3
AN10745	Glycine hydroxymethyltransferase	36	90	90	-2.0	-0.7	-2.5	-2.0	0.9	-0.8	-0.9	-1.7	-0.9	0.5
AN8770	Acetylglutamate kinase	66	89	198	-1.6	-0.4	-3.6	-2.0	1.6	-1.1	-0.3	-2.3	-1.1	1.0
AN1990 (LysD)	Homocitrate synthase	48	123	191	-4.1	-2.0	-1.3	-2.0	1.5	-2.4	-0.2	-1.5	-1.5	1.1
AN1306	Gelsolin	17	19	19	-3.4	-2.0	-1.1	-2.0	1.2	-1.3	-1.1	-0.9	-1.1	0.2
AN6227	Hercynylcysteine sulfoxide lyase	77	110	69	-3.0	-1.8	-2.1	-1.9	0.7	-1.7	-0.8	3.2	-0.8	2.6
AN10298	3-phosphoserine aminotransferase	96	108	181	-2.3	-1.1	-1.9	-1.9	0.6	-1.5	-0.6	-1.1	-1.1	0.5
AN11227 (HscA)	Heat shock protein	165	233	510	-1.9	-0.7	-1.9	-1.9	0.7	-0.5	-0.1	-1.7	-0.5	0.8
AN2295	Succinate-CoA ligase	36	50	93	-1.8	-0.4	-2.0	-1.8	0.9	-0.3	-0.2	-1.7	-0.3	0.9
AN0860	Protein of unknown function	30	21	29	-2.3	-1.3	-1.8	-1.8	0.5	1.3	0.0	1.7	1.3	0.9
AN2272	Kinase	57	110	170	-1.7	-0.8	-3.0	-1.7	1.1	-0.5	-0.3	-1.6	-0.5	0.7
AN5601	Saccharopine dehydrogenase	13	57	132	-2.7	-1.4	-2.1	-1.7	0.6	-1.2	-0.4	-1.2	-1.2	0.5
AN4409 (ArgB)	Ornithine carbamoyltransferase	52	206	282	-2.3	-1.0	-2.5	-1.7	0.8	-1.9	-0.7	-0.9	-0.9	0.6
AN7625	Myo-inositol-1-phosphate synthase	104	248	668	-1.8	-0.4	-3.1	-1.7	1.3	-1.5	-0.3	-2.8	-1.5	1.3
AN0443	Alcohol dehydrogenase	59	111	178	-2.5	-1.1	-1.7	-1.7	0.7	-0.6	-5.6	-1.9	-1.9	2.6
AN1523	F1F0-ATPase complex subunit	250	419	577	-1.6	-0.4	-1.6	-1.6	0.7	-0.4	-0.5	-1.6	-0.5	0.7
AN3695	Anthranilate synthase	16	39	63	-2.3	-1.4	-1.8	-1.6	0.4	-1.0	-0.5	-0.8	-0.8	0.3
AN2436 (AclB)	ATP citrate synthase	407	500	1057	-2.0	-0.7	-1.6	-1.6	0.7	0.8	0.6	-0.8	0.6	0.9
AN3059 (PgmA)	Phosphoglycerate mutase	153	235	503	-1.6	-0.3	-1.5	-1.5	0.7	-0.5	-0.1	-1.6	-0.5	0.8
AN5793	20S proteasome beta-type subunit	9	38	36	-1.9	-0.9	-2.1	-1.5	0.7	-0.2	0.0	-1.0	-0.2	0.5
AN0240 (PppA)	Pentose-phosphate	450	621	820	-1.5	-0.4	-2.2	-1.5	0.9	-0.2	-2.4	-1.5	-1.5	1.1
AN2164	Chromatid cohesion	17	29	33	-1.9	-0.5	-1.5	-1.5	0.7	0.5	0.2	-0.7	0.2	0.6

Supplementary Table 5, is continued from page 185-198.

Supplements

Gene ID	Description	PSM			<i>laeAΔ/laeA</i>			∅	SD	<i>laeAcomp+/laeA</i>			∅	SD
		1	2	3	1	2	3			1	2	3		
AN6048	Aspartate transaminase	169	350	399	-2.2	-0.9	-2.0	-1.5	0.7	-0.9	-1.2	-1.5	-1.2	0.3
AN1177	Coatomer subunit beta	34	43	102	-1.5	-0.5	-2.1	-1.5	0.8	-0.1	-0.5	-1.4	-0.5	0.7
AN10675	Protein of unknown function	39	40	75	-1.5	-0.6	-1.6	-1.5	0.6	0.0	-0.4	-0.7	-0.4	0.4
AN10278	Electron transfer flavoprotein	8	38	59	-1.5	-0.2	-1.5	-1.5	0.7	-0.1	-0.3	-1.5	-0.3	0.8
AN2126 (KapJ)	Importin	35	19	42	-1.4	0.6	-2.0	-1.4	1.4	0.2	0.1	-1.1	0.1	0.8
AN2286 (AlcC)	Alcohol dehydrogenase III	259	384	437	-1.4	0.0	-2.1	-1.4	1.1	-0.3	0.0	-2.1	-0.3	1.1
AN8277 (CysD)	Methionin-Synthase	157	262	210	-1.6	-0.5	-2.3	-1.4	0.9	0.1	-0.5	-1.3	-0.5	0.7
AN6708 (PhdA)	Acetyltransferase	87	108	470	-1.8	-0.4	-2.5	-1.4	1.1	-0.5	-0.3	-2.1	-0.5	1.0
AN1263	Adenosylhomocysteinase	195	433	447	-1.4	-0.2	-1.4	-1.4	0.7	-0.4	-0.3	-1.7	-0.4	0.8
AN9408 (FasB)	Fatty acid synthase	81	183	578	-2.1	-0.3	-2.5	-1.4	1.2	0.0	0.8	-1.5	0.0	1.2
AN1964	40S ribosomal protein S6	24	21	143	-1.4	-0.1	-1.4	-1.4	0.8	-0.3	-0.2	-2.1	-0.3	1.1
AN0688	Transketolase	558	633	859	-1.6	-0.6	-1.3	-1.3	0.5	0.6	2.4	-1.0	0.6	1.7
AN5141	Protein of unknown function	6	12	80	-1.1	-0.3	-2.3	-1.3	1.0	-0.4	-0.3	-1.5	-0.4	0.7
AN6168 (MaeA)	Malate dehydrogenase	12	35	40	-3.3	-1.6	-1.1	-1.3	1.2	-2.4	-0.6	-0.6	-0.6	1.0
AN6010 (SgdE)	Heat shock protein	305	438	861	-2.4	-1.0	-1.7	-1.3	0.7	-1.1	-0.6	-2.3	-1.1	0.8
AN2896	Catalytic activity	10	8	16	-1.4	0.2	-1.3	-1.3	0.9	-0.5	-0.4	-1.4	-0.5	0.6
AN10148 (CphA)	CHORD-containing protein	7	5	17	-1.7	-1.3	-1.1	-1.3	0.3	0.1	-0.8	1.1	0.1	0.9
AN1013	60S ribosomal protein L5	72	56	313	-1.3	0.2	-1.8	-1.3	1.0	-0.4	-0.2	-1.3	-0.4	0.6
AN8722 (Sub2)	RNA helicase	33	42	66	-1.2	-0.6	-2.0	-1.3	0.7	-0.4	-0.1	-1.4	-0.4	0.7
AN10030	Alkaline serine protease	27	114	150	-1.3	-0.4	-1.9	-1.3	0.8	-0.2	-0.6	0.1	-0.2	0.3
AN3466 (KgdB)	Succinyl transferase	47	117	353	-1.3	0.1	-1.4	-1.3	0.8	-0.3	-0.4	-2.1	-0.4	1.0
AN2213	Proteasome	39	47	80	-1.3	-0.4	-1.7	-1.3	0.7	0.3	-0.5	-1.2	-0.5	0.7
AN5210 (PkiA)	Pyruvate kinase	207	258	440	-1.7	-0.5	-2.1	-1.3	0.8	-0.4	-0.4	-2.3	-0.4	1.1
AN5975	Dehydrogenase	459	443	359	-1.3	-0.5	-2.1	-1.3	0.8	1.0	0.4	1.7	1.0	0.7
AN1256	Protein of unknown function	52	76	130	-1.3	-0.6	-1.3	-1.3	0.4	-0.2	-0.2	-1.4	-0.2	0.7
AN3112 (UgmA)	UDP-galactopyranose mutase	91	98	182	-1.8	-0.4	-1.3	-1.3	0.7	0.4	0.2	-1.9	0.2	1.3
AN8866	Phosphoglycerate dehydrogenase	110	141	150	-1.7	-0.8	-1.7	-1.3	0.5	-0.8	-0.1	-1.4	-0.8	0.6
AN3829	Dehydrogenase	33	60	219	-1.0	0.4	-2.9	-1.3	1.6	-0.8	-1.1	-3.8	-1.1	1.6
AN5884	Orotate phosphoribosyltransferase	28	33	49	-1.5	-0.7	-1.8	-1.2	0.6	-0.3	-0.3	-1.9	-0.3	0.9
AN4163 (CpcB)	Protein with seven WD repeats	84	90	287	-1.0	-0.2	-2.3	-1.2	1.1	0.0	-0.3	-2.0	-0.3	1.1
AN3906	Protein of unknown function	51	89	182	-1.4	0.2	-2.7	-1.2	1.4	0.8	0.2	-1.3	0.2	1.0
AN4380	Ribonucleotide reductase	16	35	45	-2.0	-0.8	-1.6	-1.2	0.6	0.7	0.5	-1.5	0.5	1.2
AN6058	Protein of unknown function	51	69	102	-2.6	-1.4	-1.0	-1.2	0.8	-1.6	-1.2	-2.5	-1.6	0.7
AN0912	Dehydrogenase	32	58	115	-1.9	-0.4	-1.2	-1.2	0.7	-0.5	0.3	-1.4	-0.5	0.8
AN1638	Serine-type peptidase	280	378	473	-1.2	0.0	-1.3	-1.2	0.7	0.3	-0.1	-0.9	-0.1	0.6
AN0242	Hydrolase	56	70	222	-1.3	-0.3	-1.2	-1.2	0.5	0.0	-3.5	-1.6	-1.6	1.8
AN0840	Alpha-isopropylmalate synthase	58	107	180	-2.5	-1.2	-0.3	-1.2	1.1	-1.2	-0.4	-1.5	-1.2	0.6
AN4462 (PycA)	Pyruvate carboxylase	297	369	1671	-1.6	-0.5	-1.8	-1.2	0.7	-0.2	-0.2	-1.0	-0.2	0.5
AN2909	Arsenite-transporting ATPase	6	13	37	-1.2	-0.3	-1.6	-1.2	0.7	0.5	0.3	-1.2	0.3	0.9
AN4401	Asparagine synthase	14	53	138	-2.3	-1.1	-1.3	-1.2	0.6	-1.6	-0.3	-1.7	-1.6	0.8
AN7010	Catalytic activity	54	65	48	-3.3	-1.9	-0.5	-1.2	1.4	-2.6	-0.4	2.3	-0.4	2.5
AN1282	Protein of unknown function	41	45	114	-1.8	-0.5	-1.2	-1.2	0.7	-0.1	-0.2	-1.1	-0.2	0.6
AN4259	43S preinitiation complex	18	29	107	-1.8	-0.6	-1.7	-1.2	0.7	-0.6	-0.6	-1.9	-0.6	0.7
AN1401 (KapK)	Exportin 1	32	50	117	-1.2	-0.2	-1.4	-1.2	0.6	0.3	0.0	-1.0	0.0	0.7
AN5744	14-3-3-like protein	340	443	689	-1.2	-0.1	-2.2	-1.2	1.0	0.2	-0.3	-1.3	-0.3	0.8
AN10710	Phosphomannomutase	39	62	79	-1.2	-0.3	-1.5	-1.2	0.6	0.2	0.2	-1.6	0.2	1.0
AN5206 (LysB)	Homocitrate dehydrogenase	37	74	117	-2.2	-0.6	-1.7	-1.2	0.8	-1.0	-0.5	-2.7	-1.0	1.2
AN12465	Dihydroliipoamide dehydrogenase	113	241	358	-1.2	0.0	-1.8	-1.2	0.9	-0.8	-0.8	-2.1	-0.8	0.7
AN6391 (PphA)	Protein phosphatase	23	27	56	-1.7	-0.3	-2.0	-1.1	1.0	0.3	0.0	-1.2	0.0	0.8
AN8269 (Hsp90)	Heat shock protein	625	758	1431	-1.6	-0.4	-1.9	-1.1	0.8	0.1	-0.1	-1.5	-0.1	0.8
AN2914	Argininosuccinate lyase	35	103	151	-2.1	-1.1	-1.1	-1.1	0.5	-1.3	-0.4	-1.3	-1.3	0.5
AN10266	Ubiquitin-activating enzyme E1	111	245	299	-1.6	-0.5	-1.1	-1.1	0.6	0.3	-0.2	-0.8	-0.2	0.6
AN1923	Alanine transaminase	157	157	223	-1.4	-0.4	-1.1	-1.1	0.5	-1.6	-1.2	-2.1	-1.6	0.5
AN0359 (SgdA)	Translation initiation factor 3 (eIF3)	4	13	217	-2.5	0.2	0.5	-1.1	1.6	-0.6	2.5	-1.8	-0.6	2.2
AN4085	Serine threonine phosphatase	42	62	90	-1.3	-0.3	-2.0	-1.1	0.8	0.5	0.0	-1.1	0.0	0.8
AN6639 (McdB)	2-methylcitrate dehydratase	121	163	220	-2.0	-0.6	-1.6	-1.1	0.7	-0.3	-0.9	-1.0	-0.9	0.4
AN0753	Protein of unknown function	16	58	231	-1.1	0.2	-1.6	-1.1	1.0	2.4	1.3	-4.0	1.3	3.4
AN3236	Methyltransferase	13	20	14	-2.6	-1.1	5.0	-1.1	4.0	-2.4	-0.8	1.9	-0.8	2.2
AN1274	Oxidoreductase	11	41	20	-1.1	-0.2	-1.4	-1.1	0.6	0.4	0.1	-1.1	0.1	0.8
AN1911	Guanylyltransferase	44	42	81	-1.1	0.2	-1.6	-1.1	0.9	0.6	0.2	-1.3	0.2	1.0
AN4862 (RanGAP)	Ran GTPase activating protein	10	29	104	-1.2	0.2	-2.3	-1.1	1.2	0.3	0.2	-1.9	0.2	1.3
AN11045	D-lactate dehydrogenase	6	8	48	-1.0	-0.5	-1.8	-1.0	0.7	-0.7	-0.4	-2.3	-0.7	1.0
AN3413	Ribosomal protein S2	76	55	252	-1.0	-0.1	-1.8	-1.0	0.9	-0.3	-0.3	-2.0	-0.3	1.0
AN6346	Dihydroxy-acid dehydratase	23	61	6	-1.6	-0.2	-1.9	-1.0	0.9	-0.8	-0.2	-2.2	-0.8	1.0

Supplements

Gene ID	Description	PSM			<i>laeAΔ/laeA</i>			Ø	SD	<i>laeAcomp+/laeA</i>			Ø	SD
		1	2	3	1	2	3			1	2	3		
AN2875 (FbaA)	Fructose-bisphosphate aldolase	323	507	596	-1.0	-0.1	-1.4	-1.0	0.7	0.2	0.0	-1.5	0.0	0.9
AN7169 (FhbA)	NirA-dependent flavohemoprotein	170	252	315	-1.1	-0.1	-1.9	-1.0	0.9	0.4	-0.2	-2.0	-0.2	1.2
AN5989	Epimerase/dehydratase	459	45	41	-1.3	-1.9	-0.2	-1.0	0.8	1.0	-0.9	0.4	0.4	1.0
AN2210	ABC-transporter	58	82	20	-2.2	-1.0	-0.4	-1.0	0.9	-0.7	0.1	-1.6	-0.7	0.8
AN6202 (Rpl3)	Ribosomal protein L3	18	32	325	-1.2	-0.1	-1.9	-1.0	0.9	-0.6	-0.2	-2.1	-0.6	1.0
AN2133	Actin capping protein	45	18	23	-1.0	-0.4	-1.3	-1.0	0.5	0.6	-0.3	0.7	0.6	0.5
AN2743	Translation initiation factor 3	9	19	158	-1.0	0.1	-1.9	-1.0	1.0	-0.5	-0.3	-2.0	-0.5	0.9
AN5747	26S protease subunit	12	31	63	-0.9	-0.7	-1.3	-1.0	0.3	0.3	-0.5	-1.2	-0.5	0.7
AN2932	Eukaryotic initiation factor 4A	101	245	438	-1.5	-0.7	-1.0	-1.0	0.4	-0.3	-0.2	-1.5	-0.3	0.7
AN7430	Glutamine amidotransferase	17	47	78	-2.3	-1.9	-0.1	-1.0	1.2	-1.2	-0.7	-1.4	-1.2	0.4
AN4464	Bifunctional purine biosynthesis	146	148	338	-1.5	-0.6	-1.4	-1.0	0.5	0.2	-0.1	-1.5	-0.1	0.9
AN1810 (OtaA)	Ornithine transaminase	293	427	781	-1.8	-1.0	0.7	-1.0	1.3	-0.9	0.1	-2.3	-0.9	1.2
AN6547	Proteasome subunit	50	47	51	-0.9	0.0	-1.9	-1.0	1.0	0.2	-0.1	-1.0	-0.1	0.6
AN5746	Phosphopyruvate hydratase	20	832	963	-1.0	-0.2	-1.7	-1.0	0.7	0.1	-0.3	-1.6	-0.3	0.9
AN10079 (UreB)	Urease	81	57	51	-1.4	-0.1	-1.0	-1.0	0.7	1.5	0.4	-0.8	0.4	1.2
AN12237 (AbpA)	Actin-binding protein	62	52	62	-0.9	0.3	-1.8	-0.9	1.1	0.8	0.0	-1.1	0.0	0.9
AN4470	Regulation of translational fidelity	24	35	73	-1.4	-0.4	-1.5	-0.9	0.6	-0.3	-0.3	-1.7	-0.3	0.8
AN4769	Sulfurylase	108	263	376	-1.2	0.0	-1.9	-0.9	1.0	0.4	-0.2	-2.4	-0.2	1.5
AN0075 (TigA)	Disulfide isomerase	19	24	33	-0.9	0.1	-1.6	-0.9	0.9	1.0	0.6	-0.9	0.6	1.0
AN10279	eIF4G binding	28	27	59	-0.9	0.0	-1.4	-0.9	0.7	-0.2	-0.3	-1.8	-0.3	0.9
AN8824	Translation initiation factor (eIF-6)	43	40	29	-2.0	-0.8	-1.1	-0.9	0.6	-0.3	-0.8	-0.8	-0.8	0.3
AN2930	Protein of unknown function	4	23	20	-1.3	0.3	-0.9	-0.9	0.8	0.2	0.1	-1.2	0.1	0.8
AN2068	RNA binding effector protein	52	77	184	-1.1	-0.6	-0.9	-0.9	0.3	0.0	-0.4	-1.6	-0.4	0.8
AN0554 (AldA)	Aldehyde dehydrogenase	877	828	506	-2.0	-0.9	0.8	-0.9	1.4	-1.5	-0.9	2.1	-0.9	1.9
AN4869	20S proteasome component	30	36	48	-1.2	0.1	-1.9	-0.9	1.0	0.0	0.2	-1.1	0.0	0.7
AN8182 (AspC)	Septin	139	160	252	-0.8	0.1	-1.8	-0.9	0.9	1.1	0.4	-1.1	0.4	1.1
AN5162 (PdhB)	Pyruvate dehydrogenase	36	70	214	-2.0	-0.2	-1.5	-0.9	0.9	-0.5	-0.4	-2.1	-0.5	1.0
AN10527	Trimethyllysine dioxygenase	9	8	27	-1.6	-0.2	-0.8	-0.8	0.7	-0.7	-1.2	-2.1	-1.2	0.7
AN6267	Regulation of G0 to G1 transition	20	5	14	-1.3	-0.2	-1.5	-0.8	0.7	0.7	0.1	-0.7	0.1	0.7
AN10222	Glucose-6-phosphate 1-epimerase	57	52	59	-1.8	-0.7	-0.8	-0.8	0.6	-0.3	0.0	-0.6	-0.3	0.3
AN9403	Pyruvate dehydrogenase	75	57	225	-2.0	-0.4	-1.3	-0.8	0.8	-0.5	-0.1	-2.0	-0.5	1.0
AN6699	Electron-transfer flavoprotein	29	94	141	-1.3	-0.3	-1.4	-0.8	0.6	0.1	-0.2	-1.8	-0.2	1.0
AN8748	Palmitoyl-(protein) hydrolase	10	3	11	-1.6	-0.6	-1.1	-0.8	0.5	0.1	-0.3	-1.2	-0.3	0.6
AN1017 (HogA)	Mitogen-activated protein kinase	17	14	17	-1.3	-0.3	-0.8	-0.8	0.5	0.3	0.2	-1.3	0.2	0.9
AN2440	Ribose-5-phosphate isomerase	7	27	29	-0.8	0.2	-1.1	-0.8	0.7	0.3	0.3	-1.1	0.3	0.8
AN2968 (IppA)	Inorganic diphosphatase	239	358	473	-0.8	0.0	-1.8	-0.8	0.9	0.6	0.1	-1.1	0.1	0.9
AN3928 (ThiF)	Thiazole synthase	35	132	370	-3.2	-0.6	-1.0	-0.8	1.4	-1.8	0.5	-1.9	-1.8	1.4
AN7000	Succinate-CoA ligase	60	65	138	-1.9	-0.5	-1.1	-0.8	0.7	-0.2	0.1	-1.4	-0.2	0.8
AN4888 (PdcA)	Pyruvate decarboxylase	140	499	580	-2.6	-0.9	-0.7	-0.8	1.0	-0.9	-0.5	-2.0	-0.9	0.8
AN4174	Lactoylglutathione lyase	75	79	116	-1.0	0.0	-1.6	-0.8	0.8	0.6	-0.2	-1.4	-0.2	1.0
AN1182 (BenA)	Beta-tubulin	352	327	648	-0.8	0.0	-1.4	-0.8	0.7	0.7	0.3	-1.0	0.3	0.9
AN7107	Role in translation	18	30	210	-1.0	0.0	-1.6	-0.8	0.8	-0.3	-0.2	-2.1	-0.3	1.0
AN6630	Nascent polypeptide-associated	118	138	264	-1.1	-0.1	-1.5	-0.8	0.7	-0.1	-0.2	-1.7	-0.2	0.9
AN8435	Tyrosinase domain protein	110	58	73	1.5	-0.2	-1.4	-0.8	1.5	4.2	2.8	5.1	4.2	1.1
AN6591 (Cse1)	Essential nuclear export receptor	38	48	113	-1.0	-0.5	-1.1	-0.8	0.3	0.2	0.0	-1.2	0.0	0.8
AN2212	Ubiquitin-conjugating enzyme E2	7	2	7	-0.8	0.6	-1.6	-0.8	1.1	0.8	0.0	-1.2	0.0	1.0
AN9401	Oxidoreductase	7	14	4	-2.1	-0.5	-1.0	-0.8	0.8	-0.4	-0.7	-1.7	-0.7	0.7
AN4739	SAICAR synthetase	6	6	47	-3.0	-0.7	-0.9	-0.8	1.3	-0.8	0.1	-1.7	-0.8	0.9
AN0906 (KapB)	Nuclear transport protein	22	57	110	-1.5	-0.1	-0.8	-0.8	0.7	0.0	0.1	-1.5	0.0	0.9
AN8273	Ubiquinol-cytochrome-c reductase	45	63	126	-1.6	-0.2	-1.3	-0.7	0.7	-0.5	-0.4	-2.4	-0.5	1.1
AN2012	Protein of unknown function	117	148	175	-0.9	0.1	-0.7	-0.7	0.5	0.6	-0.1	-0.2	-0.1	0.5
AN5999	Carbamoyl-phosphate synthase	93	218	481	-2.6	-1.2	-0.3	-0.7	1.2	-1.8	-0.5	-1.7	-1.7	0.7
AN10223	1-Cys peroxidase	363	335	459	-1.6	-0.7	0.0	-0.7	0.8	0.2	-0.3	-1.4	-0.3	0.8
AN0687	Arginine metabolism	60	42	63	-1.3	-0.3	-0.7	-0.7	0.5	0.3	1.6	-1.1	0.3	1.4
AN6563	Translation elongation factor	330	445	722	-1.7	-0.7	-0.8	-0.7	0.6	-0.1	0.0	-1.2	-0.1	0.7
AN6726	Proteasome subunit	37	55	51	-0.9	0.0	-1.5	-0.7	0.8	0.2	-0.3	-1.1	-0.3	0.6
AN0179	Oxidoreductase	18	63	69	-1.7	-0.7	-0.5	-0.7	0.7	0.1	-2.5	-1.3	-1.3	1.3
AN8204	NAD+ diphosphatase	6	12	14	-1.9	-0.9	-0.6	-0.7	0.7	0.1	-0.6	-1.3	-0.6	0.7
AN5745	Translation initiation factor	425	2	35	-1.2	-0.3	-1.1	-0.7	0.4	-0.3	-0.5	-1.8	-0.5	0.8
AN7335	Protein of unknown function	8	3		-0.7	-0.3	-1.1	-0.7	0.4	0.8	0.0	-1.8	0.0	1.3
AN5571 (KgdA)	Oxoglutarate dehydrogenase	71	106	224	-1.7	-0.1	-1.3	-0.7	0.9	-0.5	-0.4	-2.0	-0.5	0.9
AN5713 (Cct7)	Chaperonin	23	24	93	-1.8	-0.5	-0.8	-0.7	0.7	-0.1	-0.3	-1.8	-0.3	0.9
AN4591	Phosphoglucomutase	81	60	68	-1.3	-0.5	-0.9	-0.7	0.4	0.3	-0.5	-0.8	-0.5	0.6
AN6921	Co-chaperone	62	61	77	-0.9	0.0	-1.3	-0.7	0.7	0.2	-0.1	-0.8	-0.1	0.5
AN7436 (PdiA)	Disulfide isomerase	118	152	204	-1.7	-0.7	-0.6	-0.6	0.6	0.6	-0.2	-0.5	-0.2	0.5
AN2904	26S proteasome regulatory subunit	25	69	99	-1.6	-0.4	-0.6	-0.6	0.6	-0.1	-0.2	-1.1	-0.2	0.5
AN6341	Coronin	137	110	194	-0.4	0.6	-1.8	-0.6	1.2	1.1	0.5	-1.2	0.5	1.2

Supplements

Gene ID	Description	PSM			<i>laeAΔ/laeA</i>			Ø	SD	<i>laeAcomp+/laeA</i>			Ø	SD
		1	2	3	1	2	3			1	2	3		
AN6508 (GskA)	Kinase	69	53	47	-1.4	-0.1	-1.2	-0.6	0.7	0.7	0.2	-0.5	0.2	0.6
AN3748	Phosphoribosyltransferase	43	95	109	-2.1	-0.9	-0.3	-0.6	0.9	-0.6	-0.3	-1.1	-0.6	0.4
AN4667 (AspA)	Septin	92	185	226	-0.9	0.2	-1.4	-0.6	0.8	0.9	0.3	-1.0	0.3	1.0
AN4102 (BglA)	Beta-glucosidase	138	100	40	-0.3	0.4	-1.7	-0.6	1.1	1.4	-0.8	1.1	1.1	1.2
AN5547	Oxidoreductase	28	21	29	-1.5	-0.4	-0.8	-0.6	0.6	-1.2	-1.2	-1.6	-1.2	0.2
AN4402	Voltage-gated anion channel	35	26	82	-1.6	-0.3	-0.9	-0.6	0.6	-0.3	-0.5	-2.9	-0.5	1.5
AN7003	60S ribosomal protein L13	18	28	159	-1.2	0.0	-1.3	-0.6	0.7	-0.3	-0.3	-2.1	-0.3	1.0
AN5973 (PkcB)	Protein kinase C	16	15	36	-1.6	0.1	-1.3	-0.6	0.9	0.5	0.3	-1.4	0.3	1.1
AN5122	Kinase	69	63	104	-1.8	-0.5	-0.7	-0.6	0.7	-0.8	-0.5	-2.0	-0.8	0.8
AN5529 (CotA)	Serine/threonine protein kinase	7	18	55	-1.4	0.0	-1.1	-0.6	0.7	0.3	-0.1	-1.4	-0.1	0.9
AN5895 (GdiA)	Rab GDP-dissociation inhibitor	112	142	251	-0.9	0.2	-1.4	-0.6	0.8	0.8	0.3	-1.4	0.3	1.2
AN6900 (TpiA)	Triose-phosphate isomerase	113	189	231	-0.9	0.0	-1.2	-0.6	0.6	-0.2	-0.3	-1.5	-0.3	0.7
AN6257	Protein of unknown function	87	107	162	-1.7	-0.3	-0.8	-0.6	0.7	0.1	0.0	-1.4	0.0	0.8
AN4087	40S ribosomal protein subunit	89	78	237	-1.2	-0.1	-1.0	-0.5	0.6	-0.3	0.0	-2.1	-0.3	1.1
AN1015	Phosphorylase	108	80	82	-1.0	-0.5	1.2	-0.5	1.2	1.5	-0.3	-0.6	-0.3	1.1
AN3954	Phosphogluconate dehydrogenase	483	863	944	-1.5	-0.3	-0.7	-0.5	0.6	-0.2	-0.2	-1.6	-0.2	0.8
AN3592 (ClxA)	Calnexin	38	33	106	-1.8	-0.2	-0.5	-0.5	0.8	0.6	0.2	-1.3	0.2	1.0
AN1993	Aspartate transaminase	151	342	498	-1.5	-0.3	-0.5	-0.5	0.6	-1.4	-0.9	-2.3	-1.4	0.7
AN10718 (RiboG)	Lumazine synthase	2	22	27	-0.5	1.1	-1.6	-0.5	1.4	1.4	0.8	-0.8	0.8	1.1
AN6004	Protein of unknown function	119	110	119	-1.3	-0.2	-0.8	-0.5	0.5	0.7	-0.2	-1.3	-0.2	1.0
AN7570 (TubB)	Alpha-tubulin	192	263	363	-0.8	0.0	-1.0	-0.5	0.5	0.9	0.1	0.4	0.4	0.4
AN2916	Succinate dehydrogenase	17	40	97	-1.0	0.3	-0.5	-0.5	0.7	0.1	-0.5	-2.3	-0.5	1.3
AN2458	Cullin binding protein	39	51	81	-1.3	-0.4	-0.5	-0.5	0.5	0.1	-0.4	-1.2	-0.4	0.7
AN1733 (PrnC)	Oxidoreductase	68	39	37	-0.5	0.2	-1.0	-0.5	0.6	1.5	-0.8	-0.4	-0.4	1.2
AN6650 (McsA)	Methylcitrate synthase	57	79	46	-1.6	-0.9	0.0	-0.5	0.8	0.2	-0.9	0.9	0.2	0.9
AN8870	40S ribosomal protein S3Ae	8	25	123	-1.3	0.0	-0.9	-0.5	0.7	-0.2	-0.2	-2.0	-0.2	1.1
AN10273 (Gst3)	Glutathione S-transferase	38	32	37	-2.4	0.5	-0.5	-0.5	1.5	0.1	0.5	-0.7	0.1	0.6
AN5602	Chaperone	38	34	47	-2.1	-0.3	-0.6	-0.5	1.0	-0.5	0.0	-1.5	-0.5	0.8
AN6499 (MdhC)	Malate dehydrogenase	437	548	429	-0.9	0.0	-0.9	-0.5	0.5	0.9	0.1	-0.1	0.1	0.5
AN6840	Hydroxyacylglutathione hydrolase	38	29	19	-1.1	-0.3	-0.6	-0.5	0.4	0.5	-0.6	-0.9	-0.6	0.8
AN4501 (ArtA)	14-3-3 protein	427	599	892	-1.0	-0.1	-0.8	-0.4	0.5	0.7	0.0	-1.0	0.0	0.9
AN5129 (Hsp70)	Heat shock protein	604	842	1322	-1.6	-0.5	-0.4	-0.4	0.7	0.0	0.0	-1.4	0.0	0.8
AN8022	Protein of unknown function	23	30	28	-0.9	0.0	-0.8	-0.4	0.5	0.3	-0.2	-1.0	-0.2	0.7
AN9497	Hydrolase	141	9	19	-1.7	-0.3	-0.5	-0.4	0.7	-0.8	-0.2	-1.1	-0.8	0.5
AN9308	Dehydrogenase	31	32	12	-2.0	-0.6	-0.2	-0.4	0.9	0.7	0.1	-0.5	0.1	0.6
AN4820	Dehydrogenase	52	51	22	0.5	1.1	-1.9	-0.4	1.6	2.0	0.2	1.7	1.7	0.9
AN11070	Metalloaminopeptidase	75	32	20	-1.2	-0.4	0.1	-0.4	0.7	0.0	-1.0	-0.9	-0.9	0.6
AN5986	Reductase	16	35	13	-1.6	1.2	-1.9	-0.4	1.7	0.5	0.3	0.3	0.3	0.1
AN5790	Isocitrate dehydrogenase	9	21	126	-0.9	0.1	-0.9	-0.4	0.6	0.2	-0.3	-2.2	-0.3	1.3
AN1426	Serine-type carboxypeptidase	34	16	14	-0.4	0.6	-0.9	-0.4	0.8	2.7	0.0	-0.1	0.0	1.6
AN4463	Clathrin	102	298	436	-1.2	0.0	-0.6	-0.3	0.6	0.4	0.1	-1.2	0.1	0.8
AN3932	Proteasome beta-5 subunit	12	28	60	-0.5	1.7	-2.3	-0.3	2.0	0.2	0.0	-1.0	0.0	0.6
AN5812	Aminopeptidase	16	19	15	-1.9	0.2	-0.8	-0.3	1.1	0.2	-0.3	-1.0	-0.3	0.6
AN10709 (GfaA)	Transaminase activity	224	451	672	-1.3	-0.3	2.5	-0.3	2.0	0.7	0.2	-1.0	0.2	0.8
AN4871 (ChiB)	Chitinase	44	62	43	-0.1	0.2	-0.8	-0.3	0.5	0.0	-1.7	-0.9	-0.9	0.9
AN5525 (AcoA)	Aconitate hydratase	339	380	55	-1.4	-0.1	-0.4	-0.3	0.7	-0.4	-0.4	-1.8	-0.4	0.8
AN3739	Protein of unknown function	18	10	63	-1.5	-0.3	-0.2	-0.3	0.7	0.0	-0.6	-0.4	-0.4	0.3
AN10020	Proteasome complex localization	44	105	105	-1.5	-0.3	3.0	-0.3	2.3	-0.3	-0.2	-1.3	-0.3	0.6
AN2142	Uracil phosphoribosyltransferase	43	66	111	-1.5	-0.2	1.0	-0.2	1.3	0.1	-0.2	-1.6	-0.2	0.9
AN4794	Ribosomal protein	3	19	129	-1.8	0.2	-0.6	-0.2	1.0	-0.6	0.0	-2.0	-0.6	1.1
AN4414	Decarboxylase	96	121	209	-2.0	-1.0	0.5	-0.2	1.3	0.5	-0.1	-0.7	-0.1	0.6
AN6525 (AciA)	Formate dehydrogenase	384	358	231	0.7	1.5	-1.9	-0.2	1.7	1.9	0.5	2.4	1.9	1.0
AN2998	Tetrahydrofolate synthase	110	143	260	-0.9	-0.2	0.3	-0.2	0.6	0.7	0.0	-1.4	0.0	1.1
AN7262	Protein of unknown function	116	84	189	-1.0	0.1	-0.4	-0.1	0.6	1.3	0.6	-1.3	0.6	1.3
AN2051 (Cdc37)	Cell division cycle 37	6	10	42	-1.5	-0.1	0.3	-0.1	1.0	0.4	-0.1	-0.7	-0.1	0.6
AN8689 (GlkA)	Glucokinase	56	72	102	-0.1	0.9	-1.1	-0.1	1.0	-0.3	0.0	-2.3	-0.3	1.2
AN3973	Peroxioredoxin	45	54	85	-2.5	-0.9	0.7	-0.1	1.6	-1.5	-0.7	-2.8	-1.5	1.0
AN8674	V-type ATPase	36	60	40	-2.6	0.1	-0.2	0.0	1.5	0.6	-0.1	-1.0	-0.1	0.8
AN6232 (VamB)	F1F0-ATPase complex subunit	112	173	234	-1.0	0.0	0.0	0.0	0.6	0.3	-0.3	-1.2	-0.3	0.7
AN2412 (CmkA)	Kinase	26	28	50	-0.4	0.6	0.0	0.0	0.5	1.2	0.5	-0.8	0.5	1.0
AN2936	Alpha-mannosidase	32	31	29	0.0	1.0	-1.3	0.0	1.1	1.3	-0.4	0.1	0.1	0.9
AN5604 (AcuG)	Fructose-bisphosphatase	33	43	3	0.7	1.4	-1.3	0.0	1.4	-0.2	-1.0	-1.0	-1.0	0.4
AN6988	Proteasome regulatory particle	20	46	66	-1.6	-0.5	0.6	0.1	1.1	0.0	-0.2	-1.1	-0.2	0.6
AN1358	Serine/threonine phosphatase	41	28	71	0.8	0.1	-1.8	0.1	1.3	1.5	0.2	-0.8	0.2	1.1
AN5916 (EchA)	Mitochondrial enoyl-CoA hydratase	2	8	8	-0.7	0.7	-0.5	0.1	0.7	0.9	-0.8	-1.2	-0.8	1.1
AN2526	Ketol-acid reductoisomerase	149	308	499	-1.2	0.2	0.1	0.1	0.8	-0.7	0.0	-2.3	-0.7	1.2
AN7708	Oxidoreductase	63	82	129	0.8	0.7	-0.4	0.1	0.6	5.2	0.5	-1.2	0.5	3.3

Supplements

Gene ID	Description	PSM			<i>laeAΔ/laeA</i>			Ø	SD	<i>laeAcomp+/laeA</i>			Ø	SD
		1	2	3	1	2	3			1	2	3		
AN3716	26S proteasome	13	48	55	-1.0	-0.1	0.4	0.2	0.7	0.0	-0.1	-1.1	-0.1	0.6
AN7111 (FoxA)	Role in fatty acid beta-oxidation	131	172	40	1.4	2.3	-1.9	0.2	2.2	1.7	-0.5	-1.3	-0.5	1.5
AN5994	Dehydratase	27	7	19	-2.0	-0.4	1.0	0.3	1.5	0.5	-0.5	-0.9	-0.5	0.7
AN2532	Amine oxidase	73	102	85	0.3	1.7	-2.3	0.3	2.0	0.8	0.1	-1.8	0.1	1.3
AN4127	Protein of unknown function	29	39	138	-2.5	-1.4	2.0	0.3	2.4	-1.7	-0.8	-3.2	-1.7	1.2
AN5977	Carbonyl reductase	27	18	34	-2.0	-0.6	1.4	0.4	1.7	0.5	-0.2	0.4	0.4	0.4
AN0824 (ScdA)	Dehydrogenase	6	10		-1.0	0.6	1.1	0.6	1.0	0.1	-0.7	-1.6	-0.7	0.8
AN7950 (EglC)	Glucosidase	13	65	71	-2.0	-0.4	1.5	0.6	1.8	-0.7	-0.9	-1.0	-0.9	0.1
AN8707	Fumarate dehydratase	88	172	258	-0.8	0.5	0.8	0.6	0.8	0.1	-0.3	-2.3	-0.3	1.3
AN6330	Elongation factor 2	896	1127	1483	-1.2	-0.3	1.6	0.6	1.4	0.0	-0.1	-1.4	-0.1	0.8
AN9124	Heat shock protein	44	113	219	-1.4	-0.3	1.7	0.7	1.6	0.6	0.1	-1.2	0.1	0.9
AN6653 (AcuE)	Malate synthase	11	15	24	0.4	0.4	1.8	1.1	0.8	0.1	-2.3	-2.9	-2.3	1.6
AN5872	Proteasome subunit	17	79	64	-0.9	0.0	2.7	1.4	1.8	0.1	-0.2	-1.0	-0.2	0.6
AN8953 (AgdB)	Alpha-glucosidase	68	164	78	3.4	3.8	-1.1	1.4	2.7	2.4	2.2	4.7	2.4	1.4
AN5626 (FacA)	Acetyl-CoA synthase	375	351	227	1.8	2.5	0.3	1.4	1.1	2.3	-0.3	-0.3	-0.3	1.5
AN8782	S-formylglutathione hydrolase	10	28	12	-0.1	0.7	2.4	1.6	1.3	0.7	-0.3	0.6	0.6	0.5
AN8664	Hydrolase	78	66	89	-0.8	0.3	2.9	1.6	1.9	-0.5	-1.0	-1.3	-1.0	0.4
AN6231 (TepB)	Tryptophan synthase	121	157	277	-3.1	-1.5	5.0	1.7	4.2	-1.8	-0.5	-0.7	-0.7	0.7
AN8233	Phosphatidylinositol transporter	94	122	176	-0.3	0.8	3.3	2.0	1.8	1.0	0.7	-1.4	0.7	1.3
AN3499	Phosphotransferase	12	26	10	NaN	-1.7	-1.6	-1.7	1.0	-2.1	-1.6	-2.1	-2.1	0.3
AN2977	Small molecule transport	17	11	10	NaN	-0.4	-1.4	-0.9	0.7	-0.8	-0.9	-1.9	-0.9	0.6
AN3626	Carboxylase	3	25	59	-2.1	NaN	-2.6	-2.6	1.4	-0.4	-2.7	-1.7	-1.7	1.1
AN10096	Hydrolase	29	27	26	-3.5	-2.0	NaN	-2.8	1.7	-2.0	-0.9	-2.4	-2.0	0.7
AN0158	2-alkenal reductase	15	35	38	-2.9	-1.9	NaN	-2.4	1.5	-1.0	-0.8	-1.9	-1.0	0.5
AN3222	5'-nucleotidase	25	25	20	-2.8	-1.9	NaN	-2.3	1.4	-0.6	-1.1	-0.5	-0.6	0.3
AN7074	Oxidoreductase	134	63	60	-2.5	-2.2	NaN	-2.2	1.4	-2.0	-1.7	1.2	-1.7	1.8
AN1883	Argininosuccinate synthase	92	175	212	-2.6	-1.5	NaN	-2.0	1.3	-1.5	-0.7	-1.4	-1.4	0.4
AN2867 (PgmB)	Phosphoglucomutase	243	240	417	-2.0	-1.0	NaN	-1.5	1.0	-0.3	-0.4	-0.5	-0.4	0.1
AN3031	Threonine synthase	24	101	177	-2.0	-0.9	NaN	-1.4	1.0	-0.9	-0.5	-2.0	-0.9	0.8
AN7141	Aldehyde dehydrogenase	71	76	72	-2.4	-1.4	NaN	-1.4	1.2	-0.7	-0.7	-0.6	-0.7	0.0
AN1045	Protein of unknown function	12	17	50	-2.1	-0.6	NaN	-1.4	1.1	-1.1	-0.3	-1.7	-1.1	0.7
AN5610	Dehydrogenase	55	128	200	-3.1	-1.3	NaN	-1.3	1.6	-1.4	-0.4	-1.4	-1.4	0.5
AN7479	Asparaginyl-tRNA synthetase	40	122	243	-1.7	-1.3	NaN	-1.3	0.9	-1.6	-0.4	-0.6	-0.6	0.7
AN2435 (AclA)	ATP citrate synthase	282	352	540	-1.8	-0.7	NaN	-1.3	0.9	0.7	0.5	-0.8	0.5	0.9
AN9339 (CatB)	Catalase	637	669	575	-1.8	-1.2	NaN	-1.2	0.9	1.2	0.3	1.6	1.2	0.7
AN2964 (PdhX)	Pyruvate dehydrogenase	17	28	48	-2.0	-0.3	NaN	-1.1	1.1	-0.6	-0.3	-2.1	-0.6	1.0
AN5701 (Arof)	DAHPh synthase	76	66	94	-2.3	-1.1	NaN	-1.1	1.1	-1.0	-0.3	-1.4	-1.0	0.6
AN1904	Chaperonin	4	10	52	-1.7	-0.5	NaN	-1.1	0.9	-0.1	-0.3	-1.8	-0.3	0.9
AN10981	GTP cyclohydrolase II	69	72	42	-1.3	-0.9	NaN	-1.1	0.7	1.3	0.1	2.4	1.3	1.1
AN1922	Proteasome	27	22	68	-1.8	-0.4	NaN	-1.1	0.9	0.0	-0.3	-1.1	-0.3	0.6
AN4376 (GdhA)	Glutamate dehydrogenase	535	710	1032	-2.2	-1.1	NaN	-1.1	1.1	-0.7	-0.2	-2.0	-0.7	0.9
AN10946	Protein of unknown function	57	65	216	-1.7	-0.4	NaN	-1.1	0.9	-0.6	-0.5	-1.4	-0.6	0.5
AN1003	Isocitrate dehydrogenase	34	151	178	-1.8	-0.3	NaN	-1.0	0.9	-0.3	-0.3	-2.3	-0.3	1.1
AN3058	Glycine hydroxymethyltransferase	94	159	233	-1.5	-0.5	NaN	-1.0	0.8	-0.6	-0.4	-2.0	-0.6	0.9
AN10540	Dipeptidyl-peptidase	166	126	187	-1.5	-0.5	NaN	-1.0	0.8	0.7	0.1	0.3	0.3	0.3
AN3172	40S ribosomal protein S0	52	55	106	-1.7	-0.3	NaN	-1.0	0.9	-0.5	-0.2	-2.1	-0.5	1.0
AN10257	Initiation factor 4G binding	32	45	80	-1.6	-0.4	NaN	-1.0	0.8	-0.4	-0.3	-1.5	-0.4	0.7
AN1700	26S proteasome regulatory subunit	17	42	139	-1.3	-0.6	NaN	-1.0	0.6	-0.1	-0.6	-1.1	-0.6	0.5
AN1635	Protein of unknown function	14	23	59	-1.6	-0.3	NaN	-0.9	0.8	-0.1	-0.3	-1.5	-0.3	0.7
AN0747	Ubiquinol-cytochrome-c reductase	28	52	72	-1.6	-0.3	NaN	-0.9	0.8	-0.5	-1.3	-2.2	-1.3	0.8
AN2225	Oxidoreductase	33	48	22	-1.2	-0.6	NaN	-0.9	0.6	1.1	-0.3	-0.1	-0.1	0.7
AN0858 (Hsp104)	Chaperone	38	100	158	-1.6	-0.2	NaN	-0.9	0.9	-0.3	-0.5	-2.0	-0.5	0.9
AN5563 (GldB)	Dehydrogenase	150	169	219	-1.7	-0.9	NaN	-0.9	0.9	0.8	0.2	-0.4	0.2	0.6
AN4793	Dehydrogenase	60	67	96	-1.9	-0.9	NaN	-0.9	1.0	-1.1	-0.6	-0.9	-0.9	0.3
AN1246 (PgkA)	Phosphoglycerate kinase	424	815	1074	-1.3	-0.3	NaN	-0.8	0.7	-0.7	-0.6	-2.1	-0.7	0.8
AN10797	Hydroxymethylglutaryl-CoA lyase	5	17	13	-1.4	-0.3	NaN	-0.8	0.7	0.0	-0.6	-1.6	-0.6	0.8
AN5731	Chorismate synthase	20	38	48	-2.5	-0.8	NaN	-0.8	1.3	-1.2	-0.5	-1.6	-1.2	0.6
AN0648 (TrpC)	Tryptophan biosynthesis	31	89	113	0.3	-1.9	NaN	-0.8	1.2	NaN	-0.7	-1.2	-0.9	0.4
AN4727 (UrgeA)	UDP-glucose 4-epimerase	144	218	272	-2.0	-0.8	NaN	-0.8	1.0	-0.8	-0.8	-1.4	-0.8	0.3
AN8800 (SgdC)	CysteinyI tRNA synthase	41	38	49	-2.2	-0.8	NaN	-0.8	1.1	0.0	0.1	-1.1	0.0	0.6
AN3712	Carboxymethylglutaminase	48	81	52	-1.5	-0.7	NaN	-0.7	0.8	1.1	0.1	0.6	0.6	0.5
AN0351 (GfdA)	Dehydrogenase	8	6	30	-1.1	-0.4	NaN	-0.7	0.5	-0.1	-1.5	-2.0	-1.5	1.0
AN10351	Aminopeptidase	180	141	158	-1.0	-0.2	NaN	-0.6	0.6	0.0	-0.4	-1.1	-0.4	0.6
AN7254	Cell division control protein 48	213	207	433	-1.7	-0.6	NaN	-0.6	0.9	0.1	-0.2	-0.7	-0.2	0.4
AN8434 (AnkG)	Ankyrin repeat domain protein	102	36	62	-1.6	-0.6	NaN	-0.6	0.8	4.0	2.9	1.1	2.9	1.5
AN2248 (GatA)	4-aminobutyrate transaminase	96	200	513	-1.1	0.0	NaN	-0.5	0.6	0.3	-0.4	-2.9	-0.4	1.7
AN2237	Carboxypeptidase C	23	14	14	-0.9	-0.2	NaN	-0.5	0.4	2.4	1.2	1.5	1.5	0.6

Supplements

Gene ID	Description	PSM			<i>laeΔ/laeA</i>			Ø	SD	<i>laeAcomp+/laeA</i>			Ø	SD
		1	2	3	1	2	3			1	2	3		
AN7517	Protein of unknown function	30	4	7	-2.3	-0.5	NaN	-0.5	1.2	0.8	-0.1	0.1	0.1	0.5
AN6037 (SwoB)	Glucose-6-phosphate isomerase	216	411	615	-1.7	-0.5	NaN	-0.5	0.9	-0.2	-0.3	-1.1	-0.3	0.5
AN9148 (GalF)	Uridyltransferase	173	299	716	-1.5	-0.4	NaN	-0.4	0.8	-0.3	-0.6	-2.3	-0.6	1.1
AN7725 (PyroA)	Pyridoxal 5'-phosphate synthase	231	227	399	-1.8	-0.4	NaN	-0.4	0.9	-1.5	-0.3	-1.8	-1.5	0.8
AN1394 (AspD)	Septin	195	170	255	-0.9	0.1	NaN	-0.4	0.6	1.0	0.4	-1.0	0.4	1.0
AN5784	Proteasome core complex	32	70	41	-1.8	-0.4	NaN	-0.4	1.0	-0.3	-0.2	-1.1	-0.3	0.5
AN10337	Proteasome regulatory particle	30	40	101	-2.1	1.4	NaN	-0.4	1.7	-0.3	-0.2	-1.2	-0.3	0.6
AN4583 (Cyp7)	Eptidyl-prolyl cis-trans isomerase D	53	87	92	-1.0	-0.3	NaN	-0.3	0.5	0.5	0.1	-0.8	0.1	0.7
AN7299	DNA-binding protein	79	98	229	-1.2	-0.3	NaN	-0.3	0.6	-0.1	-0.2	-1.4	-0.2	0.7
AN4492	Protease activity	18	6	55	-1.5	-0.2	NaN	-0.2	0.8	0.1	-0.3	-1.2	-0.3	0.7
AN2304	RAD23 homolog	44	52	31	-0.7	0.2	NaN	-0.2	0.5	0.9	0.1	-0.8	0.1	0.9
AN10399	Oxidoreductase	89	54	54	-1.0	0.6	NaN	-0.2	0.8	1.4	0.8	-0.2	0.8	0.8
AN4443 (MethH)	Methionine synthase	863	1264	16	-1.0	-0.2	NaN	-0.2	0.6	0.1	0.1	-1.7	0.1	1.0
AN6717 (MdhA)	Malate dehydrogenase	488	564	766	-1.6	-0.2	NaN	-0.2	0.9	-0.6	-0.3	-1.8	-0.6	0.8
AN4546	RNA binding activity	29	52	96	-1.2	-0.2	NaN	-0.2	0.7	0.1	-0.1	-0.9	-0.1	0.6
AN1534	F1F0-ATPase	17	143	7	-1.9	1.7	NaN	-0.1	1.8	-0.7	-0.4	-2.7	-0.7	1.3
AN1769	3'-5' bisphosphate nucleotidase	31	46	25	-0.6	0.4	NaN	-0.1	0.5	1.0	-0.1	-1.3	-0.1	1.2
AN4997	Phosphatidylinositol transporter	44	85	110	-1.0	-0.1	NaN	-0.1	0.6	0.3	0.2	-1.6	0.2	1.1
AN7944 (Ngn3)	GNAT-type acetyltransferase	62	102	70	-1.0	0.0	NaN	0.0	0.6	-0.7	0.1	0.8	0.1	0.8
AN8176	60S ribosomal protein L4	135	126	444	-1.1	0.0	NaN	0.0	0.6	-0.4	-0.2	-2.1	-0.4	1.0
AN8275 (CitA)	Citrate synthase	90	199	401	-1.6	0.0	NaN	0.0	0.9	-1.1	-0.4	-2.7	-1.1	1.2
AN6279 (AcuJ)	Carnitine acetyltransferase	21	53	64	-1.3	0.1	NaN	0.1	0.8	-0.7	-1.8	-1.8	-1.8	0.7
AN3344 (Ngn27)	GNAT-type acetyltransferase	39	62	112	-0.6	0.8	NaN	0.1	0.7	1.0	0.7	-2.2	0.7	1.7
AN4282	Metalloaminopeptidase	85	137	146	-0.8	0.1	NaN	0.1	0.5	0.7	0.0	-1.3	0.0	1.0
AN8054	20S core proteasome	61	75	83	-0.7	0.1	NaN	0.1	0.4	0.2	-0.3	-1.0	-0.3	0.6
AN10512 (MthA)	Ketoacyl-CoA thiolase	18	7	21	-0.7	1.0	NaN	0.1	0.9	0.9	-0.6	-1.6	-0.6	1.2
AN6089	Heat shock protein	107	355	650	-1.1	0.2	NaN	0.2	0.7	-0.9	-0.5	-2.9	-0.9	1.3
AN3299	Glutathione S-transferase	15	10	7	-0.2	0.9	NaN	0.3	0.6	1.4	-0.4	1.3	1.3	1.0
AN3459	Metalloidiptidase	46	61	99	0.0	0.7	NaN	0.3	0.4	1.4	0.2	-1.0	0.2	1.2
AN1689	Oxidoreductase	76	74	37	0.1	0.6	NaN	0.4	0.3	0.8	-0.3	-0.2	-0.2	0.6
AN3674	Phospholipid binding activity	628	357	615	-0.5	0.4	NaN	0.4	0.5	2.3	1.2	-0.6	1.2	1.5
AN5803 (FimA)	Fimbrin protein	76	155	165	-0.5	0.7	NaN	0.7	0.6	1.2	0.1	-0.8	0.1	1.0
AN7193	Glycerol dehydrogenase	50	127	113	-0.2	0.8	NaN	0.8	0.5	1.3	0.3	-0.4	0.3	0.8
AN1543	Succinate dehydrogenase	192	143	132	0.3	1.7	NaN	1.0	0.9	1.5	-0.4	-1.4	-0.4	1.5
AN8756	Monoxygenase	3	34	78	-0.5	1.3	NaN	1.3	0.9	-0.7	-0.6	-3.7	-0.7	1.7
AN2383	Protein of unknown function	118	150	189	1.0	2.1	NaN	1.5	1.1	3.9	4.3	2.2	3.9	1.1
AN6490	Phosphorylase	17	31	27	-0.8	1.7	NaN	1.7	1.3	0.8	0.4	-0.6	0.4	0.7
AN6031	Nitronate monooxygenase	36	90	32	0.8	1.9	NaN	1.9	0.9	1.4	-0.8	-0.4	-0.4	1.1
AN8406	Alcohol dehydrogenase	67	84	28	0.7	1.9	NaN	1.9	1.0	-0.6	-1.5	-0.9	-0.9	0.5
AN5646	Fatty acid degradation	26	46	2	1.6	2.0	NaN	2.0	1.1	1.5	-0.8	-0.9	-0.8	1.4
AN7902	Monoxygenase	19	31	6	1.9	2.1	NaN	2.1	1.2	0.6	1.0	1.2	1.0	0.3
AN2859	Dihydrodipicolinate synthase	69	47	13	1.7	3.0	NaN	2.4	1.5	1.8	-0.9	-1.0	-0.9	1.6
AN7388 (CpeA)	Laccase	450	319	63	1.9	3.1	NaN	3.1	1.6	3.2	-0.6	4.7	3.2	2.7
AN7895 (ChiB)	Oxidoreductase	155	340	241	2.7	3.9	NaN	3.9	2.0	1.5	1.6	-0.1	1.5	1.0
AN10087	Proliferating cell nuclear antigen	5		17	-1.1	-0.2	-1.2	-1.1	0.6	0.6	0.4	NaN	0.5	0.3
AN7387 (PcrA)	Proline-5-carboxylate reductase	23	23	40	-2.2	-0.8	-1.3	-1.1	0.7	-1.0	-1.0	NaN	-1.0	0.6
AN1799	Triglyceride lipase	32	22		-1.1	-0.2	-1.7	-1.1	0.8	0.1	0.0	NaN	0.1	0.1
AN2493	Alkaline phosphatase	21	42	14	-2.1	-0.8	-0.7	-0.8	0.8	1.5	1.3	NaN	1.4	0.8
AN4231	Riboflavin biosynthesis	21	9	5	-1.4	-0.1	-1.2	-0.6	0.7	0.6	0.3	NaN	0.4	0.3
AN6014 (FaaA)	Long-chain-fatty-acid-CoA ligase	29	9		-0.5	0.5	-1.8	-0.6	1.2	1.9	0.7	NaN	1.3	0.9
AN4905 (GstA)	Glutathione S-transferase	36	38		0.2	1.0	-2.1	-0.5	1.6	2.3	0.6	NaN	1.4	1.2
AN5558 (PrtA)	Alkaline protease	17	102	73	0.1	0.4	-0.7	-0.2	0.6	2.9	3.3	NaN	3.1	1.8
AN1763	Oxidoreductase	11	10		-0.6	0.4	0.1	0.1	0.5	0.5	0.1	NaN	0.3	0.2
AN2572	Dipeptidyl-peptidase	65	136	29	0.2	1.4	-2.7	0.2	2.1	1.1	-0.1	NaN	0.5	0.7
AN1378	Protein of unknown function	169	6		0.2	2.5	-1.0	0.2	1.8	1.9	0.9	NaN	1.4	0.9
AN8415 (ApdG)	Acyl-coA dehydrogenase	15	9		0.4	1.4	-0.1	0.6	0.8	0.9	-2.6	NaN	-0.8	1.8
AN5421	Monoxygenase	146	40	9	0.7	1.8	-0.4	0.7	1.1	3.5	0.6	NaN	2.0	1.9
AN8942	Protein of unknown function	21	17	10	-1.4	-0.9	2.4	0.8	2.1	0.2	-0.6	NaN	-0.2	0.4
AN9340 (TreA)	Alpha-trehalase	27	17	3	0.3	1.2	1.2	1.2	0.5	1.7	-0.6	NaN	0.6	1.2
AN8445	Amino-peptidase Y	55	58	52	-1.0	-0.3	2.9	1.3	2.1	2.9	1.5	NaN	2.2	1.4
AN6035	D-fuconate dehydratase	28	11	7	2.9	5.0	-1.8	1.6	3.5	4.1	1.0	NaN	2.6	2.2
AN2166	Phytanoyl-CoA dioxygenase	39	30	3	2.0	2.8	-1.3	2.0	2.2	2.1	1.1	NaN	1.6	1.1
AN1050	3-ketoacyl-CoA thiolase	46	33		2.3	2.6	-2.1	2.3	2.6	2.4	-1.4	NaN	0.5	1.9
AN6853	Phosphatidylinositol transporter		10	33	NaN	-1.3	-1.2	-1.3	0.7	NaN	-0.1	-1.4	-0.8	0.8
AN3593	Dehydratase	6	17	27	NaN	-0.5	-1.8	-1.2	0.9	NaN	0.6	-0.9	-0.2	0.7
AN3719 (MpkB)	Mitogen-activated protein kinase		7	43	NaN	-0.9	-0.9	-0.9	0.5	NaN	0.2	-0.2	0.0	0.2
AN5954	Translation initiation factor	8	21	116	NaN	-1.6	-0.3	-0.9	0.9	NaN	-0.4	-1.8	-1.1	1.0

Supplements

Gene ID	Description	PSM			<i>laeAΔ/laeA</i>			∅	SD	<i>laeAcomp+/laeA</i>			∅	SD	
		1	2	3	1	2	3			1	2	3			
AN1673	DAHPh synthase	4	9	18	NaN	-1.2	-1.1	-1.1	0.7	-1.6	NaN	-1.0	NaN	NaN	
AN7914	Alcohol dehydrogenase	203	159	75	-6.2	-4.9	NaN	-4.9	3.3	-1.8	-3.9	NaN	-2.8	1.9	
AN2343	Nitroreductase	97	8		-4.9	-2.8	NaN	-3.9	2.5	-3.1	-1.8	NaN	-2.4	1.5	
AN7836	Protein of unknown function	19	36	23		-3.5	-3.0	NaN	-3.0	1.9	1.2	-1.5	NaN	-0.2	1.4
AN2622 (IpnA)	Isopenicillin-N synthase	8	2		-2.1	-4.0	NaN	-3.0	2.0	2.0	0.4	NaN	1.2	1.1	
AN7268	Oxidoreductase	35	17	2	-1.1	-2.9	NaN	-2.9	1.5	2.9	0.8	NaN	1.8	1.5	
AN1539 (CsnD)	COP9 signalosome	3		4	-1.5	1.0	-2.1	-1.5	1.6	0.9	NaN	NaN	NaN	NaN	
AN3628	Peptide alpha-N-acetyltransferase	5	7	41	-1.9	NaN	-1.2	-1.2	1.0	-0.6	NaN	-1.6	-1.1	0.8	
AN2315	F1FO-ATPase complex subunit	417	515	842	-1.7	-0.3	NaN	-1.0	0.9	-0.4	-0.5	NaN	-0.4	0.3	
AN1194	Adenylyl phosphosulfate kinas	14	28	50	-1.5	-0.4	NaN	-0.9	0.8	0.6	0.2	NaN	0.4	0.3	
AN2668	Oxidoreductase	2	3		-1.2	-0.6	NaN	-0.9	0.6	-0.3	-1.0	NaN	-0.6	0.5	
AN5981	Myosin I binding activity	12	6	28	-1.2	NaN	0.9	-0.1	1.1	0.1	NaN	-1.1	-0.5	0.7	
AN3524	Galactose 1-dehydrogenase		29	43	NaN	2.1	-1.3	0.4	1.7	NaN	NaN	-4.6	-4.6	2.7	
AN5878	Thiolasas	2	5	4	1.0	1.8	-0.7	0.6	1.3	-0.9	NaN	NaN	NaN	NaN	
AN0034	Kinase	84	51		0.6	1.5	NaN	1.0	0.8	2.6	-0.4	NaN	1.1	1.6	
AN2828 (BglL)	Beta-glucosidase	58	6		1.1	1.3	-0.3	1.1	0.9	3.4	NaN	NaN	NaN	NaN	
AN10335	Oxidoreductase	5	8		1.0	2.0	NaN	1.5	1.0	3.0	-0.2	NaN	1.4	1.8	
AN0783	Carbon-nitrogen ligase	3	17	10	1.7	1.8	-1.8	1.7	2.1	2.6	NaN	NaN	NaN	NaN	
AN2577	Oxidoreductase	36	25		1.3	2.3	NaN	1.8	1.2	0.7	NaN	NaN	NaN	NaN	
AN1677	Short-chain dehydrogenase	45	48	18	2.0	3.0	NaN	2.5	1.5	1.1	NaN	NaN	NaN	NaN	
AN5695	Carbon-sulfur lyase	7	2		1.2	2.7	NaN	2.7	1.3	1.0	-0.1	NaN	0.5	0.6	
AN5373	Oxidoreductase	49	25	5	1.9	2.9	NaN	2.9	1.5	3.5	1.5	NaN	2.5	1.7	
AN5883 (MetF)	Reductase	14	5	42	NaN	-1.3	NaN	NaN	NaN	-1.4	0.3	-1.8	-1.4	1.1	
AN3591	Dehydrogenase	56	78	62	NaN	0.7	NaN	NaN	NaN	1.0	-0.8	-1.2	-0.8	1.2	
AN0651 (FadA)	Heterotrimeric G protein	5	6	3	NaN	NaN	-0.5	NaN	0.3	NaN	NaN	-1.2	NaN	NaN	
AN3594 (SogA)	Vacuolar protein-sorting protein	7	24	22	NaN	NaN	-1.5	NaN	NaN	NaN	0.0	-1.8	NaN	NaN	
AN7579	26S proteasome regulatory subunit	5		23	-1.0	NaN	-1.7	NaN	0.9	NaN	NaN	-0.8	NaN	NaN	
AN1805 (CanB)	Carbonic anhydrase		35	36	NaN	-2.0	NaN	NaN	NaN	NaN	0.1	NaN	NaN	NaN	
AN3349	Cytochrome P450	16	8	7	NaN	NaN	-3.8	NaN	NaN	0.3	NaN	NaN	NaN	NaN	
AN6078 (NadA)	Adenine deaminase	4		10	NaN	NaN	-2.3	NaN	NaN	NaN	NaN	NaN	NaN	NaN	
AN6712 (PldA)	Phospholipase D	14	5		NaN	NaN	-2.0	NaN	NaN	NaN	NaN	NaN	NaN	NaN	
AN3573	Oxidoreductase	54	6	5	1.8	NaN	NaN	NaN	NaN	5.4	NaN	NaN	NaN	NaN	
AN9103 (AifA)	Apoptosis-inducing factor (AIF)-like	48	59	17	NaN	NaN	-1.1	NaN	NaN	NaN	NaN	1.8	NaN	NaN	
AN7143	Heat shock protein	3		103	NaN	NaN	-5.6	NaN	NaN	NaN	NaN	-1.8	NaN	NaN	
AN8797 (MvlA)	Orsellinic acid gene cluster		22	14	NaN	NaN	-1.5	NaN	NaN	NaN	NaN	-1.7	NaN	NaN	
AN6838 (TubC)	Beta-tubulin	157		365	NaN	NaN	-3.7	NaN	NaN	NaN	NaN	-0.9	NaN	NaN	
AN8692	Thioredoxin-dependent peroxidase	123		6	NaN	NaN	-2.4	NaN	NaN	NaN	NaN	0.6	NaN	NaN	
AN6126 (AccA)	Acetyl-CoA carboxylase	36	156	351	NaN	NaN	-2.4	NaN	NaN	NaN	NaN	-0.8	NaN	NaN	
AN6157 (PyrG)	Decarboxylase		6	16	NaN	NaN	-2.2	NaN	NaN	NaN	NaN	-1.4	NaN	NaN	
AN8932	TIM-barrel enzyme family protein		6	2	NaN	NaN	-2.1	NaN	NaN	NaN	NaN	1.5	NaN	NaN	
AN8072	Protein of unknown function	7	6	21	NaN	NaN	-2.1	NaN	NaN	NaN	NaN	-1.1	NaN	NaN	
AN6060	Role in RNA metabolic process	7	22	107	NaN	NaN	-2.0	NaN	NaN	NaN	NaN	-2.0	NaN	NaN	
AN7008	Hydroxyacyl-CoA dehydrogenase		8	6	NaN	NaN	-2.0	NaN	NaN	NaN	NaN	-1.3	NaN	NaN	
AN6753	Oxidoreductase		15	34	NaN	NaN	-1.9	NaN	NaN	NaN	NaN	-1.8	NaN	NaN	
AN8268	Ras GTPase-activating protein	12		45	NaN	NaN	-1.8	NaN	NaN	NaN	NaN	-1.8	NaN	NaN	
AN6077	NADH dehydrogenase (ubiquinone)		5	77	NaN	NaN	-1.8	NaN	NaN	NaN	NaN	-2.6	NaN	NaN	
AN8874	Dynammin-related protein	14	8	41	NaN	NaN	-1.8	NaN	NaN	NaN	NaN	-1.9	NaN	NaN	
AN5908 (TpiB)	Triose-phosphate isomerase	12	10	11	NaN	NaN	-1.8	NaN	NaN	NaN	NaN	-0.7	NaN	NaN	
AN8036	Oxidoreductase		15	14	NaN	NaN	-1.7	NaN	NaN	NaN	NaN	0.7	NaN	NaN	
AN9407 (FasA)	Fatty acid synthase	41	144	524	NaN	NaN	-1.7	NaN	NaN	NaN	NaN	-1.6	NaN	NaN	
AN7159	Tripeptidyl-peptidase		24	22	NaN	NaN	-1.6	NaN	NaN	NaN	NaN	-1.4	NaN	NaN	
AN3629	DNA glycosylase		4	13	NaN	NaN	-1.5	NaN	NaN	NaN	NaN	-0.6	NaN	NaN	
AN6688 (AspB)	Putative Septin B	8	180	314	NaN	NaN	-1.5	NaN	NaN	NaN	NaN	-0.8	NaN	NaN	
AN7035	Peptidase		10	34	NaN	NaN	-1.5	NaN	NaN	NaN	NaN	-0.1	NaN	NaN	
AN9090 (RrmA)	RNA binding protein	22	21	86	NaN	NaN	-1.4	NaN	NaN	NaN	NaN	-1.5	NaN	NaN	
AN6006 (KapD)	Karyopherin	9	24	79	NaN	NaN	-1.4	NaN	NaN	NaN	NaN	-1.7	NaN	NaN	
AN9083	Adenine phosphoribosyltransferase	11	12	11	NaN	NaN	0.1	NaN	NaN	NaN	NaN	-0.8	NaN	NaN	
AN6705	Protein of unknown function		12	44	NaN	NaN	-1.4	NaN	NaN	NaN	NaN	-1.5	NaN	NaN	
AN8203	Hydrolase	16	10	35	NaN	NaN	-1.3	NaN	NaN	NaN	NaN	-0.9	NaN	NaN	
AN7590	Mannitol 2-dehydrogenase	18	23	17	NaN	NaN	-1.3	NaN	NaN	NaN	NaN	-1.3	NaN	NaN	
AN6741	Aspartic-type endopeptidase	2		3	NaN	NaN	-1.3	NaN	NaN	NaN	NaN	-1.3	NaN	NaN	
AN6338	Aromatic-amino-acid transaminase		14	29	NaN	NaN	-1.2	NaN	NaN	NaN	NaN	-2.3	NaN	NaN	
AN7909 (OrsA)	Polyketide synthase	13	15	45	NaN	NaN	-1.2	NaN	NaN	NaN	NaN	0.4	NaN	NaN	
AN8755 (MclA)	Methylisocitrate lyase		3	15	NaN	NaN	-1.1	NaN	NaN	NaN	NaN	-1.0	NaN	NaN	
AN6193	Peptidase		15	59	NaN	NaN	-1.1	NaN	NaN	NaN	NaN	-2.3	NaN	NaN	
AN6734 (KapF)	Karyopherin	23	31	47	NaN	NaN	-1.0	NaN	NaN	NaN	NaN	-1.2	NaN	NaN	
AN7199	Protein of unknown function		2	48	NaN	NaN	-1.0	NaN	NaN	NaN	NaN	-2.8	NaN	NaN	

Supplements

Gene ID	Description	PSM			<i>laeAΔ/laeA</i>			Ø	SD	<i>laeAcomp+/laeA</i>			Ø	SD
		1	2	3	1	2	3			1	2	3		
AN7194	Oxidoreductase	6	4	14	NaN	NaN	-0.9	NaN	NaN	NaN	NaN	-1.3	NaN	NaN
AN8869	Uracil phosphoribosyltransferase	12	11	15	NaN	NaN	-0.9	NaN	NaN	NaN	NaN	-1.0	NaN	NaN
AN9094 (UngA)	Pyrophosphorylase	147	233	287	NaN	NaN	-0.9	NaN	NaN	NaN	NaN	-0.8	NaN	NaN
AN6507	Cap binding protein		4	32	NaN	NaN	-0.9	NaN	NaN	NaN	NaN	-1.5	NaN	NaN
AN8023 (VpsA)	Required for vacuole biogenesis	17	51	111	NaN	NaN	-0.8	NaN	NaN	NaN	NaN	-1.6	NaN	NaN
AN8057 (CysB)	Cysteine synthase		15	63	NaN	NaN	-0.8	NaN	NaN	NaN	NaN	-2.4	NaN	NaN
AN6978 (Rcc1)	Nucleotide exchange factor		6	49	NaN	NaN	-0.8	NaN	NaN	NaN	NaN	-1.4	NaN	NaN
AN7441	Histone acetyltransferase	3	4	20	NaN	NaN	-0.7	NaN	NaN	NaN	NaN	-1.0	NaN	NaN
AN6512	ATPase		8	14	NaN	NaN	-0.7	NaN	NaN	NaN	NaN	-0.9	NaN	NaN
AN7498	Deoxyhypusine monoxygenase	12	14	14	NaN	NaN	-0.7	NaN	NaN	NaN	NaN	-1.2	NaN	NaN
AN6045	Chaperone	3		7	NaN	NaN	-0.6	NaN	NaN	NaN	NaN	-1.2	NaN	NaN
AN6844	3-hydroxyisobutyryl-CoA hydrolase	8	12	10	NaN	NaN	-0.6	NaN	NaN	NaN	NaN	-2.3	NaN	NaN
AN6054	Genome maintenance protein		2	3	NaN	NaN	-0.5	NaN	NaN	NaN	NaN	-2.0	NaN	NaN
AN6505 (RcoA)	WD40 repeat protein	25	39	57	NaN	NaN	-0.3	NaN	NaN	NaN	NaN	-0.4	NaN	NaN
AN8795	AP-1 adaptor complex subunit	2	7	16	NaN	NaN	-0.3	NaN	NaN	NaN	NaN	-1.7	NaN	NaN
AN7142 (PacA)	Phosphatase		7	216	NaN	NaN	0.0	NaN	NaN	NaN	NaN	-4.2	NaN	NaN
AN6033	Coat protein complex I	17		14	NaN	NaN	0.0	NaN	NaN	NaN	NaN	-1.8	NaN	NaN
AN6182 (GalD)	Uridyltransferase	5		4	NaN	NaN	0.1	NaN	NaN	NaN	NaN	-0.4	NaN	NaN
AN7491	Deubiquitinating enzymes		6	14	NaN	NaN	0.2	NaN	NaN	NaN	NaN	-0.6	NaN	NaN
AN8945	Methyltransferase		7	20	NaN	NaN	0.6	NaN	NaN	NaN	NaN	-0.7	NaN	NaN
AN7540	Role in translational initiation		263	141	NaN	NaN	0.6	NaN	NaN	NaN	NaN	-1.7	NaN	NaN
AN8790	D-xylulokinase	10	4	9	NaN	NaN	0.8	NaN	NaN	NaN	NaN	-1.0	NaN	NaN
AN8045	Role in mRNA polyadenylation	3		31	NaN	NaN	0.8	NaN	NaN	NaN	NaN	-1.0	NaN	NaN
AN6325	5'-nucleotidase		6	9	NaN	NaN	2.4	NaN	NaN	NaN	NaN	0.5	NaN	NaN
AN7105	Translation initiation factor 3 (eIF3)	7	22	237	NaN	NaN	2.5	NaN	NaN	NaN	NaN	-1.9	NaN	NaN
AN9011	Aryl-alcohol oxidase	35	12	12	NaN	NaN	2.8	NaN	NaN	NaN	NaN	3.9	NaN	NaN
AN7017	Protein of unknown function		6	14	NaN	NaN	3.5	NaN	NaN	NaN	NaN	-2.7	NaN	NaN
AN7422	Deubiquitinating enzymes	20	14	38	NaN	NaN	4.3	NaN	NaN	NaN	NaN	-0.5	NaN	NaN
AN3070	Chaperone		21	59	NaN	NaN	-1.5	NaN	NaN	NaN	NaN	-1.6	NaN	NaN
AN5737	Oxidoreductase		2	10	NaN	NaN	-1.5	NaN	NaN	NaN	NaN	0.9	NaN	NaN
AN0252	F1F0-ATPase complex gamma	43		27	NaN	NaN	-1.5	NaN	NaN	NaN	NaN	-2.1	NaN	NaN
AN3080	Coat protein complex II protein	20	11	31	NaN	NaN	-1.5	NaN	NaN	NaN	NaN	-1.2	NaN	NaN
AN1163	Chaperone		13	20	NaN	NaN	-1.5	NaN	NaN	NaN	NaN	-2.8	NaN	NaN
AN5144 (PfkZ)	6-phosphofructo-2-kinase	5	12	71	NaN	NaN	-1.5	NaN	NaN	NaN	NaN	-1.4	NaN	NaN
AN1158	Cell wall biogenesis protein	27	69	130	NaN	NaN	-1.5	NaN	NaN	NaN	NaN	-1.2	NaN	NaN
AN2441	E1 NeddH/Nedd8-activating	20	12	21	NaN	NaN	-1.5	NaN	NaN	NaN	NaN	-0.6	NaN	NaN
AN4550 (Dps1)	Asparaginyl-tRNA synthetase	90	108	207	NaN	NaN	-1.5	NaN	NaN	NaN	NaN	-1.2	NaN	NaN
AN2970	Phosphatase	2	10	11	NaN	NaN	-1.5	NaN	NaN	NaN	NaN	-1.6	NaN	NaN
AN5123	Oxidoreductase		10	7	NaN	NaN	-1.4	NaN	NaN	NaN	NaN	-0.5	NaN	NaN
AN5520	Role in ribosome biogenesis	30	32	287	NaN	NaN	-1.4	NaN	NaN	NaN	NaN	-2.2	NaN	NaN
AN10229	Dehydrogenase	7		9	NaN	NaN	-1.4	NaN	NaN	NaN	NaN	-2.6	NaN	NaN
AN4745	Rho GTPase activating	4	23	40	NaN	NaN	-1.4	NaN	NaN	NaN	NaN	-1.7	NaN	NaN
AN3804	Protein of unknown function		3	41	NaN	NaN	-1.4	NaN	NaN	NaN	NaN	-3.5	NaN	NaN
AN10164	Polyadenylated RNA-binding	12	15	46	NaN	NaN	-1.4	NaN	NaN	NaN	NaN	-0.4	NaN	NaN
AN11902	Formyltetrahydrofolate cyclo-ligase		2	4	NaN	NaN	-1.4	NaN	NaN	NaN	NaN	-0.7	NaN	NaN
AN5957	Aminotransferase	18	40	85	NaN	NaN	-1.4	NaN	NaN	NaN	NaN	-1.5	NaN	NaN
AN5717 (Kap1)	Importin subunit	21	35	88	NaN	NaN	-1.4	NaN	NaN	NaN	NaN	-1.3	NaN	NaN
AN4178 (Myg1)	Melanocyte proliferating protein		8	19	NaN	NaN	-1.3	NaN	NaN	NaN	NaN	-2.1	NaN	NaN
AN4288	Oxidoreductase	9		101	NaN	NaN	-1.3	NaN	NaN	NaN	NaN	-2.8	NaN	NaN
AN10182	Translation initiation factor 3	5	24	95	NaN	NaN	-1.3	NaN	NaN	NaN	NaN	-1.4	NaN	NaN
AN3034	Regulation of penicillin biosynthesis		12	50	NaN	NaN	-1.3	NaN	NaN	NaN	NaN	-2.6	NaN	NaN
AN2983 (Msb1)	Rho GTPase-activating protein	3		8	NaN	NaN	-1.3	NaN	NaN	NaN	NaN	-1.9	NaN	NaN
AN5130	Coproporphyrinogen oxidase	50	125	202	NaN	NaN	-1.3	NaN	NaN	NaN	NaN	-4.0	NaN	NaN
AN9509	Role in transcription termination	15	4	28	NaN	NaN	-1.3	NaN	NaN	NaN	NaN	-0.8	NaN	NaN
AN10783	Phosphogluconate dehydrogenase	32	24	28	NaN	NaN	-1.3	NaN	NaN	NaN	NaN	1.1	NaN	NaN
AN11058	Protein of unknown function	14	7	10	NaN	NaN	-1.2	NaN	NaN	NaN	NaN	0.6	NaN	NaN
AN4207	Clastrin adaptor protein	4	6	31	NaN	NaN	-1.2	NaN	NaN	NaN	NaN	-1.3	NaN	NaN
AN0317	Role in endocytosis	24	36	49	NaN	NaN	-1.2	NaN	NaN	NaN	NaN	-1.4	NaN	NaN
AN2000 (Ubi4)	Polyubiquitin	3	59	90	NaN	NaN	-1.2	NaN	NaN	NaN	NaN	-1.0	NaN	NaN
AN1084	Elongation factor EF-Tu	96	151	8	NaN	NaN	-1.2	NaN	NaN	NaN	NaN	-2.0	NaN	NaN
AN10765	Translation initiation factor		14	40	NaN	NaN	-1.2	NaN	NaN	NaN	NaN	-1.2	NaN	NaN
AN0193	Hydrolase	14		18	NaN	NaN	-1.2	NaN	NaN	NaN	NaN	-1.5	NaN	NaN
AN0295	Polyubiquitin binding activity		8	4	NaN	NaN	-1.2	NaN	NaN	NaN	NaN	-1.2	NaN	NaN
AN4323	Aminotransferase		48	108	NaN	NaN	-1.2	NaN	NaN	NaN	NaN	-2.6	NaN	NaN
AN1466	PWWP domain protein		4	27	NaN	NaN	-1.2	NaN	NaN	NaN	NaN	-1.3	NaN	NaN
AN2066	Prospore assembly	23	27	35	NaN	NaN	-1.1	NaN	NaN	NaN	NaN	-0.9	NaN	NaN
AN10519	Protein of unknown function	36	43	61	NaN	NaN	-1.1	NaN	NaN	NaN	NaN	-1.3	NaN	NaN

Supplements

Gene ID	Description	PSM			<i>laeAΔ/laeA</i>			∅	SD	<i>laeAcomp+/laeA</i>			∅	SD
		1	2	3	1	2	3			1	2	3		
AN2981 (GsdA)	Dehydrogenase	136	219	266	NaN	NaN	-1.1	NaN	NaN	NaN	NaN	-1.5	NaN	NaN
AN4563	Serine/threonine kinase	14	15	27	NaN	NaN	-1.1	NaN	NaN	NaN	NaN	-1.2	NaN	NaN
AN1409	Acetyl-CoA C-acetyltransferase		206	293	NaN	NaN	-1.1	NaN	NaN	NaN	NaN	-1.1	NaN	NaN
AN2275	Large ribosomal subunit		22	119	NaN	NaN	-1.1	NaN	NaN	NaN	NaN	-2.0	NaN	NaN
AN10281	Serine/threonine phosphatase	16	11	28	NaN	NaN	-1.1	NaN	NaN	NaN	NaN	-1.3	NaN	NaN
AN4397 (FatD)	Coenzyme A synthetase	11	5	6	NaN	NaN	-1.1	NaN	NaN	NaN	NaN	-1.5	NaN	NaN
AN10080	Siderophore biosynthetic	10		18	NaN	NaN	-1.1	NaN	NaN	NaN	NaN	-1.0	NaN	NaN
AN1404	Diacylglycerol kinase	3	4	5	NaN	NaN	-1.1	NaN	NaN	NaN	NaN	-0.4	NaN	NaN
AN5566	GMP synthase	16	38	106	NaN	NaN	-1.1	NaN	NaN	NaN	NaN	-1.6	NaN	NaN
AN4258	Kinase	28	50	67	NaN	NaN	-1.0	NaN	NaN	NaN	NaN	-1.7	NaN	NaN
AN4000 (FabM)	Poly(A)-binding protein	15	67	256	NaN	NaN	-1.0	NaN	NaN	NaN	NaN	-2.0	NaN	NaN
AN3026 (CopA)	Coatomer protein complex	25	44	53	NaN	NaN	-1.0	NaN	NaN	NaN	NaN	-1.4	NaN	NaN
AN9470	Urate oxidase		260	159	NaN	NaN	-0.9	NaN	NaN	NaN	NaN	-1.2	NaN	NaN
AN10743	Role in endocytosis	9	10	28	NaN	NaN	-0.9	NaN	NaN	NaN	NaN	-1.1	NaN	NaN
AN0717	Aminotransferase	28	29	53	NaN	NaN	-0.9	NaN	NaN	NaN	NaN	-0.6	NaN	NaN
AN1162	Guanyl-nucleotide exchange factor	212	237	513	NaN	NaN	-0.9	NaN	NaN	NaN	NaN	-1.9	NaN	NaN
AN0106 (PkcA)	Protein kinase C	11	11	27	NaN	NaN	-0.9	NaN	NaN	NaN	NaN	-0.7	NaN	NaN
AN2907	Translation initiation factor 3		16	98	NaN	NaN	-0.9	NaN	NaN	NaN	NaN	-2.0	NaN	NaN
AN2734	60S acidic ribosomal protein P0	27	29	299	NaN	NaN	-0.9	NaN	NaN	NaN	NaN	-2.2	NaN	NaN
AN5749	Metallopeptidase	8	39	23	NaN	NaN	-0.9	NaN	NaN	NaN	NaN	-0.7	NaN	NaN
AN0673	Actin assembly		32	39	NaN	NaN	-0.9	NaN	NaN	NaN	NaN	-1.2	NaN	NaN
AN5972	Coat protein complex I	12	6	48	NaN	NaN	-0.8	NaN	NaN	NaN	NaN	-1.4	NaN	NaN
AN5820 (MecA)	Cystathionine beta-synthase	63	66	97	NaN	NaN	-0.8	NaN	NaN	NaN	NaN	-1.7	NaN	NaN
AN5499 (Mlp1)	Nuclear pore complex protein	2		31	NaN	NaN	-0.8	NaN	NaN	NaN	NaN	-1.2	NaN	NaN
AN7704	Protein of unknown function	47	15	25	NaN	NaN	-0.8	NaN	NaN	NaN	NaN	-0.6	NaN	NaN
AN10469	Oxidoreductase		8	5	NaN	NaN	-0.8	NaN	NaN	NaN	NaN	-1.5	NaN	NaN
AN5799	Reductase	30		49	NaN	NaN	-0.8	NaN	NaN	NaN	NaN	-1.3	NaN	NaN
AN7721	Translocon subunit	12		27	NaN	NaN	-0.7	NaN	NaN	NaN	NaN	-1.8	NaN	NaN
AN5677	Protein of unknown function	14	12	29	NaN	NaN	-0.7	NaN	NaN	NaN	NaN	-1.2	NaN	NaN
AN5666 (MpkA)	Mitogen-activated protein kinase	44	50	98	NaN	NaN	-0.7	NaN	NaN	NaN	NaN	-0.4	NaN	NaN
AN1639	Disulfide oxidoreductase	11	7	32	NaN	NaN	-0.7	NaN	NaN	NaN	NaN	-0.1	NaN	NaN
AN11702	Protein of unknown function		2	102	NaN	NaN	-0.6	NaN	NaN	NaN	NaN	0.2	NaN	NaN
AN4547	Coat protein complex II	21	34	119	NaN	NaN	-0.6	NaN	NaN	NaN	NaN	-1.6	NaN	NaN
AN4430	Acetolactate synthase	8		46	NaN	NaN	-0.5	NaN	NaN	NaN	NaN	-2.0	NaN	NaN
AN5613 (HxA)	Xanthine dehydrogenase	4	37	27	NaN	NaN	-0.5	NaN	NaN	NaN	NaN	0.5	NaN	NaN
AN5311	Oxidoreductase		15	56	NaN	NaN	-0.5	NaN	NaN	NaN	NaN	-4.8	NaN	NaN
AN12229	Protein of unknown function	9	8	26	NaN	NaN	-0.5	NaN	NaN	NaN	NaN	-1.3	NaN	NaN
AN1150	Transaminase	17	15	62	NaN	NaN	-0.5	NaN	NaN	NaN	NaN	-1.3	NaN	NaN
AN0316 (TubA)	Alpha-tubulin	99	199	338	NaN	NaN	-0.4	NaN	NaN	NaN	NaN	-1.2	NaN	NaN
AN2243	Carbamoyl-phosphate synthase		9	44	NaN	NaN	-0.4	NaN	NaN	NaN	NaN	-2.0	NaN	NaN
AN0076	Regulation in translation	8	7	37	NaN	NaN	-0.4	NaN	NaN	NaN	NaN	-0.7	NaN	NaN
AN11102	Thioesterase	3	7	34	NaN	NaN	-0.3	NaN	NaN	NaN	NaN	-1.6	NaN	NaN
AN10695	Protein of unknown function	13		4	NaN	NaN	-0.3	NaN	NaN	NaN	NaN	2.0	NaN	NaN
AN1328 (NnaA)	GNAT-type acetyltransferase	5	5	19	NaN	NaN	-0.2	NaN	NaN	NaN	NaN	-1.9	NaN	NaN
AN10301	Protein of unknown function	5	5	11	NaN	NaN	-0.1	NaN	NaN	NaN	NaN	0.9	NaN	NaN
AN8831 (AmpB)	Role in actin filament organization	5	9	17	NaN	NaN	0.0	NaN	NaN	NaN	NaN	-1.5	NaN	NaN
AN11055	Phosphatase		4	24	NaN	NaN	0.0	NaN	NaN	NaN	NaN	-1.3	NaN	NaN
AN2871 (McnC)	Phosphoprotein	4	3	33	NaN	NaN	0.0	NaN	NaN	NaN	NaN	-1.8	NaN	NaN
AN5743	Potassium-transporting ATPase	2		11	NaN	NaN	0.0	NaN	NaN	NaN	NaN	-3.1	NaN	NaN
AN1809	Fumarylacetoacetase	17	19	13	NaN	NaN	0.1	NaN	NaN	NaN	NaN	1.1	NaN	NaN
AN10614	G-quadruplex DNA binding activity		30	175	NaN	NaN	0.3	NaN	NaN	NaN	NaN	-2.0	NaN	NaN
AN3226	Oxidoreductase	21	68	80	NaN	NaN	0.5	NaN	NaN	NaN	NaN	2.4	NaN	NaN
AN5435	Oxidoreductase		15	25	NaN	NaN	0.5	NaN	NaN	NaN	NaN	-0.7	NaN	NaN
AN9467	Serine/threonine phosphatase		6	21	NaN	NaN	0.7	NaN	NaN	NaN	NaN	-0.8	NaN	NaN
AN7659	RNA helicase	58	63	66	NaN	NaN	0.7	NaN	NaN	NaN	NaN	-1.0	NaN	NaN
AN5616	Aminotransferase	14	28	34	NaN	NaN	0.9	NaN	NaN	NaN	NaN	-0.9	NaN	NaN
AN3312	L-xylulose reductase		7	7	NaN	NaN	1.2	NaN	NaN	NaN	NaN	3.2	NaN	NaN
AN10060	Protein of unknown function	33	3		NaN	NaN	1.2	NaN	NaN	NaN	NaN	-2.4	NaN	NaN
AN0052	Oxidoreductase	6	12	6	NaN	NaN	1.4	NaN	NaN	NaN	NaN	2.5	NaN	NaN
AN7600	Oxidoreductase	6	29	283	NaN	NaN	1.5	NaN	NaN	NaN	NaN	-2.3	NaN	NaN
AN10306	N-terminal subunit of Cand1		7	3	NaN	NaN	1.7	NaN	NaN	NaN	NaN	-1.5	NaN	NaN
AN0788	Protein of unknown function		3	4	NaN	NaN	1.8	NaN	NaN	NaN	NaN	-0.2	NaN	NaN
AN6541	Ligase	24	37	60	NaN	NaN	1.9	NaN	NaN	NaN	NaN	-1.8	NaN	NaN
AN11005	Metalloexopeptidase		18	27	NaN	NaN	2.3	NaN	NaN	NaN	NaN	-1.5	NaN	NaN
AN3019	Proteasome regulatory particle	28	48	64	NaN	NaN	3.4	NaN	NaN	NaN	NaN	-0.8	NaN	NaN
AN3987	Protein of unknown function	21	16	60	NaN	NaN	4.5	NaN	NaN	NaN	NaN	-1.7	NaN	NaN
AN8009 (Nmt1)	Thiamine biosynthesis protein	64	491	953	NaN	NaN	4.8	NaN	NaN	NaN	NaN	-1.7	NaN	NaN

Supplements

Gene ID	Description	PSM			<i>laeAΔ/laeA</i>			∅	SD	<i>laeAcomp+/laeA</i>			∅	SD
		1	2	3	1	2	3			1	2	3		
AN0224	Dipeptidase	27	40	33	NaN	NaN	-1.2	NaN	NaN	NaN	NaN	NaN	NaN	NaN
AN0271	dUTP pyrophosphatase	19	6	2	NaN	NaN	-1.1	NaN	NaN	NaN	NaN	NaN	NaN	NaN
AN0182 (RasA)	Small monomeric GTPase		10	5	NaN	NaN	-0.9	NaN	NaN	NaN	NaN	NaN	NaN	NaN
AN7222	NACHT domain-containing protein	40	16	45	NaN	NaN	-2.8	NaN	NaN	NaN	NaN	NaN	NaN	NaN
AN7264	Methyltransferase	5	9		NaN	NaN	-2.7	NaN	NaN	NaN	NaN	NaN	NaN	NaN
AN7177	Protein of unknown function	52	30	63	NaN	NaN	-2.6	NaN	NaN	NaN	NaN	NaN	NaN	NaN
AN6207 (PkpC)	Kinase	8	16	22	NaN	NaN	-1.8	NaN	NaN	NaN	NaN	NaN	NaN	NaN
AN2879	Carbon-nitrogen ligase	95	4	7	NaN	NaN	-1.7	NaN	NaN	NaN	NaN	NaN	NaN	NaN
AN7350	Translation initiation factor 4B	45	29	95	NaN	NaN	-1.7	NaN	NaN	NaN	NaN	NaN	NaN	NaN
AN8074	Thiolesterase	6	17	25	NaN	NaN	-1.5	NaN	NaN	NaN	NaN	NaN	NaN	NaN
AN8168 (NmrA)	Nitrogen metabolite repression		4	5	NaN	NaN	-1.5	NaN	NaN	NaN	NaN	NaN	NaN	NaN
AN9138	Amidase/acetamidase	13	6	7	NaN	NaN	-1.4	NaN	NaN	NaN	NaN	NaN	NaN	NaN
AN7469	Riboflavin kinase		8	5	NaN	NaN	-1.3	NaN	NaN	NaN	NaN	NaN	NaN	NaN
AN6515	Protein of unknown function	11	17	37	NaN	NaN	-1.2	NaN	NaN	NaN	NaN	NaN	NaN	NaN
AN7298	Protein of unknown function	6		2	NaN	NaN	-1.2	NaN	NaN	NaN	NaN	NaN	NaN	NaN
AN7307	Protein of unknown function	13	3		NaN	NaN	-1.1	NaN	NaN	NaN	NaN	NaN	NaN	NaN
AN6980 (Nic96)	Nuclear pore complex	6		9	NaN	NaN	-1.0	NaN	NaN	NaN	NaN	NaN	NaN	NaN
AN8218 (TrxB)	Thioredoxin reductase	17	15	22	NaN	NaN	-0.9	NaN	NaN	NaN	NaN	NaN	NaN	NaN
AN7128	Oxidoreductase	21	13		NaN	NaN	-0.9	NaN	NaN	NaN	NaN	NaN	NaN	NaN
AN7511 (GelE)	1,3-beta-transglucosidase	14	17	30	NaN	NaN	-0.8	NaN	NaN	NaN	NaN	NaN	NaN	NaN
AN6438	Exopeptidase	20		6	NaN	NaN	-0.8	NaN	NaN	NaN	NaN	NaN	NaN	NaN
AN6272	Oxidoreductase		4	10	NaN	NaN	-0.6	NaN	NaN	NaN	NaN	NaN	NaN	NaN
AN6286	Protein of unknown function	4	3		NaN	NaN	-0.5	NaN	NaN	NaN	NaN	NaN	NaN	NaN
AN7998 (XptC)	GMC Oxidoreductase <i>mdp/xpt</i>	7	3		NaN	NaN	0.1	NaN	NaN	NaN	NaN	NaN	NaN	NaN
AN7051 (MetG)	Cystathionine beta-lyase		11	23	NaN	NaN	0.1	NaN	NaN	NaN	NaN	NaN	NaN	NaN
AN8433	Protein of unknown function	27	24	15	NaN	NaN	0.2	NaN	NaN	NaN	NaN	NaN	NaN	NaN
AN7911 (OrsB)	Amidohydrolase	6		3	NaN	NaN	2.4	NaN	NaN	NaN	NaN	NaN	NaN	NaN
AN9012	Lyase	11		6	NaN	NaN	3.9	NaN	NaN	NaN	NaN	NaN	NaN	NaN
AN7897	Monoxygenase		6	12	NaN	NaN	-4.2	NaN	NaN	NaN	NaN	NaN	NaN	NaN
AN10437	Protein of unknown function	13	14	21	NaN	NaN	-4.1	NaN	NaN	NaN	NaN	NaN	NaN	NaN
AN5353	Protein of unknown function		11	8	NaN	NaN	-3.9	NaN	NaN	NaN	NaN	NaN	NaN	NaN
AN3565	Hydrolase activity	7	2		NaN	NaN	-3.3	NaN	NaN	NaN	NaN	NaN	NaN	NaN
AN4058	Dihydroxy acid dehydratase		18	6	NaN	NaN	-2.9	NaN	NaN	NaN	NaN	NaN	NaN	NaN
AN1849	Protein of unknown function		2	5	NaN	NaN	-2.6	NaN	NaN	NaN	NaN	NaN	NaN	NaN
AN10942	Actin depolymerizing protein	38	39	45	NaN	NaN	-2.5	NaN	NaN	NaN	NaN	NaN	NaN	NaN
AN2244	Cytoplasmic translation		6	8	NaN	NaN	-2.5	NaN	NaN	NaN	NaN	NaN	NaN	NaN
AN1007 (NiiA)	Nitrite reductase	7	69	286	NaN	NaN	-2.4	NaN	NaN	NaN	NaN	NaN	NaN	NaN
AN5688	Lipid biosynthetic process		8	10	NaN	NaN	-2.2	NaN	NaN	NaN	NaN	NaN	NaN	NaN
AN11191	Polyketide synthase (PKS)		188	197	NaN	NaN	-2.2	NaN	NaN	NaN	NaN	NaN	NaN	NaN
AN3197	Oxidoreductase	9	3		NaN	NaN	-2.1	NaN	NaN	NaN	NaN	NaN	NaN	NaN
AN3057	Oxidoreductase	5	4	9	NaN	NaN	-2.1	NaN	NaN	NaN	NaN	NaN	NaN	NaN
AN11168	Protein of unknown function	3	17	21	NaN	NaN	-2.1	NaN	NaN	NaN	NaN	NaN	NaN	NaN
AN7722	Arginine metabolism	32	25	63	NaN	NaN	-2.1	NaN	NaN	NaN	NaN	NaN	NaN	NaN
AN8274	Alpha-ketoglutarate transport	10		17	NaN	NaN	-2.0	NaN	NaN	NaN	NaN	NaN	NaN	NaN
AN2335	Dehydrogenase		30		NaN	NaN	-1.9	NaN	NaN	NaN	NaN	NaN	NaN	NaN
AN12022	Monoxygenase		8	2	NaN	NaN	-1.9	NaN	NaN	NaN	NaN	NaN	NaN	NaN
AN3416	Syntaxin	39	27	50	NaN	NaN	-1.8	NaN	NaN	NaN	NaN	NaN	NaN	NaN
AN1211	Vacuolar ATP synthase subunit H	22	7	8	NaN	NaN	-1.8	NaN	NaN	NaN	NaN	NaN	NaN	NaN
AN0628	D-lactate dehydrogenase	3	4	4	NaN	NaN	-1.8	NaN	NaN	NaN	NaN	NaN	NaN	NaN
AN9193 (LlmJ)	LaeA-like methyltransferase		4	4	NaN	NaN	-1.7	NaN	NaN	NaN	NaN	NaN	NaN	NaN
AN3456	Cystathionine gamma-synthase		13	32	NaN	NaN	-1.7	NaN	NaN	NaN	NaN	NaN	NaN	NaN
AN9149	Protein of unknown function	22		23	NaN	NaN	-1.7	NaN	NaN	NaN	NaN	NaN	NaN	NaN
AN3916	Glycerol kinase	50	9		NaN	NaN	-1.7	NaN	NaN	NaN	NaN	NaN	NaN	NaN
AN0948	ATPase activity	10	6	6	NaN	NaN	-1.7	NaN	NaN	NaN	NaN	NaN	NaN	NaN
AN10230	Phosphorylase	34	28	37	NaN	NaN	-1.6	NaN	NaN	NaN	NaN	NaN	NaN	NaN
AN0327	DNA helicase		5	22	NaN	NaN	-1.6	NaN	NaN	NaN	NaN	NaN	NaN	NaN
AN5831	Protein of unknown function		44	75	NaN	NaN	-1.6	NaN	NaN	NaN	NaN	NaN	NaN	NaN
AN10856	Protein of unknown function	6	3	18	NaN	NaN	-1.6	NaN	NaN	NaN	NaN	NaN	NaN	NaN
AN2091	Carboxy-lyase	12	30	22	NaN	NaN	-1.6	NaN	NaN	NaN	NaN	NaN	NaN	NaN
AN2853	Transcription regulator protein		8	2	NaN	NaN	-1.6	NaN	NaN	NaN	NaN	NaN	NaN	NaN
AN4008	Methyltransferase	20	41	33	NaN	NaN	-1.5	NaN	NaN	NaN	NaN	NaN	NaN	NaN
AN3029	AP-1 adaptor complex	17	23		NaN	NaN	-1.5	NaN	NaN	NaN	NaN	NaN	NaN	NaN
AN10533	Trehalose-6-phosphate synthase		28	23	NaN	NaN	-1.5	NaN	NaN	NaN	NaN	NaN	NaN	NaN
AN8010	Glycogen (starch) synthase	321	9		NaN	NaN	-1.5	NaN	NaN	NaN	NaN	NaN	NaN	NaN
AN2298	SUMO activating enzyme	3	14	6	NaN	NaN	-1.5	NaN	NaN	NaN	NaN	NaN	NaN	NaN
AN3161	Oxidoreductase		2	5	NaN	NaN	-1.5	NaN	NaN	NaN	NaN	NaN	NaN	NaN
AN0447	Iron-sulfur cluster binding activity		6	11	NaN	NaN	-1.4	NaN	NaN	NaN	NaN	NaN	NaN	NaN

Supplements

Gene ID	Description	PSM			<i>laeAΔ/laeA</i>			Ø	SD	<i>laeAcomp+/laeA</i>			Ø	SD
		1	2	3	1	2	3			1	2	3		
AN4483	Serine/threonine kinase		3	11	NaN	NaN	-1.4	NaN	NaN	NaN	NaN	NaN	NaN	NaN
AN1873	Protein of unknown function		10	10	NaN	NaN	-1.4	NaN	NaN	NaN	NaN	NaN	NaN	NaN
AN0665 (AneA)	Coatomer subunit epsilon		10	12	NaN	NaN	-1.4	NaN	NaN	NaN	NaN	NaN	NaN	NaN
AN0697	Septin cytoskeleton	7		16	NaN	NaN	-1.4	NaN	NaN	NaN	NaN	NaN	NaN	NaN
AN2414	NADH dehydrogenase (ubiquinone)	8	3	32	NaN	NaN	-1.4	NaN	NaN	NaN	NaN	NaN	NaN	NaN
AN4353	Protein of unknown function	33	22		NaN	NaN	-1.4	NaN	NaN	NaN	NaN	NaN	NaN	NaN
AN4575	Protein of unknown function	6	25	14	NaN	NaN	-1.4	NaN	NaN	NaN	NaN	NaN	NaN	NaN
AN4688 (IvdA)	Acyl-coA dehydrogenase	10	3		NaN	NaN	-1.4	NaN	NaN	NaN	NaN	NaN	NaN	NaN
AN12209	Protein of unknown function	2		3	NaN	NaN	-1.4	NaN	NaN	NaN	NaN	NaN	NaN	NaN
AN4916	Role in ribosome biogenesis	13		4	NaN	NaN	-1.4	NaN	NaN	NaN	NaN	NaN	NaN	NaN
AN4268	Nitronate monooxygenase	5	6	3	NaN	NaN	-1.3	NaN	NaN	NaN	NaN	NaN	NaN	NaN
AN4965	Protein of unknown function		6	24	NaN	NaN	-1.3	NaN	NaN	NaN	NaN	NaN	NaN	NaN
AN3961	Protein of unknown function		38	10	NaN	NaN	-1.3	NaN	NaN	NaN	NaN	NaN	NaN	NaN
AN4439	Adenylyltransferase	11		8	NaN	NaN	-1.3	NaN	NaN	NaN	NaN	NaN	NaN	NaN
AN1502 (NagA)	Chitin hydrolysis	8	8		NaN	NaN	-1.2	NaN	NaN	NaN	NaN	NaN	NaN	NaN
AN4024	Protein of unknown function	8	6	11	NaN	NaN	-1.2	NaN	NaN	NaN	NaN	NaN	NaN	NaN
AN10417	RNA helicase		11	21	NaN	NaN	-1.2	NaN	NaN	NaN	NaN	NaN	NaN	NaN
AN2860	Alcohol dehydrogenase	6	2		NaN	NaN	-1.1	NaN	NaN	NaN	NaN	NaN	NaN	NaN
AN10282	Protein of unknown function	3	9	95	NaN	NaN	-1.1	NaN	NaN	NaN	NaN	NaN	NaN	NaN
AN8396 (PdcB)	Decarboxylase	22	17		NaN	NaN	-1.1	NaN	NaN	NaN	NaN	NaN	NaN	NaN
AN8859	Aspartate kinase	4		16	NaN	NaN	-1.1	NaN	NaN	NaN	NaN	NaN	NaN	NaN
AN4532 (Prp8)	Catalytic core of the spliceosome	16	8	6	NaN	NaN	-1.1	NaN	NaN	NaN	NaN	NaN	NaN	NaN
AN2311	Phosphomevalonate kinase	44	31	44	NaN	NaN	-1.1	NaN	NaN	NaN	NaN	NaN	NaN	NaN
AN10379	Protein of unknown function	16	17	20	NaN	NaN	-1.1	NaN	NaN	NaN	NaN	NaN	NaN	NaN
AN1545	Phosphatase	18		19	NaN	NaN	-1.1	NaN	NaN	NaN	NaN	NaN	NaN	NaN
AN5718	Fumarate hydratase	8	7	16	NaN	NaN	-1.0	NaN	NaN	NaN	NaN	NaN	NaN	NaN
AN12335 (AcdA)	Acyl-CoA dehydrogenase	20	22		NaN	NaN	-1.0	NaN	NaN	NaN	NaN	NaN	NaN	NaN
AN10311 (MnpA)	Cell wall mannoprotein	20	4		NaN	NaN	-1.0	NaN	NaN	NaN	NaN	NaN	NaN	NaN
AN7805 (StcV)	Norsolorinic acid reductase	154	4		NaN	NaN	-1.0	NaN	NaN	NaN	NaN	NaN	NaN	NaN
AN4779	Protein of unknown function	4	4	4	NaN	NaN	-1.0	NaN	NaN	NaN	NaN	NaN	NaN	NaN
AN8836	Serine/threonine-protein kinase		4	13	NaN	NaN	-1.0	NaN	NaN	NaN	NaN	NaN	NaN	NaN
AN3867	Pheromone precursor	14	11	19	NaN	NaN	-0.9	NaN	NaN	NaN	NaN	NaN	NaN	NaN
AN0423	D-xylose reductase	4	6	35	NaN	NaN	-0.9	NaN	NaN	NaN	NaN	NaN	NaN	NaN
AN10350	Phosphatidylinositol binding activity	8	9	13	NaN	NaN	-0.9	NaN	NaN	NaN	NaN	NaN	NaN	NaN
AN4315	Translational elongation	7	4	15	NaN	NaN	-0.9	NaN	NaN	NaN	NaN	NaN	NaN	NaN
AN10960	Protein of unknown function	10	9	2	NaN	NaN	-0.9	NaN	NaN	NaN	NaN	NaN	NaN	NaN
AN2224 (Sog)	Vacuolar protein-sorting protein	9	18	26	NaN	NaN	-0.9	NaN	NaN	NaN	NaN	NaN	NaN	NaN
AN5800	Role in translation	160		4	NaN	NaN	-0.8	NaN	NaN	NaN	NaN	NaN	NaN	NaN
AN8801	Nitronate monooxygenase	3	4		NaN	NaN	-0.8	NaN	NaN	NaN	NaN	NaN	NaN	NaN
AN10023 (MdpL)	Member of the <i>mdp/xpt</i> gene cl.	19	14	18	NaN	NaN	-0.8	NaN	NaN	NaN	NaN	NaN	NaN	NaN
AN0847	Chaperone		4	14	NaN	NaN	-0.8	NaN	NaN	NaN	NaN	NaN	NaN	NaN
AN5634 (AcdD)	Isocitrate lyase	6	29	16	NaN	NaN	-0.7	NaN	NaN	NaN	NaN	NaN	NaN	NaN
AN1524	Dehydrogenase	3	8	28	NaN	NaN	-0.7	NaN	NaN	NaN	NaN	NaN	NaN	NaN
AN9320	Protein of unknown function		6	46	NaN	NaN	-0.6	NaN	NaN	NaN	NaN	NaN	NaN	NaN
AN1611	U1 snRNP localization		17	15	NaN	NaN	-0.6	NaN	NaN	NaN	NaN	NaN	NaN	NaN
AN3778	Gephyrin-related protein	3	9	12	NaN	NaN	-0.5	NaN	NaN	NaN	NaN	NaN	NaN	NaN
AN4602	Role in tubulin complex assembly	7	6		NaN	NaN	-0.5	NaN	NaN	NaN	NaN	NaN	NaN	NaN
AN3642	Vacuolar protein sorting protein	2		8	NaN	NaN	-0.4	NaN	NaN	NaN	NaN	NaN	NaN	NaN
AN0656	Menaquinone biosynthesis		16	11	NaN	NaN	-0.4	NaN	NaN	NaN	NaN	NaN	NaN	NaN
AN2017 (AqdA)	Alpha-glucosidase	6		8	NaN	NaN	-0.4	NaN	NaN	NaN	NaN	NaN	NaN	NaN
AN11915	Formyltetrahydrofolate cyclo ligase		4	12	NaN	NaN	-0.3	NaN	NaN	NaN	NaN	NaN	NaN	NaN
AN5778	Cytoskeleton localization	3	11	33	NaN	NaN	-0.2	NaN	NaN	NaN	NaN	NaN	NaN	NaN
AN1694	Protein of unknown function		12	5	NaN	NaN	-0.1	NaN	NaN	NaN	NaN	NaN	NaN	NaN
AN5606	ATPase subunit	14		13	NaN	NaN	-0.1	NaN	NaN	NaN	NaN	NaN	NaN	NaN
AN3709	Protein of unknown function		4	6	NaN	NaN	0.0	NaN	NaN	NaN	NaN	NaN	NaN	NaN
AN2229 (MetE)	Acetyltransferase		3	3	NaN	NaN	0.0	NaN	NaN	NaN	NaN	NaN	NaN	NaN
AN1917 (DicB)	Dicarboxylate-tricarboxylate	17	4		NaN	NaN	0.1	NaN	NaN	NaN	NaN	NaN	NaN	NaN
AN2947	Phosphodiesterase	15	11	8	NaN	NaN	0.4	NaN	NaN	NaN	NaN	NaN	NaN	NaN
AN4843 (AqdG)	Alpha-glucosidase	12		2	NaN	NaN	0.4	NaN	NaN	NaN	NaN	NaN	NaN	NaN
AN5658	Gamma-glutamyltransferase	5	5		NaN	NaN	0.4	NaN	NaN	NaN	NaN	NaN	NaN	NaN
AN0740	Oxidoreductase	9	10		NaN	NaN	0.5	NaN	NaN	NaN	NaN	NaN	NaN	NaN
AN1675	Lysophospholipase	26	15	15	NaN	NaN	0.7	NaN	NaN	NaN	NaN	NaN	NaN	NaN
AN2389	2-dehydropantoate 2-reductase		15	4	NaN	NaN	1.0	NaN	NaN	NaN	NaN	NaN	NaN	NaN
AN5635 (TreB)	Alpha-trehalase	4		27	NaN	NaN	1.2	NaN	NaN	NaN	NaN	NaN	NaN	NaN
AN0866	Heat shock protein-like	9	13	28	NaN	NaN	1.3	NaN	NaN	NaN	NaN	NaN	NaN	NaN
AN0562	Catalytic activity		6	3	NaN	NaN	2.7	NaN	NaN	NaN	NaN	NaN	NaN	NaN
AN3255	Glutathione peroxidase	24	24	18	NaN	NaN	2.8	NaN	NaN	NaN	NaN	NaN	NaN	NaN

Supplements

Gene ID	Description	PSM			<i>laeAΔ/laeA</i>			Ø	SD	<i>laeAcomp+/laeA</i>			Ø	SD
		1	2	3	1	2	3			1	2	3		
AN1897 (HmgA)	Homogentisate 1,2-dioxygenase	24	15		NaN	NaN	2.9	NaN	NaN	NaN	NaN	NaN	NaN	NaN
AN10788	Protease		9	11	NaN	NaN	3.2	NaN	NaN	NaN	NaN	NaN	NaN	NaN
AN5068	Arylformamidase	18	6	13	NaN	NaN	3.5	NaN	NaN	NaN	NaN	NaN	NaN	NaN
AN3330	Protein of unknown function	53	61	54	NaN	NaN	3.6	NaN	NaN	NaN	NaN	NaN	NaN	NaN
AN0234	Hydrolase		21	79	NaN	NaN	NaN	NaN	NaN	NaN	NaN	-4.6	NaN	NaN
AN2555	Serine-type carboxypeptidase	5	11	67	NaN	NaN	NaN	NaN	NaN	NaN	NaN	-3.7	NaN	NaN
AN10901	Dehydrogenase	17	76	221	NaN	NaN	NaN	NaN	NaN	NaN	NaN	-3.4	NaN	NaN
AN4908	Translation initiation factor subunit	5	29	185	NaN	NaN	NaN	NaN	NaN	NaN	NaN	-3.3	NaN	NaN
AN0893 (AdB)	Adenylosuccinate synthase	56	65	97	NaN	NaN	NaN	NaN	NaN	NaN	NaN	-3.1	NaN	NaN
AN6209	Adenylosuccinate lyase	4	26	38	NaN	NaN	NaN	NaN	NaN	NaN	NaN	-2.4	NaN	NaN
AN6521 (LysF)	Homoaconitate hydratase		13	31	NaN	NaN	NaN	NaN	NaN	NaN	NaN	-2.3	NaN	NaN
AN1558 (MyoA)	Myosin I	12		11	NaN	NaN	NaN	NaN	NaN	NaN	NaN	-2.3	NaN	NaN
AN11192	Cytochrome P450		28	18	NaN	NaN	NaN	NaN	NaN	NaN	NaN	-2.2	NaN	NaN
AN4064	ADP/ATP carrier protein	137	136	263	NaN	NaN	NaN	NaN	NaN	NaN	NaN	-2.1	NaN	NaN
AN1503	Dihydrodipicolinate synthase	3	2		NaN	NaN	NaN	NaN	NaN	NaN	NaN	-2.1	NaN	NaN
AN0952	Phosphatase	9	2	32	NaN	NaN	NaN	NaN	NaN	NaN	NaN	-2.1	NaN	NaN
AN12070	Carbon-nitrogen ligase	7	7	24	NaN	NaN	NaN	NaN	NaN	NaN	NaN	-2.1	NaN	NaN
AN10426	GTPase	5	19	56	NaN	NaN	NaN	NaN	NaN	NaN	NaN	-2.1	NaN	NaN
AN0595	Reductase	5	3	21	NaN	NaN	NaN	NaN	NaN	NaN	NaN	-2.1	NaN	NaN
AN2332	Succinate dehydrogenase		2	8	NaN	NaN	NaN	NaN	NaN	NaN	NaN	-2.1	NaN	NaN
AN10296	Fumarate reductase	256	297	390	NaN	NaN	NaN	NaN	NaN	NaN	NaN	-2.0	NaN	NaN
AN4038	Translation initiation factor eIF5B		8	84	NaN	NaN	NaN	NaN	NaN	NaN	NaN	-2.0	NaN	NaN
AN4956	Acetolactate synthase		16	48	NaN	NaN	NaN	NaN	NaN	NaN	NaN	-2.0	NaN	NaN
AN8121	FGAM-Synthase	7	22	36	NaN	NaN	NaN	NaN	NaN	NaN	NaN	-2.0	NaN	NaN
AN3894	Aconitate hydratase	4	16	57	NaN	NaN	NaN	NaN	NaN	NaN	NaN	-2.0	NaN	NaN
AN7386	Protein of unknown function		7	5	NaN	NaN	NaN	NaN	NaN	NaN	NaN	-1.9	NaN	NaN
AN4859 (PmaA)	Plasma membrane ATPase	11	4	61	NaN	NaN	NaN	NaN	NaN	NaN	NaN	-1.9	NaN	NaN
AN2516 (AmpA)	Actin-associated protein		2	32	NaN	NaN	NaN	NaN	NaN	NaN	NaN	-1.9	NaN	NaN
AN0432	Cytochrome-b5 reductase	22	30	35	NaN	NaN	NaN	NaN	NaN	NaN	NaN	-1.9	NaN	NaN
AN2120	Oxidoreductase	5	27	201	NaN	NaN	NaN	NaN	NaN	NaN	NaN	-1.8	NaN	NaN
AN3375	Heat shock protein	3	6	21	NaN	NaN	NaN	NaN	NaN	NaN	NaN	-1.8	NaN	NaN
AN2731	Unfolded protein binding activity	7	8	53	NaN	NaN	NaN	NaN	NaN	NaN	NaN	-1.8	NaN	NaN
AN2185 (NucA)	Endonuclease	16	12	16	NaN	NaN	NaN	NaN	NaN	NaN	NaN	-1.8	NaN	NaN
AN12221	Deoxyribose-phosphate aldolase	27	28	20	NaN	NaN	NaN	NaN	NaN	NaN	NaN	-1.7	NaN	NaN
AN0708 (AromA)	Aromatic amino acid biosynthesis	29	34	93	NaN	NaN	NaN	NaN	NaN	NaN	NaN	-1.7	NaN	NaN
AN1216 (GppA)	Glycerol 3-phosphate phosphatase		7	11	NaN	NaN	NaN	NaN	NaN	NaN	NaN	-1.7	NaN	NaN
AN8805	Ankyrin repeat protein		2	8	NaN	NaN	NaN	NaN	NaN	NaN	NaN	-1.7	NaN	NaN
AN5447	Glutamate decarboxylase	56	75	183	NaN	NaN	NaN	NaN	NaN	NaN	NaN	-1.7	NaN	NaN
AN9159	Protein of unknown function	6	11	23	NaN	NaN	NaN	NaN	NaN	NaN	NaN	-1.6	NaN	NaN
AN2882	Homoserine dehydrogenase		80	219	NaN	NaN	NaN	NaN	NaN	NaN	NaN	-1.6	NaN	NaN
AN0290	Actin filament		18	43	NaN	NaN	NaN	NaN	NaN	NaN	NaN	-1.6	NaN	NaN
AN2847	Protein of unknown function		5	2	NaN	NaN	NaN	NaN	NaN	NaN	NaN	-1.6	NaN	NaN
AN8016 (Fal1)	RNA helicase	7	20	44	NaN	NaN	NaN	NaN	NaN	NaN	NaN	-1.6	NaN	NaN
AN0183	Molybdopterin binding protein		23	23	NaN	NaN	NaN	NaN	NaN	NaN	NaN	-1.5	NaN	NaN
AN3163 (StoA)	Stomatin protein	19		13	NaN	NaN	NaN	NaN	NaN	NaN	NaN	-1.5	NaN	NaN
AN4234 (PcmA)	Phosphoacetylglucosamine mutase	21	37	106	NaN	NaN	NaN	NaN	NaN	NaN	NaN	-1.5	NaN	NaN
AN1198	Hydrolase	9	13	41	NaN	NaN	NaN	NaN	NaN	NaN	NaN	-1.4	NaN	NaN
AN0661	RNA-directed DNA polymerase	5	6		NaN	NaN	NaN	NaN	NaN	NaN	NaN	-1.4	NaN	NaN
AN4015	Translation elongation factor	63		19	NaN	NaN	NaN	NaN	NaN	NaN	NaN	-1.3	NaN	NaN
AN4317 (Sec13)	Nuclear pore complex protein	24		7	NaN	NaN	NaN	NaN	NaN	NaN	NaN	-1.3	NaN	NaN
AN8862 (MyoV)	Myosin V	8	18	36	NaN	NaN	NaN	NaN	NaN	NaN	NaN	-1.3	NaN	NaN
AN8021 (VmaA)	Vacuolar ATPase (V-ATPase)	49	57	90	NaN	NaN	NaN	NaN	NaN	NaN	NaN	-1.3	NaN	NaN
AN5662	Threonine-tRNA ligase	51	107	193	NaN	NaN	NaN	NaN	NaN	NaN	NaN	-1.2	NaN	NaN
AN3445	Chitin synthase	12	6	36	NaN	NaN	NaN	NaN	NaN	NaN	NaN	-1.2	NaN	NaN
AN7289	Actin monomer binding protein	42	50	59	NaN	NaN	NaN	NaN	NaN	NaN	NaN	-1.1	NaN	NaN
AN8853 (SnpA)	Polypeptide releasing factor	17	6	46	NaN	NaN	NaN	NaN	NaN	NaN	NaN	-1.1	NaN	NaN
AN4616	Heat shock protein	33	49	138	NaN	NaN	NaN	NaN	NaN	NaN	NaN	-1.0	NaN	NaN
AN5121	Proteasome regulatory subunit 8	48	71	78	NaN	NaN	NaN	NaN	NaN	NaN	NaN	-1.0	NaN	NaN
AN3918	Aminopeptidase	8	24	28	NaN	NaN	NaN	NaN	NaN	NaN	NaN	-0.9	NaN	NaN
AN9357	Short-chain dehydrogenase	8	14		NaN	NaN	NaN	NaN	NaN	NaN	NaN	-0.9	NaN	NaN
AN7334	Phospholipase	19	25	74	NaN	NaN	NaN	NaN	NaN	NaN	NaN	-0.8	NaN	NaN
AN3789	Protein of unknown function	26	12	13	NaN	NaN	NaN	NaN	NaN	NaN	NaN	-0.8	NaN	NaN
AN0667 (ManA)	Mannose-6-phosphate isomerase		26	27	NaN	NaN	NaN	NaN	NaN	NaN	NaN	-0.8	NaN	NaN
AN2026	Transcription factor	4	5	7	NaN	NaN	NaN	NaN	NaN	NaN	NaN	-0.8	NaN	NaN
AN9067	Protein of unknown function	18	30		NaN	NaN	NaN	NaN	NaN	NaN	NaN	-0.5	NaN	NaN
AN9297	Protein of unknown function	53	67		NaN	NaN	NaN	NaN	NaN	NaN	NaN	-0.5	NaN	NaN
AN5404	Protein of unknown function		4	15	NaN	NaN	NaN	NaN	NaN	NaN	NaN	-0.5	NaN	NaN

Supplements

Gene ID	Description	PSM			<i>laeAΔ/laeA</i>			∅	SD	<i>laeAcomp+/laeA</i>			∅	SD
		1	2	3	1	2	3			1	2	3		
AN10170	ATPase activity	89	133	180	NaN	NaN	NaN	NaN	NaN	NaN	NaN	-0.4	NaN	NaN
AN0495	Formyltetrahydrofolate deformylase		22	34	NaN	NaN	NaN	NaN	NaN	NaN	NaN	-0.2	NaN	NaN
AN2405	Methyltransferases	16	6	2	NaN	NaN	NaN	NaN	NaN	NaN	NaN	0.1	NaN	NaN
AN8430	Protein of unknown function	11	14	25	NaN	NaN	NaN	NaN	NaN	NaN	NaN	0.1	NaN	NaN
AN6985	Ribulokinase	20		2	NaN	NaN	NaN	NaN	NaN	NaN	NaN	0.6	NaN	NaN
AN7999	Oxidoreductase <i>mdp/xpt</i>	63	63	84	NaN	NaN	NaN	NaN	NaN	NaN	NaN	0.9	NaN	NaN
AN8604 (Ngn23)	GNAT-type acetyltransferase	7	8	9	NaN	NaN	NaN	NaN	NaN	NaN	NaN	1.6	NaN	NaN
AN0787 (Mns1B)	Mannosidase 1A	15	3	10	NaN	NaN	NaN	NaN	NaN	NaN	NaN	1.7	NaN	NaN
AN1117	COPII adaptor activity	21	20	22	NaN	NaN	NaN	NaN	NaN	NaN	NaN	1.9	NaN	NaN
AN5423	Protein of unknown function	16	6	19	NaN	NaN	NaN	NaN	NaN	NaN	NaN	2.1	NaN	NaN
AN0050	Picolinic acid decarboxylase	8	22	4	NaN	NaN	NaN	NaN	NaN	NaN	NaN	NaN	NaN	NaN
AN0051	Dioxygenase	14	17		NaN	NaN	NaN	NaN	NaN	NaN	NaN	NaN	NaN	NaN
AN0121 (HemC)	Porphobilinogen deaminase	6	17	22	NaN	NaN	NaN	NaN	NaN	NaN	NaN	NaN	NaN	NaN
AN0133	RNA helicase	5	2	11	NaN	NaN	NaN	NaN	NaN	NaN	NaN	NaN	NaN	NaN
AN0146 (MdpC)	Versicolorin ketoreductase	33	13	23	NaN	NaN	NaN	NaN	NaN	NaN	NaN	NaN	NaN	NaN
AN0150 (MdpG)	Polketide synthase <i>mdp/xpt</i>	17	4	5	NaN	NaN	NaN	NaN	NaN	NaN	NaN	NaN	NaN	NaN
AN0228	DNA helicase	6	9	9	NaN	NaN	NaN	NaN	NaN	NaN	NaN	NaN	NaN	NaN
AN0261 (Sec23)	Coat protein complex II	36	8	133	NaN	NaN	NaN	NaN	NaN	NaN	NaN	NaN	NaN	NaN
AN0381	Chaperonin	15	26	77	NaN	NaN	NaN	NaN	NaN	NaN	NaN	NaN	NaN	NaN
AN0410	Phosphatase	7	9	34	NaN	NaN	NaN	NaN	NaN	NaN	NaN	NaN	NaN	NaN
AN0465	Protein of unknown function	42		6	NaN	NaN	NaN	NaN	NaN	NaN	NaN	NaN	NaN	NaN
AN0574	Nucleotide binding	17	26		NaN	NaN	NaN	NaN	NaN	NaN	NaN	NaN	NaN	NaN
AN0579	IPP isomerase	40	43	38	NaN	NaN	NaN	NaN	NaN	NaN	NaN	NaN	NaN	NaN
AN0593	Dehydrogenase	21	11	3	NaN	NaN	NaN	NaN	NaN	NaN	NaN	NaN	NaN	NaN
AN0757	tRNA methylation	4	6	46	NaN	NaN	NaN	NaN	NaN	NaN	NaN	NaN	NaN	NaN
AN0922	Golgi vesicle-mediated transport	11	21	62	NaN	NaN	NaN	NaN	NaN	NaN	NaN	NaN	NaN	NaN
AN0987	Protein of unknown function	25		48	NaN	NaN	NaN	NaN	NaN	NaN	NaN	NaN	NaN	NaN
AN10108	Oxidoreductase		4	24	NaN	NaN	NaN	NaN	NaN	NaN	NaN	NaN	NaN	NaN
AN1019	SCF complex protein		4	13	NaN	NaN	NaN	NaN	NaN	NaN	NaN	NaN	NaN	NaN
AN1023 (SagA)	Cytoskeletal adaptor protein	7		7	NaN	NaN	NaN	NaN	NaN	NaN	NaN	NaN	NaN	NaN
AN10276	Initiation factor 4G binding		11	32	NaN	NaN	NaN	NaN	NaN	NaN	NaN	NaN	NaN	NaN
AN10284	Glutathione synthase	12	9		NaN	NaN	NaN	NaN	NaN	NaN	NaN	NaN	NaN	NaN
AN10476	Dehydrogenase/GMP reductase	57	39	98	NaN	NaN	NaN	NaN	NaN	NaN	NaN	NaN	NaN	NaN
AN10734	Regulation translational elongation	3	6	35	NaN	NaN	NaN	NaN	NaN	NaN	NaN	NaN	NaN	NaN
AN10864	Phosphatase	3		3	NaN	NaN	NaN	NaN	NaN	NaN	NaN	NaN	NaN	NaN
AN11052	5'-3' exonuclease		12	83	NaN	NaN	NaN	NaN	NaN	NaN	NaN	NaN	NaN	NaN
AN1122	60S ribosomal protein L1	12	22	234	NaN	NaN	NaN	NaN	NaN	NaN	NaN	NaN	NaN	NaN
AN11246	Protein of unknown function		11	31	NaN	NaN	NaN	NaN	NaN	NaN	NaN	NaN	NaN	NaN
AN1167	Protein of unknown function	21	14	40	NaN	NaN	NaN	NaN	NaN	NaN	NaN	NaN	NaN	NaN
AN11981	Aminomethyltransferase	2	11		NaN	NaN	NaN	NaN	NaN	NaN	NaN	NaN	NaN	NaN
AN12027	Protein of unknown function	26	35	16	NaN	NaN	NaN	NaN	NaN	NaN	NaN	NaN	NaN	NaN
AN12054 (SsnF)	Transcriptional co-repressor	10	10	24	NaN	NaN	NaN	NaN	NaN	NaN	NaN	NaN	NaN	NaN
AN1222	S-adenosylmethionine synthetase	144	157	357	NaN	NaN	NaN	NaN	NaN	NaN	NaN	NaN	NaN	NaN
AN12402 (XptB)	Prenyltransferase (<i>mpd/xpt</i>)	10	9	17	NaN	NaN	NaN	NaN	NaN	NaN	NaN	NaN	NaN	NaN
AN1546	Histone deacetylase		2	4	NaN	NaN	NaN	NaN	NaN	NaN	NaN	NaN	NaN	NaN
AN1547 (CoaT)	Carboxylate CoA-transferase		17	13	NaN	NaN	NaN	NaN	NaN	NaN	NaN	NaN	NaN	NaN
AN1606	Annexin		16	40	NaN	NaN	NaN	NaN	NaN	NaN	NaN	NaN	NaN	NaN
AN1851	Chaperonin	21	34	85	NaN	NaN	NaN	NaN	NaN	NaN	NaN	NaN	NaN	NaN
AN1867 (PhoB)	Cyclin-dependent protein kinase	2		5	NaN	NaN	NaN	NaN	NaN	NaN	NaN	NaN	NaN	NaN
AN1868	Glycerol dehydrogenase	11	19		NaN	NaN	NaN	NaN	NaN	NaN	NaN	NaN	NaN	NaN
AN1882	Oxidoreductase		8	4	NaN	NaN	NaN	NaN	NaN	NaN	NaN	NaN	NaN	NaN
AN1896 (FahA)	Fumarylacetoacetate hydrolase	42	49	5	NaN	NaN	NaN	NaN	NaN	NaN	NaN	NaN	NaN	NaN
AN1918 (AcuF)	Carboxykinase	16	29	39	NaN	NaN	NaN	NaN	NaN	NaN	NaN	NaN	NaN	NaN
AN1967	Fatty acid dioxygenase	22	41	87	NaN	NaN	NaN	NaN	NaN	NaN	NaN	NaN	NaN	NaN
AN1971	3'-5' DNA helicase	16	10	35	NaN	NaN	NaN	NaN	NaN	NaN	NaN	NaN	NaN	NaN
AN2080	Translation release factor eRF3		21	39	NaN	NaN	NaN	NaN	NaN	NaN	NaN	NaN	NaN	NaN
AN2092 (PapA)	Prolyl aminopeptidase		8	8	NaN	NaN	NaN	NaN	NaN	NaN	NaN	NaN	NaN	NaN
AN2149 (Cct1)	Chaperonin complex component	12	27	86	NaN	NaN	NaN	NaN	NaN	NaN	NaN	NaN	NaN	NaN
AN2208	Galactose 1-dehydrogenase	55	41	91	NaN	NaN	NaN	NaN	NaN	NaN	NaN	NaN	NaN	NaN
AN2293	Isomerase activity		2	7	NaN	NaN	NaN	NaN	NaN	NaN	NaN	NaN	NaN	NaN
AN2314	Glucan branching enzyme	43	25	22	NaN	NaN	NaN	NaN	NaN	NaN	NaN	NaN	NaN	NaN
AN2336	Phospholipase C		80	211	NaN	NaN	NaN	NaN	NaN	NaN	NaN	NaN	NaN	NaN
AN2439 (SldB)	Spindle assembly checkpoint		14	14	NaN	NaN	NaN	NaN	NaN	NaN	NaN	NaN	NaN	NaN
AN2514	Protein of unknown function		9	19	NaN	NaN	NaN	NaN	NaN	NaN	NaN	NaN	NaN	NaN
AN2523 (ChsB)	Chitin synthase	3		25	NaN	NaN	NaN	NaN	NaN	NaN	NaN	NaN	NaN	NaN
AN2525	L-serine dehydratase		3	14	NaN	NaN	NaN	NaN	NaN	NaN	NaN	NaN	NaN	NaN
AN2549 (EasD)	Acyl-CoA ligase	3	10		NaN	NaN	NaN	NaN	NaN	NaN	NaN	NaN	NaN	NaN

Supplements

Gene ID	Description	PSM			<i>laeAΔ/laeA</i>			∅	SD	<i>laeAcomp+/laeA</i>			∅	SD
		1	2	3	1	2	3			1	2	3		
AN2588	Protein of unknown function	46	21	18	NaN	NaN	NaN	NaN	NaN	NaN	NaN	NaN	NaN	NaN
AN2682	Oxidoreductase	2	4	93	NaN	NaN	NaN	NaN	NaN	NaN	NaN	NaN	NaN	NaN
AN2733	Uroporphyrinogen decarboxylase		4	5	NaN	NaN	NaN	NaN	NaN	NaN	NaN	NaN	NaN	NaN
AN2775	eIF2A subunit	2	9	43	NaN	NaN	NaN	NaN	NaN	NaN	NaN	NaN	NaN	NaN
AN2815	Mannitol 2-dehydrogenase		12	36	NaN	NaN	NaN	NaN	NaN	NaN	NaN	NaN	NaN	NaN
AN2917	Proteasome regulatory particle	29	20	49	NaN	NaN	NaN	NaN	NaN	NaN	NaN	NaN	NaN	NaN
AN2954	Protein of unknown function	71	131	96	NaN	NaN	NaN	NaN	NaN	NaN	NaN	NaN	NaN	NaN
AN2993	Protein of unknown function	34	14	11	NaN	NaN	NaN	NaN	NaN	NaN	NaN	NaN	NaN	NaN
AN3122	Clathrin-coated vesicle protein	19	13	35	NaN	NaN	NaN	NaN	NaN	NaN	NaN	NaN	NaN	NaN
AN3134	T-complex protein 1	18	24	71	NaN	NaN	NaN	NaN	NaN	NaN	NaN	NaN	NaN	NaN
AN3156	Translation initiation factor 2		9	31	NaN	NaN	NaN	NaN	NaN	NaN	NaN	NaN	NaN	NaN
AN3331	Esterase	22	21	24	NaN	NaN	NaN	NaN	NaN	NaN	NaN	NaN	NaN	NaN
AN3339	Oxidoreductase		2	7	NaN	NaN	NaN	NaN	NaN	NaN	NaN	NaN	NaN	NaN
AN3351	Dehydrogenase	6	16	19	NaN	NaN	NaN	NaN	NaN	NaN	NaN	NaN	NaN	NaN
AN3431	Pyrophosphorylase	6	7	13	NaN	NaN	NaN	NaN	NaN	NaN	NaN	NaN	NaN	NaN
AN3432	Aldose 1-epimerase		7	14	NaN	NaN	NaN	NaN	NaN	NaN	NaN	NaN	NaN	NaN
AN3590	Protein of unknown function	25	16	18	NaN	NaN	NaN	NaN	NaN	NaN	NaN	NaN	NaN	NaN
AN3830 (IleA)	L-threonine dehydratase	2		45	NaN	NaN	NaN	NaN	NaN	NaN	NaN	NaN	NaN	NaN
AN3839 (SwoF)	Peptide tetradecanoyltransferase	5	13	22	NaN	NaN	NaN	NaN	NaN	NaN	NaN	NaN	NaN	NaN
AN3853	Metalloendopeptidase	6	16	77	NaN	NaN	NaN	NaN	NaN	NaN	NaN	NaN	NaN	NaN
AN3901	Lactic acid dehydrogenase	27	31	96	NaN	NaN	NaN	NaN	NaN	NaN	NaN	NaN	NaN	NaN
AN3973	Peroxioredoxin	45	54	85	NaN	NaN	NaN	NaN	NaN	NaN	NaN	NaN	NaN	NaN
AN4051	Protein of unknown function		16	173	NaN	NaN	NaN	NaN	NaN	NaN	NaN	NaN	NaN	NaN
AN4080	Role in cytoplasmic translation		9		NaN	NaN	NaN	NaN	NaN	NaN	NaN	NaN	NaN	NaN
AN4081	Cysteine dioxygenase	14	6	24	NaN	NaN	NaN	NaN	NaN	NaN	NaN	NaN	NaN	NaN
AN4236	Proteasome regulatory particle	25	32	55	NaN	NaN	NaN	NaN	NaN	NaN	NaN	NaN	NaN	NaN
AN4270	Actin cortical patch assembly	22	6	28	NaN	NaN	NaN	NaN	NaN	NaN	NaN	NaN	NaN	NaN
AN4290	Isomerase	11	5	16	NaN	NaN	NaN	NaN	NaN	NaN	NaN	NaN	NaN	NaN
AN4303	Cytidylyltransferase	11	6	40	NaN	NaN	NaN	NaN	NaN	NaN	NaN	NaN	NaN	NaN
AN4390	Protein of unknown function		67	76	NaN	NaN	NaN	NaN	NaN	NaN	NaN	NaN	NaN	NaN
AN4647	Phytanoyl-CoA dioxygenase		16	6	NaN	NaN	NaN	NaN	NaN	NaN	NaN	NaN	NaN	NaN
AN4774	Methyltransferase		4	27	NaN	NaN	NaN	NaN	NaN	NaN	NaN	NaN	NaN	NaN
AN4775	Cullin deneddylation	45	47	101	NaN	NaN	NaN	NaN	NaN	NaN	NaN	NaN	NaN	NaN
AN4915 (SrgG)	RAB family GTPase	16	6	25	NaN	NaN	NaN	NaN	NaN	NaN	NaN	NaN	NaN	NaN
AN4929	Protein of unknown function	18	11	20	NaN	NaN	NaN	NaN	NaN	NaN	NaN	NaN	NaN	NaN
AN4934	Dehydrogenase	4	24		NaN	NaN	NaN	NaN	NaN	NaN	NaN	NaN	NaN	NaN
AN4951	Protein transporter	4	8	17	NaN	NaN	NaN	NaN	NaN	NaN	NaN	NaN	NaN	NaN
AN4987 (PkaR)	Protein kinase A	2	7	8	NaN	NaN	NaN	NaN	NaN	NaN	NaN	NaN	NaN	NaN
AN5021	Role in conidium formation		6	35	NaN	NaN	NaN	NaN	NaN	NaN	NaN	NaN	NaN	NaN
AN5132	Uncoupling protein (UCP)	6		24	NaN	NaN	NaN	NaN	NaN	NaN	NaN	NaN	NaN	NaN
AN5134 (GltA)	Glutamate synthase	75	294	789	NaN	NaN	NaN	NaN	NaN	NaN	NaN	NaN	NaN	NaN
AN5226 (AcpA)	Acetate permease	67		24	NaN	NaN	NaN	NaN	NaN	NaN	NaN	NaN	NaN	NaN
AN5257	Oxidoreductase		13	14	NaN	NaN	NaN	NaN	NaN	NaN	NaN	NaN	NaN	NaN
AN5376	Protein of unknown function	9	5	17	NaN	NaN	NaN	NaN	NaN	NaN	NaN	NaN	NaN	NaN
AN5422	Beta-lactamase	43	43	4	NaN	NaN	NaN	NaN	NaN	NaN	NaN	NaN	NaN	NaN
AN5452	Splicing factor 3b	7		29	NaN	NaN	NaN	NaN	NaN	NaN	NaN	NaN	NaN	NaN
AN5523 (TpsA)	Trehalose-phosphate synthase	28	31	31	NaN	NaN	NaN	NaN	NaN	NaN	NaN	NaN	NaN	NaN
AN5534	Glyoxylate reductase	8	6	29	NaN	NaN	NaN	NaN	NaN	NaN	NaN	NaN	NaN	NaN
AN5586	Guanylyltransferase	36	79	82	NaN	NaN	NaN	NaN	NaN	NaN	NaN	NaN	NaN	NaN
AN5607	Role in proteasome assembly		4	7	NaN	NaN	NaN	NaN	NaN	NaN	NaN	NaN	NaN	NaN
AN5690	Amine oxidase		3	4	NaN	NaN	NaN	NaN	NaN	NaN	NaN	NaN	NaN	NaN
AN5782	Fumarylacetoacetate hydrolase	24	31	17	NaN	NaN	NaN	NaN	NaN	NaN	NaN	NaN	NaN	NaN
AN6314	Oxidoreductase		15	10	NaN	NaN	NaN	NaN	NaN	NaN	NaN	NaN	NaN	NaN
AN6488	Tryptophanyl-tRNA synthetase	9	11	13	NaN	NaN	NaN	NaN	NaN	NaN	NaN	NaN	NaN	NaN
AN7181	Protein of unknown function	49	29	32	NaN	NaN	NaN	NaN	NaN	NaN	NaN	NaN	NaN	NaN
AN7231	Serine-type peptidase	21	17	5	NaN	NaN	NaN	NaN	NaN	NaN	NaN	NaN	NaN	NaN
AN7267	Oxidoreductase	179	73	27	NaN	NaN	NaN	NaN	NaN	NaN	NaN	NaN	NaN	NaN
AN7269	Dehydrogenase	26	28	25	NaN	NaN	NaN	NaN	NaN	NaN	NaN	NaN	NaN	NaN
AN7657 (GelA)	1,3-beta-transglycosidase	81	105	101	NaN	NaN	NaN	NaN	NaN	NaN	NaN	NaN	NaN	NaN
AN7900	Oxidoreductase	11	22	4	NaN	NaN	NaN	NaN	NaN	NaN	NaN	NaN	NaN	NaN
AN7912 (OrsC)	Tyrosinase	14	24		NaN	NaN	NaN	NaN	NaN	NaN	NaN	NaN	NaN	NaN
AN8102	Pepsin-like aspartic protease		5	5	NaN	NaN	NaN	NaN	NaN	NaN	NaN	NaN	NaN	NaN
AN8478	Protein of unknown function	10	4		NaN	NaN	NaN	NaN	NaN	NaN	NaN	NaN	NaN	NaN
AN8496	Metal ion binding activity	7	11		NaN	NaN	NaN	NaN	NaN	NaN	NaN	NaN	NaN	NaN
AN8528	Protein of unknown function	22	20	8	NaN	NaN	NaN	NaN	NaN	NaN	NaN	NaN	NaN	NaN
AN8815	Isoflavone reductase	11	3	45	NaN	NaN	NaN	NaN	NaN	NaN	NaN	NaN	NaN	NaN
AN8820 (CnaA)	Calcineurin A	39	28	72	NaN	NaN	NaN	NaN	NaN	NaN	NaN	NaN	NaN	NaN

Supplements

Gene ID	Description	PSM			<i>laeAΔ/laeA</i>			∅	SD	<i>laeAcomp+/laeA</i>			∅	SD
		1	2	3	1	2	3			1	2	3		
AN8843	Homoserine kinase	8	17	15	NaN	NaN	NaN	NaN	NaN	NaN	NaN	NaN	NaN	NaN
AN8863	Nap/SET family protein	12	15	137	NaN	NaN	NaN	NaN	NaN	NaN	NaN	NaN	NaN	NaN
AN9063	Oxysterol-binding protein		4	3	NaN	NaN	NaN	NaN	NaN	NaN	NaN	NaN	NaN	NaN
AN9065	Translation regulator activity		3	7	NaN	NaN	NaN	NaN	NaN	NaN	NaN	NaN	NaN	NaN
AN9220	Protein of unknown function		9	24	NaN	NaN	NaN	NaN	NaN	NaN	NaN	NaN	NaN	NaN
AN9322	Triphenylmethane Reductase	5		3	NaN	NaN	NaN	NaN	NaN	NaN	NaN	NaN	NaN	NaN
AN9425	Aldolase		10	9	NaN	NaN	NaN	NaN	NaN	NaN	NaN	NaN	NaN	NaN